



THE UNIVERSITY *of* EDINBURGH

This thesis has been submitted in fulfilment of the requirements for a postgraduate degree (e.g. PhD, MPhil, DClinPsychol) at the University of Edinburgh. Please note the following terms and conditions of use:

This work is protected by copyright and other intellectual property rights, which are retained by the thesis author, unless otherwise stated.

A copy can be downloaded for personal non-commercial research or study, without prior permission or charge.

This thesis cannot be reproduced or quoted extensively from without first obtaining permission in writing from the author.

The content must not be changed in any way or sold commercially in any format or medium without the formal permission of the author.

When referring to this work, full bibliographic details including the author, title, awarding institution and date of the thesis must be given.

***O*-Aryl Imidates, Isoureas and Thiocarbamates**



THE UNIVERSITY
of EDINBURGH

Joseph Andrew Tate

Doctor of Philosophy

University of Edinburgh

2016

Declaration

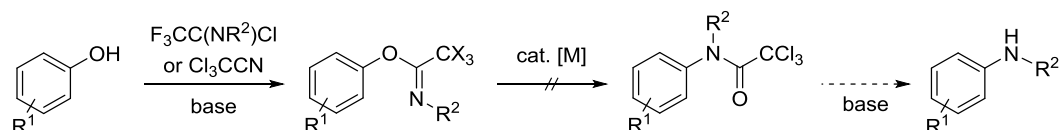
I declare that the work presented in this thesis is my own and was conducted under the supervision of Professor Guy C. Lloyd-Jones FRS. I have composed this thesis and it has not been submitted for any other degree or professional qualification.

Joseph Andrew Tate

Abstract

Phenols are some of the most readily available and easily elaborated aromatic compounds, but the strength of the C_{Ar}-O bond hampers their conversion to highly sought C_{Ar}-N, C_{Ar}-S and C_{Ar}-C analogues. Attempts have therefore been made to establish new protocols for achieving such transformations by derivatising phenols with suitable C_{Ar}-O bond activating groups. In particular, investigations have focussed on the development of reactions with the potential to enable phenols to be conveniently converted to anilines.

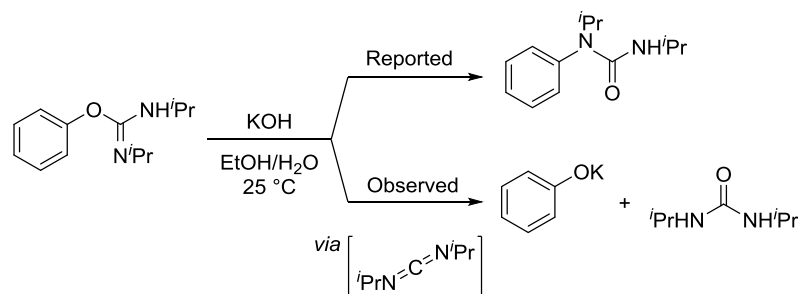
Towards this goal, the synthesis of *O*-aryl trihaloacetimidates was investigated with a view to probing their ability to rearrange to *N*-aryl trihaloacetamides *via* transition metal catalysis (Scheme 1). It was found that *O*-aryl trichloroacetimidates could be obtained from the base-catalysed reactions of phenols with trichloroacetonitrile, but only when electron-rich phenols were applied. In contrast, *N*-(4-methylphenyl)-*O*-aryl trifluoroacetimidates were generated in good yields from electron-rich and electron-poor phenols by their condensation with *N*-(4-methylphenyl)trifluoroacetimidoyl chloride. With these substrates in hand, a number of transition metal catalysts were screened for activity in the proposed rearrangement reactions, but the desired transformations were not achieved. As part of this screen, a novel mono-NHC palladium(II) precatalyst with the potential to be thermally activated was developed.



Scheme 1 The proposed strategy for converting phenols to anilines.

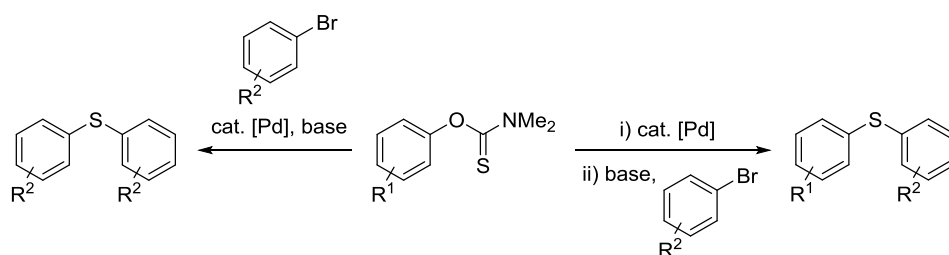
The hydroxide-catalysed rearrangement of *O*-aryl-*N,N'*-diisopropyl isoureas to *N*-aryl-*N,N'*-diisopropyl ureas was reported in 1983, but there have been no reported applications of this reaction to date. The reaction was therefore revisited with the intention of realising its unexplored synthetic potential. The reported hydroxide-catalysed rearrangement of *O*-phenyl-*N,N'*-diisopropyl isourea to *N*-phenyl-*N,N'*-diisopropyl urea was, however, discredited on the basis of ¹H NMR and UV spectrometric analyses (Scheme 2). This isourea was instead, found to be converted to phenoxide and diisopropyl urea under the reported conditions. A detailed kinetic study revealed that the isourea was not directly hydrolysed, but underwent hydroxide-mediated elimination

to produce phenoxide and diisopropyl carbodiimide. The hydrolysis of diisopropyl carbodiimide to diisopropyl urea then occurred in a slower, second step which was catalysed by hydroxide. Attempts to identify and synthesise *N*-heterocyclic isourea structures which were more disposed towards rearrangement were unsuccessful.



Scheme 2 The reported and observed reactivity of *O*-phenyl-*N,N'*-diisopropyl isourea in aqueous base.

Early attempts to use *O*-aryl-*N,N'*-dimethyl thiocarbamates as phenol-derived pseudohalides in palladium(0)-catalysed, C_{Ar}-C bond-forming cross-coupling reactions showed little promise due to the onset of their base-induced decomposition. However, the formation of a diaryl thioether side product was observed during these studies, leading to a preliminary investigation into the use of aryl thiocarbamates as hydrogen sulfide surrogates and thiophenol precursors in palladium(0)-catalysed C-S coupling reactions (Scheme 3). The promise of this approach was demonstrated by the synthesis of both symmetrical and unsymmetrical diaryl thioethers in the palladium(0)-catalysed couplings of *O*- and *S*-(4-trifluoromethyl)-*N,N*-dimethyl thiocarbamate with 1-bromo-4-fluorobenzene.



Scheme 3 The preparation of diaryl thioethers from *O*-aryl thiocarbamates and aryl bromides *via* palladium(0) catalysis.

Lay Summary

Complex synthetic organic molecules are encountered in almost all aspects of everyday life. To name but a few examples, they are present in the screens of electronic devices, are used as dyestuffs and are the active ingredients in the majority of pharmaceutical and agrochemical products. As a result, there is a great need for the development of new technologies which allow us to access these molecules more practically and efficiently from readily available, and ideally, renewable starting materials.

Almost all complex organic molecules are comprised of only six elements, namely; carbon, hydrogen, nitrogen, oxygen, phosphorus and sulfur. However, combining these elements in a predictable and efficient manner can be difficult. An efficient strategy for the synthesis of large, complex organic molecules is to piece together small molecule building blocks which have been pre-assembled by nature or well-established industrial processes.

Phenols and anilines are essentially the oxygen- and nitrogen-bound derivatives of benzene and are two different types of such building blocks. Phenols are more naturally abundant and easier to synthesise than anilines, but anilines are found more frequently in biologically active products.

This thesis details the efforts which have been made to develop a protocol for the conversion of phenols to anilines and also describes preliminary investigations into the use of phenols as starting materials for the synthesis of sulfur-containing benzene derivatives.

Acknowledgments

Firstly, I would like to thank Professor Guy Lloyd-Jones for the opportunity to work in his group. I believe that I have learnt more during my Ph.D. than I have at any other stage in my education and this is, in no small part, a result of the supervision and sound advice which has been provided by Guy and the enthusiastic support which has been offered by all of my co-workers.

My thanks also go to the Lloyd-Jones group for making my Ph.D. so enjoyable. I would like to thank Dr. Louise Evans, Dr. Alastair Lennox, Dr. Bertram Ong, Dr. Liam Ball, Dr. Tomas Racys, Dr. Carl Poree, Dr. Ruth Dooley, Dr. Rob Cox, Nick Taylor, Paul Cox, Jorge Gonzalez, Tom Corrie, Dr. Alex Cresswell, Katherine Geogheghan, Matt Robinson, Dr. Marc Reid, Dr. Eric Keske, Dr. Alba Collado, Eduardo Nieto and Magdalene Teh.

In addition, I would like to thank my industrial supervisor Dr. George Hodges for his valuable input and for giving me the opportunity to undertake a placement at Syngenta, Jealott's Hill. I am also very grateful of the entire Syngenta process studies group, and in particular Dr. Anne-Marie Hogan, for making me feel welcome during my visit.

Above all, I would like to thank my family and Amy for their unwavering confidence in me and all the encouragement they have given.

I thank Syngenta and the EPSRC for financial support.

Abbreviations

COD	1,5-cyclooctadiene
COSY	correlation spectroscopy
CuTC	copper(I) thiophene-2-carboxylate
DABCO	1,4-diazabicyclo[2.2.2]octane
dba	dibenzylideneacetone
DBU	1,8-diazabicyclo[5.4.0]undec-7-ene
DCC	<i>N,N'</i> -dicyclohexylcarbodiimide
DIC	<i>N,N'</i> -diisopropylcarbodiimide
DIPU	<i>N,N'</i> -diisopropyl urea
DMAP	4-dimethylaminopyridine
DMI	1,3-dimethyl-2-imidazolidinone
DMPU	1,3-dimethyl-3,4,5,6-tetrahydro-2(1H)-pyrimidinone
EXSY	exchange spectroscopy
HMBC	heteronuclear multiple-bond correlation spectroscopy
HMPA	hexamethylphosphoramide
H-G II	Hoveyda-Grubbs 2 nd generation catalyst
HSQC	heteronuclear single-quantum correlation spectroscopy
ms	molecular sieves
NHC	<i>N</i> -heterocyclic carbene
NKR	Newman-Kwart rearrangement
NMP	<i>N</i> -methyl-2-pyrrolidone
NOE(SY)	nuclear Overhauser effect (spectroscopy)
OMs	methanesulfonate (mesylate)

OPic	2,4,6-trinitrophenolate (picrate)
OTf	trifluoromethanesulfonate (triflate)
OTs	<i>p</i> -toluenesulfonate (tosylate)
PEPPSI	pyridine-enhanced precatalyst preparation, stabilisation and initiation
RCM	ring-closing metathesis

Contents

Declaration	i
Abstract.....	ii
Lay Summary.....	iv
Acknowledgments	v
Abbreviations	vi
Contents	viii
1 Introduction.....	1
1.1 Methods for Converting Phenols to Anilines	2
1.1.1 Historical Transformations.....	2
1.1.2 Buchwald-Hartwig Amination	3
1.1.3 The Smiles Rearrangement.....	7
1.1.4 The Chapman Rearrangement.....	9
1.1.5 The Chichibabin Rearrangement.....	11
1.2 Phenol-Derived Electrophiles in Cross-Coupling Reactions.....	12
1.2.1 Palladium-Catalysed Cross-Coupling Reactions.....	13
1.2.2 Nickel-Catalysed Cross-Coupling Reactions	14
1.2.3 Cross-Coupling Reactions Catalysed by Other Transition Metals.....	17
1.3 The Newman-Kwart Rearrangement	20
1.3.1 Practical Considerations	20
1.3.2 Catalysis	21
2 Towards a Transition Metal-Catalysed Chapman-Type Rearrangement: <i>O</i>-Aryl Trihaloacetimidates.....	25
2.1 Introduction.....	26
2.1.1 Chapter Aims.....	26
2.1.2 <i>O</i> -Allyl Trihaloacetimidates: The Overman Rearrangement.....	27

2.1.3	<i>O</i> -Glycosyl Trihaloacetimidates.....	29
2.1.4	<i>O</i> -Alkyl Trihaloacetimidates	31
2.2	Preparation of <i>O</i> -Aryl Trichloroacetimidates	32
2.2.1	Literature Procedures	32
2.2.2	Initial Optimisation: <i>O</i> -(4-Methoxyphenyl) Trichloroacetimidate	33
2.2.3	Assigning the Isomers of <i>O</i> -(4-Methoxyphenyl) Trichloroacetimidate	35
2.2.4	Other <i>O</i> -Aryl Trichloroacetimidates.....	39
2.3	Transition Metal Catalysis: <i>O</i> -Aryl Trichloroacetimidates	40
2.3.1	Considerations for Transition Metal Catalysis	40
2.3.2	Initial Attempts	42
2.3.3	Catalyst Screen	44
2.4	Palladium <i>N</i> -Heterocyclic Carbene Catalysts.....	45
2.4.1	Background and Proposal.....	45
2.4.2	Initial Investigations	48
2.4.3	SIPr-Pentafluorobenzene Adduct Thermolysis	50
2.4.4	Catalytic Activity of (SIPr)Pd(η^1 -1-PhC ₃ H ₄)(η^5 -C ₅ H ₅)	51
2.5	<i>O</i> -Aryl Trifluoroacetimidates	53
2.5.1	Concept.....	53
2.5.2	Preparation	54
2.5.3	Assigning Isomers	54
2.5.4	Catalyst Screen	58
2.6	4-Aryloxy Quinazolines	60
2.6.1	Concept.....	60
2.6.2	Catalyst Screen	61
2.7	Summary and Conclusions.....	62
2.8	Future Work	62

3	Towards a Base-Catalysed Chapman-Type Rearrangement: <i>O</i>-Aryl Isoureas.....	65
3.1	Introduction.....	66
3.1.1	Chapman-Type Rearrangements of <i>O</i> -Aryl Isoureas.....	66
3.1.2	Anionic Chapman-Type Rearrangements of <i>O</i> -Aryl Isoureas.....	68
3.1.3	Summary and Chapter Aims.....	70
3.2	Preparation of <i>O</i> -Aryl- <i>N,N'</i> -dialkyl Isoureas	70
3.2.1	Background	70
3.2.2	Literature Procedures.....	72
3.2.3	Improving the Synthetic Procedure	73
3.2.4	Mechanistic Insight into the Reaction of Phenol with DIC.....	74
3.2.5	Effect of Additives on the Reaction of Phenol with DIC	77
3.3	Revisiting the Anionic Chapman-Type Rearrangements of <i>O</i> -Aryl Isoureas.....	80
3.3.1	Background	80
3.3.2	Initial Attempts	81
3.3.3	UV-Vis Kinetics.....	82
3.4	Kinetic Analysis of Isourea Salt Solvolysis.....	86
3.4.1	Influence of Anion and <i>N</i> -Substituent	86
3.4.2	Role of Potassium Hydroxide.....	87
3.4.3	Mechanism of Isourea Salt Solvolysis.....	89
3.5	Avoiding Isourea Decomposition	94
3.5.1	Anhydrous Conditions	94
3.5.2	<i>N,N'</i> -Heterocyclic Isoureas.....	95
3.6	Summary and Conclusions.....	101
3.7	Future Work	102
4	<i>O</i>-Aryl Thiocarbamates in Palladium-Catalysed Coupling Reactions	105

4.1	<i>O</i> -Aryl Thiocarbamates as Electrophiles in Palladium-Catalysed Cross-Coupling Reactions.....	106
4.1.1	Introduction and Concept.....	106
4.1.2	Attempted Cross-Coupling Reactions Using Boronic Acids.....	108
4.1.3	Attempted Cross-Coupling Reactions Using Arylzinc Reagents	111
4.2	Synthesis of Diaryl Thioethers <i>via</i> Palladium-Catalysed Cross-Coupling Reactions.....	113
4.2.1	Introduction and Concept.....	113
4.2.2	Symmetrical Diaryl Thioethers from <i>O</i> -Aryl Thiocarbamates.....	118
4.2.3	Symmetrical Diaryl Thioethers from Aryl Bromides.....	119
4.2.4	Unsymmetrical Diaryl Thioethers from <i>O</i> -Aryl Thiocarbamates and Aryl Bromides.....	121
4.3	Summary and Conclusions.....	125
4.4	Future Work	126
5	Experimental.....	129
5.1	General Experimental Details	130
5.1.1	Techniques	130
5.1.2	Materials	130
5.1.3	Instrumentation and Analysis.....	131
5.2	Experimental Details Relevant to Chapter 2	133
5.2.1	Preparation of <i>O</i> -Aryl Trichloroacetimidates.....	133
5.2.2	Preparation of <i>N</i> -Aryl Trihaloacetamides	136
5.2.3	Initial Rearrangement Attempts	138
5.2.4	Preparation of (SIPr)Pd(η^1 -1-PhC ₃ H ₄)(η^5 -C ₅ H ₅)	140
5.2.5	Reactions of (SIPr)Pd(η^1 -1-PhC ₃ H ₄)(η^5 -C ₅ H ₅)	143
5.2.6	Preparation of <i>O</i> -Aryl- <i>N</i> -(4-methylphenyl) Trifluoroacetimidates.....	144
5.2.7	Catalyst Screening.....	145

5.3	Experimental Details Relevant to Chapter 3	147
5.3.1	Synthesis of <i>O</i> -Phenyl- <i>N,N'</i> -dialkyl Isoureas.....	147
5.3.2	Solvolysis of Isourea Salts	150
5.3.3	Elimination of Phenol and DIC from <i>O</i> -Phenyl- <i>N,N'</i> -diisopropyl Isourea.....	154
5.3.4	<i>N</i> -Heterocyclic Isoureas	155
5.4	Experimental Details Relevant to Chapter 4.....	160
5.4.1	Synthesis of Aryl- <i>N,N'</i> -dimethyl Thiocarbamates	160
5.4.2	<i>O</i> -(4-Trifluoromethylphenyl)- <i>N,N'</i> -dimethyl Thiocarbamate in Cross- Coupling Reactions.....	161
5.4.3	Coupling Reactions Forming Symmetrical Diaryl Thioethers.....	162
5.4.4	Coupling Reactions Forming Unsymmetrical Diaryl Thioethers	163
5.4.5	Diaryl Thioethers	164
6	References	167

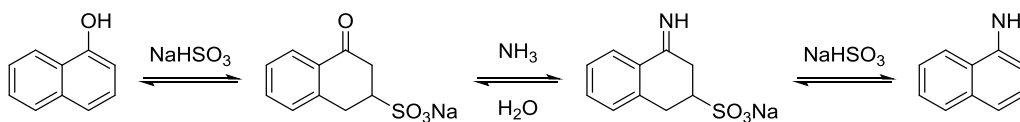
1 Introduction

1.1 Methods for Converting Phenols to Anilines

Aromatic amines and amides are among the most common chemical moieties encountered in pharmaceutical and agrochemical motifs. However, traditional strategies for accessing the C_{Ar}-N linkage, such as; electrophilic aromatic substitution (e.g. nitration), nucleophilic aromatic substitution and nucleophilic addition to arynes, tend to display poor selectivity and lack scope.¹ Therefore, whilst these methods are adequate for the synthesis of relatively simple anilines and anilides, the synthesis of more complex targets is most conveniently achieved using the extremely general palladium-catalysed Buchwald-Hartwig amination² and copper-catalysed Ullmann amination reactions.³ Importantly, these procedures are capable of producing primary anilines through the coupling of ammonia, but also typically utilize aryl halides and most efficaciously, expensive aryl iodides and aryl bromides.^{4,5} Thus, despite advances towards the coupling of cheap aryl chlorides being well documented,^{2,3,6} a general and economical procedure for the generation of primary anilines from readily obtainable phenolic precursors stands out as an attractive prospect.

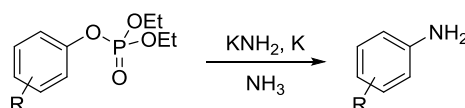
1.1.1 Historical Transformations

Methods for the preparation of primary anilines from phenols have been known for over a century, but most have been sufficiently ailed by inefficiency and poor substrate scope that they have been left largely unapplied. The Bucherer reaction was one of the earliest of these more historical transformations to be studied (Scheme 1.1) and concerns the inter-conversion of fused (hetero)aryl alcohols (e.g. naphthols and phenanthrols) with the corresponding amines. The reaction is performed by treatment of the alcohol with aqueous sodium bisulfite and ammonia, and is entirely reversible. The directionality of the process is controlled by the concentration of ammonia in the reaction mixture. The reaction proceeds *via* the partial de-aromatization of the aromatic system and as a consequence, phenols are not suitable substrates for the reaction.^{7,8} Due to the nature of those aryl alcohols which are compatible, the Bucherer reaction has found considerable application in the manufacture of dyes.⁹



Scheme 1.1 The Bucherer reaction.

The substitution of *O*-aryl diethylphosphate esters with potassium amide in liquid ammonia is compatible with non-fused aromatic alcohols (Scheme 1.2), but the substrate scope is severely limited by the strongly reducing and nucleophilic conditions.¹⁰ Aryl diethylphosphate esters are readily obtained from the reactions of phenols with diethyl chlorophosphate.



Scheme 1.2 The substitution of *O*-aryl diethylphosphate esters with potassium amide.

1.1.2 Buchwald-Hartwig Amination

The most significant development with respect to achieving a general practise for the conversion of phenols to anilines has been the innovation of the palladium(0)-catalysed amination of *O*-aryl sulfonates. This approach was pioneered by the groups of Buchwald and Hartwig, and over the last 20 years, the scope of the reaction has been expanded to encompass the coupling of amides, nitrogen heterocycles and primary, secondary and aromatic amines.¹¹ Originally, *O*-aryl triflates, the most reactive of the *O*-aryl sulfonates towards palladium(0) oxidative addition, resisted coupling due to the onset of base-induced ArO-S bond cleavage. However, the emergence of more reactive palladium(0) catalysts incorporating chelating bisphosphine ligands (e.g. dppf and BINAP)^{12,13} and the use of milder inorganic bases (e.g. lithium *tert*-butoxide and Cs₂CO₃)^{14,15} allowed such couplings to be realised. More stable, but more expensive, *O*-aryl nonaflates were also found to be competent coupling partners.^{16,17} Major advances in the efficiency and scope of the amination of aryl triflates were achieved with the emergence of more active catalysts based upon bulky and electron-rich phosphine ligands (Figure 1.1).^{11,18}

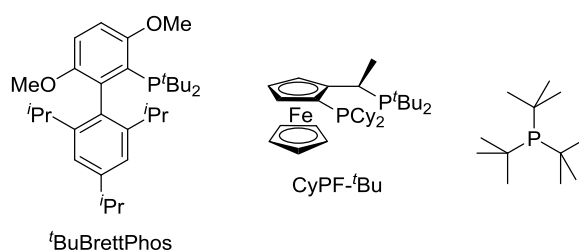
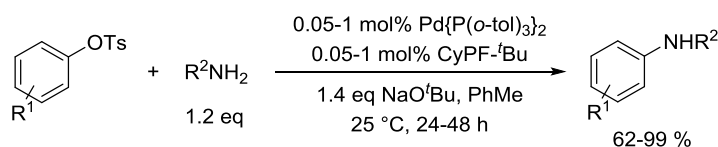


Figure 1.1 Examples of bulky and strongly electron-donating phosphine ligands.

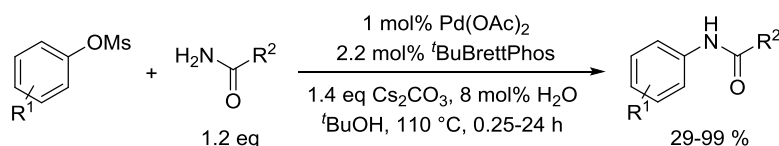
Of these ligands, dialkylbiaryl phosphines, ferrocene-derived bisphosphines and trialkyl phosphines have received the most attention. The same classes of ligands have also been

found to enable the amination of notably cheaper and more stable *O*-aryl tosylates and *O*-aryl mesylates. Of these, *O*-aryl tosylates are the most reactive and have been coupled with primary alkyl amines, primary anilines and imines even at room temperature (Scheme 1.3). Enabling this was the particularly efficient generation of an extremely active palladium(0) catalyst from a labile palladium(0) precatalyst.^{19,20}



Scheme 1.3 The palladium(0)-catalysed amination of *O*-aryl tosylates.

The amination of less reactive *O*-aryl mesylates requires significantly more forcing conditions, but is more atom-economical.^{21,22} Notably, this reaction has been extended to the cross-coupling of *O*-(hetero)aryl mesylates with amides (Scheme 1.4).²³

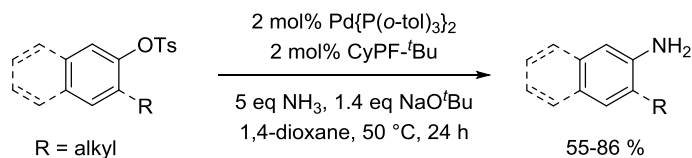


Scheme 1.4 The palladium(0)-catalysed amination of *O*-aryl mesylates with amides.

Ammonia would appear to be the ideal coupling partner for the transition metal-catalysed amination of *O*-aryl sulfonates. Ammonia is one of the simplest chemical feedstocks and its coupling with *O*-aryl sulfonates would produce highly desirable primary anilines. Unfortunately, the use of ammonia in transition metal coupling reactions is fraught with difficulty. Not only does the basicity and nucleophilicity of ammonia induce side-reactions, but its propensity to ligate transition metal centres often leads to the displacement of ligands which are essential for catalyst activity and stability. Furthermore, if coupling is achieved, the aniline products are likely to be more susceptible towards transition metal-catalysed arylation than ammonia. As a result, mixtures of mono-, di- and tri-arylated amines can be generated.^{24,25}

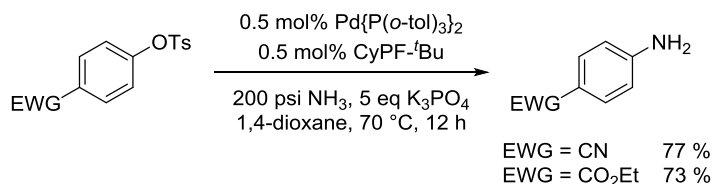
Despite these complications, the palladium(0)-catalysed coupling of ammonia with *O*-aryl tosylates has recently been accomplished. Key to achieving success was the use of a bulky and tightly-binding bisphosphine ligand. This ligand successfully resisted displacement by ammonia, promoted the reductive elimination of stable aryl palladium(II) amido complexes and dictated the selective arylation of ammonia. As a

result, the amination of *O*-naphthyl and *ortho*-substituted *O*-aryl tosylates using a 0.5 M solution of ammonia in 1,4-dioxane proceeded efficiently, without cleavage, at 50 °C (Scheme 1.5). Under the same conditions, the cleavage of *O*-aryl triflates was the dominant process.^{5,26}



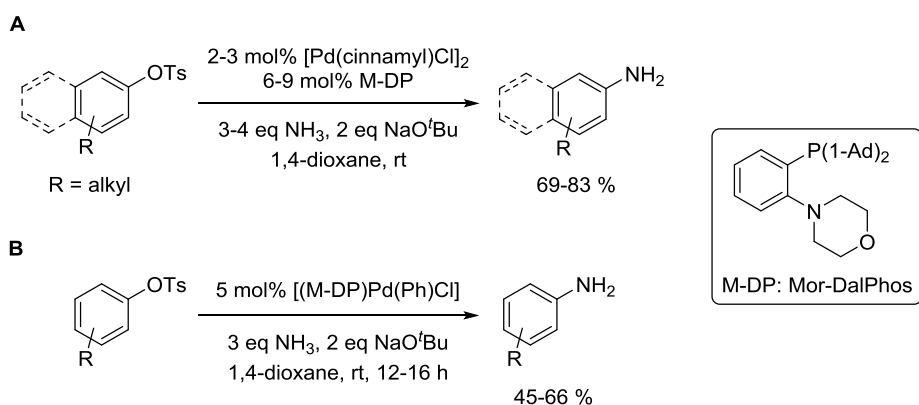
Scheme 1.5 The palladium(0)-catalysed amination of *O*-aryl tosylates using a 0.5 M solution of ammonia in 1,4-dioxane.

Using a milder base, the amination of *O*-aryl tosylates substituted with electron-withdrawing, base-sensitive functional groups in the *para*-position was also achieved, albeit only when a high pressure of ammonia was applied (Scheme 1.6).⁵



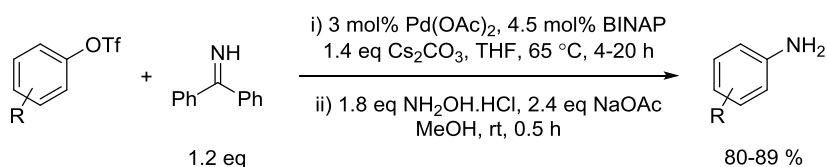
Scheme 1.6 The palladium(0)-catalysed amination of electron-deficient *O*-aryl tosylates using a high pressure of ammonia.

Later, a system capable of coupling naphthyl- and alkyl-substituted *O*-aryl tosylates with ammonia at room temperature was derived (reaction A, Scheme 1.7).²⁷ The use of an improved precatalyst allowed this reaction to be extended to a slightly wider range of *O*-(hetero)aryl tosylates. However, electron-rich and electron-poor substrates were still not tolerated, and the majority of the examples given were *ortho*-substituted (reaction B, Scheme 1.7).²⁸



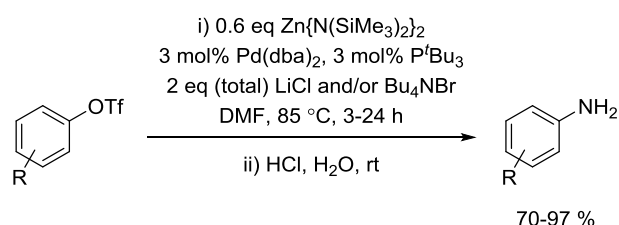
Scheme 1.7 The palladium(0)-catalysed coupling of *O*-aryl tosylates with ammonia at room temperature.

Whilst the amination of *O*-aryl sulfonates with ammonia remains limited, their coupling with ammonia surrogates provides an attractive alternative.²⁵ Ammonia surrogates are nitrogen nucleophiles which can be coupled in transition metal-catalysed amination reactions to generate products which can be readily cleaved to liberate primary anilines. A number of different types of surrogates have been coupled with aryl halides, such as; imines,^{29,30} allyl amines³¹ and silylated amines.^{32,33} However, only benzophenone imine and zinc bis(hexamethyldisilazide) have been adopted into *O*-aryl sulfonate amination protocols. Of these, benzophenone imine has received the most attention due to its higher compatibility with sensitive functional groups and the ease with which the *N*-aryl imine coupling products can be deprotected. Deprotection can be achieved *via* hydrogenation, transamination or acid-catalysed hydrolysis.³⁰ *O*-Aryl triflates (Scheme 1.8),³⁰ *O*-aryl tosylates¹⁹ and *O*-aryl benzenesulfonates³⁴ have all been successfully coupled with benzophenone imine.



Scheme 1.8 The conversion of *O*-aryl triflates to anilines *via* a palladium(0)-catalysed amination reaction using benzophenone imine.

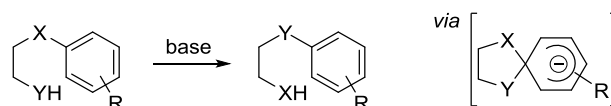
A further benefit of the benzophenone imine system is that relatively simple catalysts and conventional reaction conditions can be used. In contrast, the amination of *O*-aryl triflates with zinc bis(hexamethyldisilazide) requires the use of a highly active catalyst system and additives which increase the rate of oxidative addition in order for *O*-aryl triflate cleavage to be outcompeted (Scheme 1.9).³⁵



Scheme 1.9 The conversion of *O*-aryl triflates to anilines *via* a palladium(0)-catalysed amination reaction using zinc bis(hexamethyldisilazide).

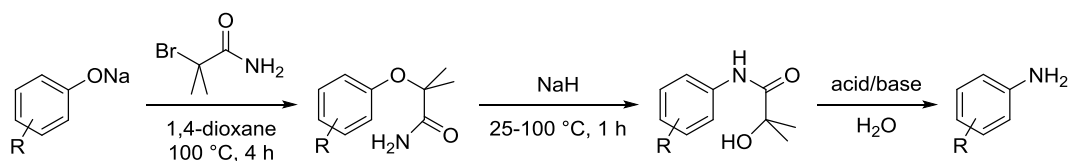
1.1.3 The Smiles Rearrangement

The Smiles rearrangement is the general name given to intramolecular nucleophilic aromatic *ipso*-substitution reactions and constitutes a diverse tool *via* which aryl heteroatom bonds can be interconverted (Scheme 1.10). As is the case with intermolecular nucleophilic aromatic substitution reactions, the Smiles rearrangement is accelerated by electron-withdrawing aromatic substituents.³⁶



Scheme 1.10 The Smiles rearrangement.

With regards to transforming C_{Ar}-O linkages to C_{Ar}-N linkages, the Smiles rearrangement has proven especially valuable. Of particular relevance to the current discussion is the base-promoted rearrangement of 2-aryloxy-2-methylpropanamides to the corresponding *N*-aryl-2-hydroxy-2-methylpropanamides (Scheme 1.11). This reaction has been refined into a practical strategy for the conversion of phenols to primary anilines.^{37,38}



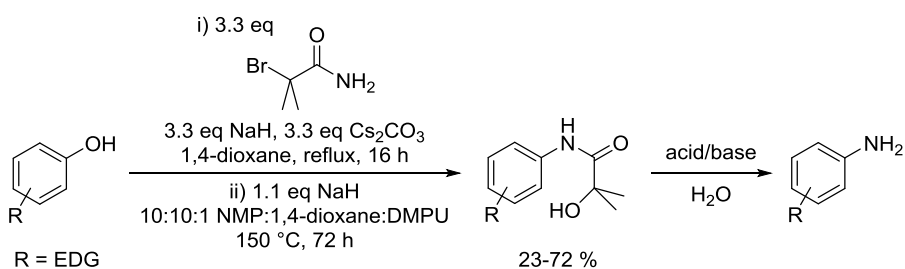
Scheme 1.11 The three-step, three-pot procedure for the conversion of phenols to anilines *via* the Smiles rearrangement of 2-aryloxy-2-methylpropanamides.

2-Aryloxy-2-methylpropanamides are routinely prepared by reacting sodium phenoxide salts with 2-bromo-2-methylpropanamide, a commercially available reagent. After isolation, the rearrangement of these substrates is most commonly induced using sodium hydride and temperatures ranging from 25-100 °C, depending upon aromatic

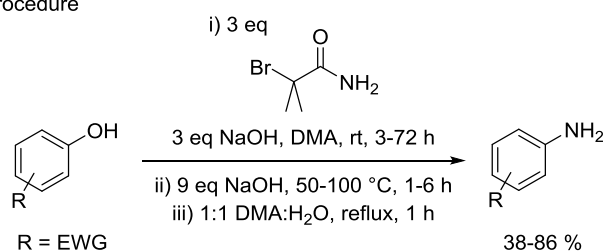
substitution and the identity of the reaction solvent. Typically, the rearrangement of substrates substituted with electron-withdrawing groups can be achieved at ambient temperature in DMF or at 100 °C in 1,4-dioxane. However, such conditions are not suitable for the rearrangement of non-activated substrates.³⁹ For the rearrangement of non-activated substrates to be achieved within the same temperature range, solvents which selectively solvate cations, such as HMPA³⁷ or DMPU,³⁸ must be employed. Such solvents even enable substrates containing electron-donating aromatic substituents to rearrange at 100 °C. The *N*-aryl-2-hydroxy-2-methylpropanamide products of rearrangement can be hydrolysed using strong acid or base to liberate the corresponding anilines.

This three-step, three-pot method for converting phenols to anilines has subsequently been adapted into three-step, two-pot⁴⁰ and three-step, one-pot procedures (Scheme 1.12).⁴¹ Beneficially, these two-pot and one-pot procedures are somewhat complimentary with respect to their substrate scope. The one-pot procedure is mild but limited to electron-deficient phenols, whereas the two-pot procedure employs forcing conditions, but has been shown to perform well with electron-rich phenols.

Two-pot procedure



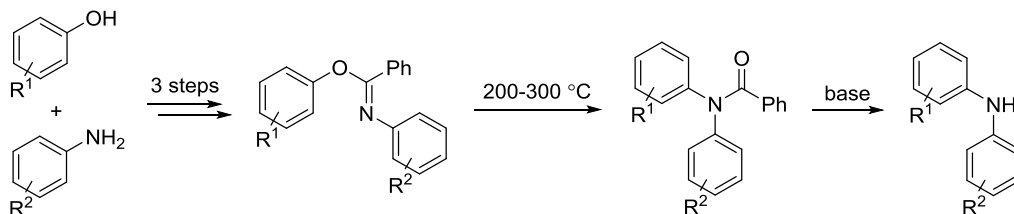
One-pot procedure



Scheme 1.12 Two- and one-pot procedures for the conversion of phenols to anilines via the Smiles rearrangement of 2-aryloxy-2-methylpropanamides.

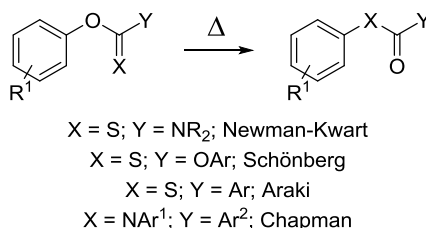
1.1.4 The Chapman Rearrangement

The Chapman rearrangement is the thermal rearrangement of *O*-aryl-*N*-aryl benzimidates to the corresponding *N,N*-diaryl benzamides, and is used in the synthesis of diaryl amines from phenols and anilines (Scheme 1.13).⁴²⁻⁴⁴



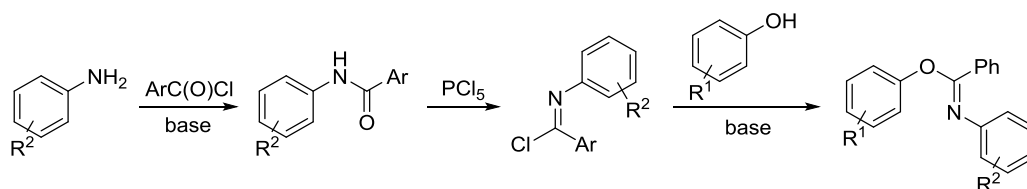
Scheme 1.13 The synthesis of diaryl amines *via* the Chapman rearrangement.

The Chapman rearrangement is part of a group of *ipso*-rearrangement reactions which involve a 1,3-aryl shift from oxygen to nitrogen or sulfur (in this case nitrogen, Scheme 1.14). The thermodynamic driving force for these rearrangement reactions is the formation of a strong C-O double bond. Like the Smiles rearrangement, these rearrangements can be viewed as intramolecular nucleophilic aromatic substitution reactions.⁴⁵



Scheme 1.14 Thermal aromatic *ipso*-rearrangement reactions involving a 1,3-aryl shift.

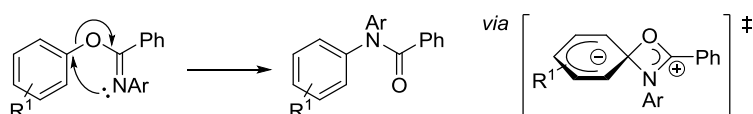
Before the emergence of transition metal-catalysed amination reactions, the Chapman rearrangement received an appreciable amount of attention for the synthesis of diaryl amines, in spite of the extreme temperatures required in the rearrangement step. Such temperatures can be difficult to achieve in a safe manner using conventional heating techniques and severely limit the substrate scope of the reaction. The rearrangement is often performed neat, although particularly high boiling solvents (e.g. diphenyl ether) can also be employed and can help to minimise the decomposition of sensitive substrates.⁴⁴ The synthesis of substrates for the Chapman rearrangement is also not routine and is typically achieved in three steps by combining a phenol, an aniline and an aroyl chloride (Scheme 1.15).⁴⁶



Scheme 1.15 The synthesis of *O*-aryl-*N*-aryl benzimidates.

Since its conception, the mechanism of the Chapman rearrangement has been a subject of considerable interest. Chapman performed the first mechanistic investigation and determined that the rearrangement was unimolecular on the basis of its adherence to first order kinetics.⁴³ In addition, electron-withdrawing *O*-aryl ring substituents were determined to accelerate the rearrangement, whilst electron-withdrawing *N*-aryl and *C*-aryl ring substituents were demonstrated to have an opposite and less significant effect.⁴⁷

Subsequent kinetic studies using more advanced experimental techniques confirmed the operation of first order reaction kinetics and also enabled the extraction of a Hammett reaction constant, $\rho = 1.63$, quantifying the electronic influence of *O*-aryl ring substituents.^{48,49} Rearrangements were also demonstrated to be associated with small and negative entropies of activation (e.g. $\Delta S^\ddagger = -7.2 \text{ cal K}^{-1} \text{ mol}^{-1}$ for *O*-phenyl-*N*-phenyl benzimidate). Overall, the collected data was consistent with an intramolecular nucleophilic aromatic substitution reaction in which a zwitterionic and 4,6-spirocyclic transition state was implicated (Scheme 1.16). The observed negative entropies of activation were justified by the lack of rotational freedom in the transition state and the positive Hammett reaction constant was explained by the transient development of a negative charge on the migrating aryl ring.⁴⁸

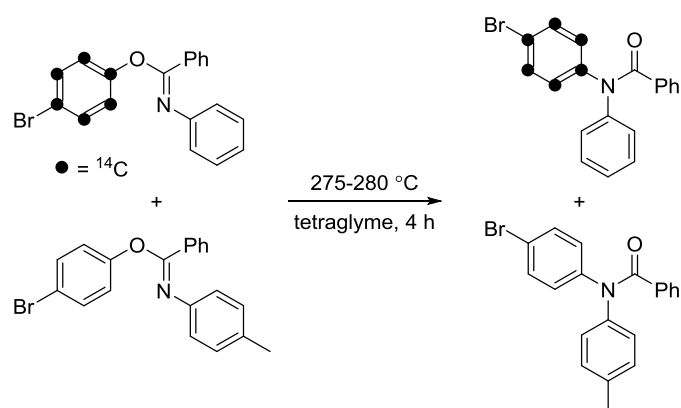


Scheme 1.16 The proposed mechanism for the Chapman rearrangement.

Counterintuitively, substrates containing *ortho*-substituted *O*-aryl rings were, in general, found to rearrange faster than their *para*-substituted counterparts. For example, *O*-(2-methylphenyl)-*N*-phenyl benzimidate was observed to rearrange 2.5 times faster than *O*-(4-methylphenyl)-*N*-phenyl benzimidate.⁴⁸ This effect was enhanced with the inclusion of a second *ortho*-substituent, but rearrangement was retarded in the presence

of *ortho tert*-butyl groups.⁵⁰ It was proposed that the rotational freedom of *O*-aryl benzimidates was restricted by *ortho*-substitution and that the rearrangement of *ortho*-substituted substrates was therefore accelerated due to the smaller entropic cost of accessing the highly-strained transition state. In support of this theory, the entropies of activation measured for *O*-(2-methylphenyl)-*N*-phenyl benzimidate and *O*-(4-methylphenyl)-*N*-phenyl benzimidate were $\Delta S^\ddagger = -3.6 \text{ cal K}^{-1} \text{ mol}^{-1}$ and $\Delta S^\ddagger = -9.7 \text{ cal K}^{-1} \text{ mol}^{-1}$ respectively.⁴⁸

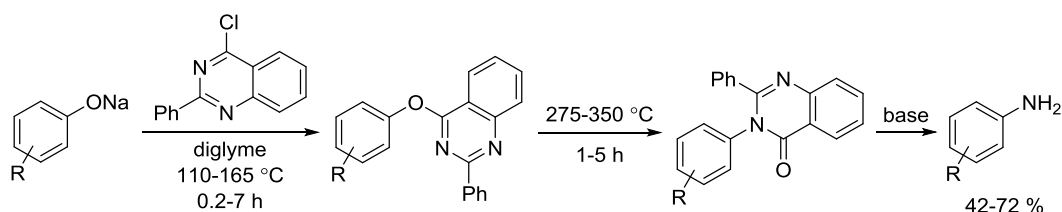
The unimolecularity of the Chapman rearrangement has been further verified by performing cross-over experiments. No cross-over was detected upon inducing rearrangement in a mixture of [¹⁴C₆]-*O*-(4-bromophenyl)-*N*-phenyl benzimidate and *O*-(4-bromophenyl)-*N*-(4-methylphenyl) benzimidate, two substrates which rearrange at almost identical rates.⁵¹



Scheme 1.17 A cross-over experiment used to prove the unimolecularity of the Chapman rearrangement.

1.1.5 The Chichibabin Rearrangement

The Chichibabin rearrangement is the thermal rearrangement of 4-aryloxy-2-phenylquinazolines to 3-(*N*-aryl-2-phenylquinazolinones (Scheme 1.18). Significantly, this derivative of the Chapman rearrangement can be utilised in a three-step procedure for the conversion of phenols to primary anilines.⁵²



Scheme 1.18 The conversion of phenols to primary anilines *via* the Chichibabin rearrangement.

The synthesis of 4-aryloxy-2-phenylquinazolines from phenols is the first step in the sequence and is achieved in high yield using the commercially available reagent 4-chloroquinazoline. The subsequent rearrangement step, like the Chapman rearrangement, adheres to first order kinetics, is accelerated by electron-withdrawing *O*-aryl substituents and can be performed neat or in a high boiling solvent (e.g. mineral oil).⁵² The hydrolysis of 3-(*N*-)aryl-2-phenylquinazolinones tends to be the lowest yielding of the three steps and has been achieved using two different methods.⁵³ The first entails heating the 3-(*N*-)aryl-2-phenylquinazolinones at 140-150 °C in a concentrated ethylene glycol solution of potassium hydroxide for 10-68 hours (depending upon aromatic substitution).^{52,54} The second and somewhat milder approach, involves treating the 3-(*N*-)aryl-2-phenylquinazolinones with sodium hydroxide in refluxing aqueous ethanol (0.5-7 hours), before acidifying the mixture with concentrated aqueous HCl and heating to 40-100 °C. Clearly, neither of these procedures are compatible with hydrolytically sensitive functional groups.^{52,55,56}

1.2 Phenol-Derived Electrophiles in Cross-Coupling Reactions

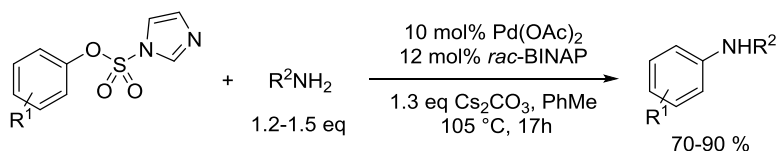
Phenol-derived electrophiles are extremely attractive alternatives to aryl halides in transition metal-catalysed cross-coupling reactions. Not only are a wide range of phenols readily available at low cost, but phenols and their derivatives are readily elaborated *via* electrophilic aromatic substitution and directed *ortho*-metalation protocols.^{57,58} Moreover, unlike aryl halides, phenols are naturally abundant and environmentally friendly. The use of 'green' phenol-derived electrophiles therefore satisfies the environmental and economical driving forces behind modern synthetic chemistry. However, cross-coupling reactions involving these species are somewhat restricted by the higher strength of the C_{Ar}-O bond relative to C_{Ar}-X bonds, where X = Cl, Br or I. As such, phenols generally have to be activated towards the oxidative addition of transition metals by derivatisation with electron-withdrawing functional groups which can be susceptible to base-mediated cleavage. Even then, often only the most reactive and electron-rich transition metal-catalysts are compatible with these systems.⁵⁹⁻⁶² These concepts were introduced in Section 1.1.2, with an emphasis on the use of aryl triflates in palladium(0) catalysed reactions. The following sections will focus on the use of alternative, more economically viable phenol-derived electrophiles, with the reactions of palladium, nickel and other transition metals treated separately. Where possible, the

use of phenol-derived electrophiles in cross-coupling reactions will be exemplified by their transition metal-catalysed amination reactions.

1.2.1 Palladium-Catalysed Cross-Coupling Reactions

In general, cross-coupling reactions which employ palladium(0) catalysts display high efficiency, wide substrate scope and a reasonable tolerance of air and moisture. As a result, palladium(0) catalysts dominate the field of aryl halide cross-coupling reactions. Their use in the cross-coupling reactions of phenol-derived electrophiles is, however, much more limited, especially when compared to the range of transformations which are amenable to nickel(0) catalysis. Indeed, prior to the last 10 years, reports detailing the palladium(0)-catalysed cross-coupling reactions of non-triflate, phenol-derived electrophiles were extremely rare. Nevertheless, such reactions were often performed using lower catalyst loadings, milder conditions and more diverse substrates than comparable processes using alternative transition metals.^{59,60}

The only class of phenol-derived electrophiles that are compatible with palladium(0)-catalysed cross-coupling reactions are the *O*-aryl sulfonates.⁵⁹ As presented in Section 1.1.2, *O*-aryl triflates are by far the most frequently applied, but more reactive catalyst systems can facilitate the coupling of cheaper and more stable *O*-aryl mesylates and *O*-aryl tosylates. Recently, the use of *O*-aryl imidazolylsulfonates has also attracted an appreciable amount of attention (Scheme 1.19).^{63,64}



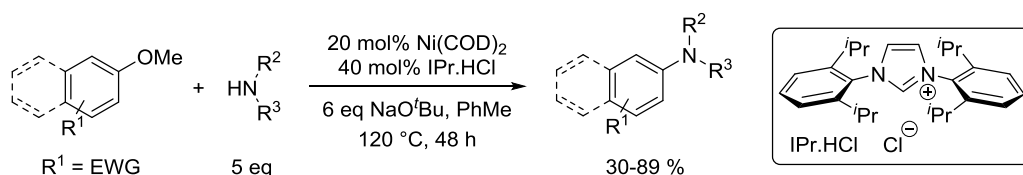
Scheme 1.19 The palladium(0)-catalysed amination of *O*-aryl imidazolylsulfonates.

Remarkably, *O*-aryl imidazolylsulfonates display a degree of stability akin to that of *O*-aryl tosylates and exhibit reactivity in cross-coupling reactions which is comparable to that of *O*-aryl triflates.⁶³ As such, these pseudohalides can be stored for extended periods of time without decomposition and can be coupled with a range of nucleophiles in high yields using conventional palladium catalysts (e.g. Pd(PPh₃)₄).^{63–66} Unfortunately, regardless of precatalyst and ligand structure, catalyst loadings tend to be high (≥ 5 mol%) and the synthesis of *O*-aryl imidazolylsulfonates from phenols is achieved using the very expensive reagent 1,1'-sulfonyldiimidazole.⁶³

1.2.2 Nickel-Catalysed Cross-Coupling Reactions

Nickel is a commodity metal and costs approximately 2,000 times less (per mole) than its group 10 relative palladium. Nickel is also smaller and more electropositive. As a result, nickel(0) complexes tend to be more reactive than palladium(0) complexes in oxidative addition reactions and have been found to activate a wide range of phenol-derived electrophiles which are inert to palladium(0) catalysis.^{61,67} Their reactivity is not however, specific to C_{Ar}-O bonds and the same complexes are usually capable of inserting into C_{Ar}-CN, C_{Ar}-NO₂ and even C_{Ar}-F bonds. Thus, the couplings of phenol-derived electrophiles containing these and other reactive functional groups often lack selectivity and achieve low yields.⁵⁹ The isolation of nickel complexes for use as precatalysts or for structural analysis and mechanistic studies is also relatively arduous.⁶¹ This again is due to the 'hard' nature of nickel and its high susceptibility to oxidative processes, as these attributes render low-valent nickel complexes particularly sensitive to air and moisture.⁵⁹ Nevertheless, the ability of nickel complexes to activate relatively simple and traditionally inert C_{Ar}-O pseudohalides has received a vast amount of attention and has been the subject of numerous reviews.^{59-62,67}

The ability of nickel(0) complexes to oxidatively add into traditionally inert C_{Ar}-O bonds is demonstrated perfectly by the nickel(0)-catalysed amination of aryl methyl ethers with secondary amines.⁶⁸

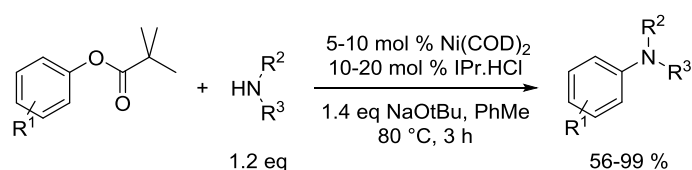


Scheme 1.20 The nickel(0)-catalysed amination of aryl methyl ethers.

Essential to the success of this transformation was the use of the very bulky *N*-heterocyclic carbene (NHC) ligand, IPr.⁶⁸ Notably, the use of this ligand and similar NHCs is typical for nickel(0)-catalysed amination reactions using phenol-derived electrophiles. Analogous C_{Ar}-C bond-forming coupling reactions are, however, more commonly achieved using somewhat less bulky and less electron-rich phosphine ligands such as; PPh₃, dppf and PCy₃, with PCy₃ being used in the more challenging reactions.⁵⁹ The requirement for NHCs to be employed in amination reactions is proposed to be a consequence of the reluctance of aryl nickel(II) amido complexes to undergo reductive elimination. In line with the higher reactivity of nickel(0) species towards oxidative

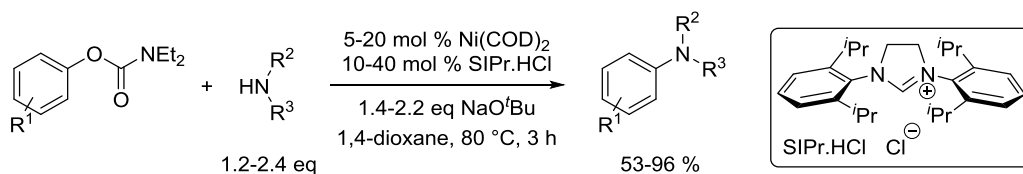
addition and the 'hard' nature of nickel, such reductive elimination reactions tend to be more difficult from nickel(II) complexes than palladium(II) complexes.⁶⁷ Indeed, reductive elimination has been identified as the rate-limiting step in nickel(0)-catalysed C_{Ar}-N and C_{Ar}-C bond-forming cross-coupling reactions.^{69,70}

Although impressive, the nickel(0)-catalysed amination of aryl methyl ethers is extremely inefficient and thus, impractical. However, the use of essentially the same system allowed for the amination of more activated *O*-aryl pivalates to be realised using substantially lower loadings of catalyst, base and amine coupling partner (Scheme 1.21). This protocol was also tolerant of a wider range of *O*-aryl substituents, but was still limited to secondary amines.⁷¹



Scheme 1.21 The nickel(0)-catalysed amination of *O*-aryl pivalates.

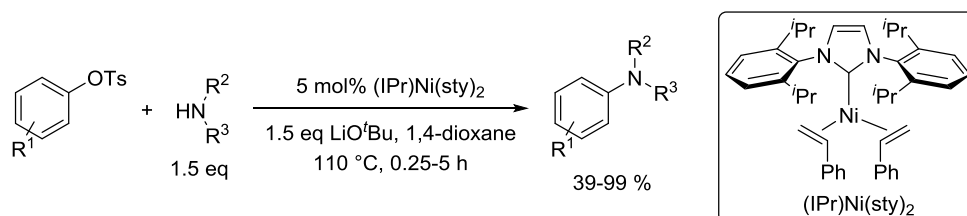
O-Aryl-*N,N*-diethyl carbamates are even more attractive pseudohalides for nickel(0)-catalysed cross-coupling reactions. Relative to *O*-aryl pivalates these substrates are significantly more stable towards cleavage and can be more readily elaborated using *ortho*-functionalisation methods.⁶² More specifically, *O*-aryl-*N,N*-diethyl carbamates are among the best directing groups for directed *ortho*-metalation reactions,^{58,72,73} iridium-catalysed *ortho*-C-H borylation reactions⁷⁴ and palladium-catalysed *ortho*-C-H arylation reactions.^{75,76} As a result, the finding that *ortho*-substituted *O*-aryl-*N,N*-diethyl carbamates were suitable substrates for nickel(0)-catalysed amination reactions was of particular importance (Scheme 1.22). This system was also compatible with the coupling of primary anilines.⁶⁹



Scheme 1.22 The nickel(0)-catalysed amination of *O*-aryl-*N,N*-diethyl carbamates.

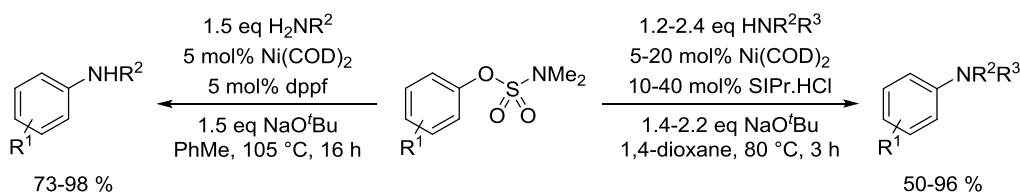
As alluded to in the previous section, the nickel(0)-catalysed cross-coupling reactions of *O*-aryl sulfonates are significantly less efficient and less general than the analogous

palladium(0)-catalysed reactions. This is demonstrated well by the nickel(0)-catalysed amination of *O*-aryl tosylates which requires relatively high catalyst loadings (loadings of palladium catalysts can be as low as 0.05 mol%, Section 1.1.2) and is only applicable to the coupling of *O*-naphthyl or *para*-substituted *O*-aryl tosylates with anilines or cyclic secondary amines (Scheme 1.23).^{77,78} Although high, these catalyst loadings are not unusual in nickel(0)-catalysed cross-coupling reactions and are a consequence of the high reactivity of nickel catalysts towards unproductive side-reactions and oxidation.⁵⁹



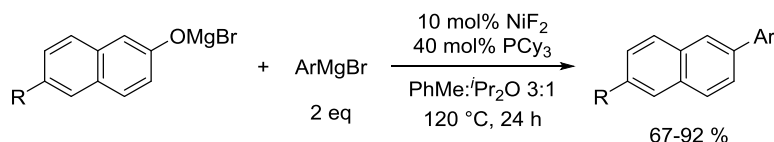
Scheme 1.23 The nickel-catalysed amination of *O*-aryl tosylates.

As an exception to the trend, the nickel(0)-catalysed cross-coupling of *O*-aryl-*N,N*-dimethyl sulfamates is much further developed than the corresponding palladium(0)-catalysed reactions. Indeed, *O*-aryl-*N,N*-dimethyl sulfamates have currently only been coupled with BOC-protected primary and secondary aminomethyltrifluoroborates *via* palladium(0) catalysis.⁷⁹ In contrast, protocols for the nickel(0)-catalysed coupling of *O*-aryl-*N,N*-dimethyl sulfamates with Grignard reagents,⁸⁰ boronic acids,^{73,81} arylzinc reagents⁸² and amines^{64,83,84} (Scheme 1.24) have all been reported. The primary advantage associated with the use of these substrates over alternative *O*-aryl sulfonates is their marked stability. *O*-Aryl-*N,N*-dimethyl sulfamates exhibit excellent stability towards base-mediated cleavage⁷² and also display stability towards benzyne formation upon *ortho*-lithiation,⁸⁰ albeit only at particularly low temperatures (-93 °C vs. -78 °C for *O*-aryl-*N,N*-diethyl carbamates).⁸⁵ The attempted *ortho*-lithiation of other *O*-aryl sulfonates leads to the formation benzyne regardless of the reaction conditions used.⁸⁰ As a result, *O*-aryl-*N,N*-dimethyl sulfamates are more readily functionalised than alternative *O*-aryl sulfonates. Furthermore, these substrates benefit from being very cheap to synthesise using *N,N*-dimethylsulfamoyl chloride.⁸³



Scheme 1.24 The nickel-catalysed amination of *O*-aryl sulfamates.

Despite the shortcomings of nickel(0)-catalysed cross-coupling reactions relative to their palladium(0)-catalysed analogues, it appears that almost any $C_{Ar}-O$ bond can be activated by nickel(0). *O*-Aryl phosphates,⁸⁶ *O*-aryl acetates,⁸⁷ *O,O'*-diaryl sulfates,⁸⁸ aryl silyl ethers⁸⁹ and, most remarkably, even the magnesium bromide salts of naphthols (Scheme 1.25) have all also been used as electrophiles in nickel(0)-catalysed cross-coupling reactions.⁹⁰

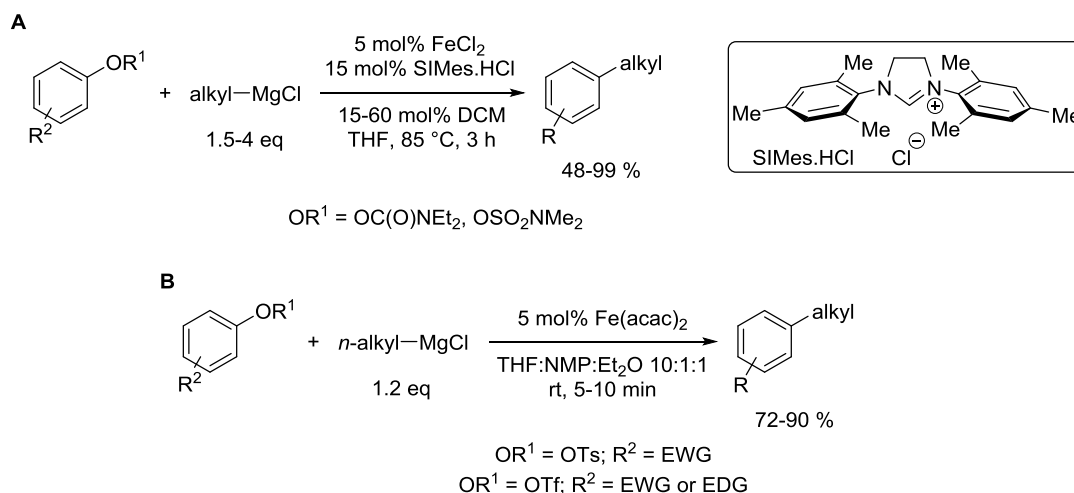


Scheme 1.25 The nickel(0)-catalysed coupling of aryl Grignard reagents with naphtholates.

1.2.3 Cross-Coupling Reactions Catalysed by Other Transition Metals

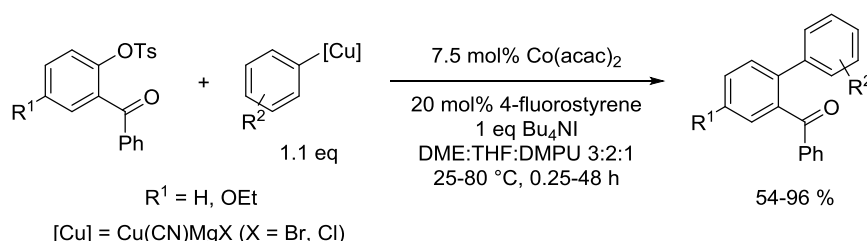
The cross-coupling chemistry of non-group 10 transition metals is far less well understood and is somewhat more unpredictable. In the majority of cases, the oxidation state of the active catalyst is not known and reaction mechanisms are ambiguous and most often, unexplored. Thus, it is hard to predict or generalise which combinations of nucleophile, $C_{Ar}-O$ electrophile and catalyst will result in productive reactions. Notably, the amination of phenol-derived electrophiles is yet to be achieved using non-group 10 transition metal catalysts.⁵⁹

Promisingly, iron catalysts have been demonstrated to activate a relatively wide range of $C_{Ar}-O$ pseudohalides, such as; *O*-aryl triflates, *O*-aryl tosylates,^{91,92} *O*-aryl-*N,N*-dimethyl sulfamates and *O*-aryl-*N,N*-diethyl carbamates.⁹³ However, such reactivity is limited to cross-coupling reactions employing alkyl Grignard reagents (Scheme 1.26). It is worth highlighting that the use of an NHC ligand is essential to the coupling of *O*-aryl-*N,N*-dimethyl sulfamates and *O*-aryl-*N,N*-diethyl carbamates (reaction A),⁹³ whereas the coupling of *O*-aryl triflates and *O*-aryl tosylates has been performed ligand-free (reaction B).^{91,92}



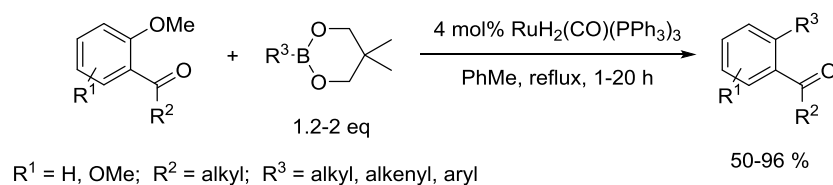
Scheme 1.26 The iron-catalysed cross-coupling of $\text{C}_{\text{Ar}}\text{-O}$ pseudohalides with alkyl Grignard reagents.

In addition, the cobalt-catalysed coupling of *O*-aryl tosylates with a diverse range of arylcopper reagents has been realised, although all *O*-aryl tosylates were required to contain an *ortho*-benzoyl group (Scheme 1.27).^{94,95} The effect of such *ortho*-substituents is to lower the barrier to oxidative addition by pre-coordinating the catalyst and directing it towards the $\text{C}_{\text{Ar}}\text{-O}$ bond. In addition to this kinetic effect, the presence of a coordinating *ortho*-substituent may also stabilise organometallic intermediates on the catalytic cycle, thus reducing the prevalence of decomposition pathways or side-reactions.⁵⁹



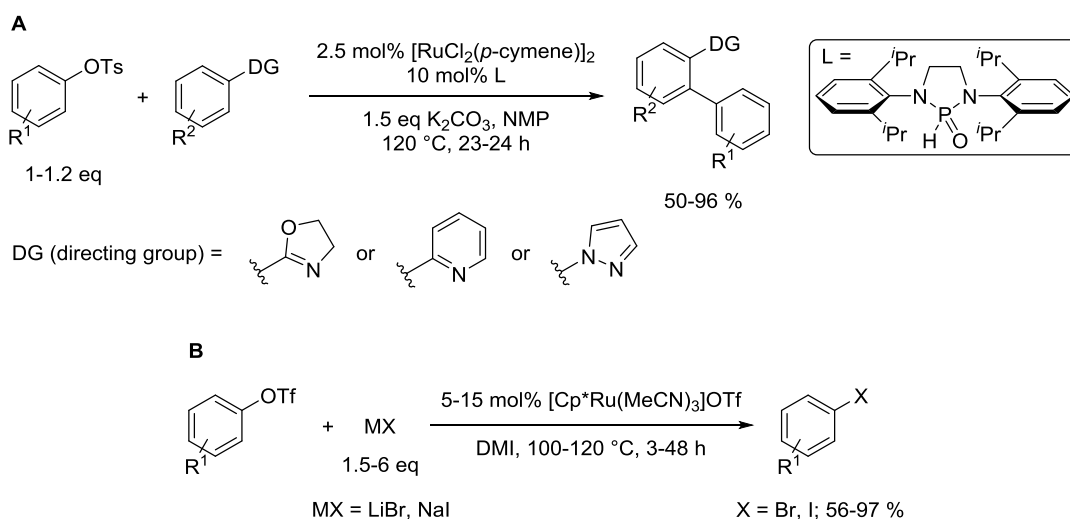
Scheme 1.27 The cobalt-catalysed cross-coupling of *O*-aryl tosylates with arylcopper reagents.

The same effect has been exploited in the ruthenium-catalysed cross-coupling of aryl methyl ethers with boronic acid neopentylglycol esters (Scheme 1.28).^{96,97}



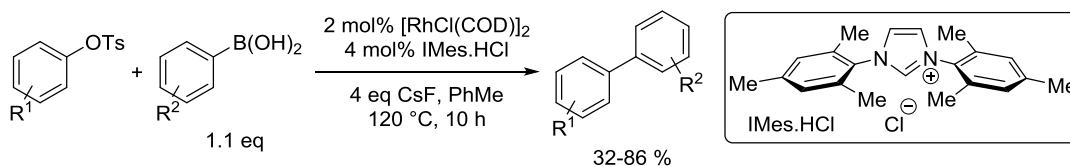
Scheme 1.28 The ruthenium-catalysed cross-coupling of aryl methyl ethers with boronic acid neopentylglycol esters.

Coordinating *ortho*-substituents were, however, not required to promote C_{Ar}-O bond activation in ruthenium-catalysed C-H arylation reactions employing *O*-aryl tosylates^{98,99} (reaction A, Scheme 1.29) or in the ruthenium-catalysed conversion of aryl triflates to aryl halides (reaction B).¹⁰⁰ Note, again, that an electron-rich ancillary ligand was used to affect the coupling of the less activated *O*-aryl tosylate substrates.



Scheme 1.29 Ruthenium-catalysed processes involving C_{Ar}-O bond activation.

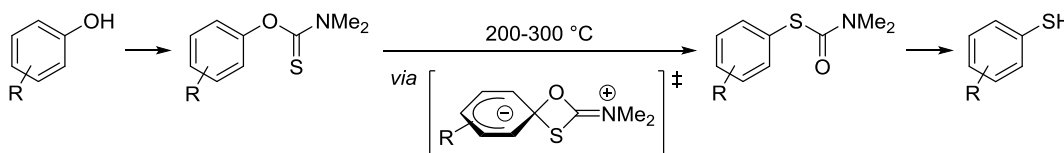
Finally, the cross-coupling of *O*-aryl tosylates with arylboronic acids using an NHC-ligated rhodium catalyst has also been reported (Scheme 1.30). *O*-Aryl benzenesulfonates were found to be poorer substrates for this reaction.¹⁰¹



Scheme 1.30 The rhodium-catalysed cross-coupling of *O*-aryl tosylates with arylboronic acids.

1.3 The Newman-Kwart Rearrangement

The Newman-Kwart rearrangement (NKR) is another more modern relative of the Chapman rearrangement and concerns the thermal rearrangement of *O*-aryl thiocarbamates to *S*-aryl thiocarbamates (Scheme 1.31). The NKR is widely used as the key step in an efficient strategy for the conversion of phenols to thiophenols.^{45,102}

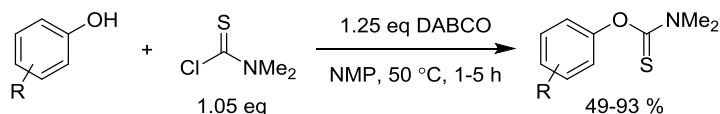


Scheme 1.31 The conversion of phenols to thiophenols *via* the Newman-Kwart rearrangement

By analogy to other Chapman-type rearrangements, the NKR was immediately identified as an intramolecular nucleophilic aromatic *ipso*-substitution reaction. In support of this conclusion, the NKR is accelerated by electron-withdrawing and *ortho*-methyl aromatic substituents ($\rho = 1.62$)^{49,103} and displays first order kinetics (Section 1.1.4).^{49,104,105}

1.3.1 Practical Considerations

It is a requirement that the *O*-aryl thiocarbamate substrates of the NKR are *N,N*-disubstituted in order to negate their ability to undergo thermal elimination to the corresponding phenols and isothiocyanates.¹⁰³ However, the nature of the *N*-substituents has been found to have very little influence over the success or rate of the rearrangement reaction.^{103,104} As a result, *O*-aryl-*N,N*-dimethyl thiocarbamates are the most commonly used substrates for the NKR due to their facile synthesis from the cheap and readily available reagent *N,N*-dimethylthiocarbamoyl chloride (Scheme 1.32).^{106,107} Notably, *O*-aryl-*N,N*-dimethyl thiocarbamates also tend to be highly crystalline.

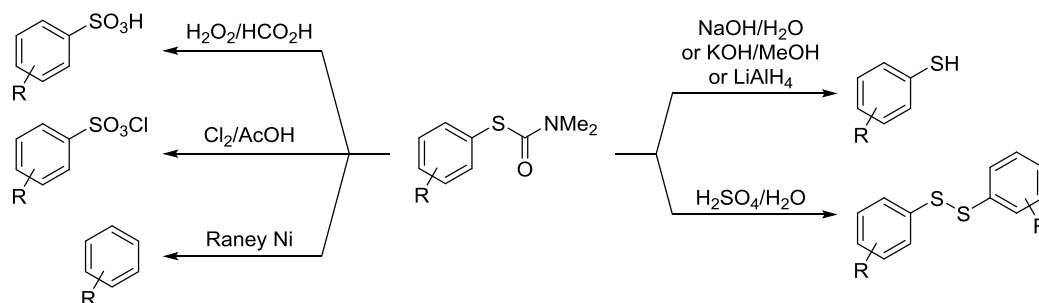


Scheme 1.32 The synthesis of *O*-aryl-*N,N*-dimethyl thiocarbamates.

Like the Chapman rearrangement, the thermal NKR is often performed neat, although the use of a high-boiling solvent can help to avoid excessive charring of substrates and products. Microwave heating has also been successfully applied to the reaction,

somewhat mitigating the concerns over convenience and safety which accompany the use of such extreme temperatures.^{106,108}

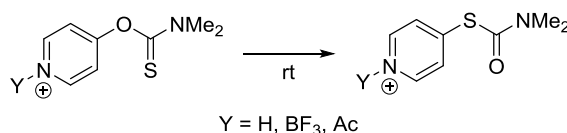
The cleavage of *S*-aryl-*N,N*-dimethyl thiocarbamate rearrangement products is readily achieved using aqueous sodium hydroxide or methanolic potassium hydroxide and proceeds in high yield.^{103,109} If non-hydrolytic conditions are required, lithium aluminium hydride can instead be employed to similar effect.¹¹⁰ It is worth highlighting that procedures for the direct conversion of *S*-aryl-*N,N*-dimethyl thiocarbamates to arylsulfonic acids,¹¹¹ arylsulfonyl chlorides,^{112,113} diaryl disulfides¹¹⁴ and desulfurised arenes^{103,115} have also been developed (Scheme 1.33).



Scheme 1.33 Reactions of *S*-aryl thiocarbamates.

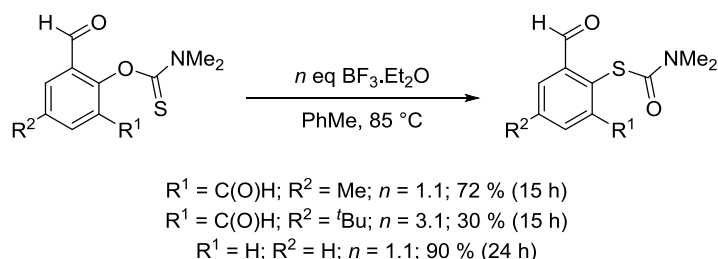
1.3.2 Catalysis

The high synthetic value of the NKR has prompted investigations into the use of catalysis to reduce reaction temperatures. A relatively simple approach involves the application of Lewis acid or Brønsted acid additives to promote the rearrangement of *O*-aryl thiocarbamates which contain *O*-aryl groups with basic coordination sites. It is proposed that the coordination of such additives reduces the electron density of the *O*-aryl ring and thus stabilises the transition state for rearrangement. Using this strategy, the temperature required to induce the rearrangement of *O*-(3-pyridyl)-*N,N*-dimethyl thiocarbamate was reduced from 250 to 190 °C (20 minute reaction time) by adding catalytic quantities of boron trifluoride or hydrogen chloride. More impressively, the boron trifluoride and hydrogen chloride salts of the corresponding *O*-(2-pyridyl) and *O*-(4-pyridyl) substrates were found to rearrange at room temperature (Scheme 1.34).¹⁰³



Scheme 1.34 The rearrangement of *O*-(4-pyridinium)-*N,N*-dimethylthiocarbamate salts.

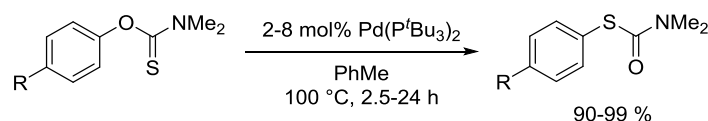
O-Aryl thiocarbamates substituted with *ortho*-formyl groups are also susceptible to boron trifluoride catalysis at 85 °C (Scheme 1.35), but *O*-aryl thiocarbamates substituted with *ortho*-acetyl and *ortho*-benzoyl groups are not.¹¹⁶



Scheme 1.35 The boron trifluoride-catalysed rearrangement of *ortho*-formyl substituted *O*-aryl thiocarbamates.

Furthermore, acceleration of the NKR by the coordination of nitro aromatic groups to magnesium bromide, nickel(0) colloids or rhodium(I) and iridium(I) complexes has been observed.^{117,118} A related rhodium(I) complex has also been shown to promote the rearrangement of an *O*-aryl thiocarbamate substituted with both an *ortho*-benzoyl group and a *para*-methoxy group.¹¹⁹

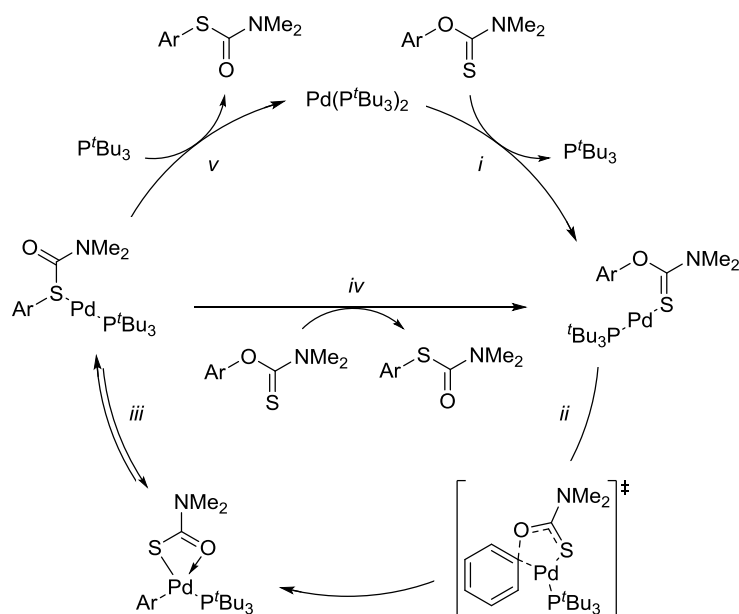
The first general catalyst system for the NKR was developed in 2009. The catalyst, $\text{Pd}(\text{P}^t\text{Bu}_3)_2$, an electron-rich palladium(0) complex, is capable of inducing the NKR of an electronically diverse range of *para*-substituted *O*-aryl-*N,N*-dimethyl thiocarbamates at 100 °C (Scheme 1.36). As observed for the thermal NKR, the palladium(0)-catalysed rearrangement is facilitated by the presence of electron-withdrawing substituents. As a result, electron-deficient substrates are transformed using lower catalyst loadings and shorter reaction times than are required for electron-rich substrates. Unfortunately, *ortho*-substituted *O*-aryl thiocarbamates are not tolerated.¹¹⁸



Scheme 1.36 The palladium(0)-catalysed NKR.

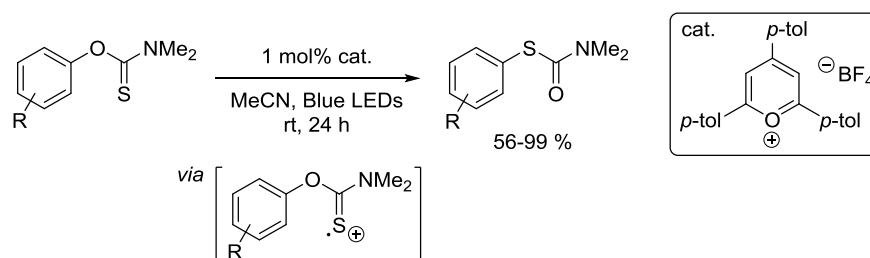
The mechanism of the palladium(0)-catalysed reaction was probed *via* kinetic analysis and computational methods. A key feature of the proposed catalytic cycle (Scheme 1.37) is the formation of a coordination complex between the palladium(0) catalyst and the *O*-aryl thiocarbamate substrate through the thiocarbonyl group. This interaction is important as it facilitates oxidative addition into the $\text{C}_{\text{Ar}}\text{-O}$ bond *via* a 5-membered ring

transition state (step *ii*), promotes catalyst activation (step *i*) and expedites catalyst turnover (step *iv*). The aryl palladium(II) thiocarbamate product of oxidative addition is proposed to be the catalyst resting state and can reversibly reductively eliminate the *S*-aryl thiocarbamate product (step *iii*).¹¹⁸ Reversible oxidative addition has been observed upon treating *S*-(4-nitrophenyl)-*N,N*-dimethyl thiocarbamate with Pd(P^{*t*}Bu₃)₂, providing evidence to suggest that the reductive elimination step (step *iii*) is relatively facile.¹¹⁷ Finally, the displacement of the product from the catalyst with either the substrate (step *iv*) or the phosphine ligand (step *v*) completes the cycle and is proposed to be the turnover-limiting step.¹¹⁸



Scheme 1.37 The proposed catalytic cycle for the palladium(0)-catalysed NKR.

Remarkably, a reasonably general method for the room temperature NKR of electron-rich *O*-aryl thiocarbamates using organic photoredox catalysis was subsequently realised (Scheme 1.38).¹²⁰



Scheme 1.38 The photoredox-mediated NKR.

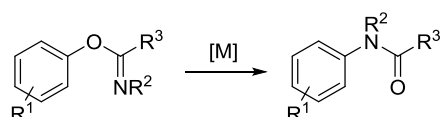
This protocol relies upon the surprisingly facile rearrangement of *O*-aryl thiocarbamates upon their single-electron oxidation, a phenomenon which had previously only been observed in the gas-phase.^{121–123} In this case, single-electron oxidation is achieved by the use of a pyrylium photoredox catalyst in conjunction with blue LED irradiation and allows the effect to be harnessed in solution, on a preparative scale. The reaction displays very good functional group tolerance, but is limited to substrates containing electron-donating *ortho*- and/or *para*-substituents. The substrate scope is therefore very complimentary to that of the palladium(0)-catalysed NKR.¹²⁰

2 Towards a Transition Metal-Catalysed Chapman-Type Rearrangement: *O*-Aryl Trihaloacetimidates

2.1 Introduction

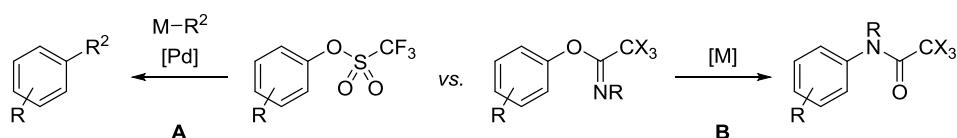
2.1.1 Chapter Aims

Inspired by the recent development of the palladium(0)-catalysed NKR, it was hoped that transition metal catalysis could be utilised to develop a more synthetically valuable, low temperature variant of the Chapman rearrangement (Scheme 2.1). Ideally, the reaction would be amenable to incorporation into a three-step strategy for the conversion of phenols to anilines. If realised, this procedure would likely be more functional group tolerant and convenient than the current technologies available to affect the same transformation (Section 1.1). For example, anilines would be generated in a protected form and the use of nucleophilic amines and strongly basic conditions (as required in Buchwald-Hartwig aminations) would be avoided. Furthermore, the key C-N bond forming reaction would be kinetically simpler than alternative metal-catalysed aryl aminations by virtue of it being a rearrangement process; no additional reagents/additives would be required and no by-products would be produced.



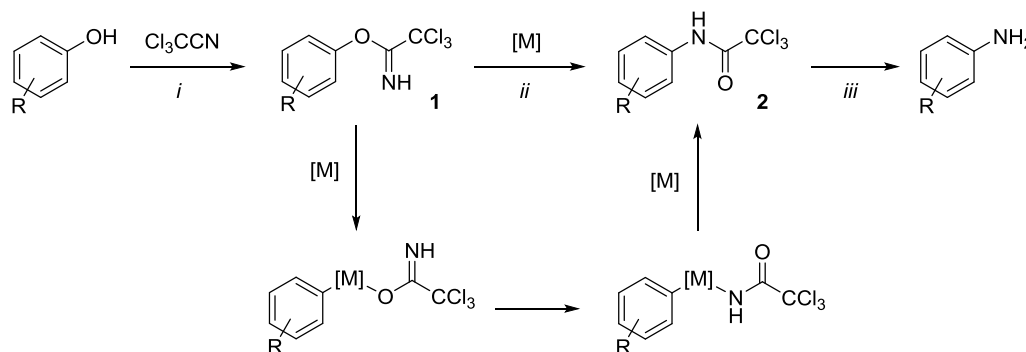
Scheme 2.1 The proposed transition metal-catalysed Chapman-type rearrangement of *O*-aryl imidates.

In order to render the imidate scaffold of the Chapman rearrangement amenable to transition metal catalysis, replacement of the *C*-phenyl ring of the archetypical *O*-aryl benzimidate substrates with a more electron-withdrawing group was desirable. It was envisioned that a reaction mechanism similar to that proposed to be operative in the palladium(0)-catalysed NKR might then be accessed, with the electron-withdrawing group aiding the difficult $C_{Ar}-O$ oxidative addition step (Section 1.2). Heeding the widespread application of *O*-aryl triflates as pseudohalides in palladium-catalysed cross-coupling reactions (reaction A, Scheme 2.2), *O*-aryl trihaloacetimidates were identified as candidate rearrangement substrates (reaction B).



Scheme 2.2 A comparison of *O*-aryl trihaloacetimidates with *O*-aryl triflates.

In an idealised scenario, *O*-aryl trichloroacetimidates **1** would be formed in the reaction of phenols with trichloroacetonitrile (step *i*, Scheme 2.3); a relatively cheap and readily accessible reagent. These trichloroacetimidates would then undergo a transition metal-catalysed rearrangement to afford *N*-aryl trichloroacetamides **2** (step *ii*) which could be cleaved, when desired, to liberate anilines under mild conditions (step *iii*).

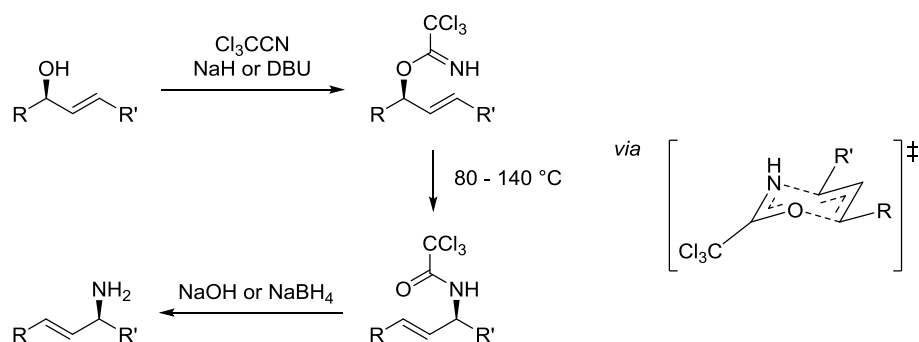


Scheme 2.3 The proposed strategy for the conversion of phenols to anilines.

Trichloroacetimidate to trichloroacetamide rearrangements allow hydroxyl groups to be transformed to amino groups in a number of organic scaffolds. These reactions are reviewed in the following sections.

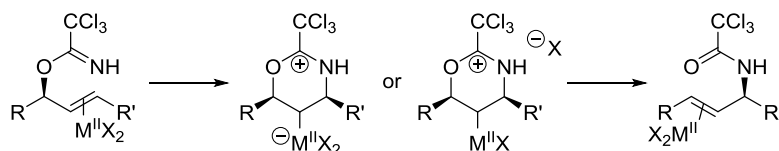
2.1.2 *O*-Allyl Trihaloacetimidates: The Overman Rearrangement

The [3,3]-sigmatropic aza-Claisen rearrangement of *O*-allyl imidates to *N*-allyl amides provides a route *via* which readily sourced allylic alcohols can be converted to the corresponding protected allylic amines. The reaction is irreversible, with the formation of the strong carbon-oxygen double bond and amide linkage providing a large thermodynamic driving force (approximately 15 kcal mol⁻¹). Due to a number of favourable attributes (easily synthesised substrates, mild conditions and wide scope) the rearrangements of allylic trihaloacetimidates have proven to be by far the most synthetically valuable subclass of these reactions (Scheme 2.4). These reactions are commonly referred to as Overman rearrangements.¹²⁴



Scheme 2.4 The thermal Overman rearrangement of *O*-allyl trichloroacetimidates.

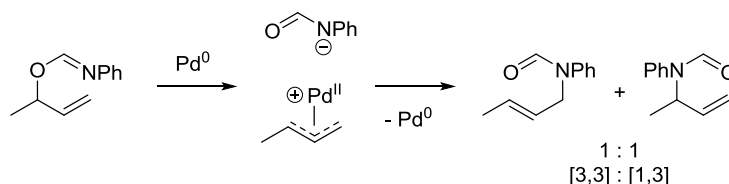
O-Allyl trichloroacetimidates are obtained by the base-mediated addition of allylic alcohols to trichloroacetonitrile. The use of catalytic quantities of DBU or the corresponding alkali metal hydroxide often provides the best results. Thermal rearrangement is most commonly promoted in aprotic solvents by heating between 80-140 °C, depending upon the degree and nature of the allylic substituents (in general, more substituted allylic imidates react faster). Due to the highly ordered nature of the chair transition state invoked (Scheme 2.4), the rearrangement usually proceeds with complete transfer of stereochemical information.¹²⁴ Soluble mercury(II) salts and palladium(II) complexes have been shown to catalyse the transformation at lower temperatures, enabling cleaner and higher yielding reactions. Coordination of the metal to the allylic double bond is proposed to increase its susceptibility to nucleophilic attack by the imidate nitrogen. Reaction *via* the cyclic intermediate thus formed ensures the selective generation of the products of [3,3]-rearrangement over the products of [1,3]-rearrangement (Scheme 2.5).¹²⁵



Scheme 2.5 The proposed mechanism for the palladium(II) or mercury(II)-catalysed Overman rearrangement.

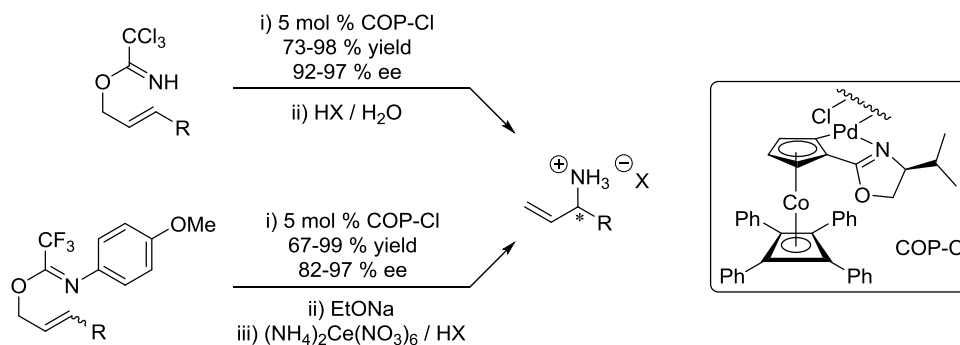
In contrast, the palladium(0)-catalysed rearrangement of *O*-allyl imidates tends to afford the regioisomeric products of both [3,3]- and [1,3]-rearrangement (Scheme 2.6). This is a consequence of a reaction mechanism whereby the palladium(0) catalyst oxidatively adds to the *O*-allyl imidate to generate a π -allyl intermediate. Subsequent nucleophilic attack of the amide anion can then occur at either end of the π -allyl system. Despite often being able to catalyse the rearrangement more efficiently, palladium(0) catalysts are

much less frequently applied than palladium(II) catalysts due to the poor selectivity of the reaction.^{126,127}



Scheme 2.6 The palladium(0)-catalysed rearrangement of *N*-phenyl formimidates.

The development of an asymmetric variant of the palladium(II)-catalysed Overman rearrangement has received a significant amount of attention. Prochiral trichloroacetimidates initially appeared to be unsuitable substrates for this transformation due to slow reaction rates and the onset of competing elimination reactions. These observations were attributed to the coordination of palladium(II) complexes to the imidate nitrogen. Supporting this, more success was achieved using prochiral *O*-allyl-*N*-(4-methoxyphenyl) trifluoroacetimidates in which the imidate nitrogen atom is less basic and more sterically hindered.¹²⁸ Following extensive tuning, the latest generation of palladium(II) catalysts are capable of catalysing highly enantioselective rearrangements of both prochiral *N*-aryl trifluoroacetimidates¹²⁹ and prochiral trichloroacetimidates (Scheme 2.7).^{128,130}

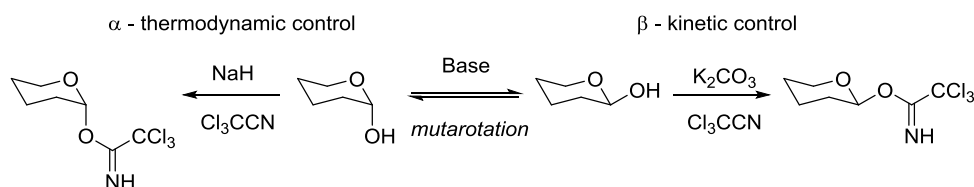


Scheme 2.7 The enantioselective palladium(II)-catalysed rearrangement of *O*-allyl *N*-aryl trifluoroacetimidates and (*E*)-*O*-allyl trichloroacetimidates enables the conversion of prochiral allylic alcohols to highly enantioenriched allylic amines.

2.1.3 *O*-Glycosyl Trihaloacetimidates

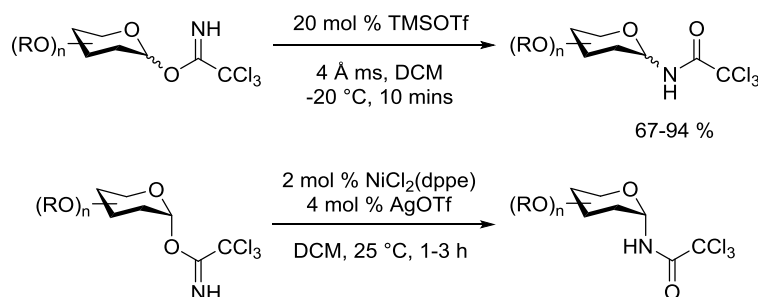
The trichloroacetimidate moiety has found widespread utility in carbohydrate chemistry as an excellent anomeric leaving group. As such, glycosyl trichloroacetimidates are potent glycosyl donors which are popularly exploited in the synthesis of 1,2-*trans*

glycosides. Stable and anomerically pure α - and β -trichloroacetimidates can be selectively prepared by virtue of the strength of the base used (Scheme 2.8).^{131,132}



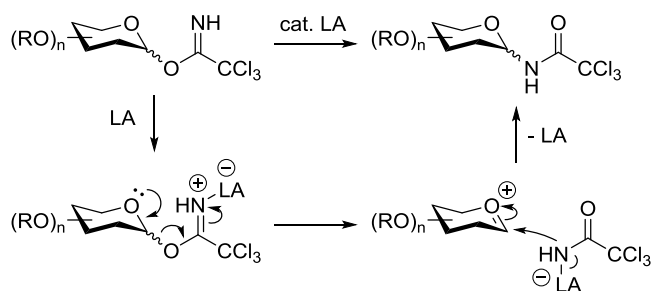
Scheme 2.8 Synthesis of O-glycosyl trichloroacetimidates.

Advantageously, *O*-glycosyl trichloroacetimidates can be activated towards condensation with glycosyl acceptors using catalytic amounts of boron trifluoride or trimethylsilyl triflate. Other common glycosyl donors can require activation with heavy metal-based reagents.¹³¹ If treated with a Lewis acid in the absence of a glycosyl acceptor, *O*-glycosyl trichloroacetimidates have been found to rearrange to the corresponding *N*-glycosyl trichloroacetamides.¹³³ In these reactions the anomeric carbon undergoes a 1,3-migration from oxygen to nitrogen. Trimethylsilyl triflate¹³⁴ and palladium(II) or nickel(II) Lewis acids^{135,136} perform well in this reaction, allowing it to be exploited in procedures for the synthesis of glycosyl amines (Scheme 2.9).



Scheme 2.9 The rearrangement of O-glycosyl trichloroacetimidates to N-glycosyl trichloroacetamides.

Presumably, the coordination of a Lewis acid to the imidate nitrogen promotes the ionisation of the acetimidate moiety which concurrently tautomerises to the more stable acetamide form (Scheme 2.10). This ionisation is facilitated by the formation of an oxocarbenium intermediate. Recombination then occurs *via* nucleophilic attack of the acetamide through nitrogen.

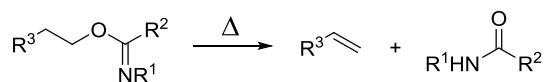


Scheme 2.10 A plausible mechanism for the Lewis acid-catalysed rearrangement of *O*-glycosyl trichloroacetimidates. LA is used to denote a Lewis acid.

When the Lewis acid-mediated coupling of *O*-glycosyl trichloroacetimidates with particularly unreactive glycosyl acceptors is attempted, rearrangement can occur as a deleterious side-reaction. In these instances, *N*-aryl-*O*-glycosyl trifluoroacetimidates can be used instead. These glycosyl donors are significantly less prone to rearrangement and β -elimination under glycosylation conditions.¹³⁷ However, their reactivity towards glycosylation is low relative to the corresponding trichloroacetimidates.^{138,139}

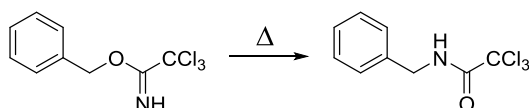
2.1.4 *O*-Alkyl Trihaloacetimidates

When heated to high temperatures, *O*-alkyl imidates containing β -hydrogen atoms are usually observed to decompose *via* elimination to the corresponding amide and olefin (Scheme 2.11).⁴⁸



Scheme 2.11 *O*-Alkyl imidates containing β -hydrogen atoms can undergo thermally-induced elimination.

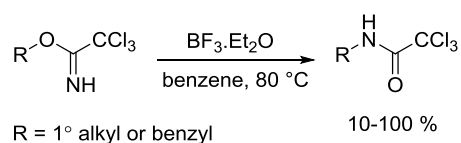
If no appropriately oriented β -hydrogen atoms are present, rearrangement can instead proceed.⁴⁴ The thermal rearrangement of *O*-benzyl trichloroacetimidate has been reported, although the reaction conditions were not detailed (Scheme 2.12).⁴⁴



Scheme 2.12 The thermal rearrangement of *O*-benzyl trichloroacetimidate to *N*-benzyl trichloroacetamide.

Although unsuitable for thermal rearrangement, *O*-alkyl imidates containing β -hydrogen atoms can rearrange upon treatment with a catalytic amount of an alkylating agent or

acid (Lewis or Brønsted). Unlike the Chapman and Overman rearrangements, this rearrangement is intermolecular.¹⁴⁰ Boron trifluoride was found to be a suitable catalyst for inducing the rearrangements of primary alkyl and benzylic trichloroacetimidates at 80 °C (Scheme 2.13).¹⁴¹

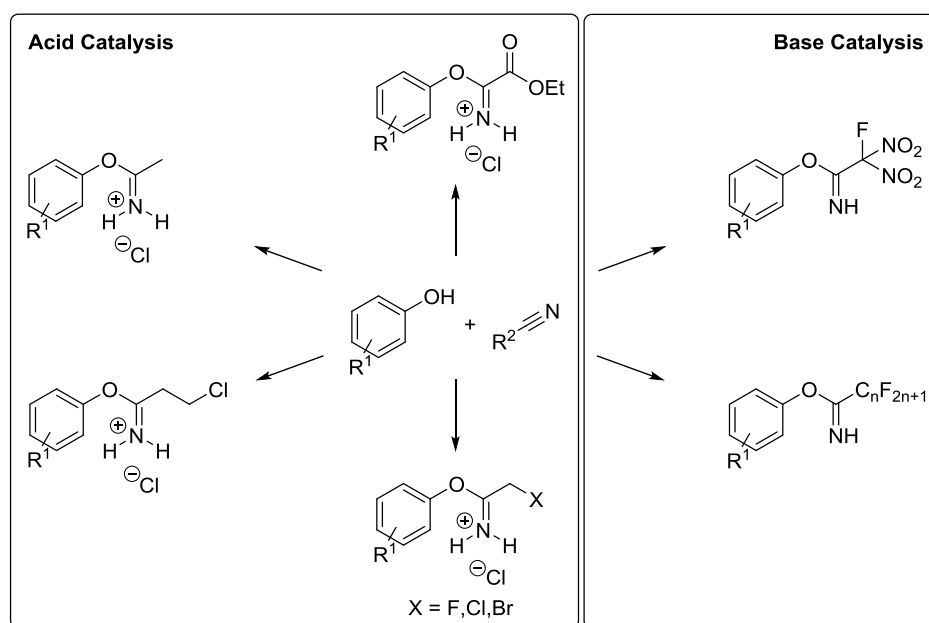


Scheme 2.13 The boron trifluoride-catalysed rearrangement of *O*-alkyl trichloroacetimidates.

2.2 Preparation of *O*-Aryl Trichloroacetimidates

2.2.1 Literature Procedures

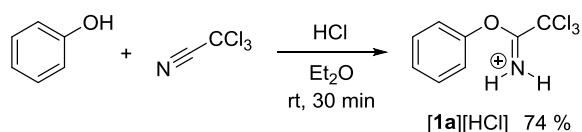
Phenols can react with nitriles under acid^{142–146} or base^{147,148} catalysis to afford *O*-aryl imidates (Scheme 2.14).



Scheme 2.14 *O*-Aryl imidates synthesised by the acid- or base-catalysed reactions of phenols with nitriles.

The acid-catalysed reaction (Pinner reaction) most commonly involves the passage of HCl gas through a diethyl ether solution of the phenol and the nitrile to generate a crystalline imidate HCl salt. Subsequent treatment of these salts with a weak base can reveal the imidate free-base.^{147,149} This method has been used to access the HCl salt of *O*-

phenyl trichloroacetimidate [**1a**][HCl] (Scheme 2.15) which was found to be relatively unstable and extremely hygroscopic.¹⁵⁰



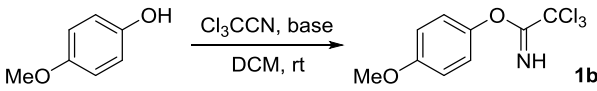
Scheme 2.15 The Pinner synthesis of O-phenyl trichloroacetimidate hydrochloride.

When the nitrile is sufficiently electron-deficient, the reaction can be effectively catalysed by base.¹⁴⁷ The base-catalysed reaction tends to be more convenient and efficient than the acid-catalysed process; substoichiometric quantities of base can be applied and neutral imidates are formed directly.

2.2.2 Initial Optimisation: O-(4-Methoxyphenyl) Trichloroacetimidate

It was hoped that base catalysis could be applied to the synthesis of *O*-aryl trichloroacetimidates **1**. With concerns over the stability of these species, the initial optimisations were performed using dried solvents and reagents under an atmosphere of nitrogen (Table 2.1). The reaction of the highly nucleophilic 4-methoxyphenol with trichloroacetonitrile was adopted as the model system. Conditions frequently used in the preparation of allyl and glycosyl trichloroacetimidates were unproductive (entry 1).¹²⁴ However, the use of a large excess of trichloroacetonitrile enabled high conversions to *O*-(4-methoxyphenyl) trichloroacetimidate **1b** to be realised on a reasonable timescale and with low base loadings (entries 4-9). Under these conditions, the reaction could be performed without anhydrous precaution, with no detriment to the outcome (entries 9 and 10). DBU proved to be an exceptionally efficient catalyst for the reaction (compare entries 8 and 10). For reactivity to be maintained at low DBU loadings, anhydrous DCM and trichloroacetonitrile had to be used (entries 11 and 12).

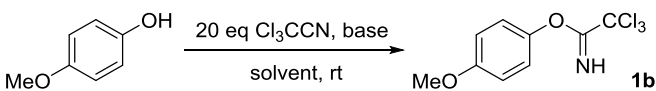
Table 2.1 Refining the synthesis of O-(4-methylphenyl) trichloroacetimidate **1b.** ^a

					
Entry	Base	mol% base	Eq. Cl ₃ CCN	<i>t</i> / h	1b / % ^b
1	DBU	110	2	1.5	0
2	DABCO	110	2	30	35
3	Et ₃ N	110	2	3	53
4	Et ₃ N	40	2	20	90
5	Et ₃ N	5	2	23	91
6	Et ₃ N	1	25	4	16
7	Et ₃ N	5	20	23	99
8	Et ₃ N	5	20	2	95
9 ^c	Et ₃ N	5	20	7.5	99
10	DBU	5	20	0.05	95
11 ^c	DBU	1	20	0.2	99
12 ^c	DBU	0.1	20	5	99

^a 0.25 mmol scale, 0.25 M, anhydrous DCM and Cl₃CCN, N₂ atmosphere. ^b Conversions determined by ¹H NMR spectroscopy. ^c No anhydrous precaution.

Inorganic bases and alternative solvents were also explored in the preparation of **1b** (Table 2.2). Potassium carbonate and potassium *tert*-butoxide could be successfully employed (entries 1-3), but more polar solvents provided extremely poor results (compare entries 1, 2 and 5 with entries 6-10). The reaction could also be performed neat (entries 3 and 4).

Table 2.2 Screen of reaction solvents and base catalysts in the synthesis of **1b.** ^a

					
Entry	Base	mol% base	Solvent	<i>t</i> / h	1b / % ^b
1	K ₂ CO ₃	10	DCM	24	99
2	KOtBu	20	DCM	16	99
3	K ₂ CO ₃	10	-	24	99
4 ^c	Et ₃ N	5	-	18.5	99
5	Et ₃ N	5	PhMe	18	100
6	Et ₃ N	10	MeCN	9	< 1
7	Et ₃ N	10	EtOAc	9	0
8	Et ₃ N	10	acetone	9	0
9	Et ₃ N	10	Et ₂ O	9	0
10	Et ₃ N	5	THF	6	0

^a 0.25 mmol scale, 0.25 M. ^b Conversions determined by ¹H NMR spectroscopy. ^c 0.5 M

Disappointingly, it was not possible to isolate **1b** from trace amounts of 4-methoxyphenol (≤ 5 mol%). However, trichloroacetoneitrile and triethylamine could be removed by evaporation *in vacuo* and potassium carbonate could be separated by filtration. Other bases could be removed by performing a HCl(aq)/DCM extraction. The samples of **1b** obtained following these manipulations were highly crystalline but were also found to be reasonably hygroscopic. As a result, **1b** was observed to liquefy and decompose to 4-methoxyphenol and trichloroacetamide upon standing in air. In general, decomposition was complete after 2-20 days, with samples which had been purified by HCl(aq)/DCM extraction being found to decompose the most rapidly. Under nitrogen, **1b** was stable for months.

2.2.3 Assigning the Isomers of O-(4-Methoxyphenyl) Trichloroacetimidate

Analysis of **1b** by ¹H and ¹³C NMR spectroscopy revealed a mixture of two isomers in an approximate 7:3 ratio (Figure 2.1). *O*-Aryl fluorodinitroacetimidates have also been reported to form as a mixture of two isomers.¹⁴⁸ In both cases it was proposed that the isomers differed in the geometry of the imide carbon-nitrogen double bond.

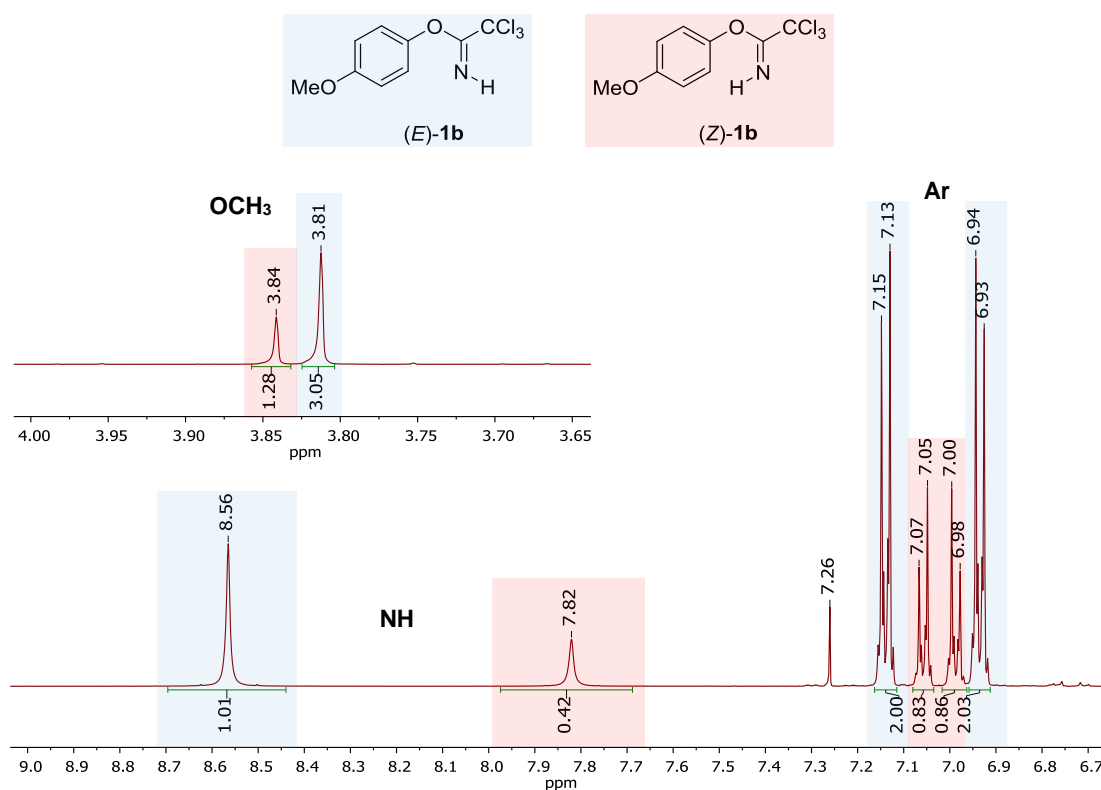


Figure 2.1 The ^1H NMR spectrum (CDCl_3) of **1b**.

Assignment of the isomers of **1b** was attempted using NOESY NMR experiments as it was hypothesised that the NH proton should reside much closer to the *ortho* aromatic protons in the *Z* isomer than it does in the *E* isomer (Figure 2.2). A nuclear Overhauser effect (NOE) was therefore, only expected to be observed between these protons in the *Z* isomer.

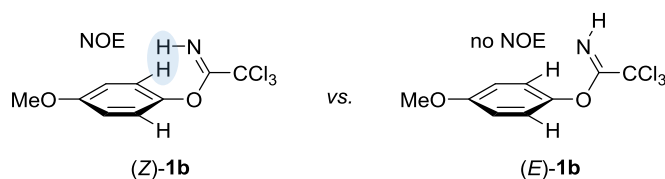


Figure 2.2 The *E* and *Z* isomers of **1b**.

A series of 1D NOESY experiments were performed (Figure 2.3), irradiating in-turn each of the aromatic signals and the two NH proton signals. In none of the spectra recorded was an NOE-derived signal observed. However, all spectra revealed extensive exchange of the excited nuclei during the mixing time (0.5 s). These experiments demonstrated that the isomers were in equilibrium and could easily interconvert.

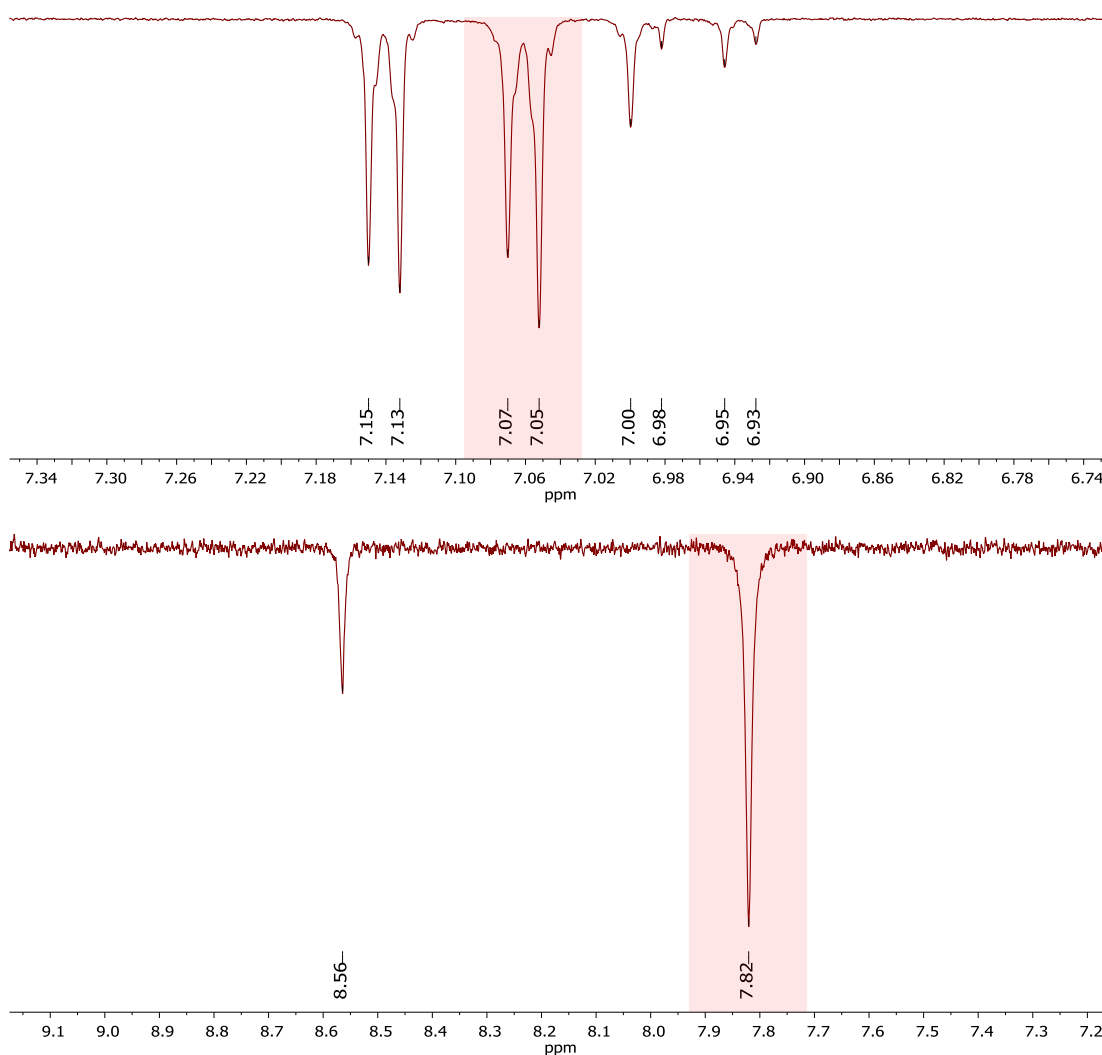
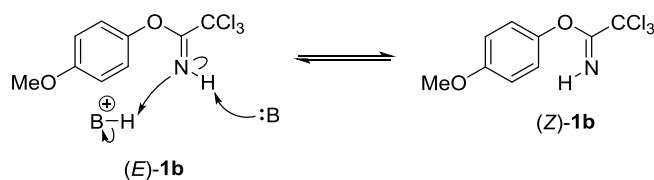


Figure 2.3 1D NOESY spectra (CDCl_3 ; mixing time: 0.5 s) of **1b** recorded with selective irradiation of the highlighted protons (above: aromatic; below: NH) of the minor isomer. The exchange of these protons with the corresponding protons in the major isomer (above: 7.14 ppm; below: 8.56 ppm) is demonstrated.

The rate of isomerisation was found to be highly dependent upon the identity of the base used to prepare the sample and the quantity of 4-methoxyphenol which was present. Therefore, it is likely that isomerisation can proceed *via* a proton shuttling pathway mediated by trace phenol, water or base (Scheme 2.16).



Scheme 2.16 (*E*)-**1b** and (*Z*)-**1b** are in dynamic equilibrium.

Subsequently, the assignment of the isomers was attempted by measuring the $^3J_{\text{CH}}$ coupling constants between the CCl_3 groups and the NH protons in a ^1H -coupled ^{13}C NMR spectrum (Figure 2.4).

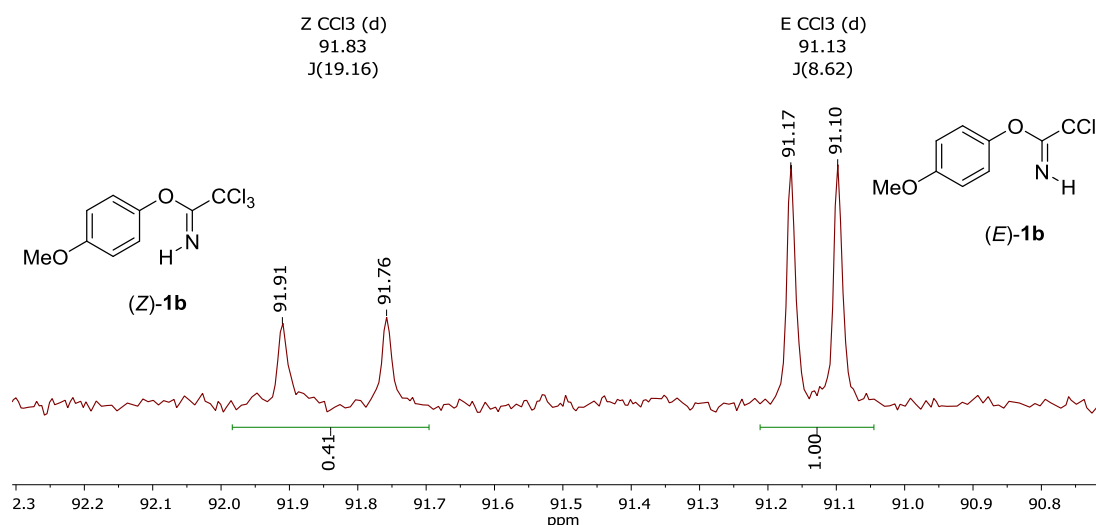


Figure 2.4 The CCl_3 signals in the ^1H -coupled ^{13}C NMR spectrum (CDCl₃) of **1b**.

Pleasingly, different values, $^3J_{\text{CH}} = 8.6$ and 19.2 Hz, were observed for the two observed CCl_3 resonances. The signal displaying the smaller coupling constant was unambiguously associated with the major isomer of **1b** by virtue of a ^1H - ^{13}C HMBC NMR experiment (Figure 2.5). This allowed the assignment of the *E* double bond geometry (*cis* relationship between the CCl_3 group and the NH proton) to the major isomer of **1b**.

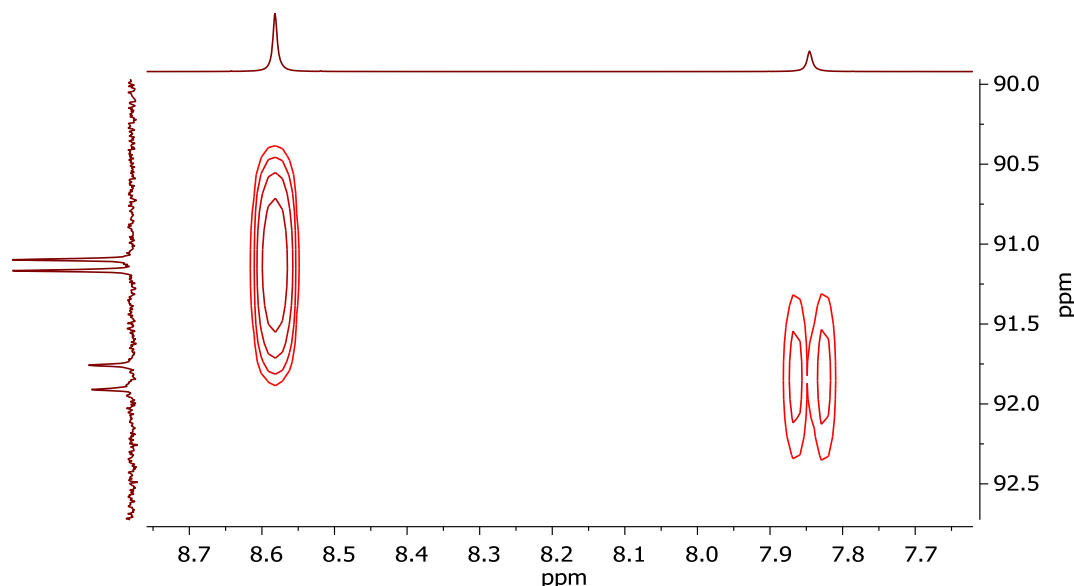
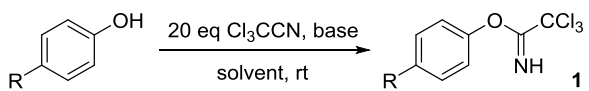


Figure 2.5 A portion of the ^1H - ^{13}C HMBC NMR spectrum (CDCl₃) of **1b**. Coupling between the NH protons and the CCl_3 carbon nuclei is demonstrated.

2.2.4 Other O-Aryl Trichloroacetimidates

The optimised conditions for preparing **1b** were evaluated in the reaction of trichloroacetonitrile with a range of phenols (Table 2.3). Other electron-rich phenols were found to perform well. Phenol and 4-*tert*-butylphenol were converted almost quantitatively to their trichloroacetimidate derivatives **1a** and **1c** (entries 1 and 2). *O*-Phenyl trichloroacetimidate **1a** was isolated as an oil and *O*-(4-*tert*-butylphenyl) trichloroacetimidate **1c** was isolated as a crystalline solid. Both were slightly contaminated with the corresponding phenol.

Table 2.3 Scree of 4-substituted phenols in the preparation of O-aryl trichloroacetimidates **1**. ^a

						
Entry	R	Base	mol% base	Solvent	<i>t</i> / h	1 / % ^b
1	H	Et ₃ N	5	DCM	21	97
2	^t Bu	Et ₃ N	5	DCM	21	98
3 ^c	NO ₂	Et ₃ N	5	DCM	67	29
4	CN	Et ₃ N	5	DCM	31	40
5	Ac	Et ₃ N	5	DCM	4	43
6 ^d	CN	Et ₃ N	5	-	7	39
7 ^e	NO ₂	Et ₃ N	5	-	47	21
8	NO ₂	Et ₃ N	5	PhMe	5	19
9 ^f	NO ₂	Et ₃ N	5	THF	4	0
10	NO ₂	K ₂ CO ₃	10	DCM	9	19
11	Cl	K ₂ CO ₃	10	DCM	7	93
12	Br	K ₂ CO ₃	10	DCM	7	95

^a 0.25 M. ^b Conversions determined by ¹H NMR spectroscopy. ^c 0.2 M. ^d 0.5 M. ^e 0.36 M. ^f 0.17 M.

Conversions were extremely low when phenols substituted with electron-withdrawing groups were employed. Such phenols were only partially soluble in the 1:1 DCM:Cl₃CCN medium typically applied (entries 3-5), but were more soluble in neat Cl₃CCN (entries 6 and 7) and were completely soluble in 1:1 PhMe:Cl₃CCN (entry 8). As no competing processes were observed and conversions did not increase over extended reaction times (entry 3), the equilibrium positions of these reactions are clearly unfavourable. If Cl₃CCN was removed from the product mixtures under reduced pressure, complete

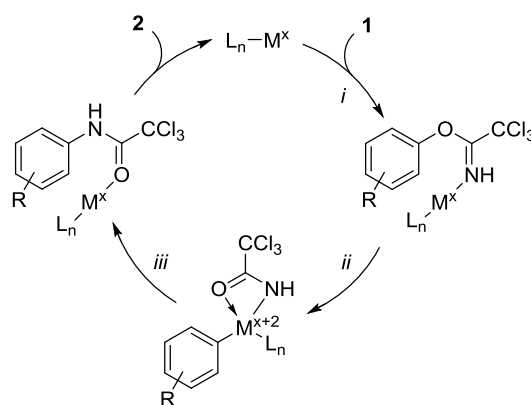
decomposition of the imidate **1** to the corresponding phenol was observed. If, however, an HCl(aq)/DCM extraction was performed prior to Cl₃CCN removal, the imidate **1** could be obtained as the minor component in an inseparable mixture with the corresponding phenol.

High conversions were achieved with less electron-deficient, halogenated phenols, but a number of unidentified side products were formed when isolation of the imidates **1** was attempted (entries 11 and 12).

2.3 Transition Metal Catalysis: *O*-Aryl Trichloroacetimidates

2.3.1 Considerations for Transition Metal Catalysis

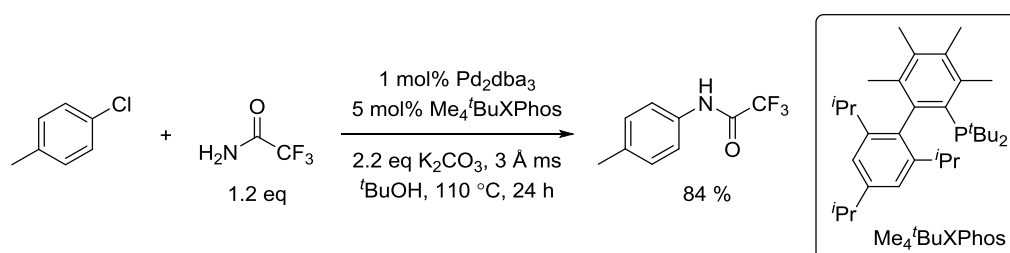
If *O*-aryl trichloroacetimidates **1** were to undergo transition metal-catalysed rearrangement, it was suspected that successful oxidative addition into the C_{Ar}-O bond (step *ii*, Scheme 2.17) would be key. As discussed in Section 1.2, only the most electron-rich and reactive low-valent metal centres will add into these strong bonds. Transition metal complexes with these characteristics would therefore be the focus of the catalyst screen for the desired reaction. In order to afford such species, bulky, strongly electron-donating phosphine ligands are often utilised. Conveniently, the same bulky phosphines also tend to be effective in promoting C_{Ar}-N reductive elimination reactions (step *iii*, Scheme 2.17).¹⁵¹



Scheme 2.17 Hypothetical catalytic cycle for the transition metal-catalysed rearrangement of *O*-aryl trichloroacetimidates **1**.

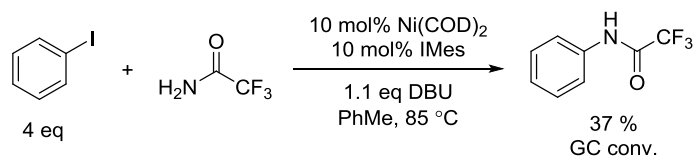
The proposed catalytic cycle for the transition metal-catalysed rearrangement of *O*-aryl trichloroacetimidates **1** (Scheme 2.17) closely resembles that operative in transition metal-catalysed cross-coupling reactions. As such, it might be predicted that catalysts

based upon the group 10 transition metals at the fore of cross-coupling chemistry, would be ideal candidates for the desired rearrangement reaction. Despite literature precedent suggesting that even the most electron-rich palladium(0) catalysts might struggle in the oxidative addition step (Section 1.2.1), it was hoped that this might be facilitated by prior coordination of the metal centre to the imidate nitrogen atom (step *i*).^{69,81,118} Such an interaction should favour this step kinetically, by effectively delivering the metal into the bond which is to be activated and by stabilising the transition state (Section 1.2.3).⁵⁹ The reductive elimination step from the palladium(II)-amidate intermediate (step *iii*) was expected to be relatively facile as the palladium-catalysed coupling of (pseudo)aryl halides with amides, including trifluoroacetamide, is well known (Scheme 2.18).¹⁵²



Scheme 2.18 The palladium(0)-catalysed coupling of trifluoroacetamide with an aryl chloride.

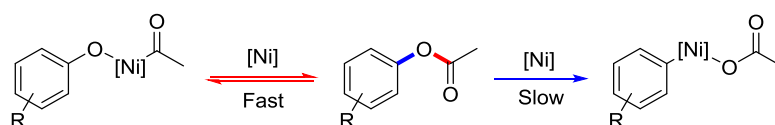
In contrast, nickel(0) complexes readily undergo oxidative addition into relatively unactivated C_{Ar}-O bonds (Section 1.2.2), but little support for the proposed reductive elimination reaction (step *iii*) can be found in the literature. The nickel-catalysed amidation of aryl halides has only been reported once and extremely poor results were achieved, even when employing high temperatures and extended reaction times. Nevertheless, the use of trifluoroacetamide was again reported, albeit with little success (yields of $\leq 37\%$ were achieved, Scheme 2.19). This reaction was only suitable for coupling aryl iodides.¹⁵³



Scheme 2.19 The nickel(0)-catalysed amidation of an aryl iodide with trifluoroacetamide.

Further complicating the proposed reaction is the possibility that low-valent transition metal catalysts might also be capable of oxidative addition into the C_{imidoyl}-O bond of *O*-aryl trichloroacetimidates **1**. A detailed computational study into the nickel-catalysed

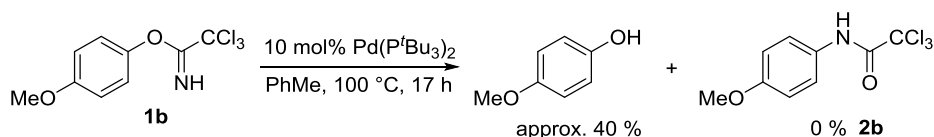
Suzuki-Miyaura cross-coupling of *O*-aryl carboxylates determined that oxidative addition into the C_{acyl}-O bond (red, Scheme 2.20) was faster than oxidative addition into the stronger C_{Ar}-O bond (80 vs. 106 kcal mol⁻¹; blue, Scheme 2.20). Oxidative addition into the C_{acyl}-O bond was however found to be reversible, allowing for productive turnover to proceed *via* irreversible addition into the C_{Ar}-O bond.¹⁵⁴ Nevertheless, insertion of a metal into the C_{imido}-O of *O*-aryl trichloroacetimidates **1** could potentially lead to undesirable side-reactions and/or catalyst deactivation. Again, it was hoped that the imidate nitrogen atom might act as a directing group and deliver the transition metal catalyst into the C_{Ar}-O bond, thus mitigating this issue.^{69,81,118}



Scheme 2.20 The oxidative addition of a PCy₃-ligated nickel(0) complex to *O*-aryl acetates.

2.3.2 Initial Attempts

It was proposed that the conditions successful in promoting the palladium(0)-catalysed NKR might also be applicable to the desired transition metal-catalysed Chapman-type rearrangement.¹¹⁸ The palladium(0)-catalysed NKR was found to be extremely sensitive to ligand structure, with only three very similar phosphine ligands out of an extensive screen; P^tBu₃, di-*tert*-butylneopentylphosphine and Q-Phos, furnishing catalysts of reasonable activity. Of these, the two trialkyl phosphines proved to be the most active, with P^tBu₃ being the most easily applied by the use of the stable palladium(0) precatalyst, Pd(P^tBu₃)₂.¹¹⁷ This was therefore the first catalyst to be evaluated in the attempted rearrangement of **1b** at 100 °C. Disappointingly, palladium black precipitated throughout the reaction and no rearrangement could be detected by ¹H NMR spectroscopy after 17 hours (Scheme 2.21). Instead, the partial decomposition of **1b** to 4-methoxyphenol and other unidentified species was revealed.



Scheme 2.21 The attempted rearrangement of **1b** with Pd(P^tBu₃)₂.

The possibility that 4-methoxyphenol was formed as a result of the simple thermal degradation of **1b** was discounted after 4-methoxyphenol was not formed under the

same conditions in the absence of $\text{Pd}(\text{P}^t\text{Bu}_3)_2$. The potential for **1b** to undergo decomposition *via* reaction with P^tBu_3 was also probed by exposing **1b** to 0.5 equivalents of P^tBu_3 . Even at room temperature this resulted in a corresponding amount of 4-methoxyphenol being liberated (Scheme 2.22). Further analysis of the reaction mixture by ^{31}P NMR spectroscopy suggested that P^tBu_3 had been protonated (peak at 123 ppm) and it was therefore proposed that P^tBu_3 had deprotonated **1b**, causing it to eliminate 4-methoxyphenol and Cl_3CCN . The protonation of the phosphine in this manner was also proposed to explain the observed catalyst and substrate decomposition in the rearrangement attempt.



Scheme 2.22 P^tBu_3 deprotonates **1b**, causing it to eliminate 4-methoxyphenol.

In an effort to minimise the concentration of free phosphine in the reaction mixture, the rearrangement of **1b** was attempted using a 10:9 ratio of $\text{Pd}(\text{dba})_2$ and P^tBu_3 . However, again, substrate and catalyst decomposition were observed and the expected product of rearrangement **2b** could not be identified.

The potential $\text{Pd}(\text{P}^t\text{Bu}_3)_2$ -catalysed rearrangements of *O*-phenyl trichloroacetimidate **1a** and *O*-(4-nitrophenyl) trichloroacetimidate **1d** were subsequently investigated (Table 2.4). These less electron-rich substrates were expected to be more susceptible to oxidative addition and it was therefore hoped that rearrangement might be able to compete with deleterious side-reactions. The reactions were conducted using equilibrium mixtures of imidate **1**, phenol and trichloroacetonitrile which had been formed as described in Section 2.2. In all cases, no conversion to **2a** or **2d** was observed.

Table 2.4 Conditions applied to the attempted rearrangements of 1a and 1d. ^a

$\text{R} = \text{H}; \mathbf{1a}$
 $\text{R} = \text{NO}_2; \mathbf{1d}$

$\text{R} = \text{H}; \mathbf{2a}$
 $\text{R} = \text{NO}_2; \mathbf{2d}$

Entry	R	Base (mol%)	% 1 ^b	Solvent	t / h	2 / % ^b
1	NO ₂	Et ₃ N (5)	19	PhMe	17	0
2	NO ₂	K ₂ CO ₃ (20)	32	-	18.5	0
3	H	K ₂ CO ₃ (20)	98	-	18.5	0

^a 0.25 mmol scale, 0.25 M ^b Conversions determined by ¹H NMR spectroscopy.

2.3.3 Catalyst Screen

The potential for **1b** to undergo rearrangement was further probed in a catalyst screen. Many of the catalysts evaluated in the screen were selected based upon their activity in cross-coupling reactions, in particular those involving the coupling of aryl-oxygen electrophiles and/or amide nucleophiles (Section 1.2). Often the metal precatalysts used in these reported reactions were reduced to the active catalyst *in situ* by the action of an organometallic reagent or a base. Such precatalysts were unsuitable for use in the proposed rearrangement reaction due to the sensitivity of *O*-aryl trichloroacetimidates **1** to basic species. As a result, the generation of catalyst species was achieved by combining labile complexes of the metal in its reduced state with the chosen ligands in an appropriate ratio.

Conditions capable of facilitating the palladium(0)-catalysed NKR were adopted (Table 2.5).¹¹⁸ Unfortunately, none of the catalyst systems tested were capable of promoting the desired reaction.

Table 2.5 Catalyst screen for the rearrangement of 1b. ^a

Precatalyst	Ligand (mol%)	2b / %
Pd(dba) ₂	XPhos (10)	0
Pd(dba) ₂	^t BuXPhos (10)	0
Pd(dba) ₂	Me ₄ ^t BuXPhos (10)	0
Pd(dba) ₂	BrettPhos (10)	0
Pd(dba) ₂	Xantphos (10)	0
Pd(dba) ₂	dppf (10)	0
Ni(COD) ₂	PCy ₃ (20)	0
Ni(COD) ₂	P(C ₆ F ₅) ₃ (20)	0
Ni(COD) ₂	P(O-2,4-(C(CH ₃) ₃) ₂ C ₆ H ₃) ₃ (20)	0
Ni(COD) ₂	Xantphos (10)	0
Ni(COD) ₂	dppf (10)	0

^a 0.2 mmol scale, 0.2 M. ^b Conversions determined by ¹H NMR spectroscopy

2.4 Palladium *N*-Heterocyclic Carbene Catalysts

2.4.1 Background and Proposal

Given that phosphines had been observed to react with **1b**, the use of *N*-heterocyclic carbenes (NHC) as ligands for potential rearrangement catalysts was explored (Figure 2.6). NHCs are extremely good σ -donors and advantageously form strong, thermally stable bonds to transition metals.^{155–157} Despite being strong bases in isolation, their low lability once complexed inhibits their tendency to react as such in the presence of metals. Relative to phosphines, NHCs show much less diversity in their electron-donating ability. This property is however somewhat dependent on both the saturation state of the *N*-heterocyclic ring and the substitution pattern of the ring backbone. Increasing unsaturation and aromaticity decreases the electron-donating power.¹⁵⁸ NHCs also have a large steric influence over the transition metal centres to which they bind. This influence is rather more anisotropic than that exerted by phosphines and is dictated by the NHCs *N*-substituents.¹⁵⁹

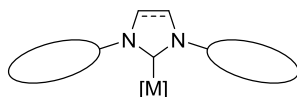


Figure 2.6 A generalised depiction of a metal imidazol(in)-2-ylidene complex.

Due to the size of NHCs, mono-NHC metal complexes tend to be the most active catalysts.¹⁶⁰ Such species based upon palladium and nickel are capable of activating traditionally inert bonds and undergoing rapid reductive elimination reactions. As a result, NHCs are often employed in the most challenging cross-coupling reactions.¹⁶¹ Active catalysts can be generated by the activation of a preformed metal NHC complex or by combining a metal source with the NHC ligand *in situ*. In palladium catalysis, the *in situ* method most commonly involves the treatment of either $\text{Pd}(\text{dba})_2$ or $\text{Pd}_2(\text{dba})_3$ with an imidazol(in)ium salt and an alkoxide base.¹⁶² Whilst convenient, better performance is often achieved using well-defined mono-NHC palladium precatalysts. Of these, palladium(II) precatalysts are the most attractive due to their ease of preparation, excellent stability and high activity in cross-coupling reactions (Figure 2.7).¹⁶³

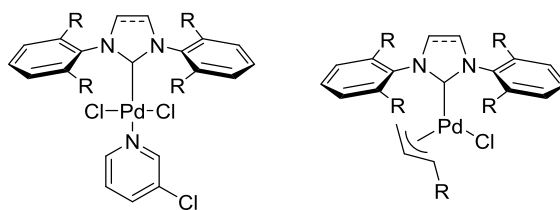


Figure 2.7 Exemplary palladium(II) mono-NHC precatalysts.

The generation of active palladium(0) catalysts from these complexes usually occurs readily under typical cross-coupling conditions and occurs through reaction with a base or the homocoupling of organometallic reagents.^{164,165} This reduction step is however not always well understood and is therefore not entirely predictable.¹⁶⁶ It might be expected that the use of palladium(0) precatalysts might alleviate this issue (Figure 2.8).^{167–169} Unfortunately, the stability of such species is reliant on the coordination of supporting ligands which bind to the metal centre tightly and thus cause low catalytic activity.^{170,171} Furthermore, the synthesis of these complexes generally necessitates that the extremely sensitive free carbene ligand is isolated.¹⁶⁰

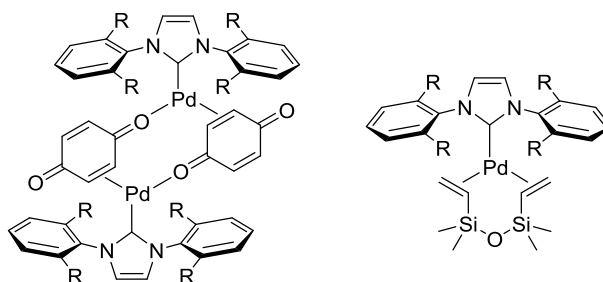
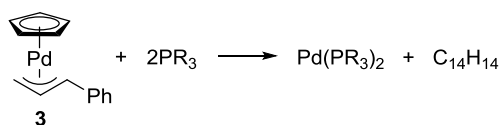


Figure 2.8 Exemplary palladium(0) mono-NHC precatalysts.

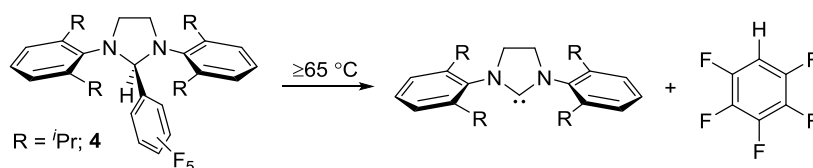
With a view to screening their activity in the proposed transition metal-catalysed rearrangement of *O*-aryl trichloroacetimidates **1**, a procedure for generating active palladium(0) mono-NHC catalysts in the absence of base was sought. It was hypothesised that this might be achieved by combining NHC ligands with $\text{Pd}(\eta^3\text{-1-PhC}_3\text{H}_4)(\eta^5\text{-C}_5\text{H}_5)$ **3**. This palladium(II) complex efficiently reductively eliminates its cyclopentadienyl (Cp) and cinnamyl ligands upon treatment with phosphines to generate very active palladium(0)-phosphine cross-coupling catalysts (Scheme 2.23).^{172–175} The high activity of the catalysts formed in this way has been attributed to their efficient formation in the absence of additional supporting ligands (e.g. dba) which can inhibit catalytic activity (i.e. when $\text{Pd}(\text{dba})_2$ is used).¹⁶⁶



Scheme 2.23 Bisphosphine palladium(0) cross-coupling catalysts can be efficiently generated from $\text{Pd}(\eta^3\text{-1-PhC}_3\text{H}_4)(\eta^5\text{-C}_5\text{H}_5)$ **3.**

It was anticipated that the steric influence of a single NHC ligand might be sufficient to stimulate the reductive elimination of the Cp and cinnamyl ligands from **3** and furnish a reactive mono-NHC palladium(0) species. Wishing to avoid the difficulties associated with synthesising and handling free NHC ligands, the validation of this theory was first attempted utilising a thermally labile NHC adduct. A number of such NHC precursors have been reported,¹⁷⁶ but pentafluorobenzene NHC adducts were selected for this study due to their stability, crystallinity and ease of synthesis. These adducts need to be heated to 65 °C or above for the elimination of pentafluorobenzene and the liberation of the free NHC to occur on reasonable timescales (Scheme 2.24).¹⁷⁷ The pentafluorobenzene adduct of 1,3-bis(2,6-diisopropylphenyl)imidazolin-2-ylidene (SIPr) **4** was chosen for

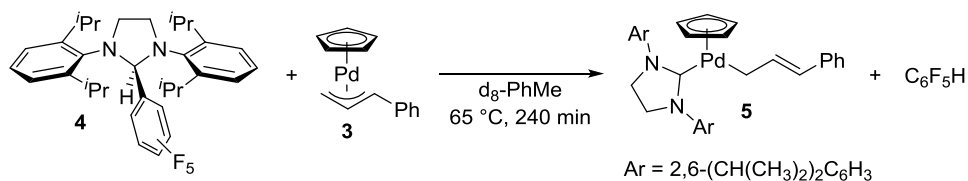
use in these studies as this NHC is large and furnishes highly active catalysts for Buchwald-Hartwig coupling reactions.¹⁷⁸



Scheme 2.24 Imidazolin-2-ylidines are liberated upon thermolysis of their pentafluorobenzene adducts.

2.4.2 Initial Investigations

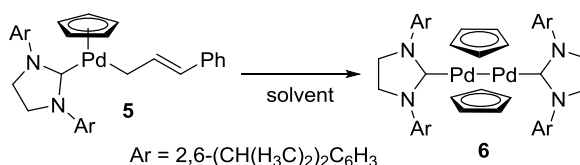
The reaction of $\text{Pd}(\eta^3\text{-1-PhC}_3\text{H}_4)(\eta^5\text{-C}_5\text{H}_5)$ **3** and **4** in a 1:1 ratio was monitored at 65 °C by ^1H NMR spectroscopy (Scheme 2.25). After 4 hours **3** had been completely consumed. The complexation of SIPr to palladium was confirmed after the characteristic downfield signal of the palladium-bound NCN carbon nucleus was observed by ^{13}C NMR spectroscopy. Despite this, it was clear from the ^1H NMR spectrum that the Cp and cinnamyl moieties remained coordinated. The cinnamyl ligand had clearly switched from an η^3 - to an η^1 -bonding mode, allowing the new structure to be tentatively identified as $(\text{SIPr})\text{Pd}(\eta^1\text{-1-PhC}_3\text{H}_4)(\eta^5\text{-C}_5\text{H}_5)$ **5**. The hapticity of the Cp ligand in **5** was somewhat more ambiguous. The chemical shifts measured in the ^1H and ^{13}C NMR spectra (5.10 and 98.5 ppm) were outside the ranges which are typically observed when η^5 - (4.0-4.8 and 70-93 ppm) or η^1 -coordination (5.6-6.2 and 113-118 ppm) is present.^{179,180} However, the measured shifts were very similar to those reported for $(\text{SIPr})\text{Pd}(\eta^5\text{-C}_5\text{H}_5)\text{Cl}$, supporting the above assignment.¹⁸¹



Scheme 2.25 The formation of a novel SIPr palladium(II) complex **5**.

The thermolysis reaction allowed **5** to be afforded with few contaminants; **4**, palladium black and the $\text{C}_{14}\text{H}_{14}$ products of Cp-cinnamyl reductive elimination. These impurities could be easily separated, however attempts to isolate **5** were complicated by its slow decomposition in solution. Solid samples of **5** could be obtained, but were often contaminated with approximately 10 % of one of the decomposition products. During a recrystallisation attempt, this decomposition product was found to be insoluble in

diethyl ether, enabling its isolation and characterisation. The NMR spectra of this material suggested that the impurity was a palladium complex containing only SIPr and Cp ligands and mass spectrometry enabled the assignment of a dimeric structure, formulated as $[(\text{SIPr})\text{Pd}(\text{C}_5\text{H}_5)]_2$. Overall, the data was consistent with a Cp-bridged palladium(I) dimer flanked by SIPr ligands **6** (Scheme 2.26). The IPr-supported variant of **6** has recently been isolated and characterised.¹⁸²



Scheme 2.26 The decomposition of **5** to the palladium(I) dimer **6**.

The filtration of diethyl ether solutions of **5** allowed for much purer samples of this product to be afforded (generally $\geq 98\%$), albeit in only moderate yields (60 %). Once isolated, **5** showed no signs of decomposition after storage in air at room temperature for a year. The recrystallization of **5** could be achieved by layering a toluene solution with hexane, but was extremely irreproducible, possibly due to the accelerated onset of reductive dimerization in supersaturated solutions. Crystals of **5** of suitable quality to be analysed by single crystal X-ray diffraction were grown by slow evaporation of a diethyl ether solution (Figure 2.9). In the solid state the cinnamyl and Cp ligands display η^1 - and η^5 -coordination respectively.

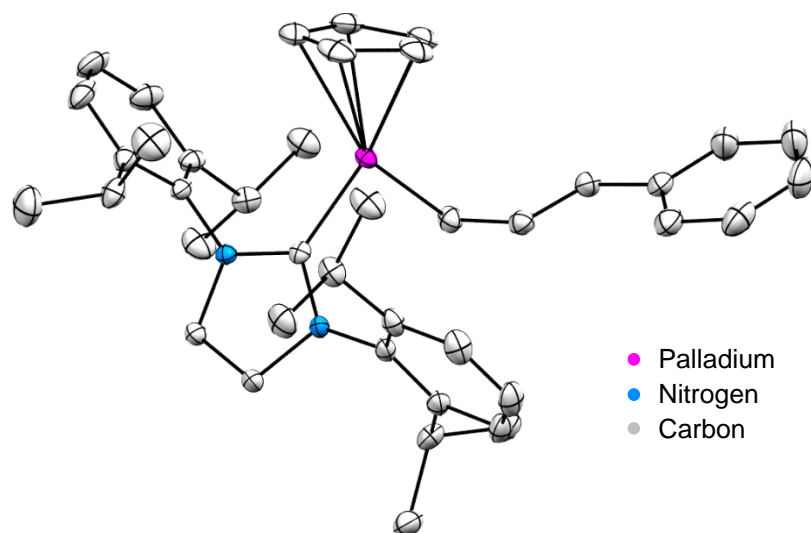


Figure 2.9 Crystal structure of **5**. Ellipsoids at the 50 % probability level.

2.4.3 SIPr-Pentafluorobenzene Adduct Thermolysis

The possibility of liberating SIPr from **4** at 65 °C prior to the addition of $\text{Pd}(\eta^3\text{-1-PhC}_3\text{H}_4)(\eta^5\text{-C}_5\text{H}_5)$ **3** at room temperature was investigated. In order to gauge the rate at which SIPr was produced at this temperature, the thermolysis of **4** was monitored by ^1H NMR spectroscopy (blue circles, Figure 2.10).

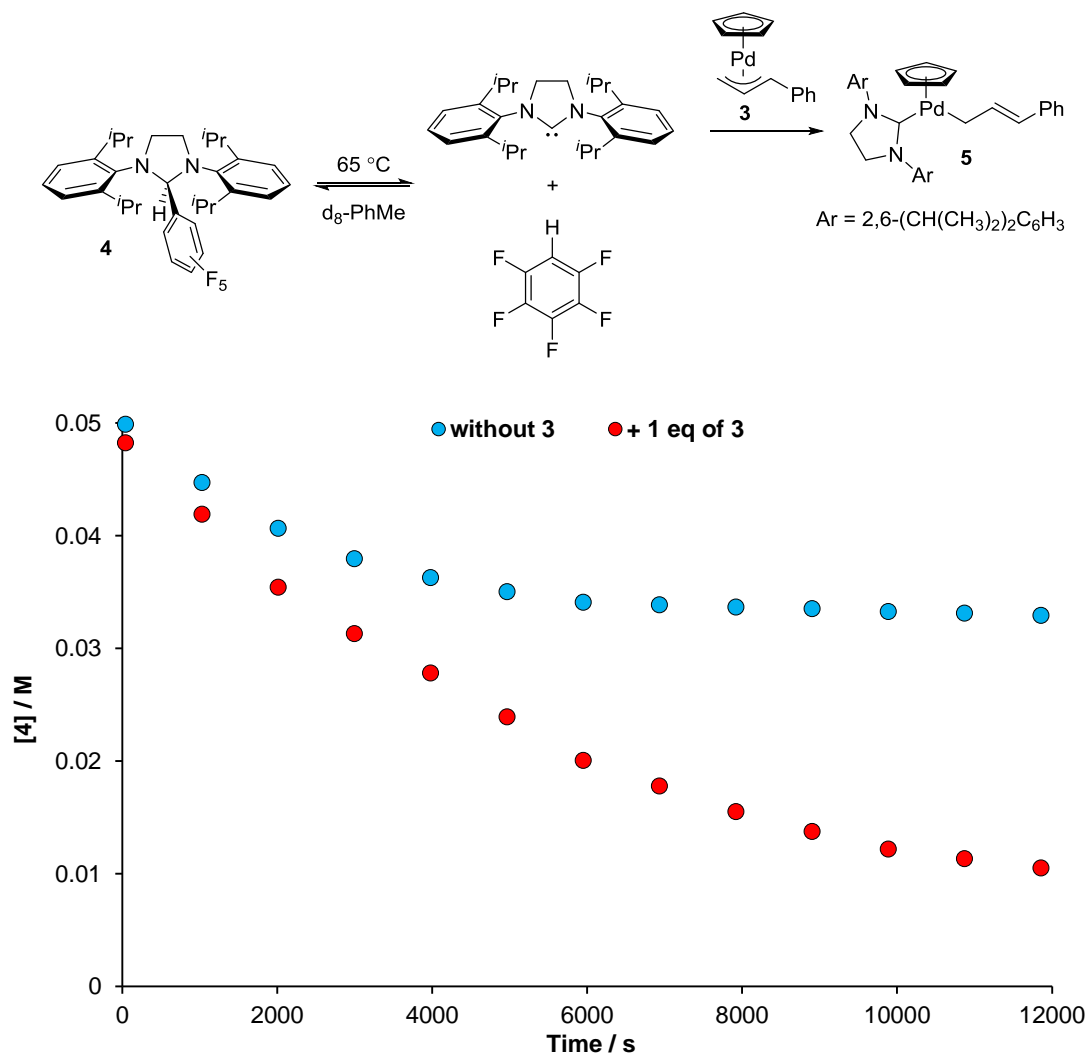


Figure 2.10 ^1H NMR spectroscopy-derived temporal concentration data for the thermolysis of **4** (0.050 M) at 65 °C in $d_8\text{-toluene}$ (blue circles). The reaction was repeated in the presence of $\text{Pd}(\eta^3\text{-1-PhC}_3\text{H}_4)(\eta^5\text{-C}_5\text{H}_5)$ **3** (0.046 M, red circles).

Surprisingly, the reaction appeared to reach equilibrium after 2 hours when a **4**:SIPr ratio of approximately 2:1 was reached. When the solution was cooled, **4** was regenerated. Although the reversible insertion of NHCs into the C-H bond of chloroform is well understood,¹⁸³ the elimination of pentafluorobenzene from NHC adducts has been treated as being irreversible.^{184,185} This is likely a consequence of the contradictory

results of Waymouth, who reported that no reaction took place upon combining SIMes and pentafluorobenzene.¹⁷⁷ The thermolysis of **4** in the presence of **3** adheres to first-order kinetics, highlighting the efficient sequestration of SIPr in this system (red circles, Figure 2.10).

The synthesis of **5** from SIPr.HCl, base (NaH or KO^tBu) and **3** was also explored, but met with very little success.

2.4.4 Catalytic Activity of (SIPr)Pd(η^1 -1-PhC₃H₄)(η^5 -C₅H₅)

It was envisioned that **5** could be used as a thermally activated precatalyst if the reductive elimination of the cinnamyl and Cp ligands could be induced at temperatures above 65 °C. As an initial test of this theory, a sample of **5** was heated to 80 °C for 3 hours in d₈-PhMe. Promisingly, minimal palladium black formation occurred and analysis of the resulting solution by ¹H NMR spectroscopy revealed that approximately 90 % of **5** had been consumed, with only 25 % having undergone dimerization. Further characterisation of the products of this reaction was not performed.

In order to assess whether the thermal decomposition of **5** afforded catalytically active palladium(0) species, **5** was applied to a Suzuki-Miyaura cross-coupling reaction at 80 °C. The conditions which were adopted had been reported to promote the coupling of aryl chlorides with arylboronic acids using catalysts formed *in situ* from Pd(OAc)₂ or Pd(dba)₂ and IMes.HCl or IPr.HCl.¹⁸⁶ Here however, the **5**-promoted coupling of 4-fluorophenylboronic acid with 3,5-bis(trifluoromethyl)bromobenzene was investigated, allowing for the reaction to be monitored by ¹⁹F NMR spectroscopy (blue circles, Figure 2.11). The reaction was complete within 2.5 hours, confirming the activation of **5** to a palladium(0) catalyst under the reaction conditions.

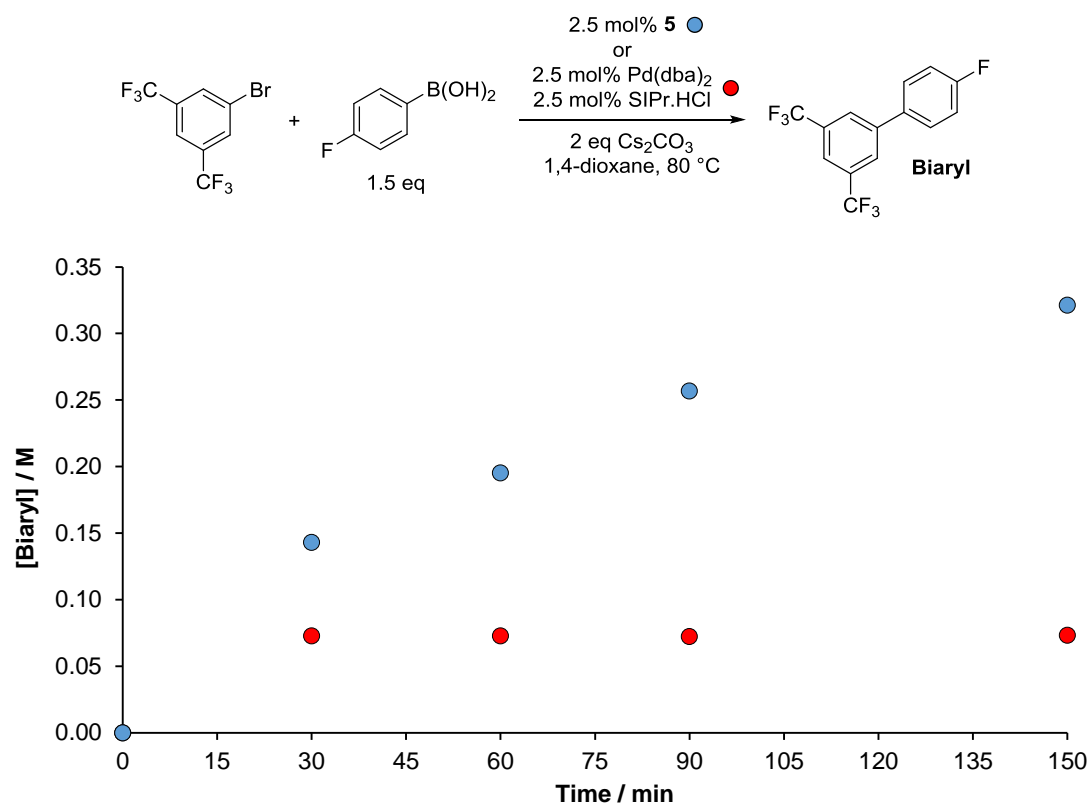
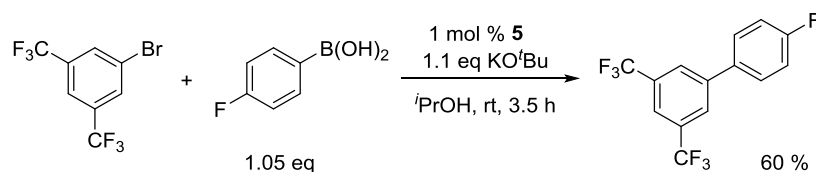


Figure 2.11 ^{19}F NMR spectroscopy-derived temporal concentration data for the Suzuki-Miyaura cross-coupling of 3,5-bis(trifluoromethyl)bromobenzene (0.33 M) with 4-fluorophenylboronic acid (0.5 M) using two different precatalyst systems.

The reaction was repeated in parallel using an ill-defined catalyst formed *in situ* from Pd(dba)_2 and SIPr.HCl (red circles, Figure 2.11). Clearly the use of **5** provides better results. It is notable that when using Pd(dba)_2 and SIPr.HCl almost all of the boronic acid had been diverted to unidentified side-products within 30 minutes.

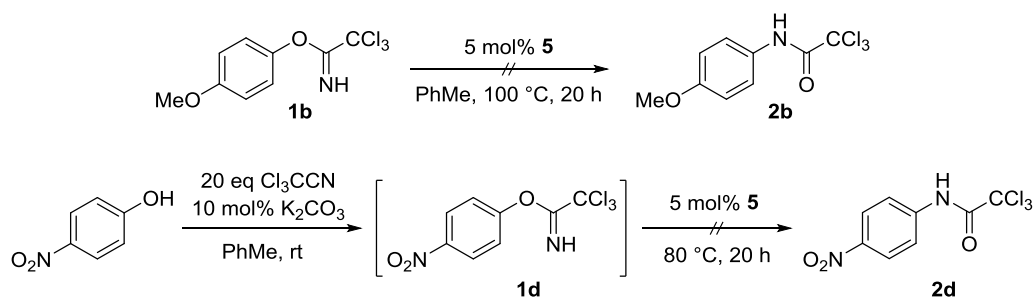
Surprisingly, under different conditions, **5** was found to catalyse the same coupling reaction at room temperature (Scheme 2.27).^{164,165}



Scheme 2.27 The room temperature Suzuki-Miyaura cross-coupling of 4-fluorophenylboronic acid with 3,5-bis(trifluoromethyl)bromobenzene catalysed by **5**.

This result demonstrated that **5** could be activated at low temperatures and in order to explain this it was hypothesised that the coordination of alkoxide to the palladium centre had stimulated the facile reductive elimination of the cinnamyl and Cp ligands. However,

no evidence was obtained to suggest that the activation mechanism accessed at room temperature was not also operative in the coupling reaction conducted at 80 °C (Figure 2.11). Nevertheless, the potential for **5** to be used as a precatalyst for the rearrangements of **1b** and **1d** was probed (Scheme 2.28). Again, none of the desired products **2** were detectable.



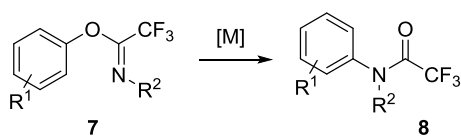
Scheme 2.28 Attempts to induce the rearrangement of **1b** and **1d** using the novel palladium(II) NHC precatalyst **5**.

Given that a range of catalyst systems had showed little promise in the proposed transition metal-catalysed Chapman-type rearrangement of *O*-aryl trichloroacetimidates **1**, modification of the trihaloacetimidate scaffold was next considered.

2.5 *O*-Aryl Trifluoroacetimidates

2.5.1 Concept

Heeding the precedent for *N*-substituted trifluoroacetimidates to be exploited as more stable analogues of trichloroacetimidates (Sections 2.1.2 and 2.1.3), the potential transition metal-catalysed rearrangement of *N*-substituted *O*-aryl trifluoroacetimidates **7** to *N*-aryl trifluoroacetamides **8** was identified as a promising avenue for investigation (Scheme 2.29).



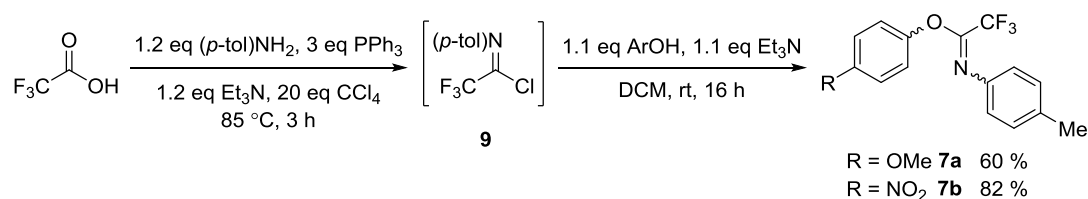
Scheme 2.29 The proposed transition metal-catalysed rearrangement of *N*-substituted *O*-aryl trifluoroacetimidates to *N*-aryl trifluoroacetamides.

Advantageously, it was proposed that the absence of an NH proton would render these substrates more resistant to base-mediated decomposition and that the presence of the strongly electron-withdrawing trifluoromethyl group would aid the oxidative addition

of catalysts into the C_{Ar}-O bond. It was recognised, however, that these benefits might be somewhat offset by the reduced ability of *N*-substituted trifluoroacetimidates to coordinate to transition metals (Sections 2.1.2 and 2.1.3).¹²⁸ It should also be highlighted that in order for primary anilines to be accessed *via* the rearrangement of **7** to **8**, the *N*-substituent would be required to be a removable protecting group.

2.5.2 Preparation

N-Substituted *O*-allyl and *O*-glycosyl trifluoroacetimidates are typically prepared by the condensation of the corresponding alcohols (or hemi-acetal) with *N*-substituted trifluoroacetimidoyl chlorides **9** under basic conditions.^{137,187} Such imidoyl chlorides **9** are not commercially available, but can be synthesised in high yield from trifluoroacetic acid and primary amines or anilines using readily available reagents.¹⁸⁸ Although imidoyl chlorides are usually isolated before use,¹⁸⁹ it was hoped *O*-aryl trifluoroacetimidates **7** might be accessed by forming an imidoyl chloride **9** and condensing it with a phenol in one pot (Scheme 2.30). Pleasingly, this approach proved feasible for the preparation of *N*-(4-methylphenyl) trifluoroacetimidates from electron-rich and electron-poor phenols. Indeed, the *O*-(4-methoxyphenyl) **7a** and *O*-(4-nitrophenyl) **7b** derivatives were synthesised in reasonable yields and proved sufficiently stable to be isolated (as oils) *via* silica-gel column chromatography. Both **7a** and **7b** were prone to slow hydrolysis in air, but displayed indefinite stability under nitrogen.



Scheme 2.30 A two-step, one-pot procedure for the synthesis of *O*-aryl-*N*-(4-methylphenyl) trifluoroacetimidates **7**.

2.5.3 Assigning Isomers

It was clear from NMR analyses that **7a** and **7b** were formed as a mixture of two interconverting isomers (Figure 2.12). All signals in their ¹H NMR spectra were broadened and their ¹⁹F NMR spectra consisted of two extremely broad singlets.

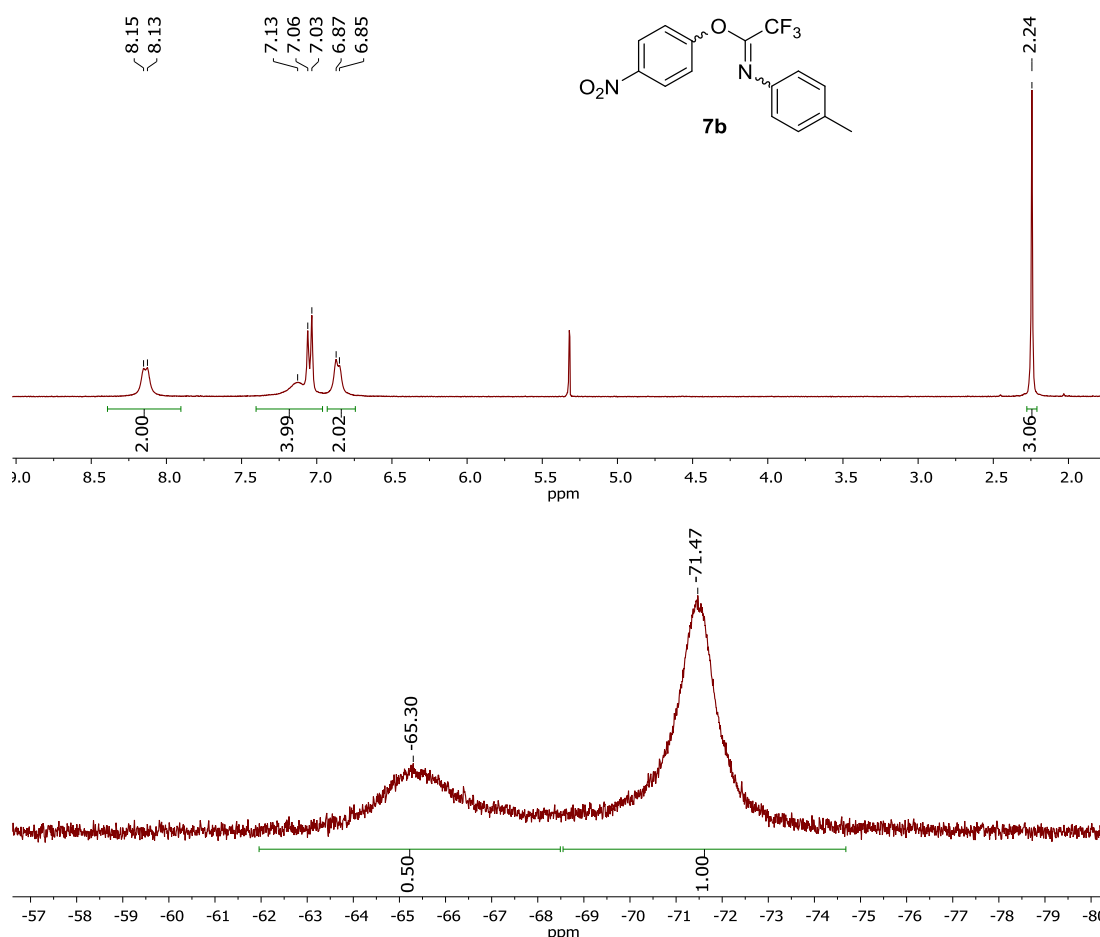


Figure 2.12 Above: The ¹H NMR spectrum (CD₂Cl₂) of **7b** recorded at 27 °C. Below: The ¹⁹F NMR spectrum (CDCl₃) of **7b** recorded at 25 °C.

As in the case of *O*-aryl trichloroacetimidates, it seemed reasonable that the two isomers differed by the geometry of their C-N double bonds (compare *E* and *Z* isomers, Figure 2.13). However, the possibility that conformational isomerism of *O*-aryl trifluoroacetimidates was responsible for the aforementioned spectroscopic observations could not be ruled out. Conformational isomerism would most likely be manifest in the geometry of the C_{imidoyl}-O bond. Two low energy conformations involving a *syn*-periplanar (*sp*) or *anti*-periplanar (*ap*) relationship between the *O*-aryl group and the CF₃ group would be expected (compare *ap* and *sp* isomers, Figure 2.13).¹⁹⁰

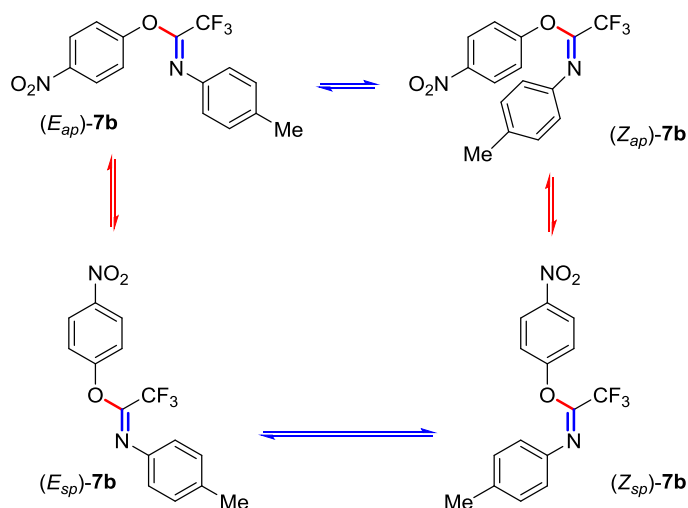
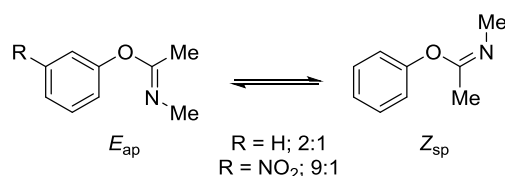


Figure 2.13 Possible configurations and conformations of **7b.**

Supporting the proposed geometrical isomerism of **7a** and **7b**, *O*-phenyl-*N*-methyl acetimidate has been shown to exist as a mixture of slowly interconverting *E* and *Z* isomers on the basis of the $^5J_{\text{HH}}$ coupling constants measured between the two methyl groups. The *E* configuration was found to dominate (*E*:*Z* 2:1, Scheme 2.31).¹⁹¹ The preference for this isomer was enhanced in *O*-(3-nitrophenyl)-*N*-methyl acetimidate (*E*:*Z* 9:1).¹⁹¹ Similarly, **7a** and **7b** existed in isomer ratios of 1:1 and 2:1 respectively.



Scheme 2.31 Isomers of *O*-phenyl-*N*-methyl acetimidate.

The aromatic ^1H NMR signals of the two isomers of **7b** were found to be well resolved at $-60\text{ }^\circ\text{C}$ in $\text{d}_2\text{-DCM}$ (spectrum A, Figure 2.14) and therefore, in an attempt to learn more about the isomerisation of this species, a 2D NOESY NMR experiment was conducted under the same conditions (spectrum C, Figure 2.14). The exchange of the isomers was confirmed but an NOE contact between the two aryl rings was not observed.

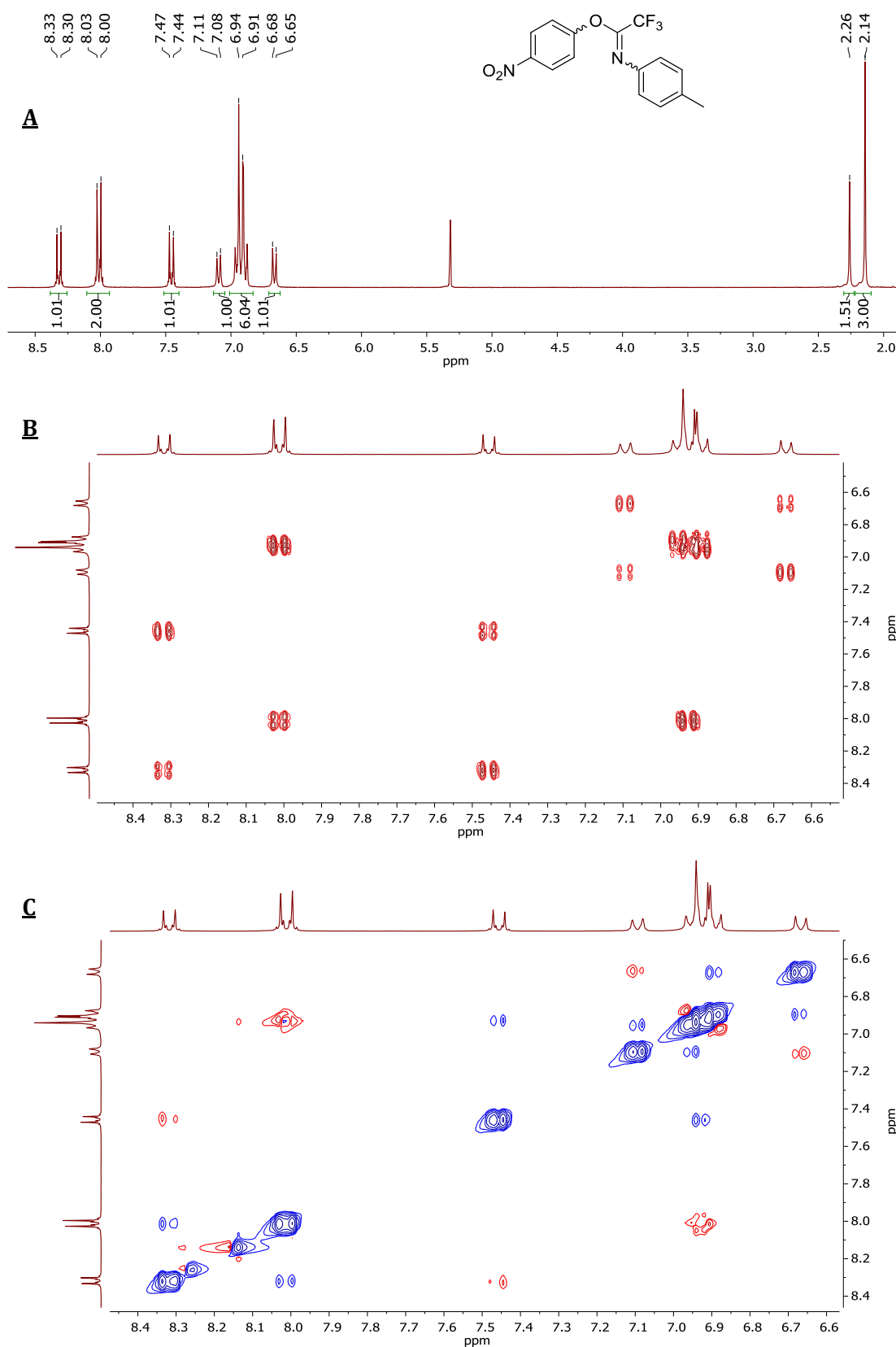


Figure 2.14 **A:** The ^1H NMR spectrum (CD₂Cl₂) of 7b recorded at -60 °C. **B:** The ^1H - ^1H COSY NMR spectrum (CD₂Cl₂) of 7b recorded at -60 °C. **C:** The 2D NOESY NMR spectrum (CD₂Cl₂) of 7b recorded at -60 °C. NOESY cross peaks are displayed in red and EXSY (exchange) cross-peaks are displayed in blue. NOE contacts are only made between protons on the same aromatic ring.

An NOE contact might have been expected if one of the two isomers had been in the Z_{ap} configuration (Figure 2.13). The existence of this isomer was therefore deemed unlikely and the presence of at least one *E* isomer was shown to be probable. Access to an *E* isomer was expected to be essential if the proposed transition metal-catalysed Chapman-type rearrangement was to proceed *via* pre-coordination of the catalyst to the substrate before oxidative addition.

2.5.4 Catalyst Screen

Many of the general considerations discussed in relation to screening catalysts for the rearrangement of *O*-aryl trichloroacetimidates **1** (Section 2.3.3) were also relevant to the catalyst screen conducted in an attempt to realise the rearrangement of *O*-aryl trifluoroacetimidates **7**. The screen focused on low oxidation state cross-coupling catalysts to activate the strong C_{Ar}-O bond and avoided the use of strongly basic and nucleophilic conditions due to the high electrophilicity of the substrates. In addition to the palladium(0) and nickel(0) catalysts previously introduced (Section 2.3.1), low-valent rhodium catalysts which have been shown to react with C_{Ar}-O electrophiles (Section 1.2.3) were also explored.

The catalyst screen was performed using **7b** as it was hoped that the presence of the electron-withdrawing *para*-nitro group would aid oxidative addition. Conditions effective in promoting the palladium(0)-catalysed NKR were adopted (Table 2.6).

Table 2.6 Catalyst screen for the rearrangement of **7b.^a**

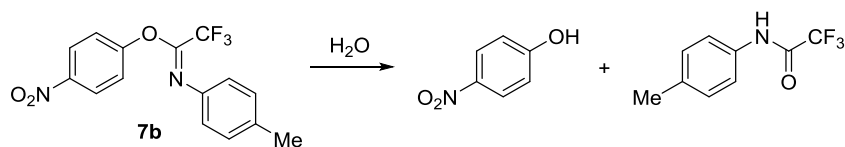
Reaction scheme: **7b** (N-(4-nitrophenyl)-N-(4-methylphenyl)trifluoroacetamide) $\xrightarrow[\text{PhMe, 100 } ^\circ\text{C, 18-24 h}]{\text{precatalyst, ligand}}$ **8b** (N-(4-nitrophenyl)-N-(4-methylphenyl)trifluoroacetamide)

Precatalyst (mol%)	Ligand (mol%)	8b / % ^b
Pd(P ^t Bu ₃) ₂ (10)	-	0
(SIPr)Pd(η^1 -1-PhC ₃ H ₄)(η^5 -C ₅ H ₅) (10)	-	0
Pd(dba) ₂ (10)	CyPF- ^t Bu (10)	0
Pd(dba) ₂ (10)	BrettPhos (10)	0
Pd(dba) ₂ (10)	dppf (10)	0
Pd(dba) ₂ (10)	^t BuXPhos (10)	0
Pd(dba) ₂ (10)	IPr (10) ^{c,f}	0
Ni(COD) ₂ (10)	Xantphos (10)	0
Ni(COD) ₂ (10)	dppf (10)	0
Ni(COD) ₂ (10)	CyPF- ^t Bu (10)	0
Ni(COD) ₂ (10)	Me ₄ ^t BuXPhos (20)	0
Ni(COD) ₂ (10)	P(C ₆ F ₅) ₃ (20)	0
Ni(COD) ₂ (10)	P(O-2,4-(C(CH ₃) ₃) ₂ C ₆ H ₃) ₃ (20)	0
Ni(COD) ₂ (10)	IPr (20) ^{d,f}	0
RhCl(PPh ₃) ₃ (5)	-	0
[Rh(COD)dppf][PF ₆] (5)	-	0 ^g
[RhCl(COD)] ₂ (2.5)	SPhos (5)	0 ^g
[RhCl(COD)] ₂ (2.5)	IMes (5) ^{e,f}	0 ^{g,h}
[RhCl(COD)] ₂ (2.5)	P(<i>o</i> -tol) ₃ (10)	0
[IrCl(COD)] ₂ (2.5)	P(OEt) ₃ (5)	0

^a 0.25 mmol scale, 0.25 M. ^b Conversions determined by ¹⁹F NMR spectroscopy. ^c 10 mol% IPr.HCl and 11 mol% ^tBuOK. ^d 20 mol% IPr.HCl and 22 mol% ^tBuOK. ^e 5 mol% IMes.HCl and 20 mol% CsF. ^f Precatalyst, imidazolium salt and base stirred for 30 min at room temperature prior to substrate addition and heating. ^g Similar results were obtained using 1,4-dioxane as the solvent. ^h T = 120 °C.

Disappointingly, the desired product, *N*-(4-nitrophenyl)-*N*-(4-methylphenyl) trifluoroacetamide **7b**, was not formed using any of the catalyst systems trialed (Table 2.6). In the majority of cases, **7b** was recovered with only minor hydrolysis to 4-

nitrophenol and *N*-(4-methylphenyl) trifluoroacetamide having been observed (determined by ^{19}F and ^1H NMR spectroscopy; Scheme 2.32).



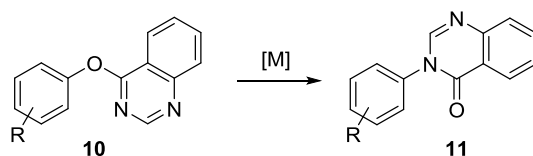
Scheme 2.32 The hydrolysis of **7b**.

When $\text{Pd}(\text{P}^t\text{Bu}_3)_2$ was applied, the reaction mixture was also analysed by ^{31}P NMR spectroscopy (without prior air exposure). Notably, a significant proportion of $\text{Pd}(\text{P}^t\text{Bu}_3)_2$ was found to have remained intact and the only other species detectable were free and oxidised phosphine.

2.6 4-Aryloxy Quinazolines

2.6.1 Concept

Having failed to promote the transition metal-catalysed Chapman-type rearrangement of *O*-aryl trihaloacetimidates, attempts were made to catalyse the Chichibabin rearrangement of 4-aryloxy quinazolines **10** to *N*-aryl quinazolinones **11** (Scheme 2.33).



Scheme 2.33 The proposed transition metal-catalysed rearrangement of 4-aryloxy quinazolines **10** to *N*-aryl quinazolinones **11**.

4-Aryloxy quinazolines **10** were expected to be less susceptible than trihaloacetimidates towards oxidative addition *via* a 3-membered ring transition state due to the relatively poor leaving group ability of the quinazolinide anion (Figure 2.15). However, it was proposed that they would more readily pre-coordinate transition metal catalysts and might therefore be more susceptible towards oxidative addition *via* a 5-membered ring transition state. Computational studies have implicated such 5-membered ring transition states in the oxidative addition of palladium(0) and nickel(0) species into the $\text{C}_{\text{Ar}}\text{-O}$ bonds of *O*-aryl (thio)carbamates and sulfamates.^{69,81,118}

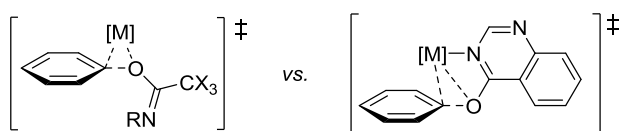


Figure 2.15 Possible 3- and 5-membered ring transition states for the oxidative addition of transition metal catalysts to O-aryl trihaloacetimidates and 4-aryloxy quinazolines 10.

Beneficially, 4-aryloxy quinazolines **10** are crystalline and are readily prepared in high yield by reacting alkali metal phenoxides with 4-chloroquinazoline.⁵² 4-Chloroquinazoline is commercially available, although relatively expensive.

2.6.2 Catalyst Screen

A catalyst screen for the rearrangement of 4-phenoxy quinazoline **10a** to *N*-phenyl quinazolinone **11a** was conducted in a similar manner to that described for the *O*-aryl trihaloacetimidates (Sections 2.3.3 and 2.5.4). Unfortunately, none of the catalysts applied were effective in promoting this reaction (Table 2.7). No substrate decomposition was observed.

Table 2.7 Catalyst screen for the rearrangement of 4-phenoxy quinazoline 10a. ^a

Precatalyst (mol%)	Ligand (mol%)	11a / % ^b
Pd(P ^{<i>t</i>} Bu ₃) ₂ (10)	-	0
Pd(dba) ₂ (10)	CyPF- <i>t</i> Bu (10)	0
Ni(COD) ₂ (10)	PCy ₃ (20)	0
Ni(COD) ₂ (10)	P(4-(CF ₃)C ₆ H ₄) ₃ (20)	0
Ni(COD) ₂ (10)	dppf (10)	0
Ni(COD) ₂ (10)	IPr (20) ^{c,e}	0
RhCl(PPh ₃) ₃ (10)	-	0
[RhCl(COD)] ₂ (5)	PCy ₃ (10)	0
[RhCl(COD)] ₂ (5)	IMes (10) ^{d,e}	0

^a 0.1 mmol scale, 0.1 M. ^b Conversions determined by ¹⁹F NMR spectroscopy. ^c 20 mol% IPr.HCl and 22 mol% KO^{*t*}Bu. ^d 10 mol% IMes.HCl and 11 mol% KO^{*t*}Bu. ^e Precatalyst, imidazolium salt and base stirred for 30 min at room temperature prior to substrate addition and heating.

2.7 Summary and Conclusions

The development of a transition metal-catalysed Chapman-type (or Chichibabin) rearrangement has been pursued to no avail.

Towards this goal, the base-catalysed reaction of phenols with trichloroacetonitrile to provide *O*-aryl trichloroacetimidates **1** as potential substrates was investigated. Although these imidates **1** were readily formed, their separation from the corresponding phenols could not be achieved. This was little issue when electron-rich phenols were employed as conversions were almost quantitative. However, when electron-deficient phenols were utilised, the reaction equilibria established were typically in favour of the phenols.

Attempts to induce the rearrangement of *O*-aryl trichloroacetimidates **1** through transition metal catalysis were hampered by their base sensitivity. This led to the development of a novel, mono-NHC palladium(II) precatalyst, (SIPr)Pd(η^1 -1-PhC₃H₄)(η^5 -C₅H₅) **5**. This precatalyst was demonstrated to display activity in Suzuki-Miyaura cross-coupling reactions, even at room temperature, but failed to promote the rearrangement of *O*-aryl trichloroacetimidates **1**. In solution, **5** was observed to slowly decompose to a bis-Cp-bridged palladium(I) dimer, (SIPr)₂Pd₂(μ -C₅H₅)₂ **6**, somewhat complicating its isolation.

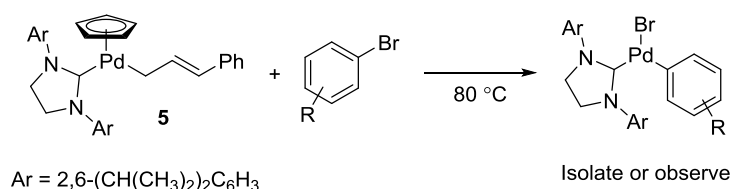
O-Aryl-*N*-(4-methylphenyl) trifluoroacetimidates **7** and 4-aryloxy quinazolines **10** were investigated as more robust substrates for the proposed rearrangement reaction. Enabling this, a one-pot, two-step procedure for accessing trifluoroacetimidates **7** from both electron-rich and electron-deficient phenols was established. Disappointingly, despite screening palladium, nickel and rhodium complexes that are typically used in challenging cross-coupling reactions, catalysts capable of inducing the rearrangement of *O*-aryl trifluoroacetimidates **7** or 4-aryloxy quinazolines **10** were not identified.

2.8 Future Work

In order to direct future attempts to promote a transition metal-catalysed Chapman-type rearrangement or develop novel phenol-derived cross-coupling electrophiles, an understanding of why *O*-aryl trihaloacetimidates resisted rearrangement would be valuable. It is proposed that stoichiometric reactions between the appropriate *O*-aryl imidates and catalysts could shed light on this matter.

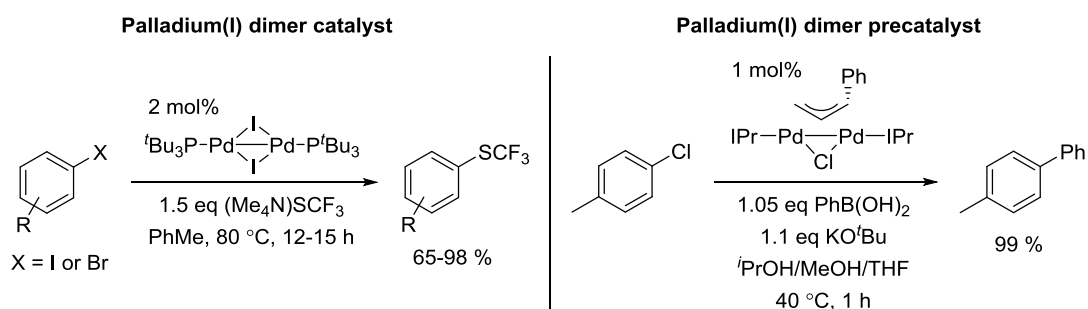
It is also envisioned that if complexes of the general formula $(\text{NHC})\text{Pd}(\eta^1\text{-1-PhC}_3\text{H}_4)(\eta^5\text{-C}_5\text{H}_5)$ are to find use as precatalysts, their synthesis and stability must be assessed with a wide range of sterically and electronically diverse NHC ligands. If the isolation of these complexes is found to be practical, their activity in various cross-coupling reactions should then be compared with existing mono-NHC palladium(II) precatalyst systems.

Provided that the feasibility of a thermal activation pathway can be confirmed, these precatalysts could also prove to be extremely valuable in base-free palladium(0)-catalysed transformations, such as telomerisation reactions.¹⁹² It is proposed that the viability of this activation pathway could be determined by examining whether oxidative addition occurs upon thermolysing $(\text{SIPr})\text{Pd}(\eta^1\text{-1-PhC}_3\text{H}_4)(\eta^5\text{-C}_5\text{H}_5)$ **5** in the presence of an aryl bromide (Scheme 2.34).



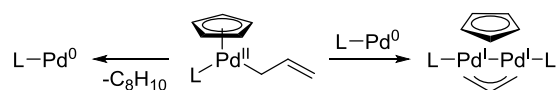
Scheme 2.34 The proposed assay for the thermal activation of **5**.

It is worth noting, however, that the pursuit of the aforementioned goals would benefit from first understanding the impact that the formation of $(\text{NHC})_2\text{Pd}_2(\mu\text{-C}_5\text{H}_5)_2$ palladium(I) dimers has upon the ability of $(\text{NHC})\text{Pd}(\eta^1\text{-1-PhC}_3\text{H}_4)(\eta^5\text{-C}_5\text{H}_5)$ complexes to act as precatalysts. Although a detrimental effect on catalyst activity is possible, it is hypothesised that the dimers could be catalytically competent or could act as reservoirs or precursors to mono-NHC palladium(0) species. These phenomena have both been observed for related dimeric palladium(I) species (Scheme 2.35).^{193,194}



Scheme 2.35 The use of palladium(I) dimers as catalysts or precatalysts in the coupling reactions of aryl halides.

The decomposition of $(\text{SI}Pr)\text{Pd}(\eta^1\text{-1-PhC}_3\text{H}_4)(\eta^5\text{-C}_5\text{H}_5)$ **5** to $(\text{SI}Pr)_2\text{Pd}_2(\mu\text{-C}_5\text{H}_5)_2$ **6** was entirely unexpected. Typically, palladium(II) complexes containing two different allyl- or Cp-type ligands decompose to generate palladium(I) dimers bridged by one of each of those two different ligands.^{182,195,196} A mechanism has been proposed which explains this observation well (Scheme 2.36).^{195,197,198}



Scheme 2.36 The proposed mechanism for the formation of $(\text{L})_2\text{Pd}_2(\mu\text{-C}_5\text{H}_5)(\mu\text{-C}_3\text{H}_5)$ palladium(I) dimers from $(\text{L})\text{Pd}(\eta^5\text{-C}_5\text{H}_5)(\eta^1\text{-C}_3\text{H}_5)$ palladium(II) complexes.

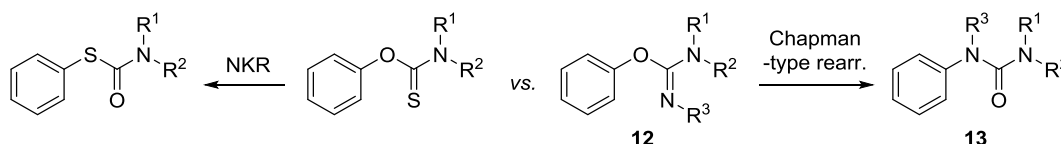
In line with this trend, bis-Cp-bridged palladium(I) dimers have only been generated from bis-Cp palladium(II) complexes.^{180,182,199} The mechanism for the decomposition of **5** is clearly different and is worthy of investigation along the $(\text{NHC})\text{Pd}(\eta^1\text{-1-PhC}_3\text{H}_4)(\eta^5\text{-C}_5\text{H}_5)$ series.

3 Towards a Base-Catalysed Chapman-Type Rearrangement: O-Aryl Isoureas

3.1 Introduction

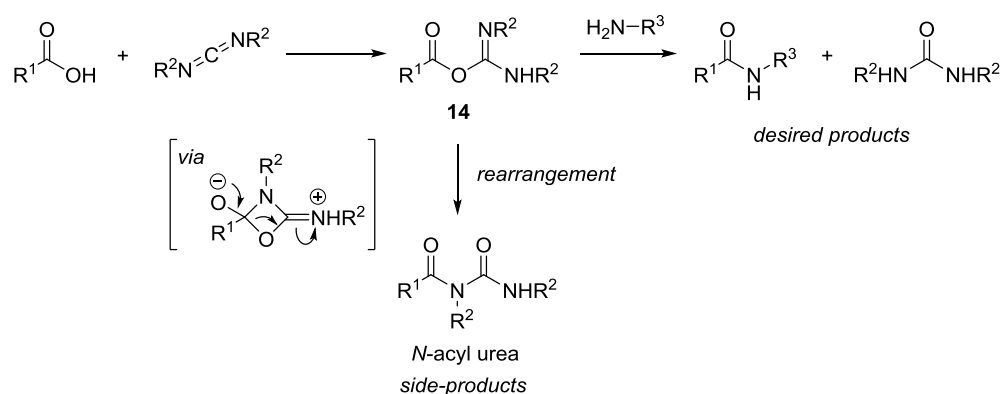
3.1.1 Chapman-Type Rearrangements of *O*-Aryl Isooureas

Given their resemblance to the *O*-aryl thiocarbamate substrates of the NKR, it is unsurprising that certain *O*-aryl isoureas **12** have been found to undergo Chapman-type rearrangements to the corresponding *N*-aryl ureas **13** (Scheme 3.1).²⁰⁰⁻²⁰³



Scheme 3.1 A comparison of *O*-aryl thiocarbamates with *O*-aryl isoureas **12**.

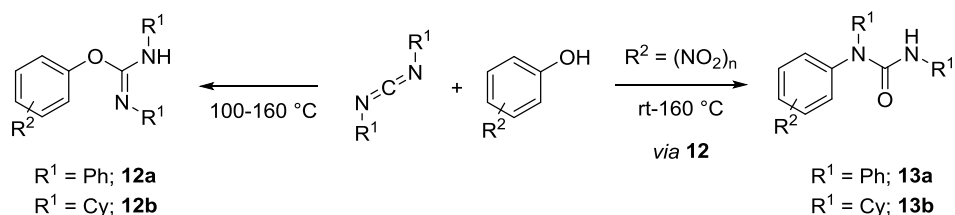
The rearrangement of *O*-aryl isoureas **12** also shares similarities with the rearrangement of *O*-acyl isoureas **14**. The rearrangement of *O*-acyl isoureas **14** to *N*-acyl ureas is a frequently encountered side-reaction in carbodiimide-mediated amide bond-forming reactions between carboxylic acids and amines (Scheme 3.2).^{204,205} The rearrangement of *O*-acyl isoureas **14** can occur under very mild conditions due to the high electrophilicity of the acyl group.



Scheme 3.2 The rearrangement of *O*-acyl isoureas **14** is a side-reaction in carbodiimide-mediated amide bond forming processes.

The rearrangement of *O*-aryl isoureas **12** to *N*-aryl ureas **13** was first observed by Busch, Blume and Pungs in their seminal work on the reactions of diaryl carbodiimides.²⁰⁰ Importantly, this study described the reactions of a number of electronically diverse phenols with diphenyl carbodiimide and demonstrated that electron-withdrawing aromatic substituents were required in order for the rearrangement reaction to be observed (at reasonable temperatures). The neat reactions of relatively weakly acidic

phenols (e.g. *p*-cresol) with diphenyl carbodiimide at 150-160 °C were shown to afford stable *O*-aryl-*N,N'*-diphenyl isoureas **12a** (Scheme 3.3) whilst more acidic, nitrated phenols reacted to afford *N,N,N'*-triaryl ureas **13a**. Diphenyl carbodiimide reacted with picric acid (2,4,6-trinitrophenol, PicOH) to form the corresponding triaryl urea even at room temperature. The analogous reaction with 2,4-dinitrophenol only proceeded in refluxing benzene whilst 4-nitrophenol and diphenyl carbodiimide had to be heated neat at 160 °C for the urea to be produced. The urea products **13a** were proposed to form *via* Chapman-type rearrangement of the corresponding isoureas **12a** after evidence was obtained for the generation of *O*-(4-nitrophenyl)-*N,N'*-diphenyl isourea upon refluxing 4-nitrophenol with diphenyl carbodiimide in benzene.²⁰⁰

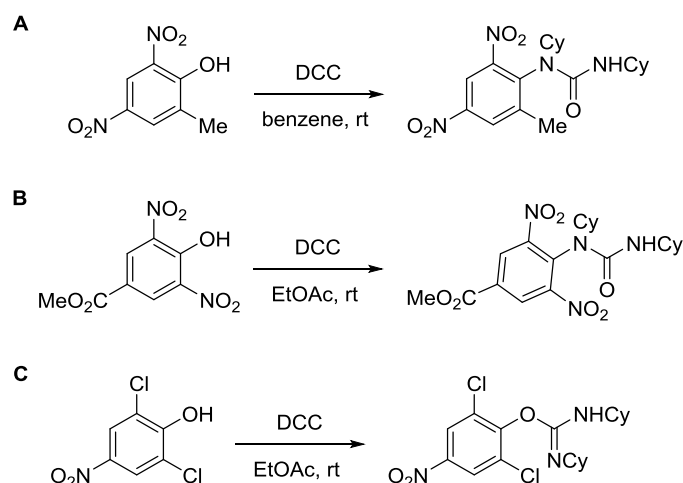


Scheme 3.3 The reactions of carbodiimides with phenols.

Over half a century later, following the discovery of stable dialkyl carbodiimides, Vowinkel assessed the reactivity of phenols with dicyclohexyl carbodiimide (DCC; Scheme 3.3). Again, the reactions of weakly acidic phenols afforded *O*-aryl isoureas **12b**, whilst those of nitrated phenols produced *N*-aryl ureas **13b**. The same relationship between the degree of phenol nitration and rate of urea **13b** formation was observed as described above (for the corresponding reactions with diphenyl carbodiimide); picric acid reacted at room temperature, 2,4-dinitrophenol reacted in refluxing ether and 4-nitrophenol reacted in refluxing benzene. Although the corresponding isoureas **12b** could not be isolated from these reactions, they were implicated as intermediates after an indicative IR band was observed upon analysing a chloroform solution of 4-nitrophenol and DCC.²⁰¹

2,4,6-Trisubstituted phenols containing one non-nitro group (e.g. a methyl²⁰² or methoxycarbonyl²⁰³ substituent) have also been found to afford urea **13b** products of rearrangement at room temperature upon treatment with DCC (reactions A and B, Scheme 3.4). Interestingly, 2,6-dichloro-4-nitrophenol combines with DCC to afford the corresponding isourea with no signs of rearrangement under comparable conditions

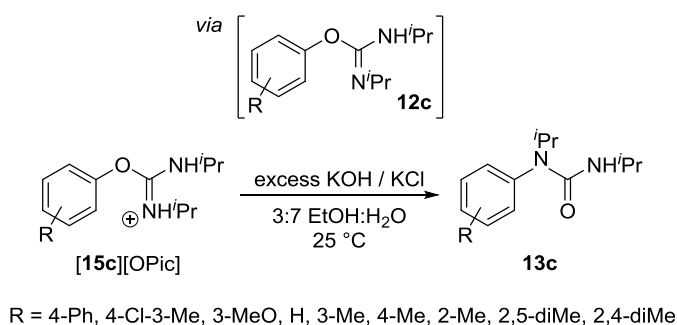
(reaction C).²⁰⁶ These results serve to highlight the sensitivity of the rearrangement to electronic effects.



Scheme 3.4 The reactions of electron-deficient 2,4,6-trisubstituted phenols with DCC.

3.1.2 Anionic Chapman-Type Rearrangements of *O*-Aryl Isooureas

Suttle and Williams reported that *O*-aryl isoureas **12** containing more electron-rich aromatic systems could also undergo room temperature rearrangement if an anionic, base-catalysed reaction manifold was invoked. Specifically, the rearrangement of *O*-aryl-*N,N'*-diisopropyl isoureas **12c** (isolated as their picrate salts [**15c**][OPic], Section 3.2.1) was reported to proceed upon treatment with an excess of potassium hydroxide in aqueous ethanol (Scheme 3.5).²⁰⁷



Scheme 3.5 The KOH-catalysed Chapman-type rearrangement of *O*-aryl-*N,N'*-diisopropyl isoureas **12c**.

Reactions were carried out using extremely low concentrations of [**15c**][OPic] (0.1 – 1 μM) allowing for the kinetics of the reaction to be measured using UV-Vis spectroscopy. The second-order rate constants for the rearrangements of a series of *O*-aryl isoureas **12c** derived from phenols within a narrow *pK_a* range (9.5 – 10.6) were obtained. Using

this data, a Brønsted-type linear free-energy relationship was derived. The extremely large Brønsted β_{LG} value extracted, $\beta_{LG} = -2.3$, was consistent with an S_NAr -type mechanism, but was significantly larger than the value determined for the thermal Chapman rearrangement, $\beta_{LG} = -0.78$. This difference in sensitivity was attributed to the different charge distributions in the transition states of these two reactions (Figure 3.1). In the base-catalysed reaction, deprotonation at nitrogen precedes nucleophilic attack and an anionic transition state is accessed. The nitrogen nucleophile in the thermal rearrangement is neutral and thus, a zwitterionic transition state is invoked. Although negative charge accumulates in the aryl rings of both transition states, the adjacent positive charge in the latter is suggested to draw some of the electron density away from the aromatic substituents.

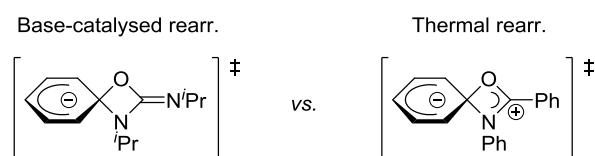
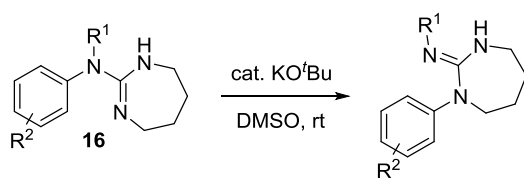


Figure 3.1 Transition states for the base-catalysed and thermal Chapman rearrangements.

It was further proposed that the higher nucleophilicity of the nitrogen anion implicated in the base-catalysed reaction was responsible for its greatly reduced thermal demand. In addition, Eyring analysis of the temperature dependence of the rearrangement revealed a small, negative entropy of activation that was consistent with intramolecular reaction. Indeed, the value determined ($\Delta S^{\ddagger} = -13.5 \text{ cal K}^{-1} \text{ mol}^{-1}$; *O*-phenyl-*N,N'*-diisopropyl isourea **12c'**) was comparable to that measured for the thermal Chapman rearrangement ($\Delta S^{\ddagger} = -9.7 \text{ cal K}^{-1} \text{ mol}^{-1}$; *O*-(4-methylphenyl)-*N*-phenyl benzimidate).²⁰⁷

Later, cyclic *N*-aryl guanidines **16** were shown to be susceptible to a related room temperature anionic Chapman-type rearrangement under comparable conditions (Scheme 3.6). In contrast to the *O*-aryl isourea **12c** substrates investigated in the study described above, all of the *N*-aryl guanidine **16** substrates examined were somewhat activated towards rearrangement by the presence of electron-withdrawing aromatic substituents. The most activated substrates (those substituted with a nitro group) were also shown to undergo relatively low temperature thermal rearrangement when heated to 100-120 °C in DMF. The products of rearrangement were unambiguously identified by X-ray crystallography.²⁰⁸



Scheme 3.6 The base-catalysed Chapman-type rearrangement of cyclic *N*-aryl guanidines **16**.

3.1.3 Summary and Chapter Aims

In summary, a collection of reports detailing the surprisingly low-temperature Chapman-type rearrangements of *O*-aryl isoureas **12** have been identified. These first of these reports concerned the spontaneous generation of *N*-aryl ureas **13** when (poly)nitrated phenols were reacted with dialkyl or diaryl carbodiimides.^{200,207} Later, the related room temperature, KOH-catalysed Chapman-type rearrangement of unactivated *O*-aryl-*N,N'*-diisopropyl isoureas **12c** was disclosed.²⁰⁷ Whilst impressive, this latter reaction was not been performed on synthetically useful scales or extended to the rearrangement of isoureas incorporating alternative *N*-substituents. This chapter will describe the efforts made to optimise the synthesis of *O*-aryl *N,N'*-dialkyl isourea salts and assess the scope and limitations of anionic Chapman-type rearrangements. Ultimately, it was hoped that establishing practical relevance in this process would lead to a viable method for the conversion of phenols to anilines.

3.2 Preparation of *O*-Aryl-*N,N'*-dialkyl Isoureas

3.2.1 Background

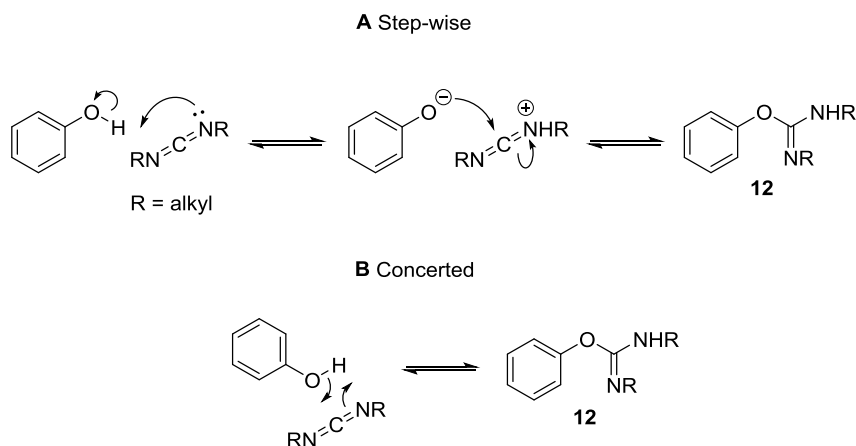
The synthesis of *O,N,N'*-trisubstituted isoureas is most commonly achieved by the reaction of phenols with carbodiimides, however, different combinations of aliphatic or aromatic alcohols and dialkyl or diaryl carbodiimides exhibit extremely different reactivity under identical reaction conditions (Table 3.1). For example, diaryl carbodiimides will react with aliphatic alcohols at high temperatures or with added alkoxide catalysts,^{209,210} whereas the reaction of dialkyl carbodiimides with aliphatic alcohols necessitates the use of an acid catalyst (Brønsted or Lewis).^{211–213} In contrast, the reactions of both diaryl and dialkyl carbodiimides with phenols proceed thermally and are retarded by the addition of a base.^{201,214}

Table 3.1 Reactivity patterns in the preparation of *O,N,N'*-trisubstituted isoureas.

Alcohol	Diaryl Carbodiimide			Dialkyl Carbodiimide		
	Thermal	Acid Cat.	Base Cat.	Thermal	Acid Cat.	Base Cat.
Aryl	✓ ²⁰⁰	✓ ²¹⁵	✗ ²¹⁶	✓ ²⁰¹	— ²¹⁶	✗ ²⁰¹
Alkyl	✓ ²¹⁰	✓ ²¹⁷	✓ ²⁰⁹	✗ ²¹⁰	✓ ²¹²	✗ ²⁰⁹
<div> <div>✓ Reaction promoted</div> <div>✗ Reaction inhibited</div> <div>— Effect unclear</div> </div>						

The different reactivity of aliphatic alcohols with dialkyl and diaryl carbodiimides can be justified by the different electrophilicities of these classes of carbodiimides. The C=N π -bond in diaryl carbodiimides is conjugated with the adjacent aromatic systems which increases the electrophilicity of these carbodiimides relative to dialkyl carbodiimides. The difference in electrophilicity is sufficiently large that, in the absence of a Brønsted or Lewis acid catalyst, only diaryl carbodiimides will react with aliphatic alcohols. Acidic catalysts are proposed to activate carbodiimides towards nucleophilic attack by protonating or complexing one of the nitrogen-based lone pairs.

In order to explain why phenols undergo thermal reactions with dialkyl carbodiimides whilst aliphatic alcohols do not, the relatively high acidity of phenols must be considered. Phenols are sufficiently acidic that they can reversibly protonate carbodiimides and the phenoxide/protonated carbodiimide ion pairs generated in this process react more rapidly than the corresponding neutral species (mechanism A, Scheme 3.7). Aliphatic alcohols are not capable of protonating carbodiimides and therefore this relatively low energy reaction pathway is not available. The addition of base to the reactions of phenols with carbodiimides inhibits this pathway by reducing the concentration of phenolic (acidic) protons.²¹⁴ Whether protonation and nucleophilic attack occur in a concerted (mechanism B) or a step wise manner (mechanism A) is unclear (Scheme 3.7).²⁰¹



Scheme 3.7 The proposed mechanisms for the reaction of phenols with carbodiimides.

As a consequence of the mechanism discussed above (Scheme 3.7), phenols are found to react with more basic dialkyl carbodiimides at lower temperatures than they react with less basic diaryl carbodiimides.^{200,201} Similarly, the rate of reaction is increased by the use of more acidic phenols (i.e. those substituted with electron-withdrawing functional groups).^{200,214}

Although they are formed rapidly, isoureas generated from reactions between acidic phenols and dialkyl carbodiimides tend to be the least thermodynamically stable. Therefore, procedures for their synthesis typically employ an excess of either the carbodiimide or the phenol in order to bias the reaction equilibrium and improve conversions.²¹⁸ However, when the isoureas generated in these reactions are subsequently isolated, they are often observed to slowly decompose to their phenol and carbodiimide components.²⁰¹ Consequently, such isoureas are typically isolated as their protonated salts by treatment with an acid which promotes crystallisation (e.g. picric acid or oxalic acid).^{200,218}

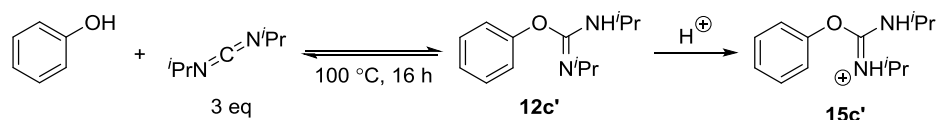
3.2.2 Literature Procedures

The synthetic route utilised by Suttle and Williams²⁰⁷ to access *O*-aryl-*N,N'*-diisopropyl isoureas **12c** was adapted from a procedure originally reported by Vowinkel and Wolff.²¹⁸ This procedure involved fusing a mixture of a phenol and a carbodiimide at temperatures between 45 and 100 °C for 1-3 days, with one of the components in excess (2-3 equivalents). In the case that the phenol was used in excess, unreacted phenol was subsequently removed by dissolving the reaction mixture in an organic solvent and washing with dilute aqueous sodium hydroxide. The organic fraction then had glacial acetic acid added to convert any unreacted carbodiimide to the corresponding urea,

which would precipitate (Scheme 3.9, Section 3.2.3). After filtration, the solution was again washed with sodium hydroxide (presumably to remove any remaining acetic acid). The solvent was then removed to afford the crude isourea which was isolated *via* precipitation from 2-propanol upon salt formation with an acid. Purification was achieved through recrystallization. If the carbodiimide was used in excess, the first sodium hydroxide wash was removed from this sequence. Following this procedure, Suttle and Williams reported isolated yields of between 30-60% for the picric acid salts of *O*-aryl-*N,N'*-diisopropyl isoureas [**15c**][OPic].²⁰⁷ Vowinkel and Wolff achieved yields of 42-96% using a wider range of carbodiimides and acids.²¹⁸

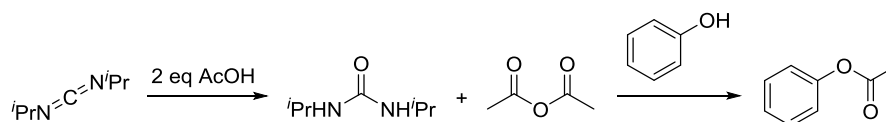
3.2.3 Improving the Synthetic Procedure

A salt of *O*-phenyl-*N,N'*-diisopropyl isourea **15c'** was sought using the procedure described above. The generation of this product as a crystalline solid was essential for its isolation and purification, however, it was hoped that the synthesis of the isourea picrate salt [**15c'**][OPic] could be avoided as picric acid is both highly explosive and toxic. It was proposed alternative acids might afford similarly crystalline, but more readily handled isourea salts. A sample of the crude isourea **12c'** was successfully prepared using an excess of diisopropyl carbodiimide (DIC, 3 equivalents, Scheme 3.8), but salt formation using *p*-toluenesulfonic acid or trifluoromethanesulfonic acid did not afford a crystalline product.



Scheme 3.8 The synthesis of *O*-phenyl-*N,N'*-diisopropyl isourea salts **15c'**.

Analysis of the crude isourea **12c'** by ¹H NMR spectroscopy prior to salt formation revealed a significant degree of contamination with phenyl acetate (approx. 4:6 phenyl acetate:**12c'**). It was rationalised that this side-product was generated by the acetylation of phenol with acetic anhydride, which itself was formed upon the decomposition of the DIC to diisopropyl urea (DIPU) upon the addition of glacial acetic acid (Scheme 3.9). Presumably, phenol had been present in the reaction mixture due to incomplete reaction or the decomposition of **12c'** during work-up. It was hypothesised that phenyl acetate was preventing the crystallisation of the sulfonate salts of **12c'**.



Scheme 3.9 The proposed route for the generation of phenyl acetate.

In order to avoid this problem, the use of excess phenol in the reaction was next explored. It was proposed that the use of excess phenol would eliminate the need for unreacted DIC to be removed from the crude isourea by the addition of acetic acid. Instead, the excess phenol would be separated by sodium hydroxide extraction. Unfortunately, the crude **12c'** obtained using this method also was not sufficiently pure for crystalline sulfonic acid salts to be prepared; varying amounts of both phenol and DIC remained.

A procedure for preparing pure samples of crude **12c'** was finally found after observing that phenol and DIC passed through a plug of silica-gel when it was eluted with DCM, whilst **12c'** was retained. The isourea **12c'** only eluted when an alternative solvent (e.g. diethyl ether) was used. This procedure was demonstrated to be compatible with the use of DIC or DCC and was found to enable the preparation of crystalline *p*-toluenesulfonic acid, trifluoromethanesulfonic acid or picric salts. Although the yields of isourea salts were consistently low (25-45%), they were very reproducible and the material which was afforded was of high analytical purity. Furthermore, this method allowed for an excess of either the carbodiimide or the phenol to be applied with no change in the outcome.

3.2.4 Mechanistic Insight into the Reaction of Phenol with DIC

During the above route development studies, attempts were made to gain an understanding of the equilibrium between isoureas and their phenol and carbodiimide components, as this reaction is poorly described in the literature. The equilibrium was investigated by reacting equimolar quantities of phenol and DIC (Scheme 3.10).



Scheme 3.10 The equilibrium established between phenol, DIC and O-phenyl-*N,N'*-diisopropyl isourea **12c'**.

Conducting this reaction in CDCl_3 in an NMR tube allowed for the concentration of DIC to be monitored using ^1H NMR spectroscopy (dataset A, Figure 3.2). At room temperature,

the reaction appeared to approach equilibrium after 500 hours (approx. 21 days), although the reaction was still proceeding slowly when analysis of the reaction was halted. Interestingly, the equilibrium concentrations of **12c'** and DIC appeared to be approximately equal (~ 0.125 M).

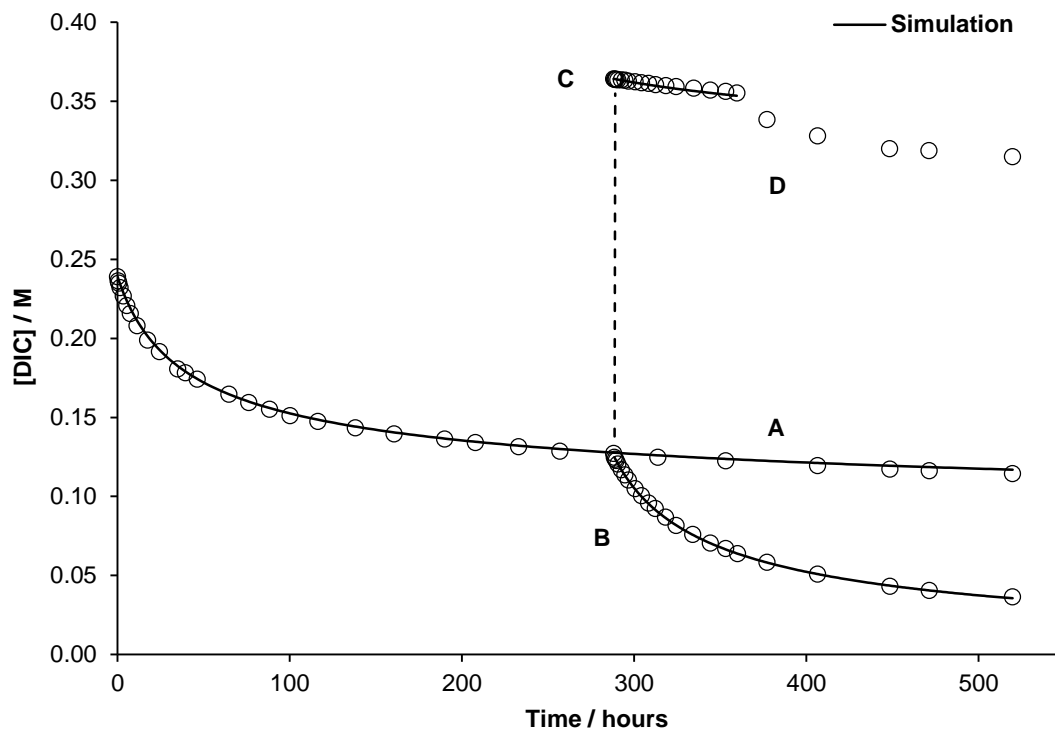


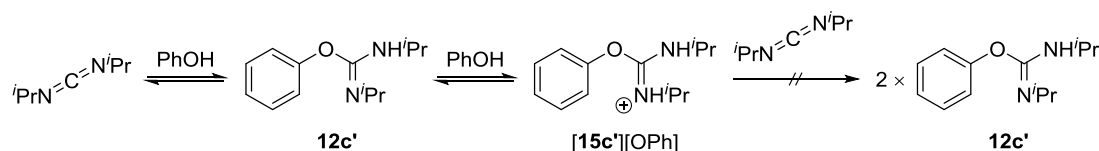
Figure 3.2 ^1H NMR spectroscopy-derived temporal concentration data for DIC (hollow circles, 0.24 M) upon reaction with phenol (PhOH; 0.25 M). A: standard reaction; B: additional phenol (0.25 M) was added after 290 hours; C: additional DIC (0.24 M) was added after 290 hours; D: sample was heated to 60 °C after 360 hours.

A separate reaction mixture, identical to that described above, was monitored in parallel for 290 hours. At this point a further equivalent of phenol was added and the ^1H NMR analyses continued (dataset B, Figure 3.2). A sharp increase in the rate of DIC consumption was observed.

A third identical reaction mixture had an additional equivalent of DIC added after 290 hours (dataset C, Figure 3.2). Surprisingly, unlike the addition of phenol, this appeared to have little influence on the rate of **12c'** formation. Only when this sample was heated to 60 °C, was the rate of **12c'** formation increased (dataset D, Figure 3.2).

The differing effects brought about by the introduction of additional quantities of phenol and DIC suggested that the isourea-forming reaction was more complex than previously reported. If it had been possible to describe the reaction as a simple equilibrium between

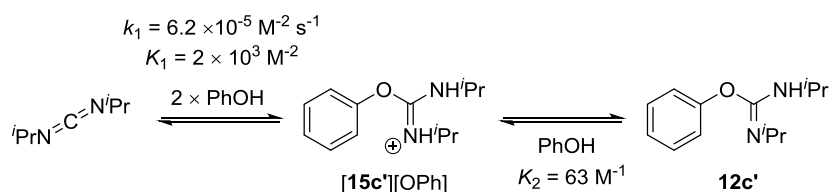
reagents and products (Scheme 3.10), increasing the concentration of either phenol or DIC should have increased the rate of **12c'** formation. Therefore, it was rationalised that upon formation, **12c'** had immediately deprotonated phenol to form the corresponding phenoxide salt **[15c']**[OPh] (Scheme 3.11). It was also proposed that without a phenolic proton, **[15c']**[OPh] would be unreactive towards reaction with DIC (compare to the effect of added base, Sections 3.2.1 and 3.2.5).



Scheme 3.11 Possible equilibria established in the reaction of phenol with DIC.

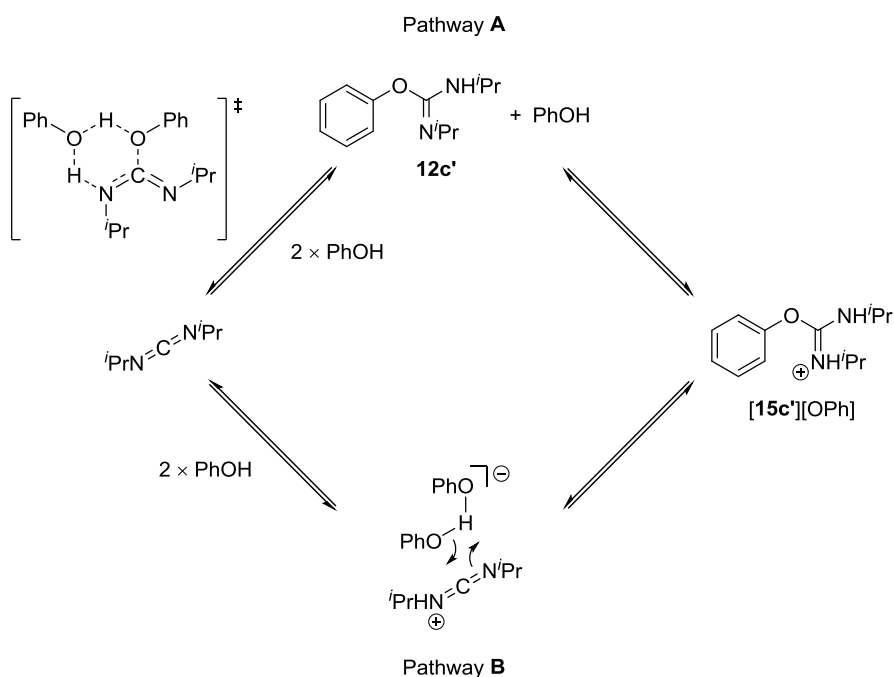
This being the case, as a 50 % conversion of DIC to **[15c']**[OPh] was approached, almost no phenol would remain and a severe deceleration of the reaction rate, as observed, would be expected (dataset A, Figure 3.2). The observed sensitivity of the reaction at this point to the concentration of phenol, but not DIC, provided support for this theory. Furthermore, the loss of the ^1H NMR signal for the phenolic OH proton as the reaction approached 50 % conversion was consistent with the generation of **[15c']**[OPh]. Analogous phenoxide salts have been identified and isolated, however only in the reactions of extremely acidic phenols (e.g. pentachlorophenol) with dialkyl carbodiimides.^{206,219}

With this hypothesis in mind, attempts were made to simulate the kinetic data using a model in which the equilibrium between **[15c']**[OPh] and **12c'** strongly favoured the formation of **[15c']**[OPh]. Significantly, a model in which the reaction was initiated by a bimolecular reaction between phenol and DIC (Scheme 3.11) did not sufficiently account for the sensitivity of the reaction to the concentration of phenol and thus gave a poor fit to the data. On the other hand, a model based upon what is formally a termolecular reaction between phenol and DIC (second order in phenol and first order in DIC, Scheme 3.12) simulated the data well (solid lines, Figure 3.2).



Scheme 3.12 The mechanistic model used to simulate the kinetics of the reaction between phenol with DIC (Figure 3.2).

It is proposed that such a reaction could occur *via* the concerted addition of a phenol dimer to DIC, either before (pathway A, Scheme 3.13) or after (pathway B) a proton transfer step. Overall, the model demonstrates that the slow attainment of equilibrium in the reaction of phenol with DIC can be justified by the formation of [15c'] [OPh] and the operation of third order kinetics. Such mechanistic features have previously not been identified and it is proposed that this is due to the acceleration of the reaction under the forcing conditions which are typically applied in literature procedures (dataset D, Figure 3.2).



Scheme 3.13 Plausible termolecular processes in the formation of [15c'] [OPh] from phenol and DIC.

3.2.5 Effect of Additives on the Reaction of Phenol with DIC

Subsequently, the influence of a number of basic or acidic (Lewis and Brønsted) additives on the model system was investigated (Figure 3.3).

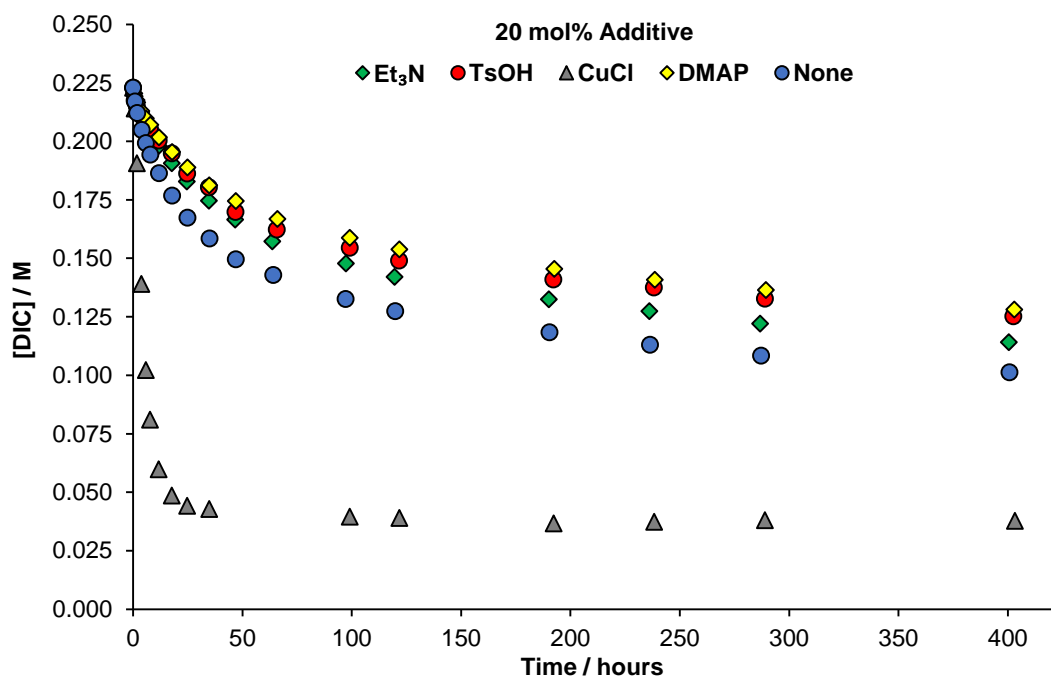
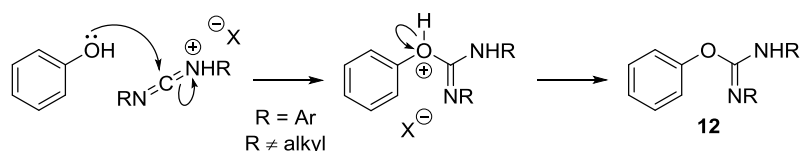


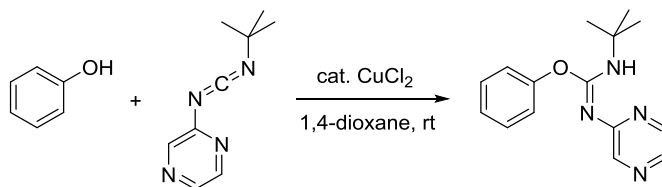
Figure 3.3 ^1H NMR spectroscopy-derived temporal concentration data for DIC (0.22 M) upon reaction with phenol (0.25 M) in the presence of a range of additives.

As expected, both triethylamine and DMAP reduced the rate of reaction. More surprisingly, *p*-toluenesulfonic acid also had an inhibitory effect. This finding contrasts with the reported observation that phenol reacts with the hydrochloride salt of diphenyl carbodiimide at lower temperatures than it reacts with the corresponding free base.²¹⁵ However, it is maybe somewhat revealing that reactions of phenol with dialkyl and mixed *N*-alkyl-*N'*-aryl carbodiimides have only been performed with added hydrogen chloride under reaction conditions which are comparable to those typically adopted in the absence of added acid.²¹⁶ Considering these points, it is proposed that Brønsted acids can promote reactions between phenols and diaryl carbodiimides, but that they inhibit reactions between phenols and dialkyl carbodiimides. In order to explain this, it is hypothesised that due to the inherent difference in their electrophilicities, protonated diaryl carbodiimides can be attacked by phenols whereas protonated dialkyl carbodiimides cannot (Scheme 3.14). Instead, the protonation of dialkyl carbodiimides is proposed to reduce the concentration of carbodiimide available for reaction with phenol *via* the proton transfer/nucleophilic addition mechanism discussed previously.



Scheme 3.14 The proposed mechanisms for the reaction of phenols with protonated diaryl carbodiimides.

Copper(I) chloride is clearly an efficient catalyst for the reaction of phenol with DIC, allowing for equilibrium to be established extremely quickly (Figure 3.3). Copper(I) and copper(II) chloride salts have previously been reported to effectively catalyse the difficult additions of aliphatic alcohols to dialkyl and diaryl carbodiimides at room temperature.^{210,211,220,221} It is worth noting however, that the ability of copper halides to catalyse reactions between phenols and carbodiimides has only been demonstrated for the reaction of phenol with *N*-(2-pyrazinyl)-*N'*-(*tert*-butyl) carbodiimide, and in this example, the mode of carbodiimide activation is ambiguous (Scheme 3.15).²²²



Scheme 3.15 The copper(II) chloride-catalysed reaction of phenol with *N*-(2-pyrazinyl)-*N'*-(*tert*-butyl) carbodiimide.

It is generally proposed that copper halides catalyse the addition of alcohols to carbodiimides by transiently coordinating to the carbodiimides and increasing their susceptibility to nucleophilic attack (Figure 3.4).²¹⁰

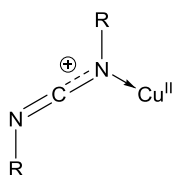


Figure 3.4 The coordination of carbodiimides to copper salts is proposed to enhance their electrophilicity.

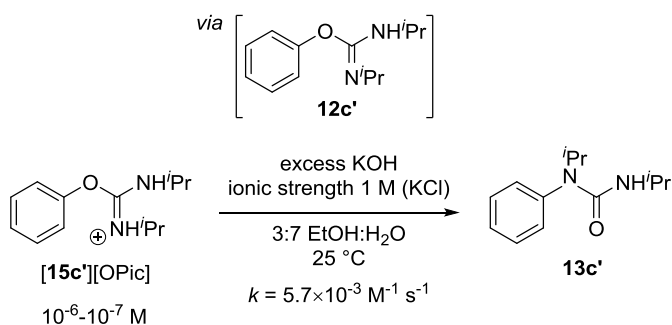
Although catalysis *via* this mechanism could have been operative in the *N*-(2-pyrazinyl)-*N'*-(*tert*-butyl) carbodiimide system, the possibility that the copper(II) chloride catalyst was activating the carbodiimide by coordination to the pyrazine ring can not be ruled out. The successful copper(I) chloride-catalysed addition of phenol to DIC therefore

serves to illustrate that copper halides can catalyse the reactions of phenols with carbodiimides which do not contain additional coordinating atoms.

3.3 Revisiting the Anionic Chapman-Type Rearrangements of *O*-Aryl Isooureas

3.3.1 Background

Before the scope and limitations of anionic Chapman-type rearrangements were probed in detail, attempts were made to reproduce some of the results reported by Suttle and Williams. These authors collected the majority of their data using the picrate salt of *O*-phenyl-*N,N'*-diisopropyl isourea [**15c'**][OPic] (Scheme 3.16), which was presumed to be rapidly deprotonated in the basic medium to liberate **12c'**. The same salt was chosen for our initial investigations in spite of the desire to utilise sulfonate salts in subsequent reaction optimisation studies on the grounds of safety.



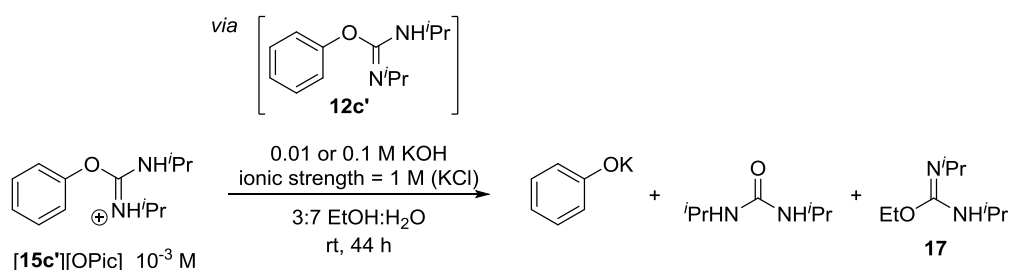
Scheme 3.16 The KOH-catalysed Chapman-type rearrangement of **12c'**.

Unfortunately, the reaction conditions reported to induce rearrangement were somewhat ambiguous and had been adopted with the sole intention of recording kinetic data using UV-Vis spectroscopy. As such, reactions were conducted in a cuvette under thermostatic control (25 °C) and commenced by adding a small unknown volume of an ethanolic isourea salt stock solution to “2.5 mL KOH buffer in 30% ethanol-water maintained at an ionic strength of 1 M with KCl”.²⁰⁷ Although the exact quantity of isourea salt used in each reaction was not measured, typical reaction concentrations were quoted as being between 10^{-6} and 10^{-7} M. It was also reported that the pH of the reaction mixtures was recorded after each reaction, however, these values (nor any other details regarding the concentrations of KOH used) were not provided. Reasonable approximations of these values were therefore extrapolated from the second order rate constants that were provided as the results of their kinetic analyses.²⁰⁷ For [**15c'**][OPic],

a rate constant of $k = 5.7 \times 10^{-3} \text{ M}^{-1} \text{ s}^{-1}$ could be translated into a reaction half-life of $t_{1/2} = 202 \text{ min}$ at a KOH concentration of 0.01 M or a reaction half-life of $t_{1/2} = 20.2 \text{ min}$ at a KOH concentration of 0.1 M. Such half-lives are practically convenient for kinetic studies and therefore KOH concentrations in this region were assumed. When Suttle and Williams used **[15c']**[OPic] as the substrate for their kinetic measurements, the formation of the product of rearrangement, *N*-phenyl-*N,N'*-diisopropyl urea **13c'** (90.1 %) and phenol (2.7 %) were reported based on analysis of the product mixture by HPLC.

3.3.2 Initial Attempts

Considering all of the above, initial investigations were carried out at a concentration of 10^{-3} M by adding **[15c']**[OPic] to a solution of KOH and KCl in 3:7 ethanol:water. The 1,000-fold increase in the reaction concentration relative to that used by Suttle and Williams allowed for the outcome of the reaction to be assessed by ^1H NMR spectroscopy. Two different KOH concentrations were applied; 0.1 and 0.01 M, with a total ionic strength of 1 M achieved in both cases by the addition of KCl. The reactions were allowed to proceed for 44 hours at room temperature before work-up and ^1H NMR analysis, which revealed the complete consumption of **12c'**. Unexpectedly, the only reaction products detectable were potassium phenoxide, DIPU and minor quantities of *O*-ethyl-*N,N'*-diisopropyl isourea **17** (Scheme 3.17). These products were proposed to arise from the base mediated solvolysis of **12c'**.



Scheme 3.17 The KOH-promoted solvolysis of **12c'**.

It was hypothesised that the elevated reaction concentration was responsible for the unexpected reaction outcome. More specifically, it was proposed that **12c'** might have formed hydrogen-bonded dimers at 10^{-3} M , causing a decrease in the acidity of the NH bond and thus, a reduced susceptibility towards deprotonation and base-catalysed rearrangement (red arrows, Figure 3.5). In support of this theory, urea has been demonstrated to form hydrogen-bonded dimers in aqueous solutions due to the hydrophobic effect, with concentration having a notable effect on the degree of

aggregation.²²³ With the rearrangement reaction inhibited, it appeared reasonable that the solvolysis of **12c'** (green arrow, Figure 3.5) would become the dominant process.

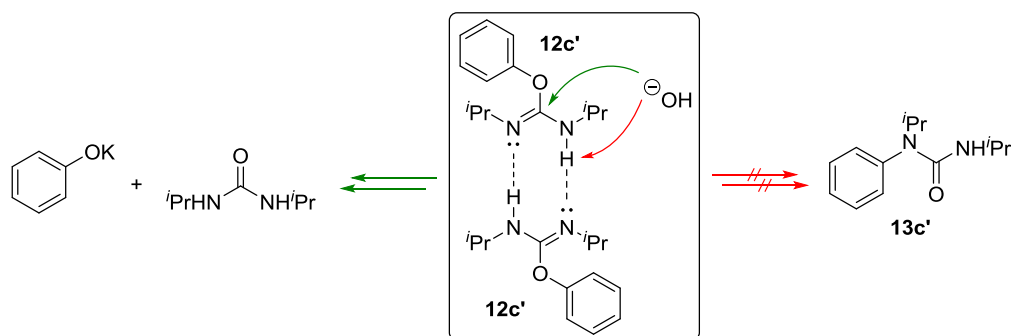


Figure 3.5 The proposed pathways for the reaction of hydrogen bonded **12c'** dimers with KOH.

3.3.3 UV-Vis Kinetics

Reducing the concentration of **12c'** in reaction mixtures was expected to restore reactivity towards rearrangement, but also necessitated that the reaction outcome be assessed using UV-Vis spectroscopy. However, despite resorting to this more sensitive analytical technique, the reaction concentration could only be reduced as low as 10^{-5} M due to the sensitivity limits of the spectrometer used. Such reactions were monitored by measuring the absorbance at 290 nm as a function of time (blue circles, Figure 3.6). Suttle and Williams also recorded their temporal absorbance data at this wavelength when studying the rearrangement of **12c'**.²⁰⁷

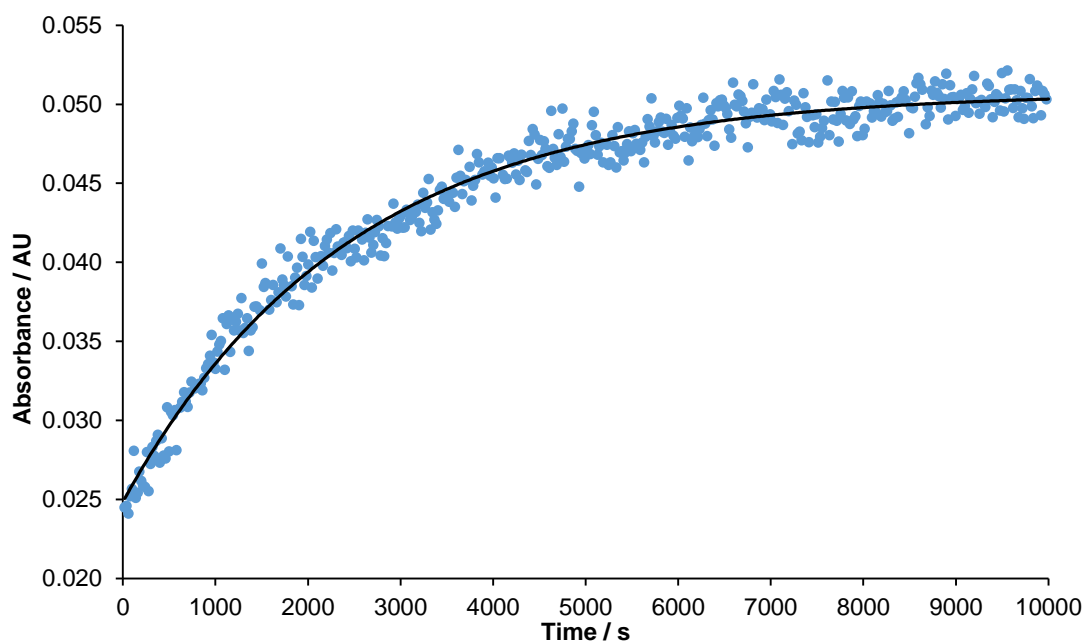


Figure 3.6 Temporal absorbance data (290 nm, 25 °C; blue circles) for the reaction of **[15c']**[OPic] (10^{-5} M) with KOH (0.1 M; KCl 0.9 M) in 3:7 ethanol:H₂O. A first order exponential was fitted to the data (black line).

The reaction appeared to be almost complete after 10,000 seconds (~ 2.8 hours). A first order exponential equation (black line, Figure 3.6) was accurately fitted to the data, suggesting that the reaction was catalysed by KOH or adhered well to the pseudo-first order approximation; a vast excess of KOH was used (10,000 equivalents). The fit allowed an observed first order rate constant, $k_{\text{obs}} = 4.12 \times 10^{-4} \text{ s}^{-1}$, to be extracted. Accounting for the concentration of KOH, a second order rate constant was calculated, $k = 4.12 \times 10^{-3} \text{ M}^{-1} \text{ s}^{-1}$. This value is in good agreement with that measured by Suttle and Williams under the same conditions, $k_{\text{lit}} = 5.7 \times 10^{-3} \text{ M}^{-1} \text{ s}^{-1}$, suggesting that the system had been well reproduced.²⁰⁷ An almost identical reaction profile was observed when the reaction was repeated at a substrate concentration of 10^{-4} M. Analysis of this data produced a calculated second order rate constant, $k = 4.63 \times 10^{-3} \text{ M}^{-1} \text{ s}^{-1}$, which was even closer to the reported value.

Whilst the kinetic data implied that the anionic Chapman-type rearrangement of **12c'** had been successful at low concentrations, further evidence for the identity of the reaction products was sought. The UV-Vis spectra of **[15c']**[OPic], **13c'** and the *p*-toluenesulfonic acid salt of *O*-phenyl-*N,N'*-diisopropyl isourea **[15c']**[OTs], were recorded and compared to the UV-Vis spectrum of the reaction products of a kinetic run at the same concentration (10^{-4} M, Figure 3.7). It should be noted that in the KOH

solutions used to measure the UV-Vis spectra, it is likely that **[15c']**[OPic] and **[15c']**[OTs] will have been deprotonated to liberate **12c'** and either potassium picrate or potassium tosylate prior to analysis.

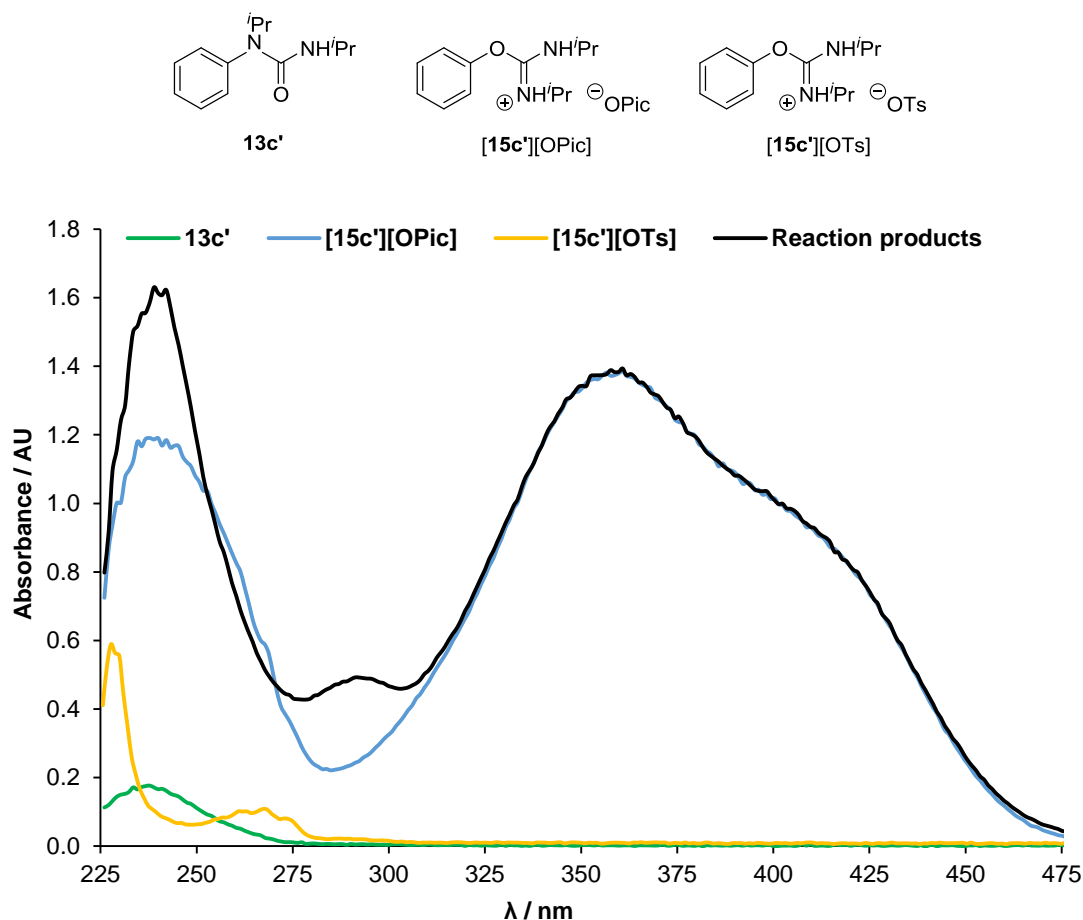


Figure 3.7 Reference UV-Vis spectra recorded at analyte concentrations of 10^{-4} M in solutions of 0.1 M KOH/0.9 M KCl in 3:7 EtOH:H₂O.

It is apparent upon comparing the spectra of **[15c']**[OPic] (blue line) and **[15c']**[OTs] (yellow line), that the strongly absorbing picrate anion dominates the UV profile of the reaction mixture (black line, Figure 3.7). Surprisingly, it was also clear that **13c'** does not absorb at 290 nm; the wavelength used in the kinetic analysis. A different species that does absorb between 280 and 300 nm must have been being formed throughout the course of the reaction. A likely candidate was identified as potassium phenoxide, which displays strong absorbance at 290 nm (red line, Figure 3.8). In order to gain further evidence for this, the absorbance spectrum of potassium phenoxide (10^{-4} M) was added to that of **[15c']**[OPic] to produce a combined spectrum (purple line, Figure 3.8). The combined spectrum accurately reproduced the profile recorded for the reaction

products above 280 nm. This suggested that potassium picrate and potassium phenoxide had been formed quantitatively in the kinetic run.

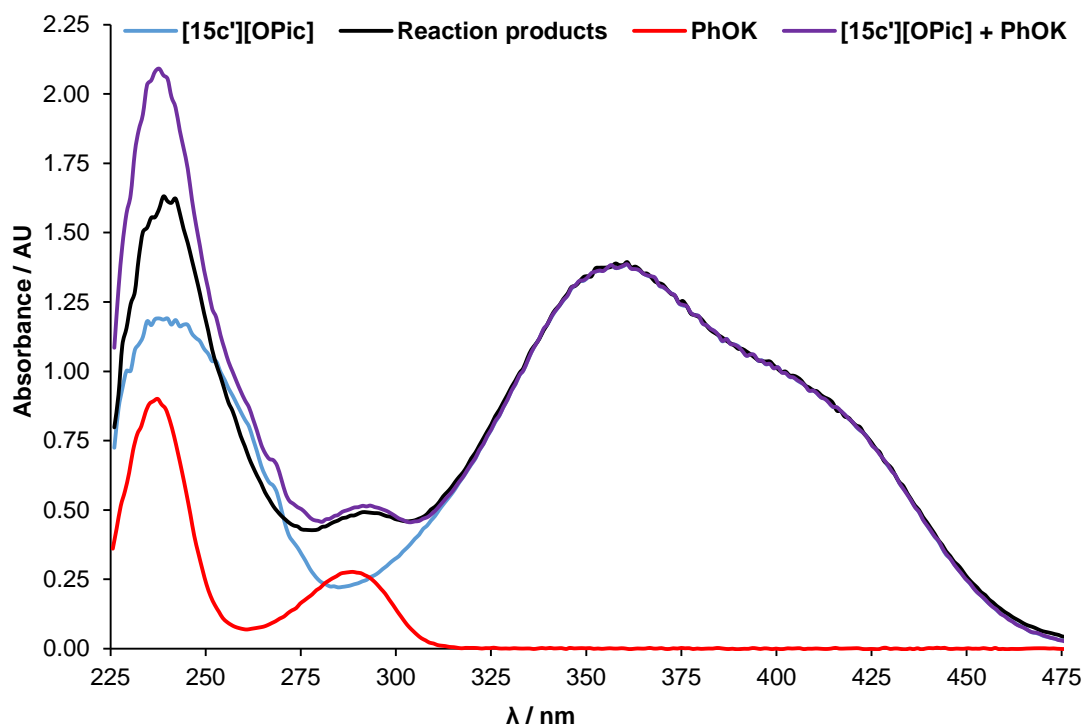


Figure 3.8 Reference UV-Vis spectra recorded at analyte concentrations of 10^{-4} M in solutions of 0.1 M KOH/0.9 M KCl in 3:7 EtOH:H₂O.

These spectra strongly suggested that Suttle and Williams might have misinterpreted their data and had probed the kinetics of isourea solvolysis rather than rearrangement. In order to confirm this, the reaction of **[15c']**[OPic] with KOH was repeated at 10^{-4} M, but on a much larger scale. This allowed for both the reaction kinetics to be measured by UV-Vis spectroscopy and the product mixture to be analysed by ^1H NMR spectroscopy. Again, the kinetic analyses revealed a second order rate constant, $k = 4.40 \times 10^{-3} \text{ M}^{-1} \text{ s}^{-1}$, in good agreement with the published value.²⁰⁷ The ^1H NMR spectrum of the reaction mixture however, enabled the products of **12c'** solvolysis (potassium phenoxide, DIPU and **17**) to be unambiguously identified as the sole products of the reaction.

Suttle and Williams may have been misled into believing that they were monitoring isourea rearrangement by the kinetic parameters they extracted from their data. Both the Brønsted relationship, $\beta_{\text{LG}} = -2.3$, they derived and the entropy of activation, $\Delta S^\ddagger = -13.5 \text{ cal K}^{-1} \text{ mol}^{-1}$, they measured were consistent with the rearrangement reaction. However, the Brønsted relationship they obtained would also be expected to be consistent with isourea solvolysis due to phenoxide acting as a leaving group in this

reaction. The small, negative entropy of activation that was calculated is less well explained by the solvolysis reaction. Indeed, the entropy of activation for the related hydrolysis of *O*-phenyl-*N*-phenyl carbamate has been found to be small and positive, $\Delta S^\ddagger = 5.0 \text{ cal K}^{-1} \text{ mol}^{-1}$.²²⁴ This discrepancy led us to re-examine the calculations which Suttle and Williams performed in order to obtain their value for ΔS^\ddagger . Upon doing so, it appeared that the rate constants that they had used in these calculations were one order of magnitude lower than the rate constants that they had measured. After correcting for this error, the activation parameters for the reaction of **12c'** were recalculated as $\Delta H^\ddagger = 19.4 \text{ kcal mol}^{-1}$ and $\Delta S^\ddagger = -3.4 \text{ cal K}^{-1} \text{ mol}^{-1}$. Although still negative, the recalculated entropy of activation is very small and is much closer to that reported for the hydrolysis of *O*-phenyl-*N*-phenyl carbamate.

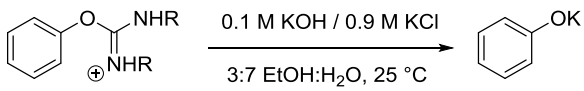
Whilst Suttle and Williams might have easily misinterpreted their kinetic data, it is harder to understand why the HPLC analyses they performed on their reaction mixtures produced false positive results. It appears that the expected product of rearrangement, *N*-phenyl-*N,N'*-diisopropyl urea **13c'**, must have displayed the same retention time as DIPU under the HPLC method they adopted. In addition, phenol must have been consumed or lost prior to, or during, sample preparation.

3.4 Kinetic Analysis of Isourea Salt Solvolysis

3.4.1 Influence of Anion and *N*-Substituent

As [**15c'**][OPic] did not undergo the desired KOH-catalysed Chapman-type rearrangement, focus was placed on gaining a deeper understanding of the unexpected solvolysis pathway. With a procedure for measuring the kinetics of the solvolysis reaction already having been established, the sensitivity of the rate of solvolysis to the identity of the *N*-substituents and the anions present in isourea salts was explored. Using the reaction conditions described in Section 3.3.3, the kinetics of the solvolysis of [**15c'**][OTs] and the trifluoromethanesulfonate salt of *O*-phenyl-*N,N'*-dicyclohexyl isourea [**15b'**][OTf] were measured using UV-Vis spectroscopy. The second order rate constants for these reactions at two different substrate concentrations (10^{-4} and 10^{-5} M) are presented in Table 3.2 alongside those previously detailed for the solvolysis of [**15c'**][OPic].

Table 3.2 Second order rate constants for the KOH-promoted solvolysis of isourea salts 15.^a

<div> <div> <div>[15c'] [OPic] R = <i>i</i>Pr</div> <div>[15c'] [OTs] R = <i>i</i>Pr</div> <div>[15b'] [OTf] R = Cy</div> </div> <div>  </div> </div>		
Substrate	$k \times 10^3 / \text{M}^{-1} \text{s}^{-1}$	
	10^{-5} M^b	10^{-4} M^b
[15c'] [OPic]	4.17 ^c	4.63
[15c'] [OTs]	4.89	4.55 ^c
[15b'] [OTf]	3.93	4.10

^a Calculated by fitting first order exponential equations to kinetic data measured using UV-Vis spectroscopy. ^b [Isourea salt]. ^c Average of three repeats.

Clearly the identity of the *N*-substituents and the anions present in the isourea salts does not have a significant influence on the rate of solvolysis. The majority of the variation in the data is likely attributable to experimental error. The only observation worthy of note is the slightly reduced rates achieved by [15b'] [OTf], which suggests that there might be a minor steric retardation of the solvolysis reaction.

3.4.2 Role of Potassium Hydroxide

So far it has been assumed that the solvolysis reaction is first order in KOH. In order to validate this assumption, kinetic analysis of the solvolysis of [15c'] [OTs] (10^{-4} M) at different KOH concentrations were performed (Figure 3.9).

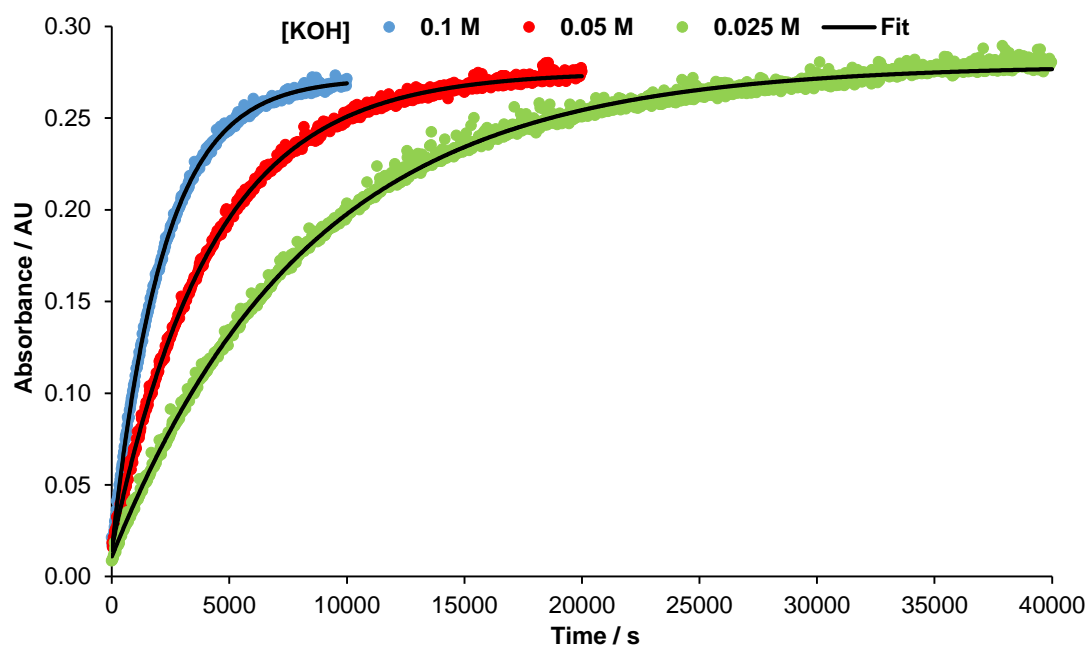


Figure 3.9 Temporal absorbance data (290 nm, 25 °C; coloured circles) for the reaction of [15c']OTs (10^{-4} M) with KOH ([KOH] + [KCl] = 1 M) in 3:7 EtOH:H₂O. First order exponentials were fitted to the data (black lines).

First order rate constants were derived as previously described (Section 3.3.3). A linear relationship was observed between these rate constants and the concentration of KOH, confirming a first order dependence of the reaction rate upon KOH concentration (Figure 3.10).

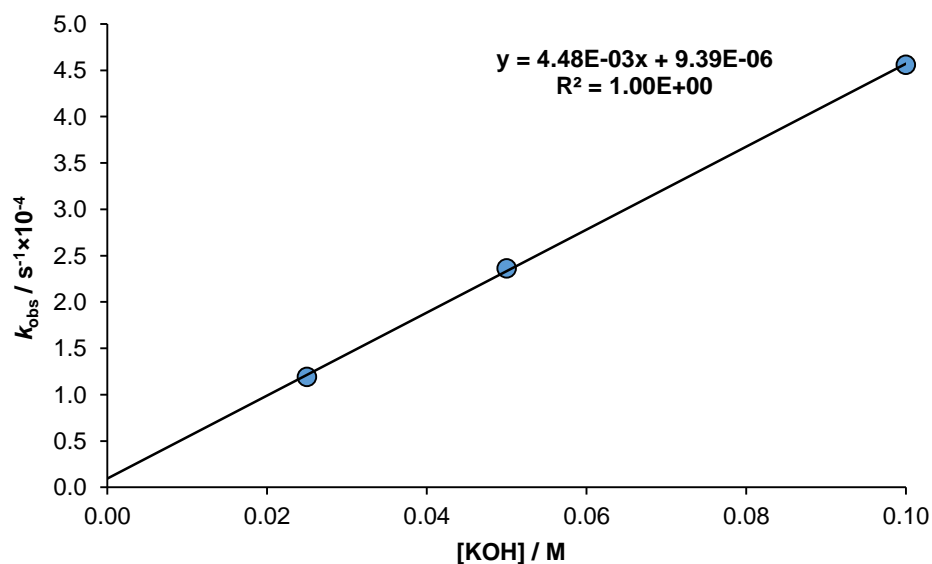
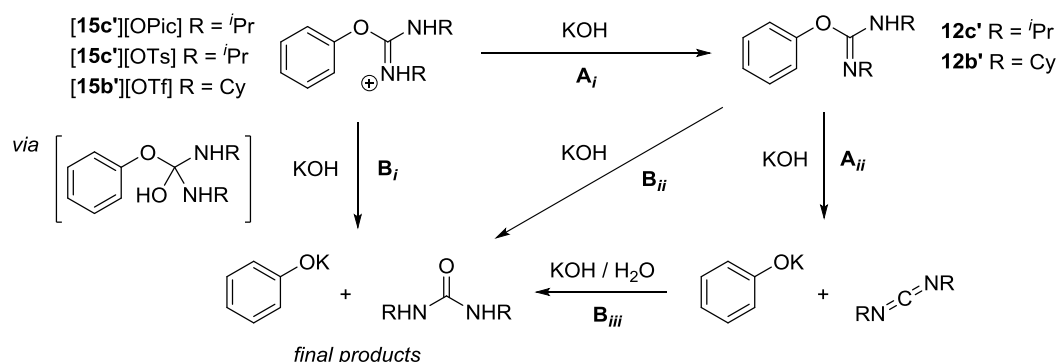


Figure 3.10 Pseudo-first order rate constants for the solvolysis of [15c']OTs as a function of KOH concentration.

The second order rate constant extracted from the gradient of the trend line, $k = 4.48 \times 10^{-3} \text{ M}^{-1} \text{ s}^{-1}$, was in good agreement with that calculated using kinetic data recorded at a single KOH concentration (see Table 3.2). Furthermore, by extrapolation, the rate of solvolysis in the absence of KOH was predicted to be slow, in accordance with observations. Under the pseudo-first order conditions applied (2,500-10,000 eq of KOH), this kinetic data could not be used to distinguish whether KOH had acted as a reagent or catalyst in the reaction. However, it was assumed that two equivalent of KOH were consumed during the reaction (i.e. KOH was acting as a reagent) due to the formation of potassium phenoxide and potassium tosylate.

3.4.3 Mechanism of Isourea Salt Solvolysis

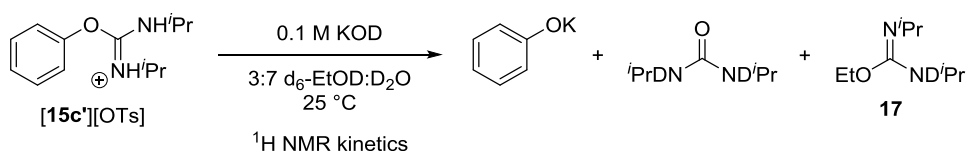
The UV-Vis spectroscopy-derived kinetic data obtained thus far could not be used to differentiate between three plausible pathways for the solvolysis reaction (Scheme 3.18).



Scheme 3.18 Three possible mechanisms for the KOH-mediated hydrolysis of isourea salts **15**. All (A) steps involve hydroxide reacting as a base. All (B) steps involve hydroxide reacting as a nucleophile. The corresponding ethanolysis reactions to form **17** are omitted for clarity.

In the first scenario (pathway B_i), solvolysis is initiated *via* direct nucleophilic attack of hydroxide or ethoxide on the isourea salt **15** (at the quaternary isourea carbon centre to form a tetrahedral intermediate). In the second (pathway A_i + B_{ii}), the isourea salt **15** is deprotonated at nitrogen to liberate the free base of the isourea **12**, which is then subject to nucleophilic attack by hydroxide or ethoxide. The third possibility (pathway A_i + A_{ii} + B_{iii}) involves generating **12** as an intermediate in the same manner as described above, before a second deprotonation causes **12** to eliminate phenoxide and a carbodiimide. The carbodiimide then undergoes hydroxide/ethoxide mediated solvolysis.

The possibility of monitoring the solvolysis of $[15c'']$ [OTs] by ¹H NMR spectroscopy under standard reaction conditions was assessed (Scheme 3.19).



Scheme 3.19 The KOD-mediated solvolysis of $[15c'] [OTs]$ (0.01 M) was monitored by $^1\text{H NMR}$ spectroscopy.

Pleasingly, it was found that potassium phenoxide, DIC, DIPU and **12c'** gave rise to signals which were distinguishable from one another in a 0.1 M solution of KOD in $d_6\text{-EtOD/D}_2\text{O}$. When the solvolysis reaction was investigated under these conditions all of these species were identified at some point, giving some early indication of the mechanism(s) under operation. Although the characteristic signals of some of the species were not available for integration throughout the duration of the reaction, the concentrations of phenoxide and DIC could be tracked accurately (Figure 3.11).

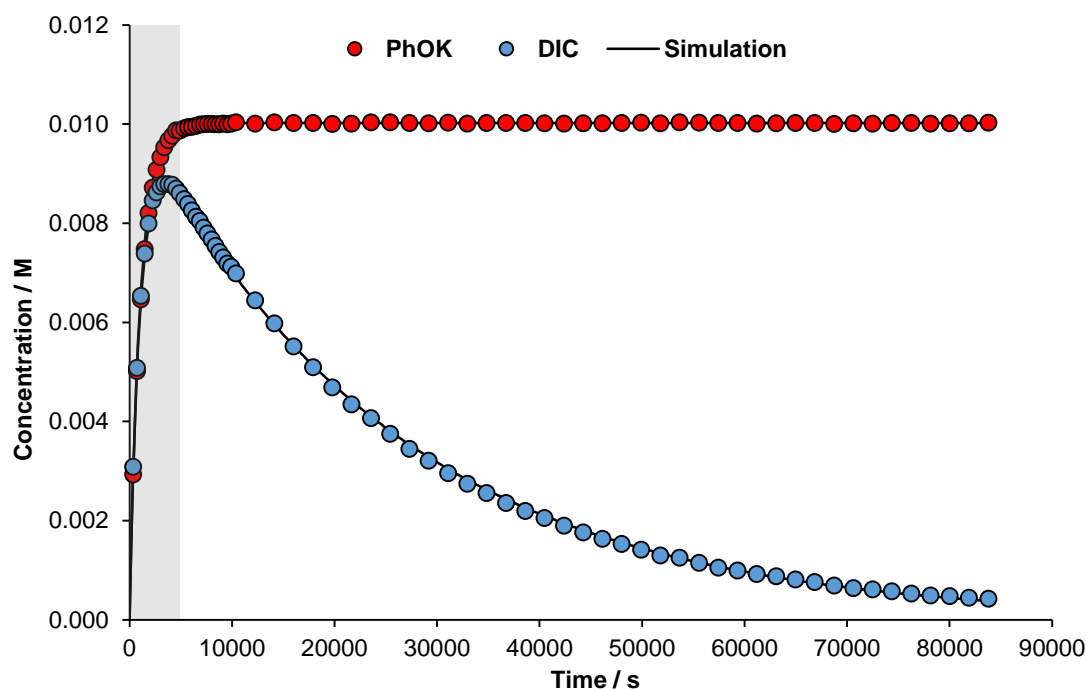


Figure 3.11 $^1\text{H NMR}$ spectroscopy-derived temporal concentration data (25 °C) for the solvolysis of $[15c'] [OTs]$ (0.01 M) in a 3:7 $d_6\text{-EtOD:D}_2\text{O}$ solution of KOD (0.1 M). The grey shaded region is expanded in Figure 3.12.

The absence of separate $^1\text{H NMR}$ signals for $[15c'] [OTs]$ or any change in the chemical shifts observed for **12c'** in the first 10 minutes of the reaction demonstrated that $[15c'] [OTs]$ was deprotonated extremely quickly. Indeed the consumption of $[15c'] [OTs]$ was much faster than phenoxide production, precluding significant reaction flux *via* pathway B_i (Scheme 3.18). In contrast, the formation of substantial quantities of DIC

during the reaction confirmed that pathway $A_i + A_{ii} + B_{iii}$ was operational to some extent. It can be seen that phenoxide and DIC are produced at approximately equal rates in the first phase of the reaction before phenoxide liberation halts due to the complete consumption of **12c'** (Figure 3.12). In the second phase, DIC is consumed in a slower reaction to form DIPU and **17** (Figure 3.11). The partitioning between DIPU and **17** was constant throughout the reaction, with these products being observed to form in a 13:1 ratio.

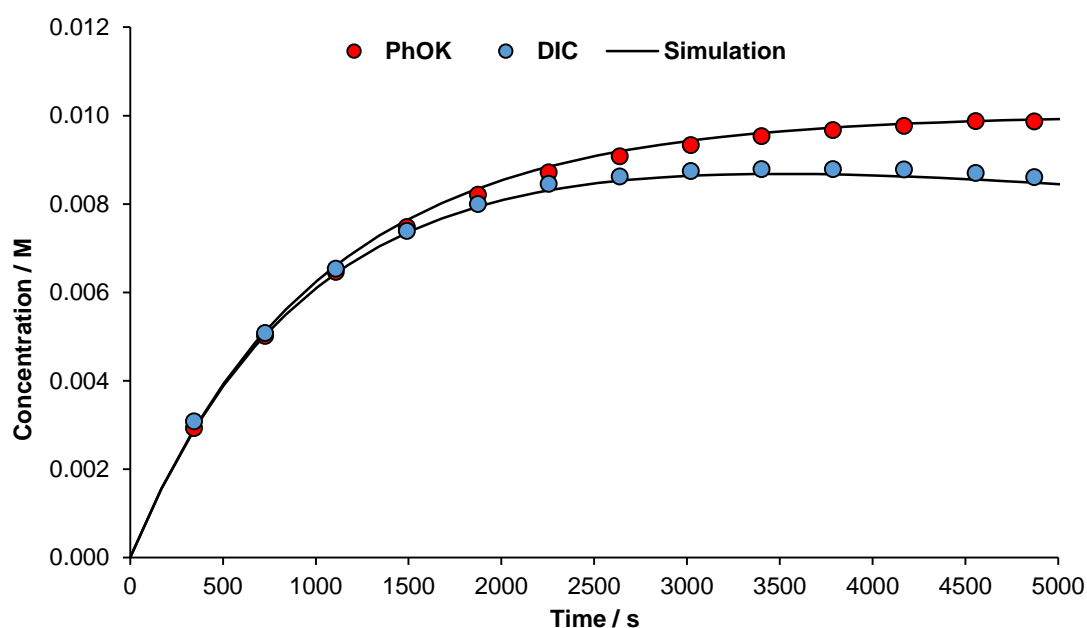
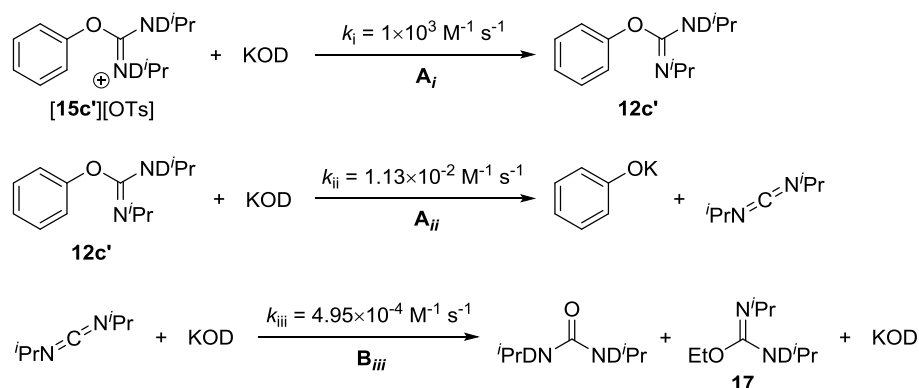


Figure 3.12 An expansion of the grey shaded region in Figure 3.11.

The observation that the maximum intermediate concentration of DIC (8.8×10^{-3} M) approaches the limiting concentration of [**15c'**][OTs] (0.01 M) used in the reaction suggests that there is little or no reaction flux *via* pathway $A_i + B_{ii}$ (Scheme 3.18). In order to further probe the significance of pathway $A_i + A_{ii} + B_{iii}$ in the solvolysis reaction, a kinetic model of this mechanism was built.

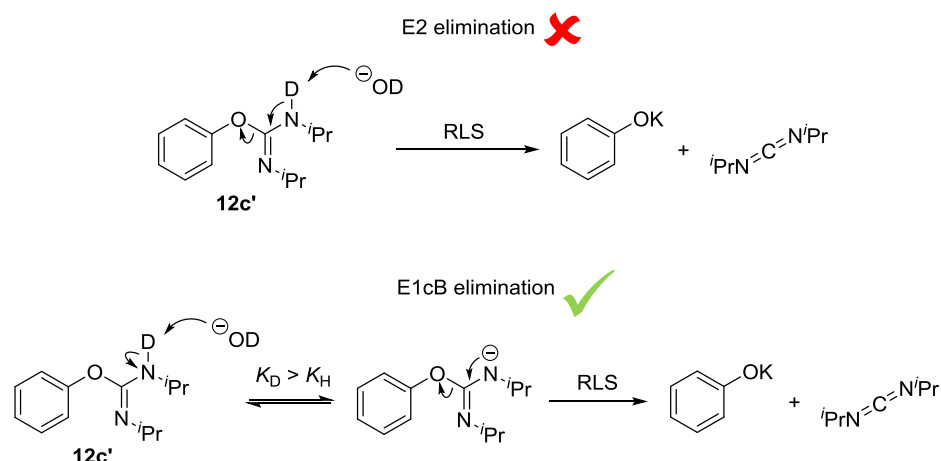
In the model, the mechanism was described using the series of irreversible reactions presented in Scheme 3.20 with the hydrolysis and ethanolysis of DIC being described by a single rate constant for simplicity. Despite being too fast to observe by ^1H NMR kinetics, step *i* was included as it consumes KOD. The rate constant for this reaction, $k_i = 1 \times 10^3 \text{ M}^{-1} \text{ s}^{-1}$, was fixed at an arbitrary, large value. Step *ii* also consumes KOD due to the formation of potassium phenoxide, whilst step *iii*, which formally constitutes the addition of D_2O or $\text{d}_6\text{-EtOD}$ to DIC, is catalysed by KOD. The rate constants for the second and third steps (k_{ii}

and k_{iii} were minimised to fit the data presented in Figure 3.11 and Figure 3.12 using kinetic modeling software. The simulated data is included in these plots (black lines) and the simulated rate constants are included in Scheme 3.20.



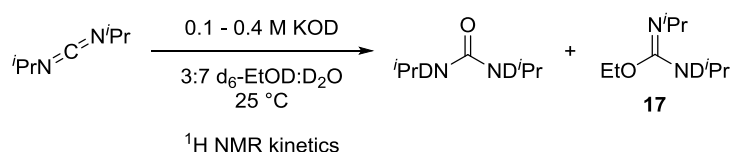
Scheme 3.20 The series of reactions used in a kinetic model describing the solvolysis of **[15c'] [OTs]**.

It was surprising to find that the simulated value for k_{ii} ($1.13 \times 10^{-2} \text{ M}^{-1} \text{ s}^{-1}$) was 2-3 times larger than the value recorded using UV-Vis spectroscopy for the same reaction (e.g. $k = 4.55 \times 10^{-3} \text{ M}^{-1} \text{ s}^{-1}$ when using **[15c'] [OTs]** at 10^{-4} M , Table 3.2). It was therefore speculated that the reaction might be subject to a solvent kinetic isotope effect. In order to test this, the kinetics of **[15c'] [OTs]** solvolysis at 10^{-4} M in deuterated solvents (3:7 d_1 -EtOD: D_2O) were measured by UV-Vis spectroscopy. The second order rate constant extracted from this experiment ($k = 1.18 \times 10^{-2} \text{ M}^{-1} \text{ s}^{-1}$) agrees extremely well with the simulated value, strongly supporting the proposed mechanism. This result also confirmed the manifestation of an inverse solvent kinetic isotope effect of ($k_D/k_H = 2.6$), suggesting that elimination does not proceed *via* an E2 mechanism involving rate-limiting deprotonation of **12c'** (Scheme 3.21). With consideration of the large β_{LG} value (-2.3) measured by Suttle and Williams, it is therefore likely that elimination occurs *via* an E1cB mechanism, in which the expulsion of phenoxide from the aza-anion derived from **12c'** is rate-limiting. In this regime, the inverse solvent isotope effect can be justified by the different equilibrium populations of the aza-anion in KOH/ H_2O and KOD/ D_2O .



Scheme 3.21 Possible mechanisms for the KOD-mediated elimination of phenoxide and DIC from $12c'$. RLS: rate-limiting step.

Next, the legitimacy of the simulated value for k_{iii} was explored. This was achieved by independently monitoring the solvolysis of DIC at a range of KOD concentrations by ^1H NMR spectroscopy, under otherwise identical conditions to those which had been applied to $[15c']$ [OTs] (Scheme 3.22).



Scheme 3.22 The KOD-mediated solvolysis of DIC (0.01 M) was monitored by ^1H NMR spectroscopy.

A linear relationship can be observed between KOD concentration and the measured pseudo-first rate constants (blue data points, Figure 3.13). When plotted alongside these rate constants, the corresponding simulated pseudo-first order rate constant (red data point, Figure 3.13) is within experimental error of the observed trend. Again, this is strong evidence in support of the proposed solvolysis mechanism. The simulated pseudo-first order rate constant ($k_{\text{obs}} = 3.96 \times 10^{-5} \text{ s}^{-1}$) was calculated from the simulated k_{iii} value ($k_{iii} = 4.95 \times 10^{-4} \text{ M}^{-1} \text{ s}^{-1}$) from the mechanistic model by accounting for the concentration of KOD which remains after steps *i* and *ii* (Scheme 3.20).

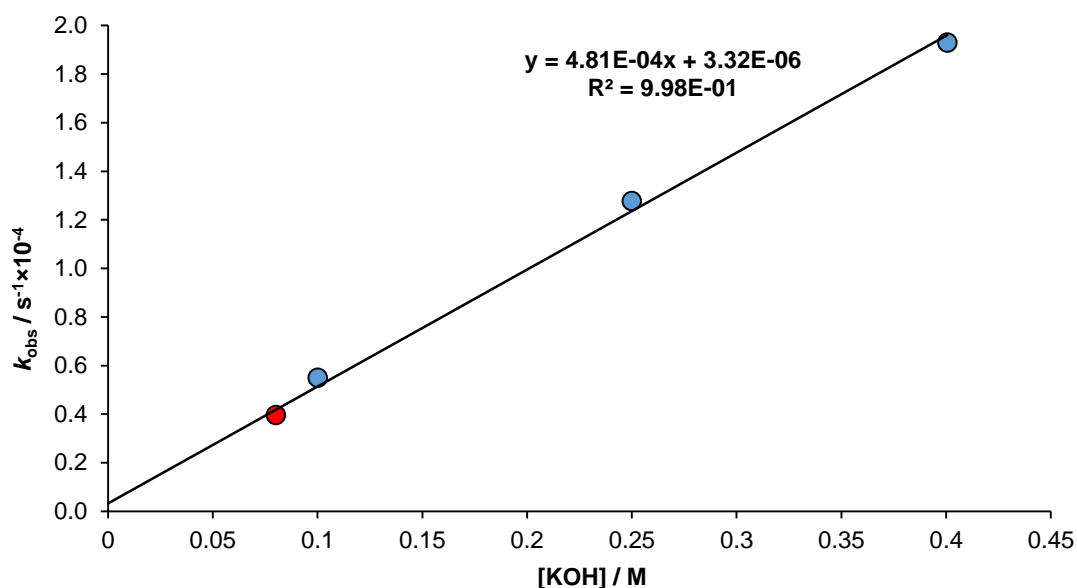


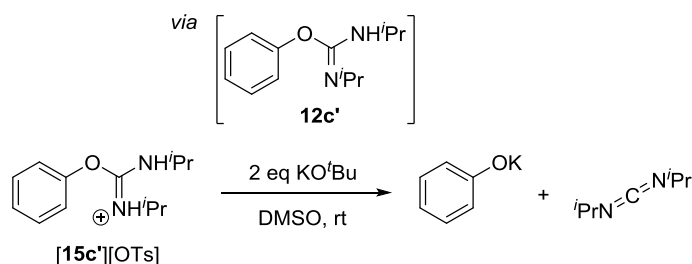
Figure 3.13 Pseudo-first order rate constants for the solvolysis of DIC as a function of KOD concentration.

In summary, the simulated values of k_{ii} and k_{iii} in the proposed mechanistic model map accurately onto the rate constants for the elimination of **12c'** and the solvolysis of DIC which have been measured in isolation. The contribution of any other solvolysis mechanism (i.e. pathway B_i or pathway $A_i + B_{ii}$) towards the overall reaction rate must therefore be extremely small (if present at all).

3.5 Avoiding Isoorea Decomposition

3.5.1 Anhydrous Conditions

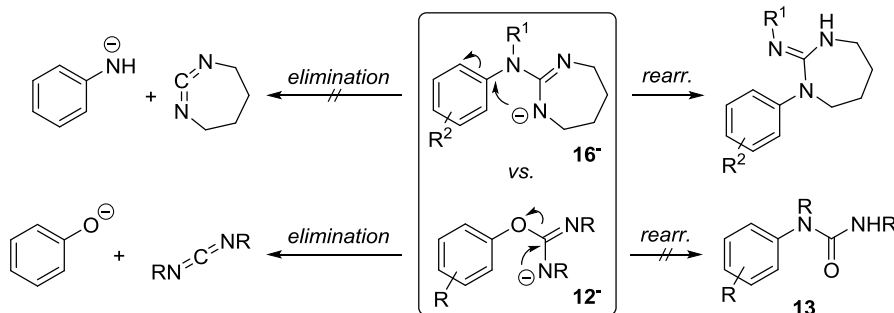
Now confident that the anionic Chapman-type rearrangement of **12c'** did not proceed under the reported conditions, an effort was made to explore related systems which might be more amenable to low temperature, base-catalysed rearrangement. These studies were encouraged by the base-catalysed, room temperature, Chapman-type rearrangement of *N*-aryl guanidines **16** which was introduced in Section 3.1.2 (see Scheme 3.6). This reaction could be performed by reaction of the substrate with catalytic quantities of potassium *tert*-butoxide in anhydrous DMSO.²⁰⁸ It was hoped that applying similar conditions to *O*-aryl isoureas **12** would avoid their solvolysis in favour of anionic rearrangement. Considering the results presented in the previous section, it was not surprising, however, that upon exposing [**15c'**][OTs] to these conditions the products of **12c'** elimination, potassium phenoxide and DIC, were detected (Scheme 3.23). The same outcome was observed when [**15c'**][OTs] was treated with sodium hydride at -78 °C.



Scheme 3.23 The base-mediated elimination of **12c'** to potassium phenoxide and DIC.

3.5.2 *N,N'*-Heterocyclic Isoureas

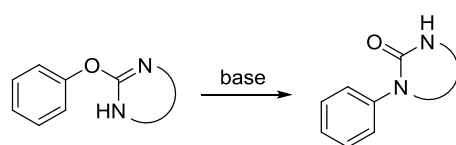
A number of theories were considered to justify why under identical conditions cyclic *N*-aryl guanidines **16** were susceptible to base-catalysed rearrangement whilst *O*-aryl isoureas **12** were not. In both cases, it was presumed that the base could deprotonate the substrate at nitrogen to produce a reactive anion (Scheme 3.24). In the case of **16**, this anion **16⁻** undergoes the desired nucleophilic *ipso*-substitution reaction, whereas with **12**, this anion **12⁻** undergoes elimination faster than nucleophilic attack can occur.



Scheme 3.24 The differing behaviour of cyclic *N*-aryl guanidine anions **16⁻** and *O*-aryl isourea anions **12⁻**.

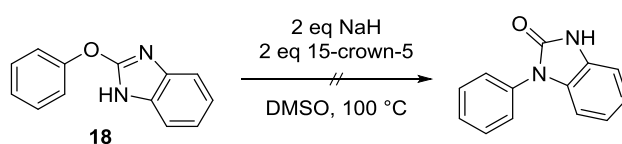
The differing reactivity between the two anions could be explained by the *N*-aryl guanidine anion **16⁻** being more susceptible to rearrangement and/or less susceptible to elimination. Regarding the first of these possibilities, the *N*-aryl guanidines **16** which have been reported to undergo rearrangement were activated towards rearrangement by substitution with electron-withdrawing groups.²⁰⁸ They would therefore, be expected to undergo rearrangement faster than the phenol derived *O*-aryl isoureas **12** considered thus far. The absence of competing elimination reactions in the guanidine system however, would necessitate that rearrangement was significantly faster than elimination. It is unlikely that aryl substituent effects would provide such a large bias as electron-withdrawing groups would also be expected to make the anilide a better leaving

group and accelerate the elimination reaction. Instead, it is proposed that the inherent difference in leaving group ability between anilides and phenoxides has a larger bearing on reactivity. A comparison of the pK_a of phenol²²⁵ and aniline²²⁶ (18.0 and 30.7 respectively, in DMSO) highlights the vast difference in the stability of their conjugate bases. In addition, cyclic *N*-aryl guanidines **16** would have to eliminate severely strained 7-membered ring cyclic carbodiimides, further rendering elimination an unfeasibly high-energy process.²²⁷ As a result of these effects, the *N*-aryl guanidine anion **16**[−] is proposed to be sufficiently stable towards elimination that facile rearrangement can occur. Inspired by the stability of the cyclic guanidine anion, the reactivity of *O*-aryl-*N,N'*-heterocyclic isoureas towards base-catalysed rearrangement was investigated (Scheme 3.25).



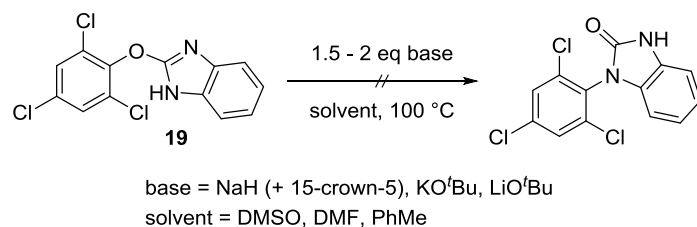
Scheme 3.25 The proposed base-mediated rearrangement of *O*-aryl-*N,N'*-heterocyclic isoureas.

2-Phenoxy benzimidazole **18** was identified as an ideal substrate for these studies, but unfortunately an anionic Chapman-type rearrangement could not be induced, despite the application of forcing conditions (Scheme 3.26). It had been hoped that the use of sodium hydride as a base in combination with 15-crown-5 (a sodium-selective crown ether) would form a particularly reactive, ‘naked’ anion in DMSO; a solvent which is poor at solvating anions. However, even upon heating such mixtures to 100 °C, **18** was recovered unchanged after work-up.



Scheme 3.26 The attempted base-mediated rearrangement of **18**.

Subsequently, attempts were made to further bias the desired rearrangement reaction by adopting 2-(2,4,6-trichlorophenoxy) benzimidazole **19** as the test substrate (Scheme 3.27). In this case, along with the forcing conditions employed above, alternative bases ($KOtBu$ and $LiOtBu$) and reaction solvents (DMF and toluene) were sampled to probe whether different cations or solvent properties might be beneficial to the reaction. However, again, **19** did not rearrange.



Scheme 3.27 The attempted base-mediated rearrangement of **19**.

A plausible hypothesis for the lack of reactivity in the benzimidazole systems is that the planar 5,6-fused ring system lacks the flexibility to enable access to the 4,6-spirocyclic transition state invoked in Chapman-type rearrangements (Figure 3.14).

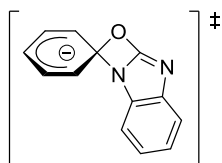


Figure 3.14 The proposed transition state for the anionic Chapman-type rearrangement of **18**.

The 7-membered ring cyclic *N*-aryl guanidines **16** discussed above appear much more accommodating to such a strained transition state ring-system (Figure 3.15). It is revealing that an analogous 6-membered ring cyclic *N*-aryl guanidine was reported to resist rearrangement under typical reaction conditions.²⁰⁷

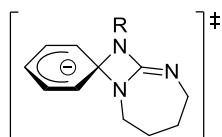
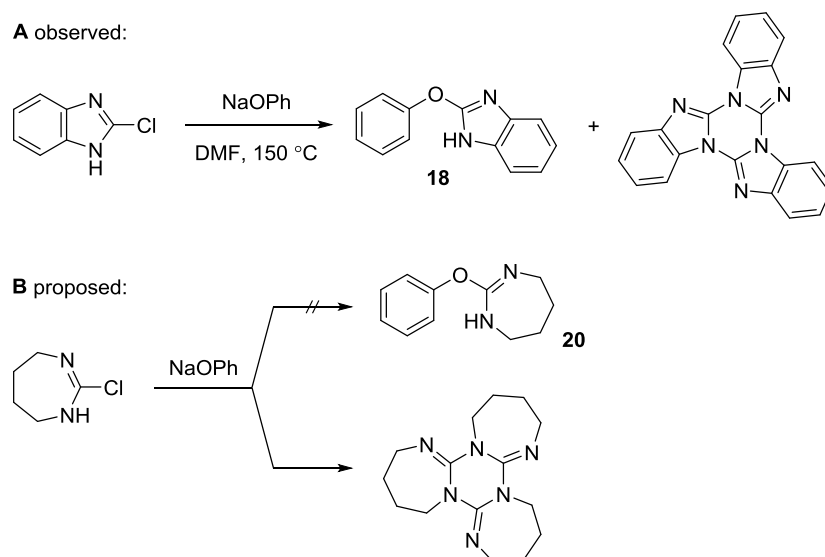


Figure 3.15 The proposed transition state for the anionic Chapman-type rearrangement of **16**.

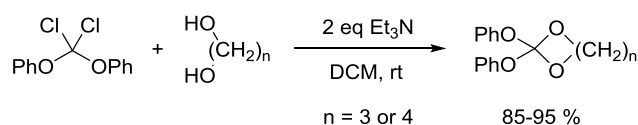
The possibility of developing a 7-membered ring *N,N'*-heterocyclic isourea system was therefore explored, but provided a substantial synthetic challenge. The 2-aryloxy benzimidazoles considered above could be accessed by nucleophilic substitution of 2-chloro benzimidazole with a phenoxide²²⁸ or by condensation of a phenol with dichlorodiphenoxymethane.²²⁹ However, neither of these approaches were suitable for the synthesis of a 2-aryloxy tetrahydro-1,3-diazepine **20**. Lacking aromatic stabilisation, a 2-chloro tetrahydro-1,3-diazepine would likely be susceptible facile self-condensation (reaction B, Scheme 3.28) and would be extremely difficult to synthesise and purify.²³⁰ Indeed, even 2-chloro benzimidazole was observed to self-condense to afford a

reasonable quantity of a triazine side-product under the conditions required to induce its reaction with phenoxides (reaction A, Scheme 3.28).²²⁸



Scheme 3.28 The self-condensation of 2-chloro benzimidazole (observed) and 2-chloro tetrahydro-1,3-diazepine (proposed).

A report detailing the successful synthesis of 6- and 7-membered ring cyclic orthocarbonates by reacting diols with dichlorodiphenoxymethane gave some promise to the potential preparation of 2-aryloxy tetrahydro-1,3-diazepines **20** using the same reagent (Scheme 3.29).²³¹



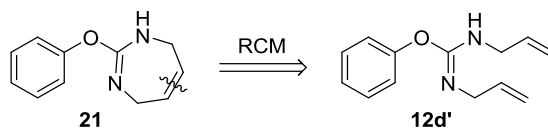
Scheme 3.29 The condensation of dichlorodiphenoxymethane with diols affords cyclic orthocarbonates.

Unfortunately, when this theory was tested by the treatment of dichlorodiphenoxymethane with either ethylenediamine or 1,3-diaminopropane in the presence of triethylamine, the desired cyclic isoureas could not be detected (Scheme 3.30).



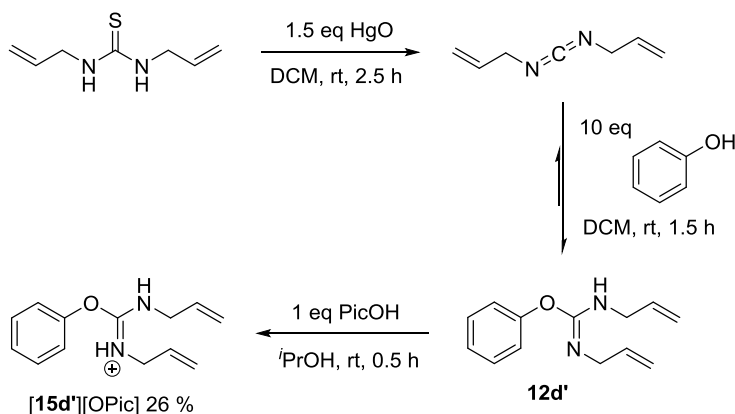
Scheme 3.30 The attempted synthesis of O-phenyl-*N,N'*-heterocyclic isoureas from dichlorodiphenoxymethane and diaminoalkanes.

Subsequently, it was proposed that 2-phenoxy 4,7-dihydro-1,3-diazepine **21** might be formed by inducing the ring-closing metathesis (RCM) of *O*-phenyl-*N,N'*-diallyl isourea **12d'** (Scheme 3.31). It was hoped that the synthesis of **12d'** would be facilitated by the knowledge gained in Section 3.2.



Scheme 3.31 The proposed strategy for preparing 2-phenoxy 4,7-dihydro-1,3-diazepine **21**.

The first challenge encountered upon exploring the viability of this route was the severe instability of diallyl carbodiimide which was required for the preparation of **12d'**. Carbodiimides with *N*-substituents containing unsaturation and/or which lack branching in the α -position are particularly susceptible to spontaneous polymerisation reactions.^{232,233} Diallyl carbodiimide was prepared by the treatment of diallyl thiourea with an excess of mercury(II) oxide (Scheme 3.32). Although the reaction proceeded to completion, the carbodiimide could not be isolated by distillation (as is typical) without initiating polymerisation.²³⁴ Instead, the reaction mixture was filtered to remove mercury-containing particulates, concentrated *in vacuo* and then directly reacted with a two-fold excess of phenol at 100 °C. Again the undesired polymerisation of the carbodiimide was promoted.

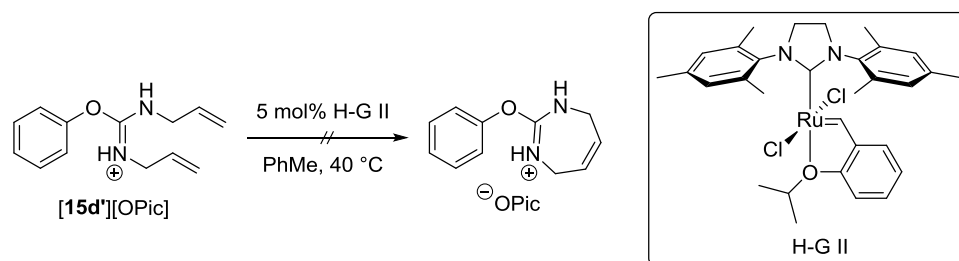


Scheme 3.32 The synthetic route used to prepare **[15d'] [OPic]**.

It was shown previously that the reaction of phenol with carbodiimides at room temperature is extremely slow (Section 3.2.4), however, the addition of a ten-fold excess of phenol to a crude solution of the carbodiimide allowed the reaction to proceed to completion within 1 hour (Scheme 3.32). The excess phenol was removed *via* filtration

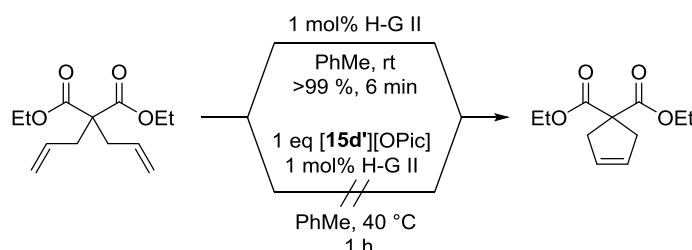
of the reaction mixture through a silica-gel column (Section 3.2.3), but the crude **12d'** thus obtained was observed to undergo extremely rapid decomposition. Attempted salt formation with sulfonic acids was therefore accompanied by the generation of inseparable contaminants. Crystallisation of the picric acid salt of the isourea **[15d']**[OPic] from a 2-propanol solution however, allowed for the troublesome impurities to be separated (Scheme 3.32).

The attempted RCM of **[15d']**[OPic] using the 2nd generation Hoveyda-Grubbs catalyst under typical conditions was unsuccessful (Scheme 3.33).



Scheme 3.33 The attempted RCM of **[15d']**[OPic] using the 2nd generation Hoveyda-Grubbs catalyst (H-G II).

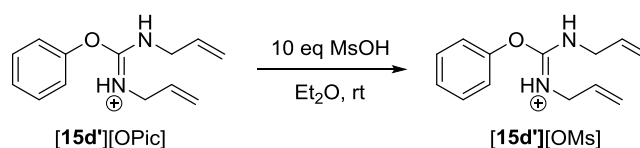
It was hypothesised that the picrate anion could be poisoning the ruthenium-based catalyst.^{235,236} To probe this, the well-precidentated RCM reaction of diethyl diallylmalonate was performed in the presence and absence of **[15d']**[OPic] (Scheme 3.34). Clearly the addition of **[15d']**[OPic] inhibited the reaction.



Scheme 3.34 The RCM of diethyl diallylmalonate in the presence and absence of **[15d']**[OPic]. See Scheme 3.33 for the structure of H-G II.

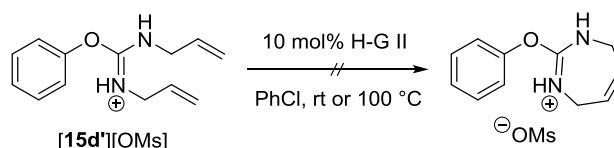
In order to alleviate the issue, the possibility of exchanging the picrate anion for a less-coordinating sulfonate anion was explored. Metathesis substrates containing basic nitrogen atoms which interfere with catalysts are often protected by protonation with sulfonic acids prior to reaction.^{237–239} A protocol for converting **[15d']**[OPic] to the corresponding methanesulfonic acid salt **[15d']**[OMs] was therefore developed (Scheme 3.35). The procedure relied upon the lower solubility of **[15d']**[OMs] than picric acid in

diethyl ether, as this enabled picric acid to be removed from the reaction mixture *via* trituration.



Scheme 3.35 The anion exchange reaction used to generate [15d'] [OMs] from [15d'] [OPic].

Unfortunately, [15d'] [OMs] also did not undergo the desired RCM reaction under the conditions evaluated (Scheme 3.36). This suggested that the protonated isourea **15d'**, rather than the picrate anion, may have been responsible for the observed catalyst inhibition.



Scheme 3.36 The attempted RCM of [15d'] [OMs]. See Scheme 3.33 for the structure of H-G II.

It is possible that *O*-phenyl-*N,N'*-diallyl isourea salts **15d'** are capable forming unreactive chelate complexes with the catalyst (Figure 3.16).^{240,241}

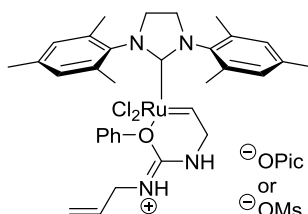


Figure 3.16 The ruthenacycle which is proposed to form upon treatment of *O*-phenyl-*N,N'*-diallyl isourea salts **15d'** with H-G II.

3.6 Summary and Conclusions

The previously documented KOH-catalysed Chapman-type rearrangement of *O*-aryl-*N,N'*-diisopropyl isoureas **12c** has been disproven. Instead, under the reported conditions, the solvolysis of *O*-aryl isourea salts **15** was identified and shown to be the subject of the previously misinterpreted mechanistic investigation. The identity of the *N*-substituents and anions in *O*-phenyl isourea salts **15** were shown to have little influence on the rate of solvolysis and the reaction was demonstrated to have a first order

dependence upon the concentration of the isourea **12** and hydroxide. In addition, experimental and simulated kinetic data have suggested that solvolysis proceeds *via* a base-promoted elimination reaction in which the isourea **12** expels potassium phenoxide and a carbodiimide. Subsequently, the carbodiimide is proposed to undergo a base-catalysed solvolysis reaction to form the corresponding urea.

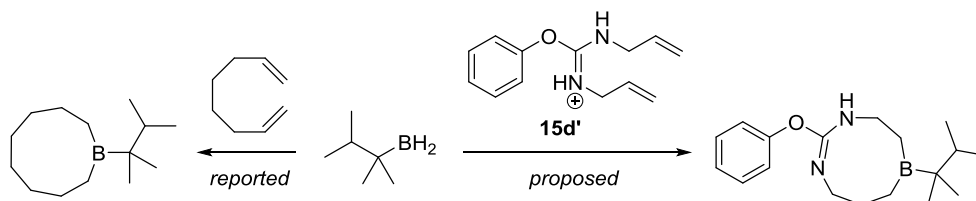
Enabling the kinetic investigation was the development of an improved, robust procedure for accessing *O*-aryl-*N,N'*-dialkyl isourea salts. As part of this study, a deeper understanding of the reaction between phenol and DIC to form *O*-phenyl-*N,N'*-diisopropyl isourea **12c'** was also pursued. It was found that this reaction was inhibited by **12c'** due to its relatively high basicity.

Numerous attempts were made to identify alternative, non-aqueous reaction conditions which would allow the low temperature, base-catalysed Chapman-type rearrangement of an isourea-type substrate to be observed. This investigation focused on inducing the rearrangement of isoureas in which the two nitrogen atoms were contained within a heterocyclic ring. Such structures were predicted to be less susceptible to undesirable base-promoted elimination reactions. Unfortunately, the rearrangement of 2-aryloxy benzimidazoles **18** and **19** which contained 5-membered ring *N,N'*-heterocyclic systems could not be induced, whilst substrates containing 7-membered ring *N,N'*-heterocyclic systems could not be prepared.

3.7 Future Work

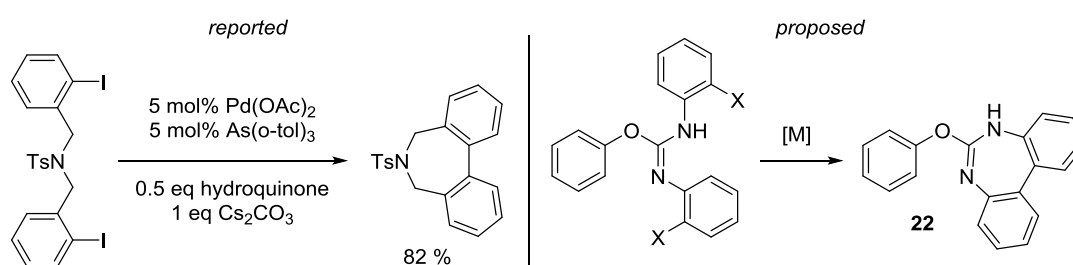
Despite the issues encountered, the development of an isourea system capable of undergoing a low temperature, base-catalysed Chapman-type rearrangement is still an enticing goal. Although the rearrangement of the 2-aryloxy benzimidazoles **18** and **19** was not achieved, their tolerance of the strongly basic reaction conditions offered promise. Given the ability of 7-membered ring cyclic guanidines **16** to rearrange, further investigation into the synthesis of isourea analogues in which the nitrogen atoms form part of a larger *N,N'*-heterocyclic ring would be worthwhile. Towards this goal, it is plausible that *O*-phenyl-*N,N'*-diallyl isourea salts **15d'** could undergo two sequential anti-Markovnikov hydroboration reactions with a mono-alkyl borane (e.g. thexyl borane) to form a 9-membered ring cyclic isourea (Scheme 3.37). The analogous reaction using 1,7-octadiene has previously been reported.²⁴² Although 9-membered ring cyclic carbodiimides are significantly more stable than their 7-membered ring analogues, the

ring-strain present in these structures might still render 9-membered ring cyclic isoureas stable to base-mediated elimination.²²⁷



Scheme 3.37 The reactions of thexyl borane with dienes to form cyclic trialkyl borane structures.

Alternatively, the preparation of an *O*-phenyl-*N,N'*-diaryl isourea containing *ortho*-halogen aromatic substituents might enable a 2-phenoxy dibenzo-1,3-diazepine **22** to be generated in an intramolecular, transition metal promoted aromatic homocoupling reaction (Scheme 3.38). Such *N*-substituents should tolerate the multi-step isourea synthesis well. Similar reductive homocoupling reactions to form 7-membered ring nitrogen heterocycles have been achieved using palladium catalysis.²⁴³



Scheme 3.38 Intramolecular, transition metal-mediated homocoupling reactions for the synthesis of nitrogen heterocycles.

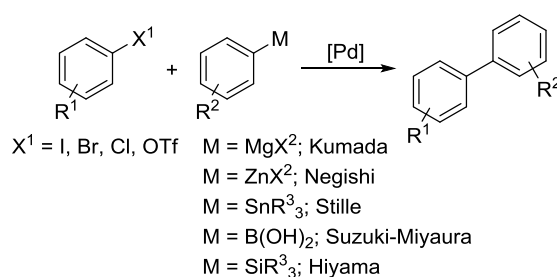
Future attempts to synthesise and isolate *O*-phenyl-*N,N'*-diaryl isoureas would benefit from a more thorough mechanistic understanding of the reactions between phenols and diaryl carbodiimides. It would also be interesting to compare the results of such a study to those acquired for the reactions of phenols with dialkyl carbodiimides as discussed in Sections 3.2.4 and 3.2.5. Finally, detailed investigations into the use of copper halide salts as catalysts for these reactions might render them more efficient and synthetically viable.

4 O-Aryl Thiocarbamates in Palladium-Catalysed Coupling Reactions

4.1 *O*-Aryl Thiocarbamates as Electrophiles in Palladium-Catalysed Cross-Coupling Reactions

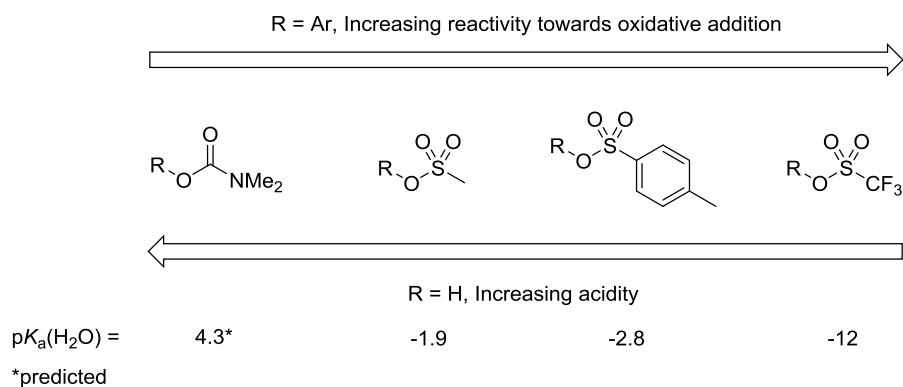
4.1.1 Introduction and Concept

Palladium(0)-catalysed cross-coupling reactions of aryl (pseudo)halides to form new C_{Ar}-C, C_{Ar}-N, C_{Ar}-O and C_{Ar}-S bonds have now been established as some of the most valuable and versatile synthetic methods.¹⁵¹ Particular success has been achieved in the palladium(0)-catalysed reaction of aryl (pseudo)halides with aryl nucleophiles to form biaryls (Scheme 4.1), which can be found in a vast number of functional and biologically active molecules (e.g. the antibiotic vancomycin).^{244,245}



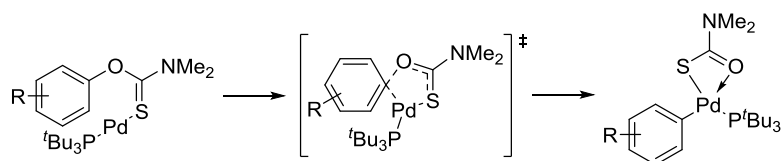
Scheme 4.1 Palladium(0) catalysed cross-coupling reactions to form biaryls.

Despite the vast amount of work which has been conducted in this field, the only class of phenol-derived pseudohalides which have, thus far, been found to be compatible with palladium(0)-catalysed cross-coupling reactions are the *O*-aryl sulfonates.⁵⁹ As discussed in Section 1.2, this observation reflects of the reluctance of strong C_{Ar}-O bonds to undergo oxidative addition reactions. Indeed, even *O*-aryl mesylates and *O*-aryl tosylates, which are some of the most activated phenol-derived electrophiles, typically require the use of harsh conditions or designer ligands to promote the oxidative addition step (Sections 1.1.2 and 1.2).^{19,23} The susceptibility of the *O*-aryl thiocarbamate **23** substrates of the NKR towards the oxidative addition of palladium(0) is therefore unexpected (Section 1.3.2).¹¹⁸ The reactivity of phenol-derived pseudohalides towards oxidative addition tends to increase as the p*K*_a of the corresponding leaving group decreases (here, it is likely that p*K*_a is acting as a proxy for bond strength; Scheme 4.2).²²



Scheme 4.2 The trend between the acidity of $\text{C}_{\text{Ar}}\text{-O}$ leaving groups and the reactivity of phenol-derived electrophiles towards oxidative addition.

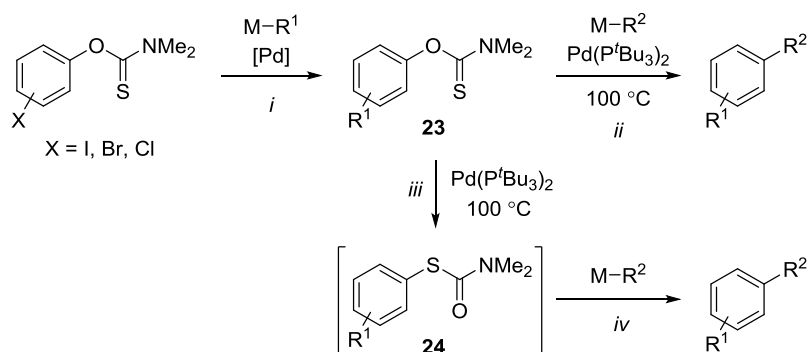
The $\text{p}K_{\text{a}}$ of *N,N*-dimethylthiocarbamic acid would be expected to be similar to that of *N,N*-dimethylcarbamic acid²⁴⁶ and significantly higher than that of any of the sulfonic acids.^{247,248} Typically, however, *O*-aryl carbamates are inert towards the oxidative addition of palladium(0) catalysts, whilst *O*-aryl thiocarbamates **23** are not.⁸¹ This suggests that the thiocarbonyl group may play a crucial role in aiding the oxidative addition reaction. As alluded to in Section 1.3.2, it is hypothesised that the thiocarbonyl group coordinates to palladium(0) catalysts and directs them towards the $\text{C}_{\text{Ar}}\text{-O}$ bond, thus providing a kinetic bias towards oxidative addition (Scheme 4.3).¹¹⁸



Scheme 4.3 The oxidative addition of palladium(0) to the $\text{C}_{\text{Ar}}\text{-O}$ bond of *O*-aryl thiocarbamates **23**.

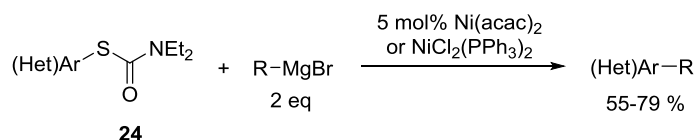
It was envisioned that the ability of palladium(0) catalysts to activate *O*-aryl thiocarbamates **23** could be exploited in $\text{C}_{\text{Ar}}\text{-C}$ bond-forming cross-coupling reactions (step *ii*, Scheme 4.4). Advantageously, *O*-aryl *N,N*-dimethylthiocarbamates are cheaper to synthesise than aryl triflates and are convenient to handle due to their high crystallinity.¹⁰⁶ Furthermore, as the palladium(0)-catalysed NKR could only be realised using a very narrow series of phosphine ligands,¹¹⁷ it was proposed that *O*-aryl thiocarbamates **23** would display orthogonal reactivity to traditional aryl (pseudo)halide coupling partners which can be coupled using a wide range of catalysis.²⁴⁵ If this was found to be the case, substrates containing both (pseudo)halide and thiocarbamate leaving groups could be subjected to iterative cross-coupling

reactions (steps *i* and *ii*, Scheme 4.4). Although the reluctance of *O*-aryl thiocarbamates **23** to undergo oxidative addition would be beneficial in this respect, it was also recognised that the high temperatures required to achieve C_{Ar}-O bond activation might somewhat limit their utility.



Scheme 4.4 The proposed palladium(0)-catalysed cross-coupling of *O*-aryl thiocarbamates **23**.

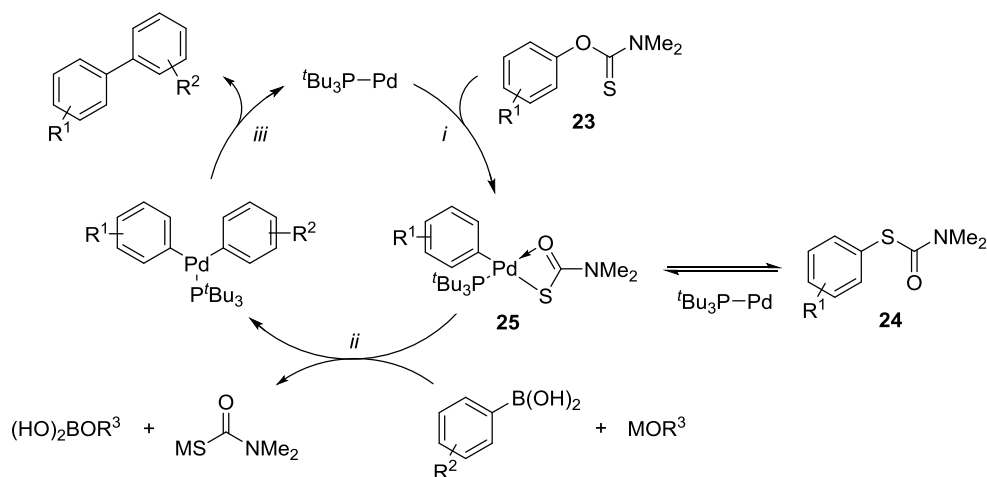
Despite the use of high temperatures, the rearrangement of *O*-aryl thiocarbamates **23** to *S*-aryl thiocarbamates **24** (step *iii*, Scheme 4.4) was not expected to interfere with the proposed coupling reaction as it was hypothesised that *S*-aryl thiocarbamates **24** would also act as competent aryl electrophiles (step *iv*). Supporting this, *S*-aryl thiocarbamates **24** have been shown to undergo reversible oxidative addition to palladium(0) at room temperature (Section 1.3.2)¹¹⁷ and have been successfully coupled with Grignard reagents *via* nickel(0) catalysis (Scheme 4.5).^{58,249}



Scheme 4.5 The nickel(0)-catalysed cross-coupling of *S*-aryl thiocarbamates **24** with Grignard reagents.

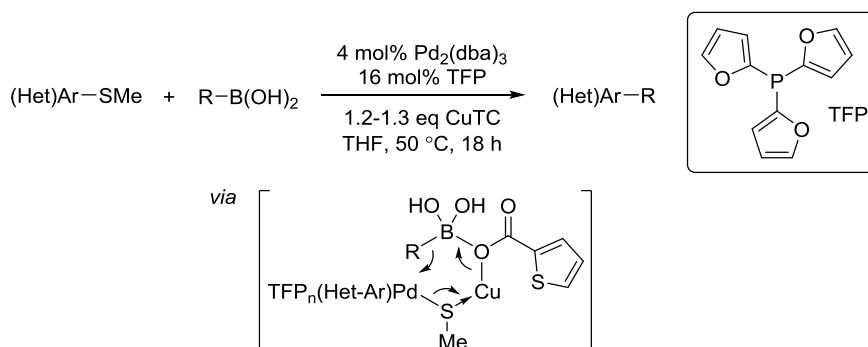
4.1.2 Attempted Cross-Coupling Reactions Using Boronic Acids

In general, the boronic acids used in the Suzuki-Miyaura reaction (Scheme 4.1) are more stable, more readily available and less toxic than the organometallic nucleophiles employed in alternative cross-coupling reactions (e.g. Grignard reagents and organostannanes). Their low intrinsic nucleophilicity of also renders the Suzuki-Miyaura reaction particularly functional group tolerant.²⁵⁰ Initial studies into the use of *O*-aryl thiocarbamates **23** as C_{Ar}-O pseudohalides therefore focused on achieving their coupling with arylboronic acids (Scheme 4.6).



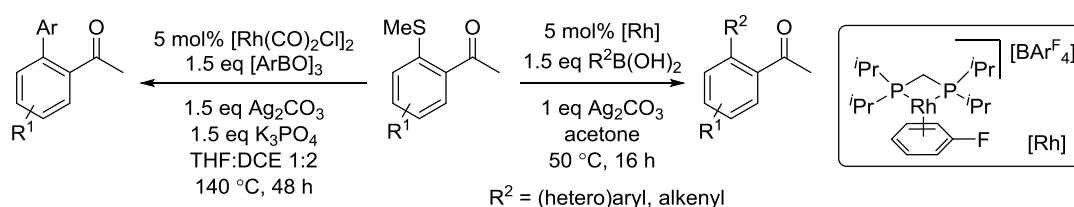
Scheme 4.6 Proposed catalytic cycle for the palladium(0)-catalysed coupling of *O*-aryl thiocarbamates **23** with arylboronic acids.

It was hypothesised that successful transmetalation between the boronic acid and the palladium(II) product of aryl thiocarbamate oxidative addition **25** would be the key obstacle to achieving productive turnover (step *ii*, Scheme 4.6). In general, there is a strong soft-soft interaction between palladium and organosulfur species and thus the displacement of the thiocarbamate anion from **25** was expected to be particularly difficult. A similar issue has been observed in the related Liebeskind-Srogl coupling of electron-deficient heteroaryl methyl sulfides with boronic acids and was overcome by the addition of stoichiometric quantities of copper(I) thiophene-2-carboxylate (CuTC). CuTC aids the difficult transmetalation step by activating both the methylthiolate leaving group and the boronic acid (Scheme 4.7).²⁵¹



Scheme 4.7 The Liebeskind-Srogl cross-coupling of heteroaryl methyl sulfides.

Silver(I) carbonate fulfils a similar role (acting as both a thiophilic scavenger and a base) in the rhodium(I)-catalysed coupling of aryl methyl thioethers with boronic acids and boroxines (Scheme 4.8).²⁵²



Scheme 4.8 Protocols for the rhodium(I)-catalysed cross-coupling of aryl methyl sulfides with boronic acids.

With these reactions in mind, catalytic quantities of CuTC were applied alongside $\text{Pd}(\text{P}^t\text{Bu}_3)_2$ and three different bases in the initial attempts to cross-couple *O*-(4-trifluoromethylphenyl)-*N,N*-dimethyl thiocarbamate **23a** with 4-fluorophenylboronic acid at 100 °C (Table 4.1). The use of these substrates allowed for reactions to be conveniently analysed using ^{19}F NMR spectroscopy.

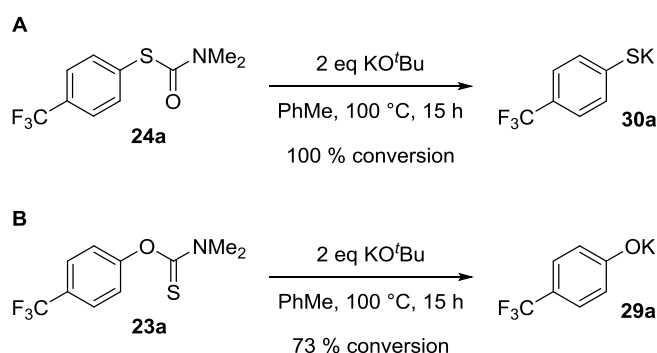
Table 4.1 Screen of bases in the attempted palladium(0)-catalysed cross-coupling of **23a** with 4-fluorophenylboronic acid. ^a

Base	Total recovery from 23a / % ^{b,c}	Conv. / % ^b				
		26	24a	27	28a	23a
KO ^t Bu	61	14	< 1	4	34	< 1
K ₂ CO ₃	119	1	12	2	29	66
KF	113	2	16	1	35	52

^a 0.25 mmol scale, 0.25 M. ^b Determined by ^{19}F NMR spectroscopy using a 1-fluoronaphthalene internal standard. ^c Calculated by summing all CF₃-containing species detected in the ^{19}F NMR spectrum.

Out of the three bases trialled, only potassium *tert*-butoxide enabled appreciable quantities (14 %) of the desired biaryl **26** to be obtained. However, the use of potassium *tert*-butoxide also resulted in the lowest total recovery of **23a**-derived products. In order to explain the latter, it was deduced that insoluble side-products had been lost by filtration of the reaction mixture prior to analysis. The major insoluble side-products were tentatively identified as potassium 4-trifluoromethylphenoxide **29a** and potassium 4-trifluoromethylphenylthiolate **30a** after these species were detected in similar

reaction mixtures following acidic work-up. The formation of these species was justified by considering that the base-mediated cleavage of **23a** and *S*-(4-trifluoromethylphenyl)-*N,N*-dimethyl thiocarbamate **24a** might occur under the reaction conditions. Evidence in support of this theory was subsequently obtained by treating **23a** and **24a** with potassium *tert*-butoxide at 100 °C in the absence of palladium (Scheme 4.9). After 3 hours, **24a** was found to have been completely cleaved (determined by ¹⁹F NMR spectroscopy; reaction A) whilst after 15 hours, 73 % of **23a** had been cleaved (reaction B). As a result, these reactions also served to highlight the higher stability of *O*-aryl thiocarbamates **23** relative to their *S*-aryl thiocarbamate **24** counterparts.



Scheme 4.9 The cleavage of **23a** and **24a** upon reaction with potassium *tert*-butoxide.

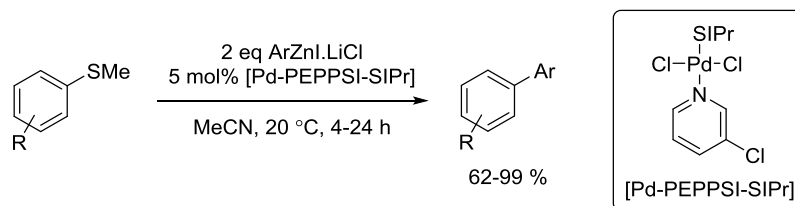
Less degradation of **23a** was observed when potassium carbonate or potassium fluoride were employed, although it was clear that the recoveries from these reactions had exceeded the theoretical maxima. In order to account for these observations, it was proposed that a significant quantity of the 1-fluoronaphthalene (b.p.: 215 °C) internal standard had been lost during work-up and most likely, upon the removal of toluene (b.p.: 110 °C) *in vacuo*. All of the conversions detailed in Table 4.1 should therefore be regarded as over-estimates.

Surprisingly, a significant quantity of bis(4-trifluoromethylphenyl)sulfide **28a** was produced in all of the attempted coupling reactions (*vide infra*, Section 4.2).

4.1.3 Attempted Cross-Coupling Reactions Using Arylzinc Reagents

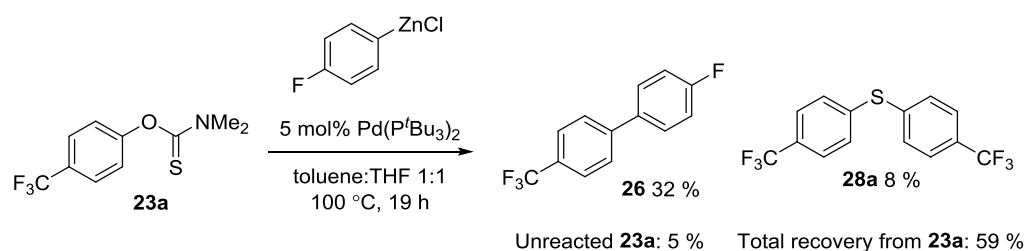
It was proposed that the use of a more reactive nucleophilic coupling partner might allow the desired C_{Ar}-C cross-coupling reaction to more effectively compete with substrate decomposition. The use of arylzinc reagents which display high reactivity in transmetallation reactions and also exhibit good functional group compatibility was therefore investigated.²⁵³ Lending promise to this approach, arylzinc reagents have been

reported to successfully couple with (hetero)aryl methyl sulfides *via* palladium catalysis (Scheme 4.10),^{254,255} with the high thiophilicity of zinc being suggested to enable the transmetallation step.^{251,256}



Scheme 4.10 The palladium(0)-catalysed coupling of aryl methyl sulfides with arylzinc reagents.

The coupling of **23a** with 4-fluorophenylzinc chloride (freshly prepared as a THF solution) was attempted under similar conditions to those sampled when applying 4-fluorophenylboronic acid (Scheme 4.11). However, to address the problems encountered previously, the 1-fluoronaphthalene ¹⁹F NMR internal standard was added after the removal of toluene *in vacuo*.



Scheme 4.11 The attempted palladium(0)-catalysed coupling of **23a** with 4-fluorophenylzinc chloride.

It was promising that a higher proportion of cross-coupled product was produced than had been achieved using 4-fluorophenylboronic acid (Table 4.1), however, **28a** was formed and the recovery of **23a**-derived species was low.

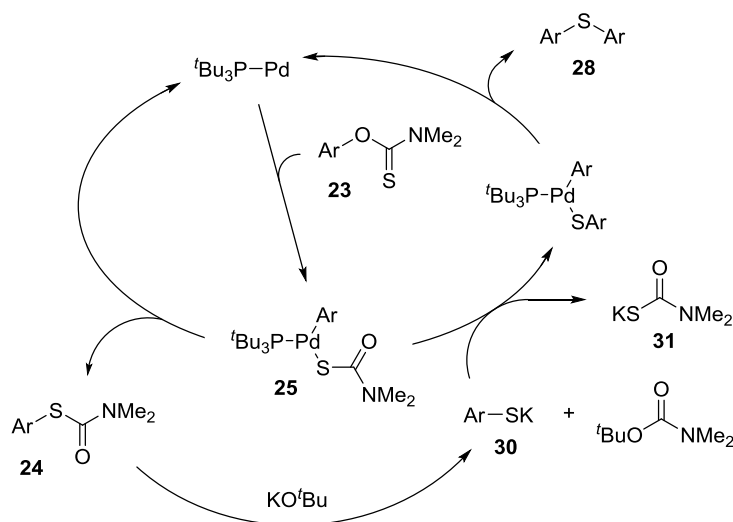
At this point the formation of **28a** from **23a** *via* palladium(0) catalysis was considered in detail with the intention of exploiting this phenomenon and developing novel synthetic route for the preparation of diaryl thioethers.

4.2 Synthesis of Diaryl Thioethers *via* Palladium-Catalysed Cross-Coupling Reactions

4.2.1 Introduction and Concept

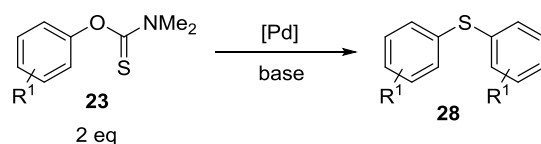
Diaryl thioethers, and their diaryl sulfoxide and sulfone derivatives, are essential structural components of pharmaceutical agents with the potential to treat cancer,^{257–259} human immunodeficiency virus (HIV),^{260,261} Alzheimer's disease^{262,263} and Parkinson's disease²⁶⁴. Diaryl thioether and sulfone linkages are also commonly found in functional, polymeric materials.^{265–267} However, whilst the diaryl thioethers and sulfones used as monomers in the production of polymeric materials are often symmetrical, those which are encountered in biologically active compounds tend to be unsymmetrical.

The observation that **28a** was produced upon attempting to cross-couple **23a** suggested that it might be possible to develop a protocol for accessing symmetrical diaryl thioethers **28** from *O*-aryl thiocarbamates **23**. A plausible mechanism for the formation of **28a** from **23a** in the attempted cross-coupling reactions was therefore considered (Scheme 4.12).



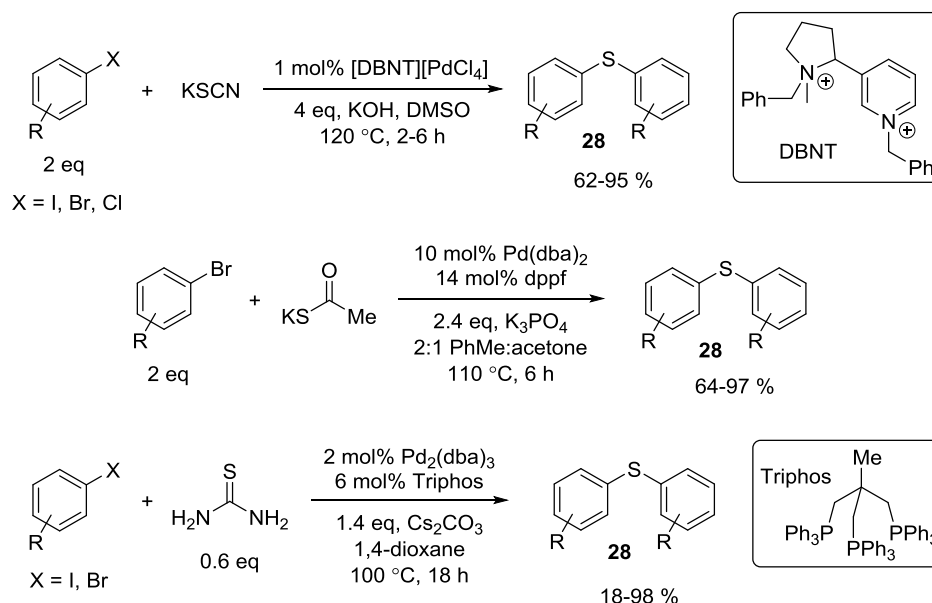
Scheme 4.12 The proposed mechanism for the formation of **28a** from **23a**.

Significantly, it was hypothesised that the formation of **28a** resulted from the palladium-catalysed coupling of **23a** or **24a** with **30a** (Scheme 4.12) and, thus, did not require the presence of an organometallic reagent. This implied that diaryl thioethers **28** might be formed from *O*-aryl thiocarbamates **23** simply upon treatment with a base in the presence of $\text{Pd(P}^t\text{Bu}_3)_2$ (Scheme 4.13).



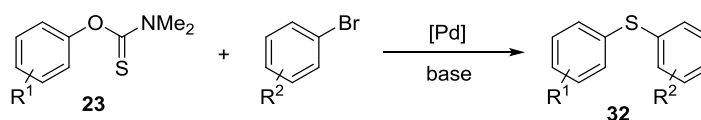
Scheme 4.13 The proposed palladium(0)-mediated synthesis of symmetrical diaryl thioethers **28** from *O*-aryl thiocarbamates **23**.

If realised, this procedure was expected to be an improvement upon other palladium-catalysed methods for the construction of symmetrical diaryl thioethers **28** (Scheme 4.14) due the ease with which *O*-aryl thiocarbamates **23** could be derived from cheap and readily available phenols.^{268–270}



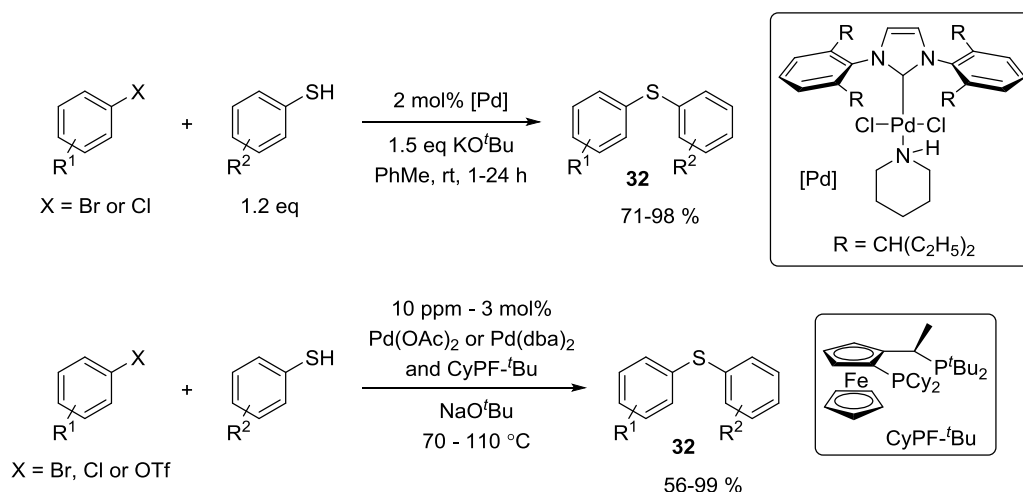
Scheme 4.14 Palladium(0)-catalysed procedures for the preparation of symmetrical diaryl thioethers **28**.

Given that **28a** was proposed to form *via* the *in situ* generation of **30a** from **23a**, it was further proposed that *O*-aryl thiocarbamates **23** might be successfully applied as labile thiophenol precursors in other coupling reactions. For example, it was anticipated that unsymmetrical diaryl thioethers **32** might be obtained in the palladium(0)-mediated reaction of *O*-aryl thiocarbamates **23** with aryl bromides under basic conditions (Scheme 4.15). Aryl bromides are more potent aryl electrophiles than *O*-aryl thiocarbamates **23** and would be expected to couple more rapidly with *in situ* generated aryl thiolates **30**.



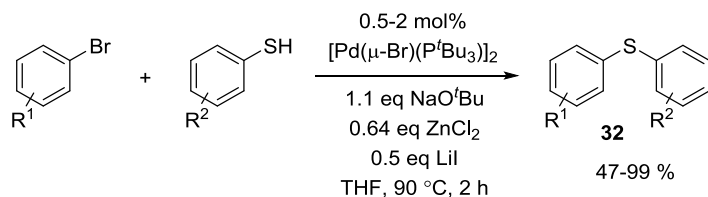
Scheme 4.15 The proposed palladium(0)-mediated synthesis of unsymmetrical diaryl thioethers **32** from *O*-aryl thiocarbamates **23** and aryl bromides.

The synthesis of unsymmetrical diaryl thioethers **32** *via* the transition metal-catalysed cross-coupling of thiophenols with aryl halides is well documented.^{271,272} The palladium(0)-catalysed variant of this reaction is the most efficient and is applicable over a wide scope of starting materials, with excellent functional group tolerance.²⁷³ Although palladium(0)-catalysed C_{Ar}-S bond-forming coupling reactions were first realised in 1978,²⁷⁴ advances in the scope and efficiency of these processes emerged slowly relative to analogous improvements in C_{Ar}-C, C_{Ar}-N and C_{Ar}-O coupling reactions.^{271,275} This observation is primarily attributable to the tendency of organosulfur compounds to poison palladium catalysts. The high affinity of transition metals for sulfur can cause organosulfur compounds to saturate the coordination sphere of the metal centre, displace ancillary ligands which are vital for catalyst activity and/or aid the clustering of metal complexes to form less reactive aggregates.²⁷⁵ A major breakthrough in this field was the deployment of bulky and strongly chelating bisphosphine ligands which resisted displacement by organosulfur species and furnished catalysts capable of activating aryl chlorides and undergoing rapid reductive elimination reactions.^{275,276} More recently, bulky NHC ligands have been used to similar effect.²⁷³ State-of-the-art palladium(0) catalysts are now capable of coupling thiophenols with aryl chlorides, bromides and iodides using extraordinarily low catalyst loadings (10-100 ppm) and promoting difficult couplings at room temperature (when higher catalyst loadings are employed; Scheme 4.16).^{273,277} The use of an aryl triflate as the electrophilic partner has also been achieved.²⁷⁸



Scheme 4.16 Summary of the most active catalyst systems for the palladium(0)-catalysed coupling of thiophenols with aryl (pseudo)halides.

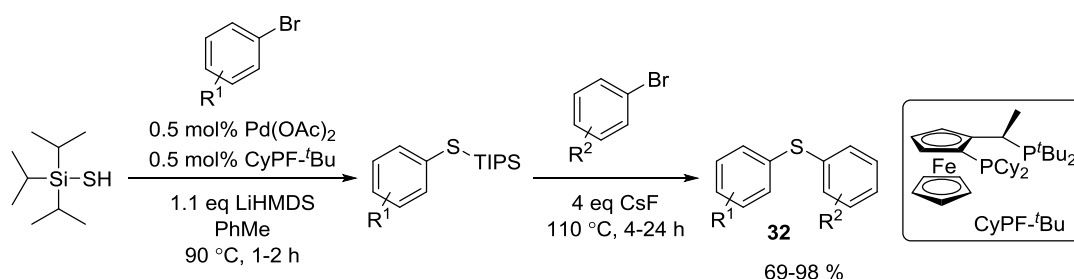
The coupling of thiophenols with aryl bromides using monodentate phosphine ligands is only viable when substantial quantities of zinc chloride are added and even then, necessitates that relatively forcing conditions are applied (Scheme 4.17).²⁷⁹ Zinc chloride acts as a sulfur scavenger and reversibly binds aryl thiolates **30**. In effect, this reduces the concentration of the aryl thiolates **30** and lessens their ability to inhibit or deactivate palladium catalysts.



Scheme 4.17 The palladium(0)-catalysed coupling of aryl bromides with thiophenols using a monodentate phosphine ligand.

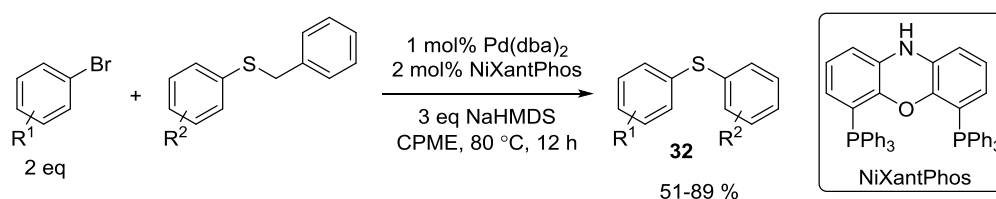
The primary drawback to the synthesis of diaryl thioethers **32** *via* the aforementioned palladium(0)-catalysed coupling reactions is the poor commercial availability of thiophenols and the inconveniences associated with their handling. Thiophenols are very unstable towards oxidation to diaryl disulfides and are extremely foul smelling.²⁸⁰ As a result, a number of procedures for generating aryl thiolate **30** coupling partners *in situ* from H_2S surrogates or protected thiophenols have been developed. Although similar, the strategy proposed above for utilising *O*-aryl thiocarbamates **23** as ‘masked’ thiophenols benefits from the ease with which *O*-aryl thiocarbamates **23** can be accessed, at low cost, from a wide range of abundant and inexpensive phenols.

The first procedure reported to exploit the *in situ* generation of aryl thiolates **30** in palladium(0)-catalysed cross-coupling reactions is performed in two steps and utilises triisopropylsilanethiol as an H₂S surrogate (Scheme 4.18).²⁸⁰ In the first step, this reagent is coupled with an aryl bromide using a particularly active catalyst based upon the chelating and electron-rich CyPF-*t*Bu Josiphos ligand. In the second step, caesium fluoride is used to cleave the TIPS-protected coupling product and liberate the aryl thiolates **30** which are then arylated with a second aryl bromide. Advantageously, low catalyst loadings are required and both of the steps can be achieved in one pot. However, the high cost of triisopropylsilanethiol limits the use of this method.



Scheme 4.18 A two-step, one-pot procedure for the synthesis of unsymmetrical diaryl thioethers **32** from two different aryl bromides.

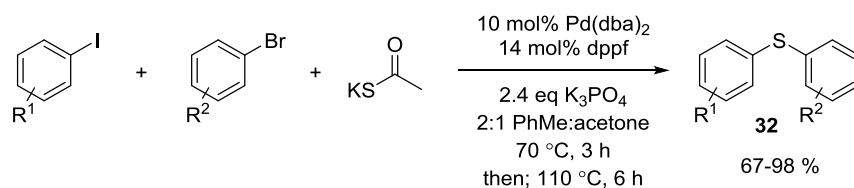
More recently, aryl thiolates **30** have been generated *in situ* by the palladium(0)-catalysed debenzoylation of aryl benzyl sulfides (Scheme 4.19).²⁸¹ The same palladium catalyst promotes the debenzoylation reaction and the coupling reaction, allowing the two processes to proceed in tandem. Although rather elegant, this approach requires 2 equivalents of the aryl bromide to be applied due to its consumption in the debenzoylation reaction. A large excess of a strong base is also used which limits the substrate scope.



Scheme 4.19 The palladium(0)-catalysed debenzoylative coupling of aryl benzyl sulfides with aryl bromides.

Unsymmetrical diaryl thioethers **32** have also been produced in the impressive one-pot, three-component couplings of potassium thioacetate with aryl iodides and aryl bromides, albeit using high catalyst loadings (Scheme 4.20).²⁶⁸ Currently, the coupling of

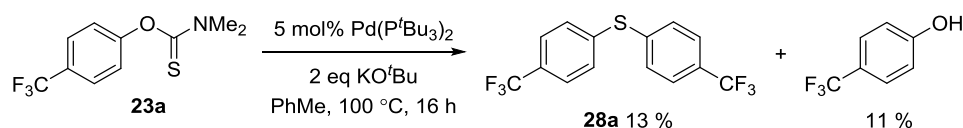
two different aryl bromides with potassium thioacetate can only be achieved using a two-step, two-pot procedure.²⁸²



Scheme 4.20 A one-pot procedure for the synthesis of unsymmetrical diaryl thioethers **32** from aryl iodides and aryl bromides.

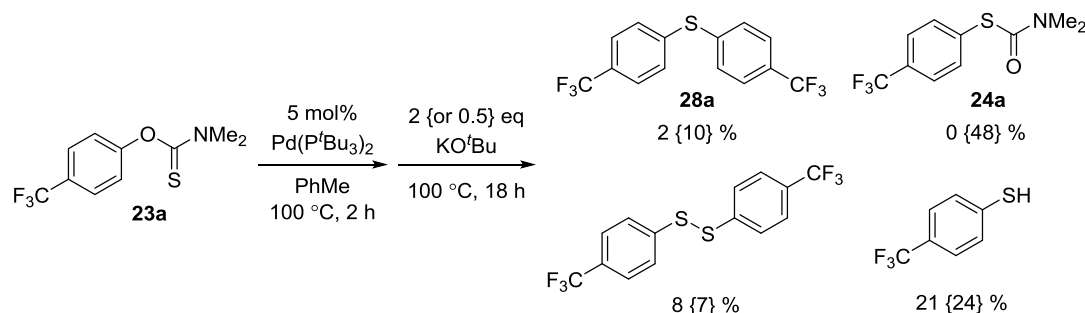
4.2.2 Symmetrical Diaryl Thioethers from *O*-Aryl Thiocarbamates

As discussed in the previous section, it was predicted that the Pd(P^{*t*}Bu₃)₂-mediated reaction of **23a** with potassium *tert*-butoxide would enable **28a** to be accessed. However, when this was attempted, the quantity of **28a** produced was very low (determined by ¹⁹F NMR spectroscopy; Scheme 4.21).



Scheme 4.21 The attempted one-step, one pot synthesis of **28a** from **23a**.

The only other product detectable after acidic work-up was 4-trifluoromethylphenol, suggesting that the decomposition of **23a** might have outcompeted productive turnover to generate **28a**. In an attempt to bias the desired reaction, the palladium-catalysed NKR of **23a** to **24a** was performed prior to the addition of potassium *tert*-butoxide to the reaction mixture (Scheme 4.22).



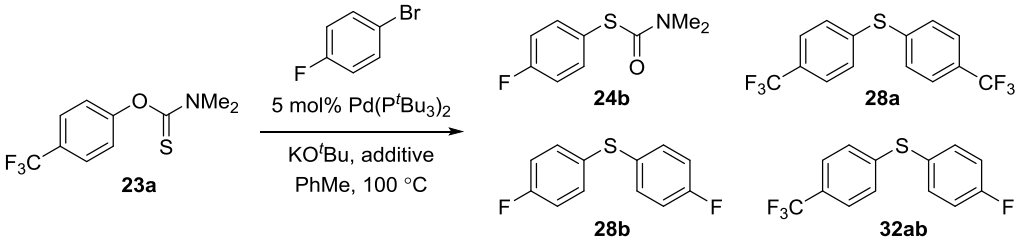
Scheme 4.22 The attempted two-step, one pot synthesis of **28a** from **23a**.

When 2 equivalents of potassium *tert*-butoxide were applied, again, very little **28a** was formed. Now, it was suspected that the base-mediated cleavage of **24a** was outcompeting productive turnover. The use of 0.5 equivalents of potassium *tert*-butoxide was therefore investigated, expecting that this would enable a maximum of 0.5 equivalents of **30a** to be generated whilst leaving 0.5 equivalents of **24a** intact. In practise, approximately half of the total amount of **24a** did appear to be cleaved, however, the desired coupling reaction did not proceed. It is possible that rapid cleavage of **24a** produced a sufficiently high concentration of the arylthiolate **30a** to poison the catalyst.

4.2.3 Symmetrical Diaryl Thioethers from Aryl Bromides

Although the reactions detailed in the previous section were unsuccessful, the results were promising with regards to achieving selectivity for unsymmetrical diaryl thioether **32** generation in the couplings of *O*-aryl thiocarbamates **23** with aryl bromides. At this point, the Pd(P^{*t*}Bu₃)₂-catalysed reaction of **23a** with 1-bromo-4-fluorobenzene in the presence of 2 equivalents of potassium *tert*-butoxide was therefore attempted (entry 1, Table 4.2). Surprisingly, the major products of the reaction were bis(4-fluorophenyl)sulfide **28b** and *S*-(4-fluorophenyl)-*N,N'*-dimethylthiocarbamate **24b**, with only minor quantities of (4-trifluoromethylphenyl)(4-fluorophenyl)sulfide **32ab** being afforded.

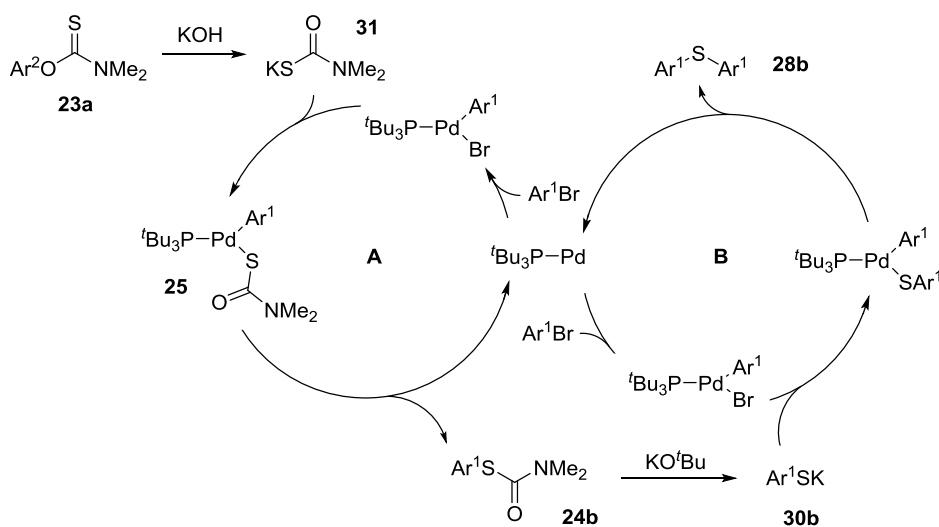
Table 4.2 The Pd(P^{*t*}Bu₃)₂-mediated reactions of **23a**, 1-bromo-4-fluorobenzene and potassium *tert*-butoxide. ^a

							
Entry	Eq. KO ^{<i>t</i>} Bu	Additives	<i>t</i> / h	Conv. / % ^b			
				32ab	28b	28a	24b
1	2	-	22	2	67	1	22
2	3	-	20	1	76	< 1	18
3	3	2 eq H ₂ O	18	15	68	4	22

^a 0.2 mmol scale, 0.2 M; 1:1 **23a**:ArBr. ^b Determined by ¹⁹F NMR spectroscopy using a 1-fluoronaphthalene internal standard.

The recovery of aryl bromide-derived products was high (97 %; calculated by summing all Ar-F-containing species observed in the ^{19}F NMR spectrum), although (as described in detail in Section 4.1.2) the conversions displayed in Table 4.2 are over-estimates due to the loss of the ^{19}F NMR internal standard (1-fluoronaphthalene) during work-up. In addition, **23a** was completely consumed in the reaction and the formation of 4-trifluoromethylphenol (6 %) was detected.

Considering all of the above observations, it was hypothesised that **23a** was cleaved under the reaction conditions to produce potassium *N,N'*-dimethyl thiocarbamate **31** which was then coupled with 1-bromo-4-fluorobenzene to form **24b**. Subsequent cleavage of **24b** would have produced 4-fluorophenylthiolate **30b** which could also have coupled with 1-bromo-4-fluorobenzene to form **28b** (Scheme 4.23). It was proposed that traces of water in the reaction mixture caused the base-mediated cleavage of **23a** to yield **31** rather than *O*-(*tert*-butyl)-*N,N'*-dimethyl thiocarbamate, as might have been expected. Overall, these results appeared to indicate that **23a** could behave as an H_2S surrogate in a similar manner to potassium thioacetate^{268,282} and triisopropylsilanethiol (Section 4.2.1).²⁸⁰



Scheme 4.23 The proposed mechanism for the formation of **28b** and **24b** in the $\text{Pd}(\text{P}^t\text{Bu}_3)_2$ -mediated reaction of **23a**, 1-bromo-4-fluorobenzene and potassium *tert*-butoxide.

As a result, attempts were made to increase the yield with which **28b** could be obtained. With the proposed mechanism for the formation of **28b** in mind, it seemed likely that the base-mediated cleavage of **24b** to 4-fluorophenylthiolate **30b** was the bottleneck for turnover *via* cycle B and the production of **28b** (Scheme 4.23). The reaction was therefore repeated using 3 equivalents of potassium *tert*-butoxide, both with and

without the addition of 2 equivalents of water (entries 2 and 3, Table 4.2). Whilst the application of a greater quantity of potassium *tert*-butoxide slightly improved the selectivity of the reaction, the inclusion of water lessened this effect and also lead to an increase in the amount of **32ab** produced.

It is predicted that a more successful approach to achieving higher yields of **28b** would be to employ a 1:2 ratio of **23a** and 1-bromo-4-fluorobenzene. Doing so should avoid the excessive consumption of 1-bromo-4-fluorobenzene in cycle A and allow for cycle B to continue until **24b** has been completely consumed.

4.2.4 Unsymmetrical Diaryl Thioethers from O-Aryl Thiocarbamates and Aryl Bromides

In the reactions described in the previous section (Table 4.2), not only were very little quantities of **32ab** yielded, but 4-trifluoromethylthiophenol and **24a** were also not detected in any quantity by ¹⁹F NMR spectroscopy. These observations suggested that the palladium(0)-catalysed NKR of **23a** was not proceeding as usual under the reaction conditions. Presumably, this was a result of the palladium(0) catalyst reacting more rapidly with 1-bromo-4-fluorobenzene than **23a** and entering cycles A and B as depicted in Scheme 4.23. It was therefore hypothesised that **32ab** would be more readily accessed if **24a** was used in place of **23a** in these reactions. Furthermore, without the need to induce the NKR of **23a**, it was expected that coupling might be observed below 100 °C. Pleasingly, at 60 °C, **24a** was selectively converted to **32ab** in high yield. The conditions applied were otherwise identical to those unsuccessful in promoting the coupling of **23a** (entry 1, Table 4.3).

Similar results were obtained when the catalyst loading was reduced to 2 mol% (entry 2), but the use of 1 mol% of catalyst caused **32ab** to be afforded in a reduced yield (entry 3). Interestingly, although only 1 equivalent of potassium *tert*-butoxide was expected to be required for reaction *via* the proposed mechanism, the desired reactivity was lost upon reducing the quantity of potassium *tert*-butoxide from 2 to 1.1 equivalents (entry 4 vs. 2). This suggested that potassium *tert*-butoxide might be protecting the catalyst from deactivation by competing with the aryl thiolate **30a** for coordination sites.

When 1.1 equivalents of potassium *tert*-butoxide were used, 4-trifluoromethylthiophenol and the corresponding disulfide were recovered in 68 % yield. These species were also afforded as side products when 1 mol% of catalyst was

used (entry 3). When 2 or 5 mol% of catalyst were employed however, these species and all other impurities were only recovered in trace amounts (< 1 %, entries 1 and 2). It was therefore proposed that when 2 or 5 mol% of catalyst were employed, the incomplete recovery of **24a**-derived material could be explained by the inherent inefficiency of the work-up procedure, rather than the diversion of **24a** in unwanted side-reactions.

Table 4.3 Screen of catalyst and base loadings for the palladium(0)-catalysed coupling of **24a with 1-bromo-4-fluorobenzene.** ^a

Entry	X	mol% Pd	Eq. KO ^t Bu	t / h	Total recovery from 24a / % ^{b,c}	Conv. / % ^b		
						32ab	28b	28a
1	Br	5	2	17	87	84	1	< 1
2	Br	2	2	17	89	85	1	< 1
3	Br	1	2	16	87	67	0	< 1
4	Br	2	1.1	19	78	1	0	0
5	Cl	2	2	23	74	0	0	0
6 ^d	Cl	2	2	18	69	8	1	3

^a 0.2 mmol scale, 0.2 M; 1:1 **24a**:ArX. ^b Determined by ¹⁹F NMR spectroscopy using a 1-fluoronaphthalene internal standard. ^c Calculated by summing all CF₃-containing species detected in the ¹⁹F NMR spectrum.

^d Reaction was performed at 100 °C.

1-Chloro-4-fluorobenzene was not a suitable substrate for the coupling reaction (entries 5 and 6). The formation of **32ab** was only observed upon performing the reaction at 100 °C and even then, the conversion was low and selectivity was poor.

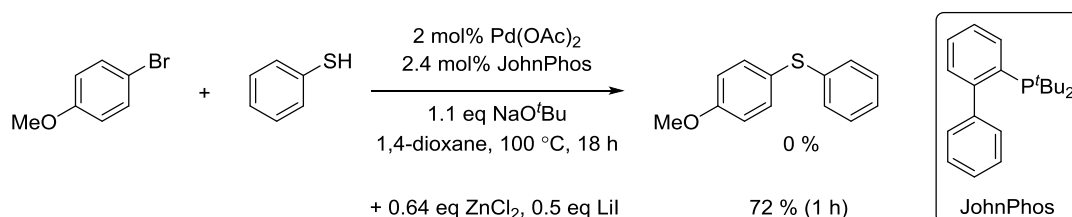
Other phosphine ligands were also found to promote the palladium(0)-catalysed coupling of **24a** with 1-bromo-4-fluorobenzene under the same conditions (Table 4.4). Buchwald's 3rd generation palladium(II) palladacycle precatalysts were used in these reactions due to the ability of these complexes to efficiently generate palladium(0) species upon treatment with a base.²⁸³ Impressively, the monophosphine dialkylbiaryl ligand, XPhos, appeared to be a feasible alternative to P^tBu₃ (entries 2 and 3), whilst the chelating bisphosphine, Xantphos, furnished a slightly less active catalyst (entry 1).

Table 4.4 Alternative catalysts for the palladium(0)-catalysed coupling of **24a with 1-bromo-4-fluorobenzene.** ^a

mol% G3-L	L	t / h	Total recovery from 24a / % ^{b,c}	Conv. / % ^b		
				32ab	28b	28a
5	Xantphos	23	79	70	2	3
5	XPhos	23	87	83	3	1
2	XPhos	19	89	83	1	1

^a 0.1 mmol scale, 0.1 M; 1:1 **24a**:ArBr. ^b Determined by ¹⁹F NMR spectroscopy using a 1-fluoronaphthalene internal standard. ^c Calculated by summing all CF₃-containing species detected in the ¹⁹F NMR spectrum.

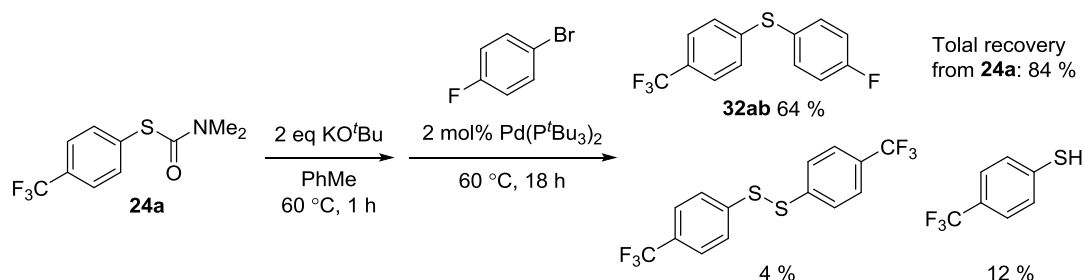
As noted in Section 4.2.1, palladium monophosphine complexes tend to be poor catalysts for the coupling of thiophenols with aryl halides. Indeed, an attempt to couple 4-bromoanisole with benzenethiol using Pd(OAc)₂ and JohnPhos (a dialkylbiaryl phosphine relative of XPhos) was reported to have failed.²⁷⁶ However, the same reaction was subsequently realised when zinc chloride and lithium iodide additives were used (Scheme 4.24).²⁷⁹



Scheme 4.24 The palladium(0)-catalysed coupling of 4-bromoanisole with benzenethiol.

Although the systems described in Table 4.4 and Scheme 4.24 differ in a number of ways, a comparison of the two sets of results raised the question of whether the use of *S*-aryl thiocarbamates **24** in place of thiophenols could lead to more successful coupling reactions. It was proposed that, under basic conditions, thiophenols would produce aryl thiolates **30** faster than the corresponding *S*-aryl thiocarbamates **24** and thus, palladium catalysts might be less prone to poisoning in reactions employing *S*-aryl thiocarbamates

24 (Section 4.2.1). As an initial test for this theory, a coupling reaction was performed in which **30a** was liberated from **24a** by reaction with potassium *tert*-butoxide, prior to the addition of 1-bromo-4-fluorobenzene and Pd(P^{*t*}Bu₃)₂ (Scheme 4.25). This two-step, one-pot procedure was expected to negate any beneficial effects that might be imparted by the slow release of **30a** from **24a**. Comparing the results of this reaction with those obtained using the standard procedure (entry 2, Table 4.3: 85 % **32ab**) suggested that the *in situ* release of the aryl thiolate from **24a** was advantageous to the outcome of the coupling reaction. Further exploration of this concept in future studies would be of interest.



Scheme 4.25 The two-step, one-pot coupling of **24a** with 1-bromo-4-fluorobenzene.

As *S*-aryl thiocarbamates **24** can be accessed from their *O*-aryl counterparts **23** *via* the NKR, the coupling of *S*-aryl thiocarbamates **24** with aryl bromides can also be viewed as the two-step, two-pot coupling of *O*-aryl thiocarbamates **23** with aryl bromides. However, although this strategy can successfully avoid the handling of thiophenols, it was clearly less valuable than the one-step, one-pot process proposed in Section 4.2.1. Efforts were therefore made to establish a more convenient two-step, one-pot procedure whereby the NKR of *O*-aryl thiocarbamates **23** and the coupling of *S*-aryl thiocarbamates **24** could be performed in succession using the same catalyst. In practise, this was probed by first carrying out the palladium(0)-catalysed NKR of **23a** at 100 °C, before adding 1-bromo-4-fluorobenzene and potassium *tert*-butoxide (Table 4.5).

Table 4.5 Initial screen of conditions for the two-step, one-pot, palladium(0)-catalysed coupling of **23a with 1-bromo-4-fluorobenzene.**

Entry	mol% Pd	T / °C	t ₁ / h	t ₂ / h	Total recovery from 23a / % ^{b,c}	Conv. / % ^b		
						32ab	28b	28a
1	5	100	2	20	95	60	13	9
2	5	60	2	4	100	84	1	10
3	2	60	4	19	78	3	0	3

^a 0.2 mmol scale, 0.2 M; 1:1 **23a**:ArBr. ^b Determined by ¹⁹F NMR spectroscopy using a 1-fluoronaphthalene internal standard. ^c Calculated by summing all CF₃-containing species detected in the ¹⁹F NMR spectrum.

Promisingly, when the entire process was performed at 100 °C, **32ab** was obtained, but with poorer selectivity and in an appreciably lower yield than when **24a** was used as the substrate. Poor selectivity in the palladium(0)-mediated synthesis of diaryl thioethers at high temperatures has been described previously and is believed to occur *via* arylthiolate ligand exchange between aryl palladium(II) complexes.^{275,276,284,285} Reducing the temperature of the second step of the reaction to 60 °C allowed for improved selectivity and a higher yield of **32ab** to be achieved (entry 2). The minor amounts of **28a** afforded in these reactions were primarily formed during the NKR step. Unfortunately, productivity was almost completely lost upon attempting to reduce the catalyst loading to 2 mol% (entry 3). Again (see discussion in Sections 4.1.2), it should be noted that all of the conversions detailed in Table 4.5 are likely to be larger than the true values due to the loss of the ¹⁹F NMR internal standard (1-fluoronaphthalene) during work-up.

4.3 Summary and Conclusions

A preliminary investigation into the use of *O*-aryl thiocarbamates **23** as novel, phenol-derived electrophiles in cross-coupling reactions was conducted. Although turnover was achieved in reactions employing both boronic acid and arylzinc reagents, *O*- and *S*-(4-trifluoromethylphenyl)-*N,N'*-dimethyl thiocarbamate, **23a** and **24a**, were found to be unstable under the reaction conditions and yields of the cross-coupled products were

low. Devising strategies to outcompete the decomposition of these species was therefore identified as the key to refining these reactions into useful processes.

Bis(4-trifluoromethylphenyl)sulfide **28a** was identified as the major side product in the attempted cross-coupling reactions. Recognising the potential benefits of being able to synthesise such structures from phenol-derived starting materials without having to handle thiophenols, attempts were made to optimise the reaction conditions to favour the formation of this product. Although this did not prove fruitful, observations were made which led to the palladium(0)-catalysed reactions of **23a** and **24a** with 1-bromo-4-fluorobenzene being investigated. It was found that **23a** could act as an H₂S surrogate in the presence of a base, allowing for bis(4-fluorophenyl)sulfide **28b** to be generated from the aryl bromide in reasonable yields. In contrast, the **24a** behaved as a precursor to the corresponding arylthiolate **30a** and coupled with the aryl bromide to form (4-trifluoromethylphenyl)(4-fluoromethylphenyl)sulfide **32ab** under the same conditions. This reaction was shown to be promoted at relatively low catalyst loadings (2 mol%) and by both monodentate and bidentate phosphine ligands. However, poor results were obtained when the coupling of 1-chloro-4-fluorobenzene was attempted. Finally, it was found that **23a** could also be coupled with the aryl bromide to form **32ab** if a two-step, one-pot procedure was adopted.

4.4 Future Work

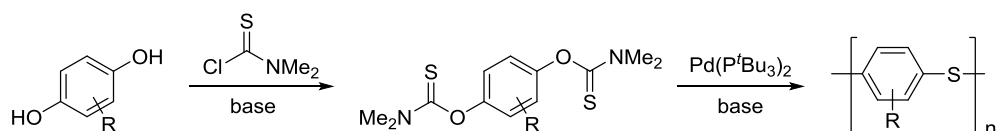
Whilst promising, the results summarised above constitute only preliminary investigations into the use of *O*-aryl thiocarbamates **23** and *S*-aryl thiocarbamates **24**, as labile thiophenol precursors in the preparation of diaryl thioethers or as phenol-derived electrophiles in cross-coupling reactions.

Of the limited number of conditions sampled for the cross-coupling of **23a**, the use of 4-fluorophenylzinc chloride provided the best results. Few improvements to this reaction can be envisioned, but it is possible that the slow addition of the arylzinc reagent could be beneficial. This strategy, however, would rely on the rate of substrate cleavage being more sensitive than the rate of productive turnover to the concentration of the arylzinc reagent (e.g. if oxidative addition was turnover-limiting). A similar approach has been successfully adopted in the palladium(0) catalysed amination of sensitive aryl triflates.^{13,14}

The coupling of *O*-aryl thiocarbamates **23** with arylboronic acids has greater scope for optimisation due to the low nucleophilicity of these reagents and the relatively mild conditions under which they can be activated. Indeed, **23a** appeared to be relatively stable in the presence of potassium fluoride and potassium carbonate under the reaction conditions described in Section 4.1.2. This suggests that a thorough screen of bases, solvents and temperatures for this coupling reaction might be fruitful. The successful cross-couplings of *O*-aryl sulfonates and *O*-aryl carbamates under forcing reaction conditions offers promise to this line of enquiry.^{81,286}

In order for the couplings of *O*-aryl thiocarbamates **23** and *S*-aryl thiocarbamates **24** with aryl halides to be established as useful methods for the preparation of diaryl thioethers, it is essential that their compatibility with electronically and sterically diverse substrates is confirmed. As 4-trifluoromethylphenyl thiocarbamates were used as the model substrates during the method development studies, it would be of particular interest to investigate how aryl thiocarbamates substituted with electron-donating groups behave under the reaction conditions.

It was surprising to find that attempts to produce bis(4-trifluoromethylphenyl)sulfide **28a** from **23a** proved unsuccessful given that this thioether was an undesired side-product in attempted C_{Ar}-C bond-forming coupling reactions using the same substrate. It would therefore be of interest to investigate how this thioether was formed in these reactions. If the preparation of symmetrical diaryl thioethers **28** from *O*-aryl thiocarbamates **23** could be realised, it could prove useful in the preparation of poly(arylenesulfide)s from aromatic diols (Scheme 4.26).



Scheme 4.26 The hypothetical synthesis of poly(arylenesulfide)s from aromatic diols in two steps.

From an atom-economical standpoint, the use of *O*-aryl thiocarbamates **23** as H₂S surrogates in the synthesis of symmetrical diaryl thioethers from aryl bromides is not ideal. However, it would be surprising if the aryloxy group was essential for this function. It is hypothesised that this reaction simply demonstrates the competency of the thiocarbamate anion as a coupling partner. Similar reactivity might therefore be displayed by lower molecular weight alcohol-derived thiocarbamates, such as *O*-methyl-

N,N'-dimethyl thiocarbamate, under the same reaction conditions. Alternatively, it is possible that *N,N'*-dimethylthiocarbamoyl chloride could be hydrolysed and coupled *in situ* or that the cheap and commercially available salt, sodium *N,N'*-diethyldithiocarbamate, could be used to similar effect.

The controlled, slow release of aryl thiolates **30** in transition metal-catalysed C-S bond forming reactions has thus far gone unexplored, despite having the potential to significantly increase the scope and efficiency of these processes. For example, by keeping the concentration of aryl thiolates low, the requirement for extremely bulky or chelating phosphine ligands to be used in palladium(0)-catalysed reactions might be avoided. A similar strategy has been employed in the Suzuki-Miyaura cross-coupling reaction in which boronic acids are often observed to take part in undesired side-reactions. In this case, the use of a number of different labile 'protected' boronic acids has enabled side-product formation to be significantly reduced and as a result, the use of these 'masked' boronic acids is now widespread.²⁵⁰ It is proposed that the coupling of *S*-aryl thiocarbamates **24** with aryl bromides would be an ideal system on which to assess the feasibility of this approach in C-S bond-forming coupling reactions. Key to achieving success would be the careful selection of reaction conditions (e.g. the quantity of base) which would allow the rate of release of the arylthiolate **30** to synchronise with catalyst turnover. These conditions could then be optimised for compatibility with other transition metal-catalysed C-S bond forming reactions.²⁸⁷

Finally, it is worth highlighting that the recent report on the use of photoredox catalysis to promote the NKR at room temperature has rendered the coupling of *S*-aryl thiocarbamates **24** with aryl bromides a much more attractive prospect. In addition, it is proposed that it might be possible to perform photoredox-catalysed NKR reactions and palladium(0)-catalysed coupling reactions in one pot (in an analogous manner to that detailed in Table 4.5). This would allow the corresponding coupling of *O*-aryl thiocarbamates **23** to be achieved under much milder conditions and thus, lead to improvements in the substrate scope of the reaction and the selectivity of the reaction for producing unsymmetrical diaryl thioethers **32**. In relation to this suggestion, it is worth noting that the coupling of *S*-aryl thiocarbamates **24** at temperatures below 60 °C has not yet been explored, but could be viable.

5 Experimental

5.1 General Experimental Details

5.1.1 Techniques

Inert Atmosphere Technique

Where indicated, oxygen and moisture sensitive manipulations were carried out under an atmosphere of anhydrous nitrogen using Schlenk line techniques (oil vacuum pump; 0.5 torr) and oven-dried glassware (200 °C). It should be assumed that when taking such precautions, anhydrous solvents were employed. $\text{Pd}(\text{P}^t\text{Bu}_3)_2$, $\text{Ni}(\text{COD})_2$, $\text{CyPF-}^t\text{Bu}$, P^tBu_3 , PCy_3 , KO^tBu , LiO^tBu and NaH were stored and weighed in an MBraun Unilab Pro SP glovebox maintained with oxygen and water levels of <1 ppm.

Chromatography

Thin-layer chromatography was conducted using silica-coated aluminium plates (Silica Gel 60 F254, Merck). Visualisation was achieved under UV light (254 nm) or by use of an aqueous, basic potassium permanganate stain. Column chromatography was performed using Davisil® 60A (35-70 m, Fisher Scientific) or Geduran® 60 (40-63 m, Merck) silica-gel.

5.1.2 Materials

Solvents

Reagent grade solvents were purchased from Fisher Technical. Toluene, DCM, hexane, THF and diethyl ether were dried using Anhydrous Engineering and MBraun Grubbs-type solvent purification systems and were stored under an atmosphere of anhydrous nitrogen. Other anhydrous solvents (1,4-dioxane, NMP, DMF and DMSO) were purchased from Sigma Aldrich. Deuterated solvents were purchased from Sigma Aldrich or Cambridge Isotope Laboratories. Deuterated solvents were dried by distillation from, and storage over, activated 3 or 4 Å molecular sieves. Organic solvents for use in reactions involving transition metals were degassed in three freeze-pump-thaw cycles. Degassed water was obtained by sparging with nitrogen.

Reagents

Reagents were purchased from commercial suppliers (Sigma Aldrich, Strem Chemicals Inc., Alfa Aesar, Acros, Fluka, Fluorochem and VWR) and used without purification unless discussed below. $\text{Pd}(\text{dba})_2$ was synthesised by Dr. Sophie Purser, sodium phenoxide was synthesised by Dr. Robert Cox and 4,4'-difluorobiphenyl and 4-fluoro-4'-

(trifluoromethyl)biphenyl were synthesised by Dr. Liam Ball. Diethyl diallylmalonate,²⁸⁸ *N,N'*-Bis(2,6-diisopropylphenyl)ethane-1,2-diamine,²⁸⁹ 4-phenoxy quinazoline **10a**,⁵² SiPr.HCl,²⁹⁰ IPr.HCl,²⁹⁰ Pd(P^{*t*}Bu₃)₂²⁹¹ and Pd(η^3 -1-PhC₃H₄)(η^5 -C₅H₅)¹⁷² **3** were prepared according to literature procedures.

Anhydrous *p*-toluenesulfonic acid was obtained by heating the monohydrate at 100 °C *in vacuo* (0.5 torr) for 24 hours. Anhydrous zinc chloride was obtained by heating at 200 °C *in vacuo* (0.5 torr) for 30 minutes.

5.1.3 Instrumentation and Analysis

NMR Spectroscopy

NMR spectra were recorded using Varian Mercury 400, Varian Mercury 500, Jeol Eclipse 400, Jeol Eclipse 300 and Jeol Lambda 300 spectrometers at the School of Chemistry, University of Bristol and Bruker AVIII 400, AVIII 500 and AVIII 600 spectrometers (fitted with nitrogen or helium cryoprobes) at the School of Chemistry, University of Edinburgh. ¹H and ¹³C NMR spectra are referenced to protiated solvent peaks and chemical shifts are reported in ppm relative to the tetramethylsilane standard. ¹⁹F and ³¹P NMR spectra were externally referenced to neat CFCl₃ and 85 % aqueous H₃PO₄ respectively and chemical shifts, in ppm, are quoted relative to these standards. Heteronuclear NMR spectra measured using non-deuterated solvents (lock off) were not referenced. Chemical shifts, coupling constants (*J*) and peak integrals were measured after spectral processing using MestReNova versions 6 to 10. The following descriptors of peak multiplicity are used: s (singlet), d (doublet), t (triplet), q (quartet), sept (septet), m (multiplet), app (apparent) and br (broad). Where necessary, the assignment of signals in ¹H and ¹³C NMR spectra was assisted by performing ¹H-¹H COSY, ¹H-¹³C HSQC, ¹H-¹³C HMBC and/or NOESY (1D or 2D) NMR experiments.

UV-Vis Spectroscopy

UV-Vis spectra (spectral width: 226-600 nm; resolution: 1 nm; integration time: 20 ms) were recorded using an Ocean Optics USB4000-UV-Vis spectrometer, an Ocean optics DH-2000-BAL light source, solarisation-resistant fiber-optic cables and Kinetic Studio version 3.5 software (TgK Scientific). Solutions of the analyte were analysed whilst being magnetically-stirred in a quartz cell (10 mm solution path length) and were maintained at 25 °C inside a temperature-regulated cell compartment.

IR Spectroscopy

The infrared spectra ($4000\text{--}600\text{ cm}^{-1}$) of neat compounds were recorded on an ATR diamond cell using a Perkin-Elmer Spectrum 1000 Series FTIR or a Bruker Alpha FTIR spectrometer. The following descriptors of relative absorption intensity are used: w (weak, 0-30 %), m (medium, 30-70 %) and s (strong, 70-100 %).

Mass Spectrometry

Mass spectra were recorded by the University of Bristol Mass Spectrometry Service (Fissons VG Analytical Autospec or Bruker Daltonics Apex IV spectrometers) or by the University of Edinburgh Mass Spectrometry Service (Bruker micrOTOF, Bruker 12 T SolariX or Thermo/Finnigan MAT 900 spectrometers).

Melting Points

Melting points were measured in open capillaries using Stuart SMP10 apparatus.

X-ray Crystallography

X-ray crystallographic structure determination was performed by Dr Mairi Haddow of the University of Bristol X-ray crystallography service using a Bruker Kappa Apex II diffractometer (Mo-anode source).

Kinetic Simulation

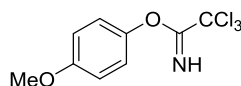
Kinetic simulations were performed using DynoChem 2011 version 4.1.

5.2 Experimental Details Relevant to Chapter 2

5.2.1 Preparation of O-Aryl Trichloroacetimidates

General Procedure A (Table 2.1, Table 2.2 and Table 2.3, entries 1 and 2)

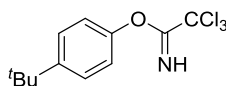
O-(4-Methoxyphenyl) Trichloroacetimidate **1b** (Table 2.1, entry 9)



General Procedure A: A solution of 4-methoxyphenol (31 mg, 0.25 mmol) and triethylamine (1.8 μ L, 0.013 mmol) in DCM (0.5 mL) had Cl_3CCN (0.5 mL, 5 mmol) added. After stirring for 7.5 hours, the reaction was concentrated *in vacuo* at 50 $^\circ\text{C}$ to afford a pale yellow, crystalline solid (129 mg). This material was identified as a mixture of the title compound **1b** and 4-methoxyphenol in a 99:1 ratio by ^1H NMR spectroscopy. The title compound **1b** was found to exist as a mixture of *E* and *Z* isomers in a 70:30 ratio.

Data for (*E*)- and (*Z*)-**1b** (NMR signals of the *Z* isomer are underlined): **^1H NMR (500 MHz, CDCl_3)**: δ 8.58 (br s, 1H, NH), 7.85 (br s, 0.42H, NH), 7.14 (d, $J_{\text{HH}} = 9.1$ Hz, 2H, Ar), 7.06 (d, $J_{\text{HH}} = 9.1$ Hz, 0.84H, Ar), 6.99 (d, $J_{\text{HH}} = 9.1$ Hz, 0.84H, Ar), 6.94 (d, $J_{\text{HH}} = 9.1$ Hz, 2H, Ar), 3.84 (s, 1.28H, OCH_3), 3.81 (s, 3H, OCH_3). **$^{13}\text{C}\{^1\text{H}\}$ NMR (126 MHz, CDCl_3)**: δ 163.6 (C=NH), 162.3 (C=NH), 158.4 (Ar), 157.5 (Ar), 146.4 (Ar), 143.4 (Ar), 122.5 (Ar), 121.9 (Ar), 115.6 (Ar), 114.6 (Ar), 91.8 (CCl_3), 91.1 (CCl_3), 55.7 (OCH_3), 55.6 (OCH_3). **ν_{max} (cm^{-1} , neat)**: 3316 (w, NH), 3214 (w, NH), 1689 (m, C=N), 1665 (m, C=N), 1594 (w), 1501 (m), 1464 (m), 1442 (m), 1315 (m), 1295 (m), 1240 (m), 1200 (m), 1181 (m), 1097 (m), 1064 (s), 1024 (m), 947 (s), 826 (s), 789 (s). **HRMS (m/z , EI^+)**: calcd. for $\text{C}_9\text{H}_8\text{Cl}_3\text{NO}_2$ [M] $^+$: 266.96151; found: 266.96132.

O-(4-*tert*-Butylphenyl) Trichloroacetimidate **1c** (Table 2.3, entry 2):

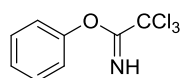


Following general procedure A, a colourless crystalline solid (73 mg) composed of the title compound **1c** and 4-*tert*-butylphenol in a 98:2 ratio was afforded. The title compound **1c** was found to exist as a mixture of two isomers in a 71:29 ratio.

Data for **1c** (NMR signals of the minor isomer are underlined): **^1H NMR (400 MHz, CDCl_3)**: δ 8.58 (br s, 1H, NH), 7.90 (br s, 0.41H, NH), 7.50 (app d, $J_{\text{HH}} = 8.8$ Hz, 0.82H, Ar),

7.44 (app d, $J_{\text{HH}} = 8.8$ Hz, 2H, Ar), 7.15 (app d, $J_{\text{HH}} = 8.8$ Hz, 2H, Ar), 7.05 (app d, $J_{\text{HH}} = 8.8$ Hz, 0.82H, Ar), 1.36 (s, 3.68H, C(CH₃)₃), 1.33 (s, 9H, C(CH₃)₃). **¹³C{¹H} NMR (101 MHz, CDCl₃):** δ 163.4 (C=NH), 162.1 (C=NH), 150.7 (Ar), 150.6 (Ar), 149.1 (Ar), 148.0 (Ar), 127.7 (Ar), 126.7 (Ar), 121.0 (Ar), 120.5 (Ar), 34.8 (C(CH₃)₃), 34.7 (C(CH₃)₃), 31.6 (C(CH₃)₃), 31.5 (C(CH₃)₃). **ν_{max} (cm⁻¹, neat):** 3328 (w, NH), 2966 (w), 1671 (m, C=N), 1506 (m), 1274 (m), 1202 (m), 1166 (m), 1106 (w), 1029 (m), 958 (m), 876 (w), 830 (s), 790 (s), 756 (m), 653 (m). **HRMS (m/z , EI⁺):** calcd. for C₁₂H₁₄Cl₃NO [M]⁺: 293.01355; found: 293.01253.

O-Phenyl Trichloroacetimidate **1a** (Table 2.3, entry 1):

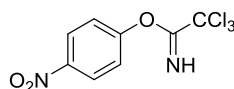


Following general procedure A, a pale yellow oil (66 mg) composed of the title compound **1a** and phenol in a 97:3 ratio was afforded. The title compound **1a** was found to exist as a mixture of two isomers in a 74:26 ratio.

Data for **1a** (NMR signals of the minor isomer are underlined): **¹H NMR (400 MHz, CDCl₃):** δ 8.62 (br s, 1H, NH), 7.85 (br s, 0.35H, NH), 7.51 (app t, $J_{\text{HH}} = 7.5$ Hz, 0.7H, Ar), 7.44 (app t, $J_{\text{HH}} = 7.5$ Hz, 2H, Ar), 7.37 (app t, $J_{\text{HH}} = 7.5$ Hz, 0.35H, Ar), 7.28 (app t, $J_{\text{HH}} = 7.5$ Hz, 1H, Ar), 7.23 (app d, $J_{\text{HH}} = 7.5$ Hz, 2H, Ar), 7.15 (app d, $J_{\text{HH}} = 7.5$ Hz, 0.7H, Ar). **¹³C{¹H} NMR (101 MHz, CDCl₃):** δ 163.3 (C=N), 161.9 (C=N), 153.0 (Ar), 150.4 (Ar), 130.9 (Ar), 129.8 (Ar), 127.5 (Ar), 126.3 (Ar), 121.7 (Ar), 121.2 (Ar). **ν_{max} (cm⁻¹, neat):** 3334 (w, NH), 3287 (w, NH), 1729 (w), 1671 (m, C=N), 1591 (m), 1491 (m), 1297 (m), 1193 (s), 1160 (m), 1051 (m), 955 (m), 861 (m), 788 (s), 761 (m), 713 (m), 685 (m), 638 (m). **HRMS (m/z , EI⁺):** calcd. for C₈H₆Cl₃NO [M]⁺: 236.95095; found: 236.94944.

General Procedure B (Table 2.3, entries 3-12)

O-(4-Nitrophenyl) Trichloroacetimidate **1d** (Table 2.3, entry 8):

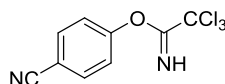


General Procedure B: A solution of 4-nitrophenol (69.6 mg, 0.5 mmol) and triethylamine (3.5 μ L, 0.025 mmol) in toluene (1 mL) had Cl₃CCN (1 mL, 10 mmol) added. After stirring for 5 hours, an aliquot (0.7 mL) of the reaction mixture was removed and analysed by ¹H

NMR spectroscopy. The title compound **1d** was formed in a 19:81 ratio with 4-nitrophenol and appeared to exist as a single isomer.

Data for **1d**: **¹H NMR (400 MHz, lock off, 1:1 DCM:Cl₃CCN)**: δ 8.93 (br s, 1H, NH), 8.31 (app d, *J*_{HH} = 9.0 Hz, 2H, Ar), 7.45 (app d, *J*_{HH} = 9.0 Hz, 2H, Ar).

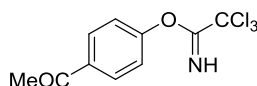
O-(4-Cyanophenyl) Trichloroacetimidate (Table 2.3, entry 4):



Following general procedure B, the title compound was formed in a 40:60 ratio with 4-cyanophenol and appeared to exist as a single isomer.

Data for *O*-(4-cyanophenyl) trichloroacetimidate: **¹H NMR (300 MHz, lock off, 1:1 DCM:Cl₃CCN)**: δ 8.88 (br s, 1H, NH), 7.74 (app d, *J*_{HH} = 8.7 Hz, 2H, Ar), 7.39 (app d, *J*_{HH} = 8.7 Hz, 2H, Ar).

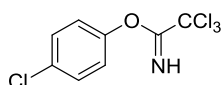
O-(4-Acetylphenyl) Trichloroacetimidate (Table 2.3, entry 5):



Following general procedure B, the title compound was formed in a 43:57 ratio with 4'-hydroxyacetophenone and appeared to exist as a single isomer.

Data for *O*-(4-acetylphenyl) trichloroacetimidate: **¹H NMR (300 MHz, lock off, 1:1 DCM:Cl₃CCN)**: δ 8.81 (br s, 1H, NH), 8.04 (app d, *J*_{HH} = 8.5 Hz, 2H, Ar), 7.34 (app d, *J*_{HH} = 8.5 Hz, 2H, Ar), 2.60 (s, 3H, CH₃).

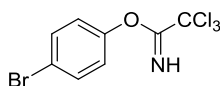
O-(4-Chlorophenyl) Trichloroacetimidate (Table 2.3, entry 11):



Following general procedure B, the title compound was formed in a 93:7 ratio with 4-chlorophenol and was found to exist as a mixture of two isomers in a 85:15 ratio

Data for *O*-(4-chlorophenyl) trichloroacetimidate (NMR signals of the minor isomer are underlined): **¹H NMR (300 MHz, lock off, 1:1 DCM:Cl₃CCN)**: δ 8.73 (br s, 1H, NH), 7.97 (br s, 0.18H, NH), 7.65 (app d, *J*_{HH} = 8.9 Hz, 0.35H, Ar), 7.55 (app d, *J*_{HH} = 8.9 Hz, 2H, Ar), 7.14 (app d, *J*_{HH} = 8.9 Hz, 2H, Ar), 7.06 (app d, *J*_{HH} = 8.9 Hz, 0.35H, Ar).

O-(4-Bromophenyl) Trichloroacetimidate (Table 2.3, entry 12):



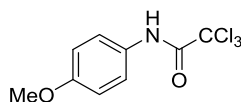
Following general procedure B, the title compound was formed in a 95:5 ratio with 4-bromophenol and was found to exist as a mixture of two isomers in a 82:18 ratio

Data for *O*-(4-bromophenyl) trichloroacetimidate (NMR signals of the minor isomer are underlined): **¹H NMR (300 MHz, lock off, 1:1 DCM:Cl₃CCN)**: δ 8.72 (br s, 1H, NH), 7.96 (br s, 0.22H, NH), 7.50 (app d, *J*_{HH} = 8.9 Hz, 0.44H, Ar), 7.41 (app d, *J*_{HH} = 8.9 Hz, 2H, Ar), 7.19 (app d, *J*_{HH} = 8.9 Hz, 2H, Ar), 7.12 (app d, *J*_{HH} = 8.9 Hz, 0.44H, Ar).

5.2.2 Preparation of *N*-Aryl Trihaloacetamides

Preparation of *N*-Aryl Trichloroacetamides

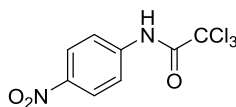
N-(4-Methoxyphenyl) Trichloroacetamide **2b**:



A solution of 4-methoxyaniline (46 mg, 0.37 mmol) and triethylamine (62 μL, 0.44 mmol) in DCM (1 mL) was cooled to 0 °C under an atmosphere of N₂. A solution of trichloroacetyl chloride (50 μL, 0.44 mmol) in DCM (1 mL) was then added dropwise over 10 minutes. The reaction was stirred at 0 °C for 1 hour and then at room temperature for a further 18 hours. Next, the reaction was diluted in EtOAc (10 mL) and washed with water (3 × 5 mL). The organic layer was dried (MgSO₄), filtered and concentrated *in vacuo* to afford the title compound **2b** (79 mg, 0.29 mmol, 79 %) as a brown solid.

¹H NMR (400 MHz, CDCl₃): δ 8.37 (br s, 1H, NH), 7.47 (app d, *J*_{HH} = 9.1 Hz, 2H, Ar), 6.90 (app d, *J*_{HH} = 9.1 Hz, 2H, Ar), 3.80 (s, 3H, OCH₃). **¹³C{¹H} NMR (101 MHz, CDCl₃)**: δ 159.4 (C=NH), 157.8 (Ar), 129.0 (Ar), 122.3 (Ar), 114.6 (Ar), 93.0 (CCl₃), 55.7 (OCH₃). **ν_{max} (cm⁻¹, neat)**: 3299 (m, NH), 3133 (w), 3069 (w), 2927 (w), 2831 (w), 1703 (m), 1687 (s, C=O), 1608 (m), 1540 (s), 1507 (s), 1460 (m), 1439 (m), 1412 (m), 1303 (w), 1241 (s), 1178 (m), 1116 (w), 1030 (m), 880 (m), 832 (s), 813 (s), 794 (s), 708 (w), 644 (s). **MS (*m/z*, EI⁺)**: calcd. for C₉H₈Cl₃NO₂ [M]⁺: 266.96; found: 267.0. **m.p. (°C)**: 108-109.

N-(4-Nitrophenyl) Trichloroacetamide **2d**:



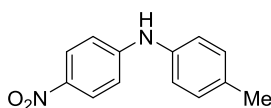
Following the procedure described above for **2b**, the title compound **2d** (91 mg, 0.32 mmol, 86 %) was afforded as an orange solid.

¹H NMR (400 MHz, CDCl₃): δ 8.66 (br s, 1H, NH), 8.29 (app d, *J*_{HH} = 9.2 Hz, 2H, Ar), 7.81 (app d, *J*_{HH} = 9.2 Hz, 2H, Ar). **¹³C{¹H} NMR (101 MHz, CDCl₃):** δ 159.6 (C=NH), 145.0 (Ar), 141.8 (Ar), 125.3 (Ar), 120.3 (Ar), 92.4 (CCl₃). **ν_{max} (cm⁻¹, neat):** 3320 (m, NH), 3114 (w), 3082 (w), 2935 (w), 1725 (s, C=O), 1614 (m), 1597 (m), 1542 (m), 1499 (s), 1489 (s), 1410 (m), 1340 (s), 1330 (s), 1302 (s), 1249 (s), 1201 (m), 1176 (m), 1114 (m), 1009 (w), 886 (m), 851 (s), 829 (m), 811 (s), 760 (m), 746 (s), 665 (s), 607 (s). **MS (*m/z*, EI⁺):** calcd. for C₈H₅Cl₃N₂O₃ [M]⁺: 281.94; found: 281.9. **m.p. (°C):** 145-146.

The data obtained is consistent with that reported in the literature.²⁹²

Preparation of *N*-(4-Nitrophenyl)-*N*-(4-methylphenyl) Trifluoroacetimidate

4-Methyl-*N*-(4-nitrophenyl)aniline:

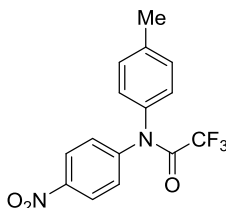


1-Bromo-4-nitrobenzene (202 mg, 1 mmol), 4-methylaniline (127 mg, 1.2 mmol), caesium carbonate (0.456 g, 1.4 mmol), Pd(dba)₂ (11.5 mg, 0.02 mmol) and BrettPhos (10.7 mg, 0.02 mmol) were dissolved in 1,4-dioxane (3 mL) under an atmosphere of N₂. This solution was stirred at 100 °C for 22 hours and then concentrated *in vacuo*. Purification by column chromatography (7:3 hexane:EtOAc) afforded the title compound as an orange solid (142 mg, 0.62 mmol, 62 %).

¹H NMR (400 MHz, CDCl₃): δ 8.10 (app d, *J*_{HH} = 9.3 Hz, 2H, Ar(NO₂)), 7.20 (app d, *J*_{HH} = 8.3 Hz, 2H, Ar(Me)), 7.11 (app d, *J*_{HH} = 8.3 Hz, 2H, Ar(Me)), 6.86 (app d, *J*_{HH} = 9.3 Hz, 2H, Ar(NO₂)), 6.19 (br s, 1H, NH), 2.36 (s, 3H, CH₃). **¹³C{¹H} NMR (101 MHz, CDCl₃):** δ 151.0 (Ar), 139.5 (Ar), 136.8 (Ar), 134.9 (Ar), 130.4 (Ar), 126.4 (Ar), 122.8 (Ar), 113.3 (Ar), 21.1 (CH₃). **MS (*m/z*, CI⁺):** calcd. for C₁₃H₁₃N₂O₂ [M+H]⁺: 229.10; found: 229.0.

The data obtained is consistent with that reported in the literature.²⁹³

N-(4-Nitrophenyl)-N-(4-methylphenyl) Trifluoroacetimidate:



A solution of 4-methyl-N-(4-nitrophenyl)aniline (57 mg, 0.25 mmol) and triethylamine (70 μ L, 0.5 mmol) in DCM (0.75 mL) was cooled to 0 °C under an atmosphere of N₂. Trifluoroacetic anhydride (70 μ L, 0.5 mmol) was then added dropwise over 2 minutes with stirring. The reaction was stirred at 0 °C for 1 hour and then at room temperature for a further 15 hours. Next, the reaction was diluted in DCM (5 mL) and washed with water (3 \times 5 mL). The organic layer was dried (Na₂SO₄), filtered and concentrated *in vacuo*. Purification by column chromatography (9:1 hexane:EtOAc) afforded the title compound (42 mg) in a 93:7 ratio with an unidentified impurity.

Data for the title compound: **¹H NMR (400 MHz, CDCl₃)**: δ 8.23 (app d, J_{HH} = 9.2 Hz, 2H, Ar(NO₂)), 7.46 (app d, J_{HH} = 9.2 Hz, 2H, Ar(NO₂)), 7.28 (app d, J_{HH} = 8.3 Hz, 2H, Ar(Me)), 7.20 (app d, J_{HH} = 8.3 Hz, 2H, Ar(Me)), 2.41 (s, 3H, CH₃). **¹³C{¹H} NMR (126 MHz, CDCl₃)**: δ 157.0 (q, $^2J_{\text{CF}}$ = 36.8 Hz, C=O), 146.7 (br, Ar), 146.2 (br, Ar), 140.1 (br, Ar), 136.0 (br, Ar), 130.7 (Ar), 128.4 (br, Ar), 126.6 (br, Ar), 124.8 (Ar), 116.3 (q, $^2J_{\text{CF}}$ = 288.6 Hz, CF₃), 21.3 (CH₃). **¹⁹F NMR (283 MHz, CDCl₃)**: δ -66.83 (s). **ν_{max} (cm⁻¹, neat)**: 3084 (w), 2926 (w), 2859 (w), 1708 (m, C=O), 1610 (w), 1592 (m), 1522 (m), 1509 (m), 1492 (m), 1381 (w), 1345 (s), 1311 (w), 1223 (m), 1202 (s), 1153 (s), 1134 (s), 1112 (m), 965 (w), 910 (w), 844 (m), 853 (m), 810 (m), 755 (m), 736 (m), 723 (m), 688 (m). **HRMS (m/z , EI⁺)**: calcd. for C₁₅H₁₁F₃N₂O₃ [M]⁺: 324.07163; found: 324.07324.

5.2.3 Initial Rearrangement Attempts

The Attempted Rearrangement of **1b**

Reaction with Pd(P^{*t*}Bu₃)₂ (Scheme 2.21):

Pd(P^{*t*}Bu₃)₂ (12.8 mg, 0.025 mmol) had a solution of **1b** (67.1 mg, 0.25 mmol) in toluene (1 mL) added under an atmosphere of N₂. The reaction was then stirred at 100 °C for 17 hours. During this time significant quantities of palladium black precipitated. Upon cooling, the mixture was concentrated *in vacuo* and analysed by ¹H NMR spectroscopy

(300 MHz, CDCl₃). 4-Methoxyphenol, **1b** and small quantities of other unidentified species were detected.

Reaction with P^tBu₃ (Scheme 2.22):

A solution of tri-*tert*-butylphosphine (19 mg, 0.094 mmol) in DCM (0.7 mL) was added to **1b** (47.2 mg, 0.176 mmol) in an NMR tube under an atmosphere of N₂. After 1 hour the solution was analysed by ¹H and ³¹P NMR spectroscopy (300/121 MHz, lock off). 4-Methoxyphenol, **1b** and protonated tri-*tert*-butylphosphine were detected.

Reaction with Pd(dba)₂ and P^tBu₃:

A solution of tri-*tert*-butylphosphine (4.6 mg, 0.023 mmol) in toluene (0.5 mL) was added to Pd(dba)₂ (14.4 mg, 0.025 mmol) under an atmosphere of N₂. This solution was stirred for 45 minutes and then a solution of **1b** (67.2 mg, 0.25 mmol) in toluene (0.5 mL) was added. The reaction was then stirred at 100 °C for 23 hours. During this time significant quantities of palladium black precipitated. Upon cooling, an aliquot (0.6 mL) was removed and analysed by ³¹P NMR spectroscopy (121 Hz, lock off). Tri-*tert*-butylphosphine oxide was detected alongside an unassignable peak at 170 ppm. The same sample was concentrated *in vacuo* and analysed by ¹H NMR spectroscopy (400 MHz, CDCl₃). 4-Methoxyphenol and **1b** were detected.

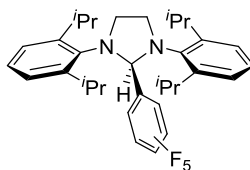
The Attempted Rearrangement of 1a and 1d Using Pd(P^tBu₃)₂ (Table 2.4)

Representative Procedure (Table 2.4, entry 1):

A solution of 4-nitrophenol (69.6 mg, 0.5 mmol) and triethylamine (3.5 µL, 0.025 mmol) in toluene (1 mL) had Cl₃CCN (1 mL, 10 mmol) added under an atmosphere of N₂. After stirring for 5 hours, an aliquot (0.7 mL) was removed and analysed by ¹H NMR spectroscopy. 4-Nitrophenol and **1d** were detected in a 81:19 ratio. The remaining solution had Pd(P^tBu₃)₂ (16.6 mg, 0.033 mmol) added and was then stirred at 80 °C for 17 hours. During this time significant quantities of palladium black precipitated. Upon cooling, an aliquot was removed and analysed by ¹H NMR spectroscopy (300 MHz, lock off). 4-Nitrophenol and **1d** were detected.

5.2.4 Preparation of (SIPr)Pd(η^1 -1-PhC₃H₄)(η^5 -C₅H₅)

1,3-Bis(2,6-diisopropylphenyl)-2-(pentafluorophenyl)imidazoline 4:



A mixture of pentafluorobenzaldehyde (0.33 g, 1.7 mmol), *N,N'*-bis(2,6-diisopropylphenyl)ethane-1,2-diamine (0.38 g, 1 mmol) and 3 Å molecular sieves (approx. 60 mg) had glacial acetic acid (0.3 mL) added. After stirring for 30 min the reaction was diluted in hexane (5 mL) and extracted with MeOH (5 mL). The MeOH layer was then washed with hexane (2 × 5 mL) and the combined hexane fractions were concentrated *in vacuo* (without heating). The resulting oil was diluted in Et₂O (approx. 0.5 mL) at 0 °C and layered with MeOH (approx. 1 mL) to afford the title compound **4** (0.41 g, 0.74 mmol, 74 %) as colourless crystals.

In order to avoid the decomposition of **4**, the CDCl₃ used for the NMR analyses had to be neutralised by passage through aluminium oxide (basic, Brockmann I).

¹H NMR (400 MHz, CDCl₃): δ 7.22-7.14 (m, 4H, Ar), 7.03 (app dd, *J*_{HH} = 2.0 and 7.7 Hz, 2H, Ar) 6.31 (s, 1H, NCHN), 3.94-3.86 (m, 2H, CHHCHH), 3.70-3.60 (m, 4H, CH(CH₃)₂ and CHHCHH), 3.53 (sept, ³*J*_{HH} = 6.8 Hz, 2H, CH(CH₃)₂), 1.42 (d, ³*J*_{HH} = 6.8 Hz, 6H, CH(CH₃)₂), 1.30 (d, ³*J*_{HH} = 6.8 Hz, 6H, CH(CH₃)₂), 1.18 (d, ³*J*_{HH} = 6.8 Hz, 6H, CH(CH₃)₂), 0.80 (d, ³*J*_{HH} = 6.8 Hz, 6H, CH(CH₃)₂). **¹³C{¹H} NMR (101 MHz, CDCl₃):** δ 151.4 (Ar), 149.4 (Ar), 138.6 (Ar), 127.5 (Ar), 124.7 (Ar), 124.4 (Ar), 75.6 (⁴*J*_{CF} = 4.5 Hz, NCHN), 53.3 (NCH₂CH₂N), 29.0, 26.9, 26.8, 26.1, 25.6, 24.2, 23.92, 23.91. **¹⁹F NMR (377 MHz, CDCl₃):** δ -135.63 (app dd, *J*_{FF} = 7.8 and 22.6 Hz, 1F), -147.47 (app dd, *J*_{FF} = 8.2 and 23.0 Hz, 1F), -155.82 (app dt, *J*_{FF} = 2.4 and 21.0 Hz, 1F), -162.46 (m, 1F), -163.36 (m, 1F). **MS (*m/z*, EI⁺):** calcd. for C₃₃H₃₉F₅N₂ [M]⁺: 558.30; found: 558.3.

The data obtained is consistent with that reported in the literature.²⁹⁴

Reaction Between **4** and Pd(η^3 -1-PhC₃H₄)(η^5 -C₅H₅) **3**; ¹H NMR Monitoring (Scheme 2.25):

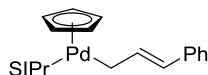
Pd(η^3 -1-PhC₃H₄)(η^5 -C₅H₅) **3** (8.6 mg, 0.03 mmol) and **4** (16.6 mg, 0.03 mmol) were dissolved in d₈-toluene (0.6 mL) in an NMR tube under an atmosphere of N₂. The NMR tube was loaded into an NMR spectrometer and spun at 65 °C whilst ¹H NMR spectra (500 MHz) were recorded over 4 hours.

Thermolysis of 4: ^1H NMR Kinetics (Figure 2.10):

4 (16.8 mg, 0.03 mmol) was dissolved in d_8 -toluene (0.6 mL) in an NMR tube under an atmosphere of N_2 . The NMR tube was loaded into an NMR spectrometer ($t = 0$) and spun at 65 °C whilst ^1H NMR spectra (500 MHz) were recorded at regular intervals.

This process was repeated with **3** (8.6 mg, 0.03 mmol) being added before the NMR tube was inserted into the spectrometer.

$(\text{SiPr})\text{Pd}(\eta^1\text{-1-PhC}_3\text{H}_4)(\eta^5\text{-C}_5\text{H}_5)$ **5**:



A solution of **3** (43 mg, 0.15 mmol) and **4** (84 mg, 0.15 mmol) in toluene (3 mL) was stirred at 65 °C for 4 hours under an atmosphere of N_2 . Upon cooling, the reaction was concentrated *in vacuo*, re-dissolved in Et_2O (3 mL) and stirred for 15 minutes. The solution was then filtered and concentrated *in vacuo*. The resulting oily solid was suspended in hexane (3 mL), again concentrated *in vacuo* and then triturated with hexane (3×0.6 mL). After drying *in vacuo* (0.5 torr), the title compound **5** (61 mg, 0.15 mmol, 60 %) as a red powder.

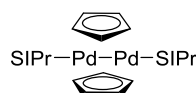
Crystals of suitable quality for analysis by single-crystal X-ray diffraction were obtained by the slow evaporation of a Et_2O solution of **5** (Table 5.1).

^1H NMR (500 MHz, d_8 -toluene): δ 7.28-6.98 (m, 11H, Ar, obscured by residual protiated toluene), 6.06 (d, $^3J_{\text{HH}} = 15.4$ Hz, 1H, $\text{CH}=\text{CHPh}$), 5.68 (dt, $^3J_{\text{HH}} = 15.4$ Hz, $^3J_{\text{HH}} = 8.8$ Hz, 1H, $\text{CH}=\text{CHPh}$), 5.10 (s, 5H, Cp), 3.48 (s, 4H, $\text{NCH}_2\text{CH}_2\text{N}$) 3.26 (sept, $^3J_{\text{HH}} = 6.8$ Hz, 4H, $\text{CH}(\text{CH}_3)_2$) 2.41 (d, $^3J_{\text{HH}} = 8.8$ Hz, 2H, PdCH_2CH), 1.44 (d, $^3J_{\text{HH}} = 6.8$ Hz, 12H, $\text{CH}(\text{CH}_3)_2$), 1.11 (d, $^3J_{\text{HH}} = 6.8$ Hz, 12H, $\text{CH}(\text{CH}_3)_2$). **$^{13}\text{C}\{^1\text{H}\}$ NMR (101 MHz, d_8 -toluene):** δ 211.6 (NCN), 147.2 (Ar), 141.29 ($\text{CH}=\text{CHPh}$), 141.26 (Ar), 137.9 (Ar), 129.3 (Ar), 128.6 (Ar, obscured by d_8 -toluene), 125.2 (Ar), 124.70 (Ar), 124.67 (Ar), 119.6 ($\text{CH}=\text{CHPh}$), 98.3 (Cp), 53.4 ($\text{NCH}_2\text{CH}_2\text{N}$), 29.1, 26.3, 23.4, 4.2 (PdCH_2).

Table 5.1 Crystal data and structure refinement for 5

Colour, habit	Red blocks
Empirical Formula	C ₄₁ H ₅₂ N ₂ Pd
<i>M</i>	679.31
Crystal system	Triclinic
Space group	P $\bar{1}$
<i>a</i> /Å	8.9642(2)
<i>b</i> /Å	12.4779(3)
<i>c</i> /Å	16.8810(4)
α /°	70.7220(10)
β /°	86.0630(10)
γ /°	86.7090(10)
<i>V</i> /Å ³	1776.92(7)
<i>Z</i>	2
μ /mm ⁻¹	0.552
<i>T</i> /K	100(2)
Reflections (measured/unique/observed)	58961/8185/7713
<i>R</i> _{int}	0.0222
<i>R</i> ₁ (observed reflections) [<i>I</i> > 2σ (<i>I</i>)]	0.0201
w <i>R</i> ₂ (all reflections)	0.0505

(SIPr)₂Pd₂(μ-C₅H₅)₂ 6:



A solution of **3** (43 mg, 0.15 mmol) and **4** (84 mg, 0.15 mmol) in toluene (3 mL) was stirred at 65 °C for 4 hours under an atmosphere of N₂. Upon cooling, the reaction was concentrated *in vacuo*, re-dissolved in Et₂O (2.5 mL) and stirred for 47 hours. The solution was then cooled to -80 °C and cannula filtered. The remaining solid was washed with cold Et₂O (3 × 0.2 mL), dried *in vacuo*. Next, toluene (2 mL) was added and the solution filtered through a pad of Celite. The eluent was concentrated *in vacuo* to give a sticky yellow solid which was triturated with hexane (2 × 0.5 mL). After drying *in vacuo* (0.5 torr), the title compound **6** was afforded as a yellow solid (11 mg, 13 %).

¹H NMR (400 MHz, d₈-toluene): δ 7.14-7.02 (m, 12H, Ar, obscured by residual protiated toluene), 4.32 (s, 10H, Cp), 3.65 (sept, ³J_{HH} = 6.8 Hz, 4H, CH(CH₃)₂), 3.64 (s, 4H, NCH₂CH₂N), 1.22 (d, ³J_{HH} = 6.8 Hz, 12H, CH(CH₃)₂), 1.19 (d, ³J_{HH} = 6.8 Hz, 12H, CH(CH₃)₂). **¹³C{¹H} NMR (101 MHz, d₈-toluene):** δ 213.4 (NCN), 146.9 (Ar), 139.1 (Ar), 128.6 (Ar, obscured by d₈-toluene), 124.5 (Ar), 86.9 (Cp), 54.3 (NCH₂CH₂N), 28.8, 26.3, 23.9. **HRMS (m/z, EI⁺):** calcd. for C₆₄H₈₈N₄¹⁰⁶Pd₂ [M]⁺: 1124.50730; found: 1124.50698.

5.2.5 Reactions of (SIPr)Pd(η^1 -1-PhC₃H₄)(η^5 -C₅H₅)

Activity of **5** in a Suzuki-Miyaura Cross-Coupling Reaction at 80 °C (Figure 2.11):

Caesium carbonate (0.33 g, 1 mmol), 4-fluorophenylboronic acid (105 mg, 0.75 mmol) and 1,4-dioxane were added to **5** (8.5 mg, 0.013 mmol) or Pd(dba)₂ (7.2 mg, 0.013 mmol) and SIPr.HCl (5.3 mg, 0.013 mmol), with stirring, under an atmosphere of N₂. 3,5-Bis(trifluoromethyl)bromobenzene (86 µL, 0.5 mmol) was then added and the reaction immediately heated to 80 °C (*t* = 0). Aliquots (0.1 mL) of the mixture were removed at time intervals over 2.5 hours and were analysed by ¹⁹F NMR spectroscopy (283 MHz, lock off) after being diluted with 1,4-dioxane (0.5 mL).

Activity of **5** in a Room Temperature Suzuki-Miyaura Cross-Coupling Reaction (Scheme 2.27):

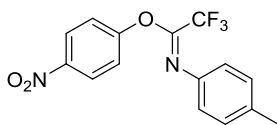
Potassium *tert*-butoxide (62 mg, 0.55 mmol), 4-fluoroboronic acid (74 mg, 0.53 mmol) and **5** (3.4 mg, 5×10⁻⁶ mol) were dissolved in 2-propanol (0.5 mL) under an atmosphere of N₂. Bis(trifluoromethyl)bromobenzene (86 µL, 0.5 mmol) was then added with stirring. After 3.5 hours an aliquot (0.1 mL) was removed, diluted in 2-propanol (0.5 mL) and analysed by ¹⁹F NMR spectroscopy (283 MHz, lock off).

Attempted Rearrangement of *O*-Aryl Trichloroacetimidates **1** Using **5** (Scheme 2.28):

The representative procedures described in Section 5.2.3 for the use of Pd(P^{*t*}Bu₃)₂ were followed.

5.2.6 Preparation of O-Aryl-N-(4-methylphenyl) Trifluoroacetimidates

O-(4-Nitrophenyl)-N-(4-methylphenyl) Trifluoroacetimidate **7b** (Scheme 2.30):

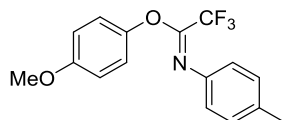


Triphenylphosphine (7.87 g, 30 mmol) and triethylamine (1.67 mL, 12 mmol) were dissolved in CCl₄ (5 mL, 50 mmol) under an atmosphere of N₂. This solution was cooled to 0 °C and trifluoroacetic acid (0.77 mL, 10 mmol) was added dropwise over 2 minutes. After stirring for 10 minutes, a solution of 4-methylaniline (1.29 g, 12 mmol) in CCl₄ (5 mL, 50 mmol) was added over 10 minutes. The reaction was allowed to warm to room temperature and was then heated to 90 °C for 3 hours. Next, the mixture was cooled and a solution of 4-nitrophenol (1.53 g, 11 mmol) and triethylamine (1.53 mL, 11 mmol) in DCM (5 mL) was added over 10 minutes. The reaction was stirred at room temperature for 16 hours and then diluted in hexane (20 mL) and filtered. The retentate was washed with additional hexane (2 × 10 mL) and the combined hexane fractions were concentrated *in vacuo*. The resulting oil was purified *via* column chromatography (19:1 petroleum ether (b.p.: 60-80 °C):Et₂O) to afford the title compound **7b** (2.66 g, 8.2 mmol, 82 %) as a pale yellow oil.

The title compound **7b** appeared to exist as a mixture of two interconverting isomers in an approximate 2:1 ratio (by ¹⁹F NMR spectroscopy) and displayed very broad NMR peaks due to its conformational mobility.

¹H NMR (400 MHz, CDCl₃): δ 8.21-8.10 (br app d, *J*_{HH} = 7.2 Hz, 2H, Ar), 7.21-6.97 (br m, 4H, Ar [including br app d, *J*_{HH} = 8.1 Hz, 2H]), 6.87 (br app s, 2H, Ar), 2.26 (s, 3H, CH₃). **¹³C{¹H} NMR (101 MHz, CDCl₃):** δ 156.9 (br, C=N), 144.6 (br, Ar), 140.2 (br, Ar) 139.0 (br, Ar), 136.6 (br, Ar), 129.6 (Ar), 125.6 (Ar), 121.7 (br, Ar), 118.8 (br, Ar), 116.8 (br q, ¹*J*_{CF} = 280.6 Hz, CF₃), 20.9 (CH₃). **¹⁹F NMR (377 MHz, CDCl₃):** δ -65.30 (br s, 1F, CF₃), -71.47 (br s, 2F, CF₃). ***ν*_{max} (cm⁻¹, neat):** 3085 (w), 2926 (w), 2859 (w), 1705 (m, C=N), 1616 (w), 1590 (m), 1523 (m), 1506 (m), 1488 (m), 1345 (m), 1319 (m), 1215 (s), 1152 (s), 1112 (s), 1070 (s), 1011 (w), 917 (w), 888 (w), 849 (m), 822 (m), 747 (m), 711 (m). **MS (*m/z*, EI⁺):** calcd. for C₁₅H₁₁F₃N₂O₃ [M]⁺: 324.07; found: 324.1.

O-(4-Methoxyphenyl)-N-(4-methylphenyl) Trifluoroacetimidate **7a** (Scheme 2.30):



Following the procedure described above for **7b**, the title compound **7a** (187 mg, 0.60 mmol, 60 %) was afforded as a pale yellow oil.

The title compound **7a** appeared to exist as a mixture of two interconverting isomers in an approximate 1:1 ratio (by ^{19}F NMR spectroscopy).

^1H NMR (300 MHz, CDCl_3): δ 7.10-6.90 (br m, 4H, Ar [including br app d, $J_{\text{HH}} = 8.2$ Hz, 2H]), 6.80 (br app s, 4H, Ar), 3.76 (s, 3H, OCH_3), 2.27 (s, 3H, CH_3). **$^{13}\text{C}\{^1\text{H}\}$ NMR (101 MHz, CDCl_3):** δ 129.3 (Ar), 114.6 (Ar), 55.7 (OCH_3), 21.0 (CH_3). **^{19}F NMR (283 MHz, CDCl_3):** δ -65.09 (br s, 1.5F, CF_3), -70.11 (br s, 1.5F, CF_3).

5.2.7 Catalyst Screening

Transition Metal-NHC/Phosphine Precatalysts and *In Situ* Transition Metal-Phosphine Catalyst Systems (Table 2.5, Table 2.6 and Table 2.7)

Representative Procedure (Table 2.7, entry 3):

Bis(1,5-cyclooctadiene)nickel (2.8 mg, 0.01 mmol) and tricyclohexylphosphine (5.6 mg, 0.02 mmol) were dissolved in toluene (0.5 mL) under an atmosphere of N_2 . After stirring for 10 minutes, a solution of 4-phenoxy quinazoline **10a** (0.1 mmol) in toluene (0.5 mL; 0.2 M stock) was added and the solution was stirred at 100 $^\circ\text{C}$ for 18 hours. Once cooled, the reaction was filtered through a short pad of Celite, eluting with toluene (3×1 mL). The filtrate was concentrated *in vacuo* and analysed by ^1H NMR spectroscopy (500 MHz, CDCl_3). Only **10a** was detected.

***In Situ* Transition Metal-NHC Catalyst Systems (Table 2.6 and Table 2.7)**

Representative Procedure (Table 2.6, entry 18):

Chloro(1,5-cyclooctadiene)rhodium dimer (3.1 mg, 6.3×10^{-6} mol), IMes.HCl (4.3 mg, 1.25×10^{-5} mol) and caesium fluoride (7.6 mg, 5×10^{-5} mol) were stirred in toluene (0.5 mL) under an atmosphere of N_2 for 30 minutes. A solution of **7b** (0.25 mmol) in toluene (0.5 mL; 0.5 M stock) was then added and the reaction was stirred at 120 $^\circ\text{C}$ for 19.5 hours. Once cooled, the reaction was concentrated *in vacuo* and analysed by ^{19}F and ^1H

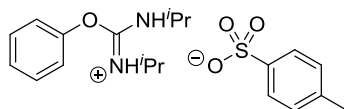
NMR spectroscopy (376/400 MHz, CDCl₃). Only **7b**, 4-nitrophenol and *N*-(4-methylphenyl) trifluoroacetamide were detected.

5.3 Experimental Details Relevant to Chapter 3

5.3.1 Synthesis of O-Phenyl-*N,N'*-dialkyl Isoureas

Preparation of Salts of O-Phenyl-*N,N'*-dialkyl Isoureas

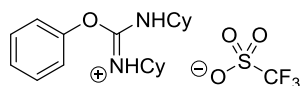
O-Phenyl-*N,N'*-diisopropyl Isourea *p*-Toluenesulfonic Acid Salt [**15c'**][OTs]:



Phenol (0.47 g, 5 mmol) and DIC (2.32 mL, 15 mmol) were heated at 100 °C for 16 hours under an atmosphere of N₂ with stirring. Once cooled, the reaction was diluted in DCM (5 mL) and loaded onto a short column of silica-gel. DCM was passed through the column until the elution of phenol had halted (as determined by TLC, approx. 400 mL DCM). Et₂O (approx. 100 mL) was used to flush the remaining material off the column and was then removed *in vacuo*. The resulting residue had petroleum ether (b.p.: 40-60 °C, 20 mL) added and was filtered. The filtrate was concentrated *in vacuo* to yield the crude isourea (0.71 g, 3.2 mmol) which was dissolved in DCM (20 mL) and had *p*-toluenesulfonic acid (monohydrate; 0.61 g, 3.2 mmol) added portion-wise over 5 minutes with rapid stirring. After 1 hour, the mixture was further diluted with DCM (10 mL) and washed with water (3 × 20 mL). The organic phase was dried (MgSO₄), filtered and concentrated *in vacuo*. Trituration of the resulting oil with Et₂O (10 mL) caused it to solidify. The solid was collected by Büchner filtration, washed with Et₂O (3 × 10 mL) and air dried. Recrystallisation from *tert*-butyl methyl ether afforded the title compound [**15c'**][OTs] (0.52 g, 1.3 mmol, 26 %) as colourless needles.

¹H NMR (400 MHz, CDCl₃): δ 10.30 (br s, 2H, NH), 7.83 (app d, *J*_{HH} = 8.2 Hz, 2H, Ar(OTs)), 7.46 (m, 2H, Ph), 7.28 (m, 1H, Ph), 7.20 (app d, *J*_{HH} = 8.2 Hz, 2H, Ar(OTs)), 7.09 (m, 2H, Ph), 3.68 (br m, 2H, CH(CH₃)₂), 2.37 (s, 3H, CH₃), 1.20 (d, ³*J*_{HH} = 6.6 Hz, 12H, CH(CH₃)₂). **¹³C{¹H} NMR (101 MHz, CDCl₃):** δ 156.9 (C=N), 153.2 (Ar), 142.3 (Ar), 140.1 (Ar), 130.9 (Ar), 128.9 (Ar), 126.12 (Ar), 126.07 (Ar), 115.8 (Ar), 46.3 (CH(CH₃)₂), 22.6 (CH(CH₃)₂), 21.5 (ArCH₃). **ν_{max} (cm⁻¹, neat):** 3177 (w, NH), 2979 (w), 2872 (w), 1668 (m, C=N), 1572 (m), 1487 (m), 1382 (m), 1219 (m), 1177 (m), 1123 (m), 1035 (m), 1012 (m), 815 (m), 754 (m), 679 (s), 561 (m). **HRMS (*m/z*, EI⁺):** calcd. for C₁₃H₂₁N₂O [M]⁺: 221.16484; found: 221.16450. **m.p. (°C):** 91-92.

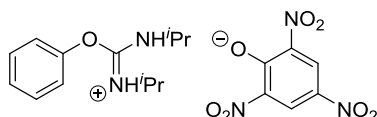
O-Phenyl-*N,N'*-dicyclohexyl Isoourea Trifluoromethanesulfonic Acid Salt [**15b'**][OTf]:



After heating a mixture of phenol (0.47 g, 5 mmol) and DCC (3.1 g, 15 mmol) at 100 °C for 18 hours the crude isourea (0.67 g, 2.2 mmol) was obtained as described above for [**15c'**][OTs]. This material was dissolved in petroleum ether (b.p.: 40-60 °C, 10 mL) and had a solution of trifluoromethanesulfonic acid (0.21 mL, 2.4 mmol) in Et₂O (5 mL) added over 5 minutes with rapid stirring. A colourless precipitate formed throughout the addition. The suspension was stirred for a further 30 minutes. The solid was then isolated by Büchner filtration, washed with Et₂O (3 × 10 mL) and air dried. Recrystallisation was achieved by layering a hot, saturated DCM solution with Et₂O and afforded the title compound [**15b'**][OTf] (0.77 g, 1.7 mmol, 34 %) as colourless needles.

¹H NMR (400 MHz, CDCl₃): δ 8.95 (br s, 2H, NH), 7.50 (app t, *J*_{HH} = 8.0 Hz, 2H, Ar), 7.35 (br m, 1H, Ar), 7.10 (app d, *J*_{HH} = 8.0 Hz, 2H, Ar), 3.31 (br s, 2H, NCH), 1.92-0.93 (br m, 20H, CH₂). **¹³C{¹H} NMR (101 MHz, CDCl₃):** δ 157.2 (br, C=N), 153.3 (Ar), 131.1 (Ar), 126.6 (br, Ar), 120.4 (q, *J*_{CF} = 318.7 Hz, CF₃), 116.1 (br, Ar), 53.6 (br, NCH), 32.5 (br, CH₂), 24.7 (2 × overlapping br s, 2C, CH₂). ***ν*_{max} (cm⁻¹, neat):** 3216 (w, NH), 3094 (w), 2941 (m), 2860 (w), 1662 (m, C=N), 1593 (m), 1486 (m), 1281 (m), 1240 (s), 1225 (m), 1183 (m), 1154 (s), 1031 (s), 761 (m), 670 (m), 635 (s), 515 (m). **HRMS (*m/z*, EI⁺):** calcd. for C₁₉H₂₉N₂O [M]⁺: 301.22744; found: 301.22760. **m.p. (°C):** 150.

O-Phenyl-*N,N'*-diisopropyl Isoourea Picric Acid Salt [**15c'**][OPic]:



After heating a mixture of phenol (0.94 g, 10 mmol) and DIC (0.77 mL, 5 mmol) at 100 °C for 21 hours the crude isourea (0.76 g, 3.5 mmol) was obtained as described for [**15c'**][OTs]. This material was dissolved in *i*PrOH (5 mL) and added to a solution of picric acid (0.8 g, 3.5 mmol) in *i*PrOH (75 mL) over 5 minutes with rapid stirring. A yellow precipitate formed throughout the addition. The suspension was stirred for a further 30 minutes and the solid subsequently isolated by Büchner filtration. After washing with *i*PrOH (3 × 10 mL) and air drying, the title compound (0.99 g, 2.2 mmol, 44 %) was afforded as a bright yellow powder.

^1H NMR (400 MHz, $\text{d}_6\text{-DMSO}$): δ 8.98 (br s, 2H, NH), 8.58 (s, 2H, Ar(OPic)), 7.53 (app t, $J_{\text{HH}} = 7.6$ Hz, 2H, Ph), 7.36 (app t, $J_{\text{HH}} = 7.6$ Hz, 1H, Ph), 7.29 (app d, $J_{\text{HH}} = 7.6$ Hz, 2H, Ph), 3.96 (br s, 2H, $\text{CH}(\text{CH}_3)_2$), 1.20 (br s, 12H, $\text{CH}(\text{CH}_3)_2$). **$^{13}\text{C}\{^1\text{H}\}$ NMR (126 Hz, $\text{d}_6\text{-DMSO}$):** δ 160.8 (C=N), 155.4 (Ar), 151.8 (Ar), 141.8 (Ar), 130.5 (Ar), 126.4 (Ar), 125.1 (Ar), 124.1 (Ar), 118.7 (Ar), 45.4 (br app d, $\text{CH}(\text{CH}_3)_2$), 21.7 (br app d, $\text{CH}(\text{CH}_3)_2$). **ν_{max} (cm^{-1} , neat):** 3196 (w, NH), 3063 (w), 2978 (w), 1677 (m, C=N), 1633 (m), 1535 (m), 1463 (m), 1317 (m), 1271 (m), 1192 (m), 1164 (m), 1129 (m), 1077 (w), 926 (w), 912 (w), 804 (w), 742 (m), 709 (w), 685 (w). **HRMS (m/z , EI^+):** calcd. for $\text{C}_{13}\text{H}_{21}\text{N}_2\text{O}$ [M] $^+$: 221.16484; found: 221.16435.

Reactions Between Phenol and DIC: ^1H NMR Monitoring

Probing the Reaction Mechanism (Figure 3.2):

Phenol (94.1 mg, 1 mmol) was dissolved in CDCl_3 (4 mL) under an atmosphere of N_2 . DIC (150 μL , 0.97 mmol) was added ($t = 0$) and the resulting mixture very briefly stirred. An aliquot of this solution (0.6 mL) was then transferred to each of three J. Young valve NMR tubes. The ^1H NMR spectra (400 MHz) of these samples were repeatedly recorded between $t = 20$ minutes to $t = 520$ hours.

At $t = 288$ hours, one of these samples had additional phenol (14.1 mg, 0.15 mmol) added, whilst a second had additional DIC (23 μL , 0.15 mmol) added.

From $t = 360$ hours to $t = 520$ hours, the sample containing additional DIC was heated to 60 $^\circ\text{C}$ in an oil bath during the intervals between ^1H NMR experiments.

Values for $[\text{DIC}]_t$ were extracted from ^1H NMR spectra using MestReNova. DynoChem was used to fit the mechanistic model described in Scheme 3.12 to this data by allowing freedom in k_1 , k_{-1} and k_{-2} . The value of k_2 was arbitrarily fixed at $1 \times 10^3 \text{ M}^{-1} \text{ s}^{-1}$. The fitted rate constants (Scheme 3.12) were used to generate the simulated data displayed in Figure 3.2.

Data for *O*-phenyl-*N,N'*-diisopropyl isourea **12c'**: **^1H NMR (400 MHz, CDCl_3):** δ 7.31 (app t, $J_{\text{HH}} = 7.5$ Hz, 2H, Ar), 7.07 (app t, $J_{\text{HH}} = 7.5$ Hz, 1H, Ar), 7.01 (app d, $J_{\text{HH}} = 7.5$ Hz, 2H, Ar), 3.74 (sept, $^3J_{\text{HH}} = 6.4$ Hz, 2H, $\text{CH}(\text{CH}_3)_2$), 1.11 (d, $^3J_{\text{HH}} = 6.4$ Hz, 12H, $\text{CH}(\text{CH}_3)_2$).

Effect of Additives (Figure 3.3):

Phenol (94.4 mg, 1 mmol) was dissolved in CDCl_3 (4 mL) under an atmosphere of N_2 . DIC (136 μL , 0.88 mmol) was added ($t = 0$) and the resulting mixture very briefly stirred. An

aliquot of this solution (0.6 mL) was then added to each of five J. Young valve NMR tubes, four of which contained different additives (0.03 mmol). The ^1H NMR spectra (400 MHz) of these samples were repeatedly recorded between $t = 30$ minutes and $t = 404$ hours.

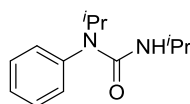
Additives (0.03 mmol): triethylamine (4.2 μL); 4-dimethylaminopyridine (3.7 mg); *p*-toluenesulfonic acid (anhydrous; 5.2 mg); copper(I) chloride (3.0 mg).

Values for $[\text{DIC}]_t$ were extracted from ^1H NMR spectra using MestReNova.

5.3.2 Solvolysis of Isourea Salts

Preparation of Reference Compounds

N-Phenyl-*N,N'*-diisopropyl Urea **13c'**:

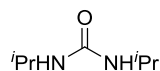


Isopropyl isocyanate (0.20 mL, 2 mmol) was diluted in Et_2O (2 mL) under an N_2 atmosphere. *N*-Isopropyl aniline (0.29 mL, 2 mmol) was then added dropwise over 2 minutes with stirring. After 30 minutes, the reaction was diluted with EtOAc (10 mL) and washed with HCl (10 % aqueous; 10 mL) and water (2×10 mL). The organic layer was dried (MgSO_4), filtered and concentrated *in vacuo*. The resulting crude solid was recrystallised from petroleum ether (b.p.: 60-80 $^\circ\text{C}$) to afford the title compound **13c'** (127 mg, 0.58 mmol, 29 %) as colourless needles.

^1H NMR (400 MHz, CDCl_3): δ 7.45-7.36 (m, 3H, Ar), 7.16-7.13 (m, 2H, Ar), 4.88 (sept, $^3J_{\text{HH}} = 6.8$ Hz, 1H, $\text{CH}(\text{CH}_3)_2$), 3.93 (sept, $^3J_{\text{HH}} = 6.5$ Hz, 1H, $\text{CH}(\text{CH}_3)_2$), 3.62 (br s, 1H, NH), 1.04 (d, $^3J_{\text{HH}} = 6.8$ Hz, 6H, $\text{CH}(\text{CH}_3)_2$), 0.99 (d, $^3J_{\text{HH}} = 6.5$ Hz, 6H, $\text{CH}(\text{CH}_3)_2$). **$^{13}\text{C}\{^1\text{H}\}$ NMR (101 Hz, CDCl_3):** δ 156.5 (C=O), 138.2 (Ar), 131.4 (Ar), 129.6 (Ar), 128.3 (Ar), 46.3 ($\text{CH}(\text{CH}_3)_2$), 42.4 ($\text{CH}(\text{CH}_3)_2$), 23.5 ($\text{CH}(\text{CH}_3)_2$), 21.8 ($\text{CH}(\text{CH}_3)_2$). **ν_{max} (cm^{-1} , neat):** 3438 (w, NH), 2964 (w), 2930 (w), 2876 (w), 1647 (m, C=O), 1489 (m), 1466 (m), 1452 (m), 1321 (m), 1267 (m), 1254 (m), 1170 (m), 1116 (m), 760 (m), 709 (m), 585 (m). **HRMS (m/z , EI^+):** calcd. for $\text{C}_{13}\text{H}_{20}\text{N}_2\text{O}$ $[\text{M}]^+$: 220.15701; found: 220.15596. **m.p. ($^\circ\text{C}$):** 66-67.

The data obtained is consistent with that reported in the literature.²⁰⁷

N,N'-Diisopropyl Urea:

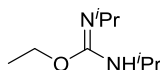


A solution of DIC (155 μ L, 1 mmol) in petroleum ether (b.p.: 40-60 $^{\circ}$ C, 4 mL) had glacial acetic acid (150 μ L, 2.6 mmol) added dropwise over 2 minutes, with rapid stirring. A colourless precipitate formed throughout the addition. After 1 hour, the solid was isolated by Büchner filtration, washed with petroleum ether (b.p.: 40-60 $^{\circ}$ C, 3 \times 5 mL) and air dried. Recrystallisation from EtOH afforded the title compound (100 mg, 0.69 mmol, 69 %) as colourless needles.

^1H NMR (400 MHz, d_6 -DMSO): δ 5.47 (d, $^3J_{\text{HH}}$ = 7.6 Hz, 2H, NH), 3.63 (dsept, $^3J_{\text{HH}}$ = 7.6 Hz and 6.5 Hz, 2H, $\text{CH}(\text{CH}_3)_2$), 1.00 (d, $^3J_{\text{HH}}$ = 6.5 Hz, 12H, $\text{CH}(\text{CH}_3)_2$). **$^{13}\text{C}\{^1\text{H}\}$ NMR (101Hz, d_6 -DMSO):** δ 156.8 (C=O), 40.7 ($\text{CH}(\text{CH}_3)_2$), 23.3 ($\text{CH}(\text{CH}_3)_2$). **ν_{max} (cm^{-1} , neat):** 3341 (w, NH), 2967 (w), 2873 (w), 1616 (m, C=O), 1556 (m), 1464 (w), 1384 (w), 1360 (w), 1325 (w), 1244 (m), 1166 (m), 1129 (m), 628 (m). **MS (m/z , EI $^{+}$):** calcd. for $\text{C}_7\text{H}_{16}\text{N}_2\text{O}$ [M] $^{+}$: 144.13; found: 144.1.

The data obtained is consistent with that reported in the literature.²⁹⁵

O-Ethyl-*N,N'*-diisopropyl Isourea **17**:



A suspension of copper(I) chloride (5 mg, 0.05 mmol) in EtOH (1 mL) had DIC (155 μ L, 1 mmol) added with stirring. After 21 hours, the mixture was diluted in brine (10 mL) and extracted with Et₂O (3 \times 10 mL). The combined organic fractions were dried (MgSO₄), filtered and concentrated to approx. 5 mL *in vacuo* (750 mbar, 40 $^{\circ}$ C). The remaining solvent was removed by passing a stream of nitrogen over the solution to afford the title compound **17** (26 mg, 0.15 mmol, 15 %) as a pale yellow oil.

The product was observed to darken over time to a pale green/blue colour, most likely indicating the presence of minor quantities of copper-based contaminants.

^1H NMR (400 MHz, d_6 -DMSO): δ 4.84 (br s, 1H, NH), 3.93 (q, $^3J_{\text{HH}}$ = 7.0 Hz, 2H, OCH₂), 3.64 (br m, 1H, $\text{CH}(\text{CH}_3)_2$), 3.34 (br m, 1H, $\text{CH}(\text{CH}_3)_2$), 1.13 (t, $^3J_{\text{HH}}$ = 7.0 Hz, 3H, CH₂CH₃), 1.04 (br d, $^3J_{\text{HH}}$ = 6.4 Hz, 6H, $\text{CH}(\text{CH}_3)_2$), 0.95 (br d, $^3J_{\text{HH}}$ = 6.1 Hz, 6H, $\text{CH}(\text{CH}_3)_2$). **$^{13}\text{C}\{^1\text{H}\}$ NMR (101Hz, d_6 -DMSO):** δ 150.4 (C=N), 59.5 (OCH₂), 44.4 (br, $\text{CH}(\text{CH}_3)_2$), 42.7 (br,

CH(CH₃)₂), 24.7 (br, CH(CH₃)₂), 23.4 (br, CH(CH₃)₂), 14.5 (CH₂CH₃). ν_{max} (cm⁻¹, neat): 2964 (m, NH), 2931 (w), 2871 (w), 1659 (s, C=N), 1464 (w), 1448 (w), 1366 (m), 1311 (s), 1169 (m), 1123 (w), 1085 (m), 1026 (w), 711 (w), 609 (w), 577 (w), 494 (w). HRMS (*m/z*, EI⁺): calcd. for C₉H₂₀N₂O [M]⁺: 172.15701; found: 172.15763.

Preparative-Scale Solvolysis of [15c']⁺[OPic] (Scheme 3.17)

A solution of KOH (28.1 mg or 281 mg, 0.5 or 5 mmol) in water (35 mL) and EtOH (9 mL) had [15c']⁺[OTs] (22.5 mg, 0.05 mmol) in EtOH (6 mL) added with rapid stirring. After 44 hours, the reaction was extracted with EtOAc (2 × 25 mL). The organic phase had d₆-DMSO (1 mL) added and was then carefully concentrated by passing a stream of nitrogen over the solution whilst it was rapidly stirred. The resulting solution was analysed by ¹H NMR spectroscopy (400 MHz) without further purification. Potassium phenoxide, DIPU, picric acid and **17** were the only species detected.

UV-Vis Kinetics

Stock Solutions:

Stock solutions were prepared using volumetric glassware. A single stock solution of a given concentration of reagent was used throughout the kinetic experiments. Dilute stock solutions of isourea salts (0.2 and 0.02 mM) were prepared by sequential-dilution of a 2 mM stock solution. The volumes of stock solutions used in UV-Vis experiments were measured using Gilson pipettes.

Background Spectra:

Background spectra were recorded after combining a stock solution of 6:4 EtOH:water (1 mL) with an aqueous KOH/KCl stock solution (1 mL) of the appropriate concentration. Background spectra were subsequently subtracted from the UV-Vis absorption spectra of analytes in solutions of the same composition.

Reference Spectra (Figure 3.7 and Figure 3.8):

UV-Vis absorption spectra were recorded immediately after combining stock solutions of the reference compounds (2×10⁻⁷ mol) in 6:4 EtOH:water (1 mL; 0.2 mM stock) with aqueous KOH/KCl (1 mL, 0.2 mmol/1.8 mmol; 0.2/1.8 M stock). The stock solution of DIC in 6:4 EtOH:water was used immediately after preparation.

Representative Procedure for a Kinetic Experiment (Figure 3.6, Figure 3.9 and Table 3.2):

Aqueous KOH/KCl (1 mL, 0.2 mmol/1.8 mmol; 0.2/1.8 M stock) was added to **15c'** (2×10^{-8} mol) in 6:4 EtOH:water (1 mL; 0.02 mM stock) in a cuvette. The cuvette was sealed with a stopper and briefly shaken. The UV-Vis spectrum of the solution was recorded at 20 second time intervals for 10,000 seconds.

Data Analysis:

Kinetic Studio was used to extract values for the absorbance at 290 nm as a function of time. The Microsoft Excel Solver Add-in was used to fit the following rate equation to this data: $d(A)/dt = k[\mathbf{12c'}][\text{KOH}]$ (where A = absorbance and $A_t \propto [\text{PhOH}]_t$), by assuming $[\text{KOH}] = 0.1$ M remains constant and solving the following equation for k : $A_t = -B \times e^{(-kt)} + C$ (where B and C are arbitrary fitting variables).

¹H NMR Kinetics

KOH/D₂O Stock Solutions:

A pellet of KOH was weighed under N₂. The appropriate volume of D₂O was then added to afford a stock solution of the desired concentration. Stock solutions were prepared immediately prior to performing kinetic reactions and were only used once.

Solvolysis of [**15c'**][OTs] (Scheme 3.19 and Figure 3.11):

[**15c'**][OTs] (0.006 mmol, 2.36 mg) was dissolved in d₆-EtOH (0.18 mL) in an NMR tube. KOH (0.06 mmol) in D₂O (0.42 mL; 0.143 M stock) was then added ($t = 0$) and the solution briefly shaken. The NMR tube was loaded into an NMR spectrometer and spun at 25 °C whilst ¹H NMR spectra (400 MHz) were recorded at regular time intervals.

Values for $[\text{PhOK}]_t$ and $[\text{DIC}]_t$ were extracted from ¹H NMR spectra using MestReNova. DynoChem was used to fit the mechanistic model described in Scheme 3.20 to this data by allowing freedom in k_{ii} and k_{iii} . The fitted rate constants (Scheme 3.20) were used to generate the simulated data displayed in Figure 3.11 and Figure 3.12.

Representative Procedure for the Solvolysis of DIC (Scheme 3.22 and Figure 3.13):

N-Phenyl urea (internal standard; 1.17 mg, 8.6×10^{-6} mol) and DIC (0.89 μL, 5.7×10^{-6} mol; calculated relative to *N*-phenyl urea using ¹H NMR integral analysis) were added to an NMR tube and dissolved in d₆-EtOH (0.18 mL). KOH (0.15 mmol) in D₂O (0.42 mL; 0.357 M stock) was then added ($t = 0$) and the solution briefly shaken. The NMR tube was

loaded into an NMR spectrometer and spun at 25 °C whilst ^1H NMR spectra (400 MHz) were recorded at regular time intervals.

Values for $[\text{DIC}]_t$ were extracted from ^1H NMR spectra using MestReNova. The Microsoft Excel Solver Add-in was used to fit the following rate equation to this data: $-\text{d}[\text{DIC}]/\text{dt} = k[\text{DIC}][\text{KOH}]$, by assuming $[\text{KOH}]$ remains constant and solving the following equation for k : $[\text{DIC}]_t = [\text{DIC}]_0 \times e^{(-kt)} + C$ (where C is an arbitrary fitting variable).

5.3.3 Elimination of Phenol and DIC from O-Phenyl-*N,N'*-diisopropyl Isoourea

Reaction of [15c'] [OTs] with Potassium *tert*-Butoxide in DMSO (Scheme 3.23):

Potassium *tert*-Butoxide (22.4 mg, 0.2 mmol) was dissolved in DMSO (0.5 mL) under an atmosphere of N_2 . A solution of [15c'] [OTs] (39.3 mg, 0.1 mmol) in DMSO (0.5 mL) was then added with rapid stirring. After 3.5 hours an aliquot (0.6 mL) the solution was removed and analysed by ^1H NMR spectroscopy (400 MHz, lock off). The complete conversion of 12c' to potassium phenoxide and DIC was confirmed by re-analysis of the sample after the addition of authentic samples of these products.

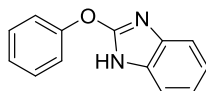
Reaction of [15c'] [OTs] with Sodium Hydride in THF:

Sodium hydride (9.6 mg, 0.4 mmol) was suspended in THF (1 mL) at -78 °C under an atmosphere of N_2 . A solution of [15c'] [OTs] (78.5 mg, 0.2 mmol) in THF (1 mL) was cooled to -78 °C and then added with rapid stirring. After 20 minutes at -78 °C, the solution was allowed to warm to room temperature. As the suspension warmed, its turbidity increased and a gas was evolved. The reaction was stirred for a further 22 hours at room temperature and then an aliquot was removed (0.2 mL), filtered and diluted in CDCl_3 (0.5 mL) for ^1H NMR analysis (400 MHz). Phenol, DCC and 12c' were the only species detected. The remaining reaction mixture was concentrated *in vacuo*, suspended in HCl (10 % aqueous; 10 mL) and extracted with EtOAc (3 \times 5 mL). The organic phase was dried (MgSO_4), filtered and concentrated *in vacuo* to afford an oil which was analysed by ^1H NMR spectroscopy (400 MHz, CDCl_3). Phenol and DIPU were the only species detected.

5.3.4 *N*-Heterocyclic Isooureas

2-Aryloxy Benzimidazoles

2-Phenoxy Benzimidazole **18**:

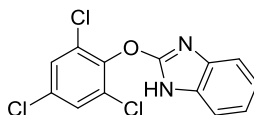


o-Phenylenediamine (0.65 g, 6 mmol) was partially dissolved in EtOAc (4 mL) under an atmosphere of N₂ and stirred rapidly. Dichlorodiphenoxymethane (0.54 g, 2 mmol) in EtOAc (2 mL) was then added dropwise over 1 hour *via* syringe pump. The mixture was stirred for a further 3 hours during which time a colourless precipitate formed. The suspension was then filtered and the solid washed with EtOAc (3 × 5 mL). The filtrate was collected and concentrated *in vacuo*. The resulting material was subjected to column chromatography (9:1, toluene: EtOAc). All product-containing fractions were combined and concentrated *in vacuo*. The crude product was recrystallised from toluene to afford the title compound **18** (0.2 g, 0.97 mmol, 49 %) as very fine, off-white plates.

¹H NMR (400 MHz, d₆-DMSO): δ 12.31 (br s, 1H, NH), 7.47 (app t, *J*_{HH} = 7.4 Hz, 2H, Ph), 7.38 (app d, *J*_{HH} = 7.4 Hz, 2H, Ph), 7.37-7.34 (m, 2H, Ar), 7.28 (app t, *J*_{HH} = 7.4 Hz, 1H, Ph), 7.12-7.08 (m, 2H, Ar). **¹³C{¹H} NMR (101 Hz, d₆-DMSO):** δ 156.4 (NCN), 153.6 (Ph), 140.5 (br, Ar), 132.6 (br, Ar), 129.7 (Ph), 125.2 (Ph), 121.2 (br, Ar), 120.1 (Ph), 117.5 (br, Ar), 110.3 (br, Ar). **ν_{max} (cm⁻¹, neat):** 3150-2400 (br), 3023 (w), 2830 (w), 2736 (w), 2631 (w), 1627 (w), 1595 (w), 1528 (m), 1486 (m), 1448 (m), 1385 (m), 1316 (w), 1259 (m), 1189 (m), 1157 (m), 1002 (m), 813 (w), 774 (m), 739 (m), 698 (m), 645 (m), 439 (m). **MS (m/z, EI⁺):** calcd. for C₁₃H₁₀N₂O [M]⁺: 210.08; found: 210.1. **m.p. (°C):** 222-223.

The data obtained is consistent with that reported in the literature.²²⁹

2-(2,4,6-Trichlorophenoxy) Benzimidazole **19**:



A stirred suspension of sodium hydride (53 mg, 2.2 mmol) in NMP (1 mL) had a solution of 2,4,6-trichlorophenol (0.43 g, 2.2 mmol) in NMP (1 mL) added dropwise over 5 minutes under an atmosphere of N₂. 2-Chlorobenzimidazole (0.31 g, 2 mmol) and 15-crown-5 (0.44 mL, 2.2 mmol) were then added and the mixture was heated to 150 °C for

20 hours. Once cooled, water (8 mL) was added with rapid stirring, causing an off-white solid to precipitate. This solid was isolated by Büchner filtration and recrystallised from EtOH to afford the title compound **19** (0.34 g, 1.1 mmol, 55 %) as very fine, off-white plates.

¹H NMR (400 MHz, d₆-DMSO): δ 12.68 (br s, 1H, NH), 7.90 (s, 2H, Ar(Cl₃)), 7.37-7.33 (m, 2H, Ar), 7.13-09 (m, 2H, Ar). **¹³C{¹H} NMR (126 Hz, d₆-DMSO):** δ 154.9 (NCN), 144.6 (Ar(Cl₃)), 140.1 (br, Ar), 133.0 (br, Ar), 131.5 (Ar(Cl₃)), 129.2 (Ar(Cl₃)), 121.5 (Ar), 121.4 (Ar), 117.6 (br, Ar), 110.6 (br, Ar). **ν_{max} (cm⁻¹, neat):** 3150-2400 (br), 3091 (w), 2838 (w), 2627 (w), 1729 (w), 1575 (w), 1529 (m), 1447 (m), 1383 (m), 1315 (m), 1243 (m), 1139 (m), 1054 (w), 1004 (w), 871 (m), 818 (m), 803 (m), 735 (m). **HRMS (m/z, EI⁺):** calcd. for C₁₃H₇Cl₃N₂O [M]⁺: 311.96185; found: 311.96366.

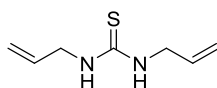
Representative Procedure for Rearrangement Attempts (Scheme 3.26 and Scheme 3.27):

Lithium *tert*-butoxide (12 mg, 0.15 mmol) had a solution of **19** (31.4 mg, 0.1 mmol) in DMSO (1 mL) added under an atmosphere of N₂. After stirring for 3.5 hours, an aliquot (0.3 mL) was removed, diluted in d₆-DMSO (0.3 mL) and was analysed by ¹H NMR spectroscopy (400 MHz). Only **19** was detected. The remaining reaction mixture was heated at 100 °C for 14 hours. Once cooled, a second aliquot was analysed as above. Again, only **19** was detected.

When toluene was used, aliquots were concentrated *in vacuo*, dissolved in d₆-DMSO (0.6 mL) and then analysed by ¹H NMR spectroscopy (400 MHz).

Attempted Synthesis of 2-Phenoxy-4,7-dihydro-1,3-diazepine **21 (Scheme 3.32)**

N,N'-Diallyl Thiourea:

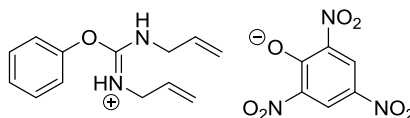


Allyl isothiocyanate (1.96 mL, 20 mmol) was diluted in DCM (10 mL) under an N₂ atmosphere. Allylamine (1.58 mL, 21 mmol) was then added dropwise over 15 minutes with rapid stirring. The addition rate was controlled such that the reaction exotherm did not cause the solution to boil. After 1 hour, the reaction was concentrated *in vacuo* and the resulting solid washed with petroleum ether (b.p.: 60-80 °C, 3 × 10 mL) and air dried. The title compound (2.93 g, 18.8 mmol, 94 %) was afforded as a sticky beige solid which was used without further purification.

¹H NMR (400 MHz, CDCl₃): δ 5.96 (br s, 2H, NH), 5.93-5.83 (m, 2H, CH=CH₂), 5.30-5.21 (m, 4H, CH=CH₂), 4.09 (br app s, 4H, NCH₂).

The data obtained is consistent with that reported in the literature.²⁹⁶

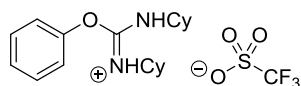
O-Phenyl-*N,N'*-diallyl Isoourea Picric Acid Salt [**15d'**][OPic]:



A mixture of *N,N'*-diallyl thiourea (0.78 g, 5 mmol) and mercury(I) oxide (1.62 g, 7.5 mmol) had DCM (5 mL) added under an atmosphere of N₂. After stirring for 2.5 hours, the resulting suspension was filtered through a pad of Celite and MgSO₄, eluting with DCM (4 × 5 mL) directly onto phenol (4.71 g, 50 mmol). This solution was allowed to stir for 1.5 hours and was then concentrated *in vacuo* until approx. 5 mL remained. This solution was loaded onto a short column of silica-gel and DCM was passed through the column until the elution of phenol had halted (as determined *via* TLC, approx. 500 mL DCM). Et₂O (approx. 100 mL) was used to flush the remaining material off the column and was then evaporated *in vacuo* until approx. 5 mL remained. The remaining solution was diluted with *i*PrOH (5 mL) and added to a solution of picric acid (0.9 g, 3.9 mmol) in *i*PrOH (75 mL) over 5 minutes with rapid stirring. A yellow precipitate formed throughout the addition. The suspension was stirred for a further 30 minutes and the solid subsequently isolated *via* Büchner filtration. After washing with *i*PrOH (3 × 10 mL) and air drying, the title compound [**15d'**][OPic] (0.57 g, 1.3 mmol, 26 %) was afforded as a bright yellow powder.

¹H NMR (400 MHz, d₆-DMSO): δ 9.38 (br s, 1H, NH), 9.01 (br s, 1H, NH), 8.58 (s, 2H, Ar(OPic)), 7.55 (app t, *J*_{HH} = 7.6 Hz, 2H, Ph), 7.43 (app t, *J*_{HH} = 7.6 Hz, 1H, Ph), 7.34 (app d, *J*_{HH} = 7.6 Hz, 2H, Ph), 5.99-5.75 (br m, 2H, CH=CH₂), 5.31-5.18 (br m, 4H, CH=CH₂), 4.02 (br s, 2H, NCH₂), 3.90 (br s, 2H, NCH₂). **¹³C{¹H} NMR (101 Hz, d₆-DMSO):** δ 160.8 (C=N), 157.6 (Ar), 150.1 (Ar), 141.9 (Ar), 133.3 (br, CH=CH₂), 131.7 (br, CH=CH₂), 130.7 (Ar), 127.6 (Ar), 125.2 (Ar), 124.2 (Ar), 120.6 (Ar), 116.8 (CH=CH₂), 43.8 (NCH₂). **HRMS (*m/z*, EI⁺):** calcd. for C₁₃H₁₇N₂O [M]⁺: 217.13354; found: 217.13195.

O-Phenyl-*N,N'*-diallyl Isoorea Methanesulfonic Acid Salt [**15d'**][OMs] (Scheme 3.35):



A suspension of [**15d'**][OPic] (89.1 mg, 0.2 mmol) in Et₂O (5 mL) had methanesulfonic acid (0.26 mL, 4 mmol) added dropwise over 5 minutes with rapid stirring. During the addition, the intense yellow colouration and the suspended solid disappeared and a colourless oil precipitated. The mixture was stirred for a further 10 minutes and then the solution above the oil was decanted. The oil was triturated with portions of Et₂O (4 × 4 mL) until no traces of picric acid remained as determined by ¹H NMR analyses. Drying *in vacuo* (0.5 torr) afforded crude [**15d'**][OMs] (38 mg), contaminated with 0.6 molar equivalents of methanesulfonic acid. This material was used in subsequent reactions without further purification.

¹H NMR (400 MHz, CDCl₃): δ 10.28 (br s, 1H, NH), 7.60-7.41 (br m, 2H, Ar), 7.33 (br app s, 1H, Ar), 7.14 (br app s, 2H, Ar), 5.77 (br app s, 2H, CH=CH₂), 5.31-5.18 (br m, 4H, CH=CH₂), 4.56 (br s, 2.9H, NH/OH), 4.29-3.59 (br m, 4H, NCH₂), 2.90 (s, 4.8H, CH₃). **¹³C{¹H} NMR (126 Hz, CDCl₃):** δ 159.0 (br, C=N), 152.6 (br, Ar), 131.3-130.8 (overlapping br s and s, 2C, Ar and CH=CH₂), 126.4 (br, Ar), 119.0 (br, CH=CH₂), 116.3 (br, Ar), 45.1 (br, NCH₂), 39.5 (CH₃). **MS (m/z, EI⁺):** calcd. for C₁₃H₁₇N₂O [M]⁺: 217.13; found: 217.1.

Representative Procedure for Attempted RCM Reactions (Scheme 3.33 and Scheme 3.36):

Hoveyda-Grubbs 2nd generation catalyst (3.1 mg, 5 × 10⁻⁶ mol) had a solution of [**15d'**][OMs] (19 mg, 6.1 × 10⁻⁵ mol) in chlorobenzene (1 mL) added under an atmosphere of N₂. The reaction was stirred for 7 hours and then concentrated *in vacuo*. The resulting residue was analysed by ¹H NMR spectroscopy (400 MHz, CDCl₃). Only [**15d'**][OMs] was detected.

When an identical reaction mixture stirred at 100 °C for 7 hours, subsequent ¹H NMR analysis revealed the formation of a number of unidentifiable products. The formation of the desired ring-closed product was discounted after analysis by mass spectrometry (ESI⁺).

Hoveyda-Grubbs 2nd generation catalyst: (1,3-Bis(2,4,6-trimethylphenyl)imidazolin-2-ylidene)dichloro(2-isopropoxybenzylidene)ruthenium.

Catalyst Inhibition by [15d']₂[OPic] (Scheme 3.34):

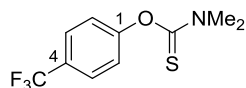
A mixture of [15d']₂[OPic] (44.5 mg, 0.1 mmol) and diethyl diallylmalonate (24 μ L, 0.1 mmol) in toluene (0.8 mL) was stirred at 40 °C under an atmosphere of N₂. A solution of Hoveyda-Grubbs 2nd generation catalyst (0.63 mg, 0.001 mmol) in toluene (0.2 mL) was then added. After 1 hour, an aliquot (0.1 mL) was removed and concentrated by passing a stream of nitrogen over the solution. The resulting residue was analysed by ¹H NMR spectroscopy (400 MHz, d₆-DMSO). Only [15d']₂[OPic] and diethyl diallylmalonate were detected.

A reaction was performed in the same manner at room temperature in the absence of [15d']₂[OPic]. An aliquot (0.1 mL) of the reaction mixture was removed 6 minutes after the addition of the catalyst. This sample was immediately filtered through a short pad of silica-gel and concentrated *in vacuo*. Analysis of the resulting residue by ¹H NMR spectroscopy (400 MHz, CDCl₃) revealed that diethyl diallylmalonate had undergone quantitative conversion to the corresponding ring-closed product (diethyl 3-cyclopentene-1,1-dicarboxylate).

5.4 Experimental Details Relevant to Chapter 4

5.4.1 Synthesis of Aryl-*N,N'*-dimethyl Thiocarbamates

O-(4-Trifluoromethylphenyl)-*N,N'*-dimethyl Thiocarbamate **23a**:

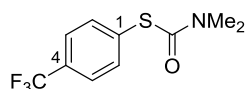


4-Trifluoromethylphenol (1.60 g, 9.9 mmol) and 1,4-diazabicyclo[2.2.2]octane (1.46 g, 13 mmol) were dissolved in NMP (7 mL) under an atmosphere of N₂. A solution of *N,N'*-dimethylthiocarbamoyl chloride (1.36 g, 11 mmol) in NMP (3 mL) was then added dropwise over 5 minutes with stirring. The reaction was heated to 50 °C for 2 hours, over which time a colourless precipitate formed. Water (20 mL) was then added over 5 minutes at 50 °C. The precipitate dissolved in the early stages, but a second precipitate formed as the addition was continued. Once cooled, the solid was isolated *via* Büchner filtration and was washed with water (20 mL). This material was dissolved in EtOAc (100 mL) and washed with brine (2 × 100 mL). The organic layer was dried (MgSO₄), filtered and concentrated *in vacuo*. After drying *in vacuo* (1 mbar) at 50 °C for 24 hours, the title compound **23a** (2.21 g, 8.9 mmol, 90 %) was afforded as a colourless powder.

¹H NMR (500 MHz, CDCl₃): δ 7.66 (app d, *J*_{HH} = 8.4 Hz, 2H, Ar), 7.19 (app d, *J*_{HH} = 8.4 Hz, 2H, Ar), 3.46 (s, 3H, CH₃), 3.36 (s, 3H, CH₃). **¹³C{¹H} NMR (126 Hz, CDCl₃):** δ 187.1 (C=S), 156.5 (C-1), 128.2 (q, *J*_{CF} = 32.8 Hz, C-4), 126.7 (q, *J*_{CF} = 3.7 Hz, C-3), 124.1 (q, *J*_{CF} = 272.0 Hz, CF₃), 123.5 (C-2), 43.5 (CH₃), 39.0 (CH₃). **¹⁹F NMR (377 MHz, CDCl₃):** δ -62.16 (s).

The data obtained is consistent with that reported in the literature.¹¹⁸

S-(4-Trifluoromethylphenyl)-*N,N'*-dimethyl Thiocarbamate **24a**:



23a (312 mg, 1.25 mmol) and Pd(P^{*t*}Bu₃)₂ (13 mg, 0.025 mmol) were dissolved in toluene (5 mL) under an atmosphere of N₂ and heated to 100 °C for 4.5 hours with stirring. Once cooled, the solution was concentrated *in vacuo* and the resulting residue purified by column chromatography (gradient: 1:0–4:1 isohexane:EtOAc). After drying *in vacuo* (0.5 torr) at 50 °C for 24 hours, the title compound **24a** (288 mg, 1.16 mmol, 92 %) was afforded as a pale yellow solid.

¹H NMR (500 MHz, CDCl₃): δ 7.64-7.60 (m, 4H, Ar), 3.11 (br s, 3H, CH₃), 3.05 (br s, 3H, CH₃). **¹³C{¹H} NMR (101 Hz, CDCl₃):** δ 165.7 (C=O), 135.8 (Ar), 133.8 (Ar), 131.1 (q, *J*_{CF} = 32.7 Hz, C-4), 125.8 (q, *J*_{CF} = 3.7 Hz, C-3), 124.1 (q, *J*_{CF} = 272.0 Hz, CF₃), 37.1 (CH₃). **¹⁹F NMR (377 MHz, CDCl₃):** δ -62.86 (s).

The data obtained is consistent with that reported in the literature.^{118,297}

5.4.2 O-(4-Trifluoromethylphenyl)-*N,N'*-dimethyl Thiocarbamate in Cross-Coupling Reactions

Cross-Coupling 23a with 4-Fluorophenylboronic Acid (Table 4.1)

Representative Procedure (Table 4.1, entry 1):

23a (62.3 mg, 0.25 mmol) and Pd(P^{*t*}Bu₃)₂ (6.4 mg, 1.25×10⁻⁵ mol) were dissolved in toluene (1 mL) under an atmosphere of N₂. After stirring for 10 minutes, this solution was added to 4-fluorophenylboronic acid (38.5 mg, 0.275 mmol), potassium *tert*-butoxide (56.1 mg, 0.5 mmol) and copper(I) thiophene-2-carboxylate (2.4 mg, 1.25×10⁻⁵ mol) and was heated to 100 °C for 17 hours. Once cooled, 1-fluoronaphthalene (0.25 mmol) in toluene (0.1 mL; 2.5 M stock) was added. An aliquot (0.2 mL) of the mixture was removed, filtered through a pad of celite and then concentrated *in vacuo* (50 mbar, 40 °C). The resulting residue was analysed by ¹⁹F NMR spectroscopy (377 MHz, CDCl₃).

Cross-Coupling of 23a with 4-Fluorophenylzinc Chloride (Scheme 4.11)

Preparation of 4-Fluorophenylzinc Chloride Stock Solution:²⁹⁸

A solution of 1-bromo-4-fluorobenzene (0.11 mL, 1 mL) in THF (2 mL) was cooled to -78 °C under an atmosphere of N₂. A solution of *n*-butyl lithium (1 mmol) in hexane (0.46 mL; 2.17 M stock) was then added dropwise over 5 minutes with stirring. After a further 5 minutes, a solution of zinc chloride (anhydrous; 204 mg, 1.5 mmol) in THF (2.5 mL) was added dropwise over 3 minutes. This mixture was then allowed to warm to room temperature, affording a solution of 4-fluorophenylzinc chloride in THF (approx. 0.2 M).

Cross-Coupling Procedure:

23a (24.9 mg, 0.1 mmol) and Pd(P^{*t*}Bu₃)₂ (2.6 mg, 5×10⁻⁶ mol) were dissolved in toluene (0.5 mL) under an atmosphere of N₂. After stirring for 10 minutes, 4-fluorophenylzinc chloride (approx. 0.1 mmol) in THF (0.5 mL; approx. 0.2 M stock) was added and the reaction was heated to 100 °C for 19 hours. Once cooled, the mixture was diluted in

EtOAc (10 mL) and washed with HCl (10 % aqueous; 10 mL). The HCl layer was extracted with EtOAc (10 mL) and the combined organic fractions were then dried (MgSO₄), filtered and concentrated *in vacuo* (145 mbar, 40 °C). The resulting residue had 1-fluoronaphthalene (0.1 mmol) in toluene (50 µL; 2 M stock) added and was analysed by ¹⁹F NMR spectroscopy (377 MHz, CDCl₃).

5.4.3 Coupling Reactions Forming Symmetrical Diaryl Thioethers

Synthesis of Bis(4-trifluoromethylphenyl)sulfide 28a from 23a

Attempted One-Step Synthesis (Scheme 4.20):

23a (62.3 mg, 0.25 mmol) and Pd(P^{*t*}Bu₃)₂ (6.4 mg, 1.25×10⁻⁵ mol) were dissolved in toluene (1 mL) under an atmosphere of N₂. After stirring for 10 minutes, this solution was added to potassium *tert*-butoxide (56.1 mg, 0.5 mmol) and was heated to 100 °C for 16 hours. Once cooled, 1-fluoronaphthalene (0.25 mmol) in toluene (0.1 mL; 2.5 M stock) was added. The mixture was then diluted with water (10 mL), acidified with HCl (10 % aqueous) and extracted with EtOAc (2 × 10 mL). The organic phase was dried (MgSO₄), filtered and concentrated *in vacuo* (100 mbar, 40 °C). The resulting residue was analysed by ¹⁹F NMR spectroscopy (377 MHz, CDCl₃).

Attempted Two-Step Synthesis (Scheme 4.21):

A solution of **23a** (49.9 mg, 0.2 mmol) and Pd(P^{*t*}Bu₃)₂ (5.1 mg, 1×10⁻⁵ mol) in toluene (1 mL) was stirred at 100 °C for 2 hours under an atmosphere of N₂. Potassium *tert*-butoxide (44.9 mg, 0.4 mmol) was then added and the reaction was heated for a further 18 hours. Once cooled, 1-fluoronaphthalene (0.2 mmol) in toluene (0.1 mL; 2 M stock) was added. This mixture was diluted in EtOAc (10 mL) and washed with HCl (10 % aqueous; 10 mL). The HCl layer was extracted with EtOAc (2 × 10 mL) and the combined organic fractions were dried (MgSO₄), filtered and concentrated *in vacuo* (40 mbar, 40 °C). The resulting residue was analysed by ¹⁹F NMR spectroscopy (377 MHz, CDCl₃).

Synthesis of Bis(4-fluorophenyl)sulfide 28b from 1-Bromo-4-fluorobenzene and 23a (Table 4.2)

Representative Procedure (Table 4.2, entry 2):

23a (49.9 mg, 0.2 mmol) and Pd(P^{*t*}Bu₃)₂ (5.1 mg, 1×10⁻⁵ mol) were dissolved in toluene (1 mL) under an atmosphere of N₂. After stirring for 10 minutes, this solution was added to potassium *tert*-butoxide (67.3 mg, 0.6 mmol) and 1-bromo-4-fluorobenzene (22 µL,

0.2 mmol) and was heated to 100 °C for 20 hours. Once cooled, 1-fluoronaphthalene (0.2 mmol) in toluene (0.1 mL; 2 M stock) was added. This mixture was diluted in EtOAc (10 mL) and washed with HCl (10 % aqueous; 10 mL). The HCl layer was extracted with EtOAc (2 × 10 mL) and the combined organic fractions were dried (MgSO₄), filtered and concentrated *in vacuo* (40 mbar, 40 °C). The resulting residue was analysed by ¹⁹F NMR spectroscopy (377 MHz, CDCl₃).

5.4.4 Coupling Reactions Forming Unsymmetrical Diaryl Thioethers

Synthesis of (4-Trifluoromethylphenyl)(4-fluorophenyl)sulfide 32ab from 1-Bromo-4-fluorobenzene and 24a (Table 4.3, Table 4.4 and Scheme 4.25)

Representative One-Step Procedure (Table 4.4, entry 1):

24a (24.9 mg, 0.1 mmol) and G3-XPhos (1.7 mg, 2×10⁻⁶ mol) were dissolved in toluene (1 mL) under an atmosphere of N₂. After stirring for 10 minutes, potassium *tert*-butoxide (22.4 mg, 0.2 mmol) and 1-bromo-4-fluorobenzene (11 µL, 0.1 mmol) were added and the reaction was heated to 60 °C for 19 hours. Once cooled, the mixture was diluted in EtOAc (10 mL) and washed with HCl (10 % aqueous; 10 mL). The HCl layer was extracted with EtOAc (10 mL) and the combined organic fractions were then dried (MgSO₄), filtered and concentrated *in vacuo* (145 mbar, 40 °C). The resulting residue had 1-fluoronaphthalene (0.1 mmol) in toluene (50 µL; 2 M stock) added and was analysed by ¹⁹F NMR spectroscopy (377 MHz, CDCl₃).

G3-XPhos: (2-Dicyclohexylphosphino-2',4',6'-triisopropyl-1,1'-biphenyl)[2-(2'-amino-1,1'-biphenyl)]palladium(II) methanesulfonate

Two-Step Procedure (Scheme 4.25):

A solution of **24a** (24.9 mg, 0.1 mmol) and potassium *tert*-butoxide (22.4 mg, 0.2 mmol) in toluene (0.5 mL) was stirred at 60 °C for 1 hour under an atmosphere of N₂. 1-Bromo-4-fluorobenzene (11 µL, 0.1 mmol) and a solution of Pd(P^{*t*}Bu₃)₂ (1.0 mg, 2×10⁻⁶ mol) in toluene (0.5 mL) were then added and the reaction was heated for a further 18 hours. Once cooled, the mixture was diluted in EtOAc (10 mL) and washed with HCl (10 % aqueous; 10 mL). The HCl layer was extracted with EtOAc (10 mL) and the combined organic fractions were then dried (MgSO₄), filtered and concentrated *in vacuo* (145 mbar, 40 °C). The resulting residue had 1-fluoronaphthalene (0.1 mmol) in toluene (50 µL; 2 M stock) added and was analysed by ¹⁹F NMR spectroscopy (377 MHz, CDCl₃).

Synthesis of 32ab from 1-Bromo-4-fluorobenzene and 23a (Table 4.5)

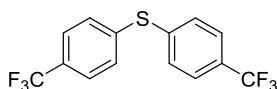
Representative Procedure (Table 4.5, entry 2):

A solution of **23a** (49.9 mg, 0.2 mmol) and Pd(P^{*t*}Bu₃)₂ (5.1 mg, 1×10⁻⁵ mol) in toluene (1 mL) was stirred at 100 °C for 2 hours under an atmosphere of N₂. Potassium *tert*-butoxide (44.9 mg, 0.4 mmol) and 1-bromo-4-fluorobenzene (22 μL, 0.2 mmol) were then added and the reaction was heated for a further 4 hours. Once cooled, 1-fluoronaphthalene (0.2 mmol) in toluene (0.1 mL; 2 M stock) was added. This mixture was diluted in EtOAc (10 mL) and washed with HCl (10 % aqueous; 10 mL). The HCl layer was extracted with EtOAc (2 × 10 mL) and the combined organic fractions were dried (MgSO₄), filtered and concentrated *in vacuo* (40 mbar, 40 °C). The resulting residue was analysed by ¹⁹F NMR spectroscopy (377 MHz, CDCl₃).

5.4.5 Diaryl Thioethers

The diaryl thioether products of the palladium(0)-catalysed coupling reactions detailed in the previous sections were not isolated, but were identified based upon the following data:

Bis(4-trifluoromethylphenyl)sulfide **28a**:

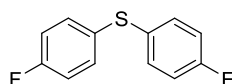


¹H NMR (500 MHz, CDCl₃): δ 7.58 (app d, *J*_{HH} = 8.2 Hz, 4H), 7.44 (app d, *J*_{HH} = 8.2 Hz, 4H).

¹⁹F NMR (376 MHz, CDCl₃): δ -62.70 (s). MS (*m/z*, EI⁺): calcd. for C₁₄H₈F₆S [M]⁺: 322.03; found: 322.

The data obtained is consistent with that reported in the literature.²⁹⁹

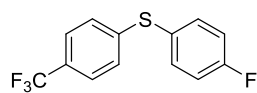
Bis(4-fluorophenyl)sulfide **28b**:



¹H NMR (500 MHz, CDCl₃): δ 7.31 (m, 4H), 7.01 (app t, *J*_{HH} = 8.7 Hz, 4H). ¹⁹F NMR (377 MHz, CDCl₃): δ -114.40 (m). MS (*m/z*, EI⁺): calcd. for C₁₂H₈F₂S [M]⁺: 222.03; found: 222.0.

The data obtained is consistent with that reported in the literature.³⁰⁰

(4-Trifluoromethylphenyl)(4-fluorophenyl)sulfide **32ab**:



¹H NMR (400 MHz, CDCl₃): δ 7.52-7.46 (m, 4H), 7.21 (app d, $J_{\text{HH}} = 8.2$ Hz, 2H), 7.11 (app t, $J_{\text{HH}} = 8.7$ Hz, 2H). **¹⁹F NMR (377 MHz, CDCl₃):** δ -62.50 (s, 3F, CF₃), -111.60 (m, 1F, ArF).

MS (m/z , EI⁺): calcd. for C₁₃H₈F₄S [M]⁺: 272.03; found: 272.1.

6 References

- (1) Fang, Y.; Zheng, Y.; Wang, Z. *Eur. J. Org. Chem.* **2012**, 2012 (8), 1495.
- (2) Hartwig, J. F. *Acc. Chem. Res.* **2008**, 41 (11), 1534.
- (3) Monnier, F.; Taillefer, M. *Angew. Chem., Int. Ed.* **2009**, 48 (38), 6954.
- (4) Xu, H.; Wolf, C. *Chem. Commun.* **2009** (21), 3035.
- (5) Vo, G. D.; Hartwig, J. F. *J. Am. Chem. Soc.* **2009**, 131 (31), 11049.
- (6) Littke, A. F.; Fu, G. C. *Angew. Chem., Int. Ed.* **2002**, 41 (22), 4176.
- (7) Seeboth, H. *Angew. Chem., Int. Ed.* **1967**, 6 (4), 307.
- (8) Laue, T.; Plagens, A. *Named Organic Reactions*, 2nd ed.; John Wiley & Sons, Ltd: Chichester, 2005.
- (9) Drake, N. L. *Org. React.* **1942**, 1, 105.
- (10) Rossi, R. A.; Bunnett, J. F. *J. Org. Chem.* **1972**, 37 (22), 3570.
- (11) Surry, D. S.; Buchwald, S. L. *Chem. Sci.* **2011**, 2 (1), 27.
- (12) Wolfe, J. P.; Buchwald, S. L. *J. Org. Chem.* **1997**, 62 (5), 1264.
- (13) Louie, J.; Driver, M. S.; Hamann, B. C.; Hartwig, J. F. *J. Org. Chem.* **1997**, 62 (5), 1268.
- (14) Barluenga, J.; Jiménez-Aquino, A.; Aznar, F.; Valdés, C. *J. Am. Chem. Soc.* **2009**, 131 (11), 4031.
- (15) Åhman, J.; Buchwald, S. L. *Tetrahedron Lett.* **1997**, 38 (36), 6363.
- (16) Anderson, K. W.; Mendez-Perez, M.; Priego, J.; Buchwald, S. L. *J. Org. Chem.* **2003**, 68 (25), 9563.
- (17) Tundel, R. E.; Anderson, K. W.; Buchwald, S. L. *J. Org. Chem.* **2006**, 71 (1), 430.
- (18) Wolfe, J. P.; Tomori, H.; Sadighi, J. P.; Yin, J.; Buchwald, S. L. *J. Org. Chem.* **2000**, 65 (4), 1158.
- (19) Ogata, T.; Hartwig, J. F. *J. Am. Chem. Soc.* **2008**, 130 (42), 13848.
- (20) Roy, A. H.; Hartwig, J. F. *J. Am. Chem. Soc.* **2003**, 125 (29), 8704.
- (21) Fors, B. P.; Watson, D. A.; Biscoe, M. R.; Buchwald, S. L. *J. Am. Chem. Soc.* **2008**, 130 (41), 13552.
- (22) So, C. M.; Zhou, Z.; Lau, C. P.; Kwong, F. Y. *Angew. Chem., Int. Ed.* **2008**, 47 (34), 6402.
- (23) Dooleweerd, K.; Fors, B. P.; Buchwald, S. L. *Org. Lett.* **2010**, 12 (10), 2350.
- (24) Klinkenberg, J. L.; Hartwig, J. F. *Angew. Chem., Int. Ed.* **2011**, 50 (1), 86.
- (25) Willis, M. C. *Angew. Chem., Int. Ed.* **2007**, 46 (19), 3402.
- (26) Shen, Q.; Hartwig, J. F. *J. Am. Chem. Soc.* **2006**, 128 (31), 10028.
- (27) Lundgren, R. J.; Peters, B. D.; Alsabeh, P. G.; Stradiotto, M. *Angew. Chem., Int. Ed.* **2010**, 49 (24), 4071.
- (28) Alsabeh, P. G.; Lundgren, R. J.; McDonald, R.; Johansson Seechurn, C. C. C.; Colacot, T. J.; Stradiotto, M. *Chem. Eur. J.* **2013**, 19 (6), 2131.
- (29) Mann, G.; Hartwig, J. F.; Driver, M. S.; Fernández-Rivas, C. *J. Am. Chem. Soc.* **1998**, 120 (4), 827.
- (30) Wolfe, J. P.; Åhman, J.; Sadighi, J. P.; Singer, R. A.; Buchwald, S. L. *Tetrahedron Lett.* **1997**, 38 (36), 6367.
- (31) Jaime-Figueroa, S.; Liu, Y.; Muchowski, J. M.; Putman, D. G. *Tetrahedron Lett.* **1998**, 39 (11), 1313.

- (32) Huang, X.; Buchwald, S. L. *Org. Lett.* **2001**, 3 (21), 3417.
- (33) Lee, S.; Jørgensen, M.; Hartwig, J. F. *Org. Lett.* **2001**, 3 (17), 2729.
- (34) Huang, X.; Anderson, K. W.; Zim, D.; Jiang, L.; Klapars, A.; Buchwald, S. L. *J. Am. Chem. Soc.* **2003**, 125 (22), 6653.
- (35) Lee, D.-Y.; Hartwig, J. F. *Org. Lett.* **2005**, 7 (6), 1169.
- (36) Truce, W. E.; Kreider, E. M.; Brand, W. W. *Org. React.* **1970**, 18, 99.
- (37) Bayles, R.; Johnson, M. C.; Maisey, R. F.; Turner, R. W. *Synthesis* **1977** (1), 33.
- (38) Coutts, I. G. C.; Southcott, M. R. *J. Chem. Soc., Perkin Trans. 1* **1990** (3), 767.
- (39) Bayles, R.; Johnson, M. C.; Maisey, R. F.; Turner, R. W. *Synthesis* **1977** (1), 31.
- (40) Weidner, J. J.; Weintraub, P. M.; Schnettler, R. A.; Peet, N. P. *Tetrahedron* **1997**, 53 (18), 6303.
- (41) Mizuno, M.; Yamano, M. *Org. Lett.* **2005**, 7 (17), 3629.
- (42) Mumm, O.; Hesse, H.; Volquartz, H. *Ber. Dtsch. Chem. Ges.* **1915**, 48 (1), 379.
- (43) Chapman, A. W. *J. Chem. Soc., Trans.* **1925**, 127, 1992.
- (44) Schulenberg, J. W.; Archer, S. *Org. React.* **1965**, 14, 1.
- (45) Lloyd-Jones, G.; Moseley, J.; Renny, J. *Synthesis* **2008** (5), 661.
- (46) Chapman, A. W. *J. Chem. Soc.* **1929**, 569.
- (47) Chapman, A. W. *J. Chem. Soc.* **1927**, 1743.
- (48) Wiberg, K. B.; Rowland, B. I. *J. Am. Chem. Soc.* **1955**, 77 (8), 2205.
- (49) Relles, H. M.; Pizzolato, G. *J. Org. Chem.* **1968**, 33 (6), 2249.
- (50) Relles, H. M. *J. Org. Chem.* **1968**, 33 (6), 2245.
- (51) Wheeler, O. H.; Roman, F.; Rosado, O. *J. Org. Chem.* **1969**, 34 (4), 966.
- (52) Scherrer, R. A.; Beatty, H. R. *J. Org. Chem.* **1972**, 37 (11), 1681.
- (53) Radu, I.-I.; Poirier, D.; Provencher, L. *Tetrahedron Lett.* **2002**, 43 (42), 7617.
- (54) Matsumoto, K.; Stark, P.; Meister, R. G. *J. Med. Chem.* **1977**, 20 (1), 17.
- (55) Morrow, D. F.; Hofer, R. M. *J. Med. Chem.* **1966**, 9 (2), 249.
- (56) Morrow, D. F.; Butler, M. E. *J. Org. Chem.* **1964**, 29 (7), 1893.
- (57) Snieckus, V. *Chem. Rev.* **1990**, 90 (6), 879.
- (58) Anctil, E. J.-G.; Snieckus, V. *J. Organomet. Chem.* **2002**, 653 (1-2), 150.
- (59) Yu, D.-G.; Luo, S.; Zhao, F.; Shi, Z.-J.; Shi, Z.-J. In *Homogeneous Catalysis for Unreactive Bond Activation*; Shi, Z.-J., Ed.; John Wiley & Sons, Inc.: Hoboken, New Jersey, 2014; pp 347–439.
- (60) Li, B.-J.; Yu, D.-G.; Sun, C.-L.; Shi, Z.-J. *Chem. Eur. J.* **2011**, 17 (6), 1728.
- (61) Rosen, B. M.; Quasdorf, K. W.; Wilson, D. A.; Zhang, N.; Resmerita, A.-M.; Garg, N. K.; Percec, V. *Chem. Rev.* **2011**, 111 (3), 1346.
- (62) Yu, D.-G.; Li, B.-J.; Shi, Z.-J. *Acc. Chem. Res.* **2010**, 43 (12), 1486.
- (63) Albaneze-Walker, J.; Raju, R.; Vance, J. A.; Goodman, A. J.; Reeder, M. R.; Liao, J.; Maust, M. T.; Irish, P. A.; Espino, P.; Andrews, D. R. *Org. Lett.* **2009**, 11 (7), 1463.
- (64) Ackermann, L.; Sandmann, R.; Song, W. *Org. Lett.* **2011**, 13 (7), 1784.
- (65) Ackermann, L.; Barfüsser, S.; Pospech, J. *Org. Lett.* **2010**, 12 (4), 724.
- (66) Luo, Y.; Wu, J. *Organometallics* **2009**, 28 (23), 6823.
- (67) Tasker, S. Z.; Standley, E. A.; Jamison, T. F. *Nature* **2014**, 509 (7500), 299.
- (68) Tobisu, M.; Shimasaki, T.; Chatani, N. *Chem. Lett.* **2009**, 38 (7), 710.

- (69) Mesganaw, T.; Silberstein, A. L.; Ramgren, S. D.; Nathel, N. F. F.; Hong, X.; Liu, P.; Garg, N. K. *Chem. Sci.* **2011**, 2 (9), 1766.
- (70) Lanni, E. L.; McNeil, A. J. *J. Am. Chem. Soc.* **2009**, 131 (45), 16573.
- (71) Shimasaki, T.; Tobisu, M.; Chatani, N. *Angew. Chem., Int. Ed.* **2010**, 49 (16), 2929.
- (72) Quasdorf, K. W.; Riener, M.; Petrova, K. V.; Garg, N. K. *J. Am. Chem. Soc.* **2009**, 131 (49), 17748.
- (73) Antoft-Finch, A.; Blackburn, T.; Snieckus, V. *J. Am. Chem. Soc.* **2009**, 131 (49), 17750.
- (74) Yamazaki, K.; Kawamorita, S.; Ohmiya, H.; Sawamura, M. *Org. Lett.* **2010**, 12 (18), 3978.
- (75) Bedford, R. B.; Webster, R. L.; Mitchell, C. J. *Org. Biomol. Chem.* **2009**, 7 (23), 4853.
- (76) Zhao, X.; Yeung, C. S.; Dong, V. M. *J. Am. Chem. Soc.* **2010**, 132 (16), 5837.
- (77) Iglesias, M. J.; Blandez, J. F.; Fructos, M. R.; Prieto, A.; Álvarez, E.; Belderrain, T. R.; Nicasio, M. C. *Organometallics* **2012**, 31 (17), 6312.
- (78) Gao, C.-Y.; Yang, L.-M. *J. Org. Chem.* **2008**, 73 (4), 1624.
- (79) Molander, G. A.; Shin, I. *Org. Lett.* **2013**, 15 (10), 2534.
- (80) Macklin, T. K.; Snieckus, V. *Org. Lett.* **2005**, 7 (13), 2519.
- (81) Quasdorf, K. W.; Antoft-Finch, A.; Liu, P.; Silberstein, A. L.; Komaromi, A.; Blackburn, T.; Ramgren, S. D.; Houk, K. N.; Snieckus, V.; Garg, N. K. *J. Am. Chem. Soc.* **2011**, 133 (16), 6352.
- (82) Tao, J.-L.; Wang, Z.-X. *Eur. J. Org. Chem.* **2015**, 2015 (29), 6534.
- (83) Ramgren, S. D.; Silberstein, A. L.; Yang, Y.; Garg, N. K. *Angew. Chem., Int. Ed.* **2011**, 50 (9), 2171.
- (84) Hie, L.; Ramgren, S. D.; Mesganaw, T.; Garg, N. K. *Org. Lett.* **2012**, 14 (16), 4182.
- (85) Sibi, M. P.; Snieckus, V. *J. Org. Chem.* **1983**, 48 (11), 1935.
- (86) Huang, J.-H.; Yang, L.-M. *Org. Lett.* **2011**, 13 (14), 3750.
- (87) Guan, B.-T.; Wang, Y.; Li, B.-J.; Yu, D.-G.; Shi, Z.-J. *J. Am. Chem. Soc.* **2008**, 130 (44), 14468.
- (88) Guan, B.-T.; Lu, X.-Y.; Zheng, Y.; Yu, D.-G.; Wu, T.; Li, K.-L.; Li, B.-J.; Shi, Z.-J. *Org. Lett.* **2010**, 12 (2), 396.
- (89) Zhao, F.; Yu, D.-G.; Zhu, R.-Y.; Xi, Z.; Shi, Z.-J. *Chem. Lett.* **2011**, 40 (9), 1001.
- (90) Yu, D.-G.; Li, B.-J.; Zheng, S.-F.; Guan, B.-T.; Wang, B.-Q.; Shi, Z.-J. *Angew. Chem., Int. Ed.* **2010**, 49 (27), 4566.
- (91) Fürstner, A.; Leitner, A. *Angew. Chem., Int. Ed.* **2002**, 41 (4), 609.
- (92) Fürstner, A.; Leitner, A.; Méndez, M.; Krause, H. *J. Am. Chem. Soc.* **2002**, 124 (46), 13856.
- (93) Silberstein, A. L.; Ramgren, S. D.; Garg, N. K. *Org. Lett.* **2012**, 14 (14), 3796.
- (94) Korn, T. J.; Schade, M. A.; Wirth, S.; Knochel, P. *Org. Lett.* **2006**, 8 (4), 725.
- (95) Korn, T.; Schade, M.; Cheemala, M.; Wirth, S.; Guevara, S.; Cahiez, G.; Knochel, P. *Synthesis* **2006** (21), 3547.
- (96) Kakiuchi, F.; Usui, M.; Ueno, S.; Chatani, N.; Murai, S. *J. Am. Chem. Soc.* **2004**, 126 (9), 2706.

- (97) Ueno, S.; Mizushima, E.; Chatani, N.; Kakiuchi, F. *J. Am. Chem. Soc.* **2006**, *128* (51), 16516.
- (98) Ackermann, L.; Althammer, A.; Born, R. *Angew. Chem., Int. Ed.* **2006**, *45* (16), 2619.
- (99) Ackermann, L.; Mulzer, M. *Org. Lett.* **2008**, *10* (21), 5043.
- (100) Imazaki, Y.; Shirakawa, E.; Ueno, R.; Hayashi, T. *J. Am. Chem. Soc.* **2012**, *134* (36), 14760.
- (101) Zhang, L.; Wu, J. *Adv. Synth. Catal.* **2008**, *350* (14-15), 2409.
- (102) Zonta, C.; De Lucchi, O.; Volpicelli, R.; Cotarca, L. In *Sulfur-Mediated Rearrangements II*; Schaumann, E., Ed.; Topics in Current Chemistry; Springer Berlin Heidelberg, 2007; Vol. 275, pp 131–161.
- (103) Newman, M. S.; Karnes, H. A. *J. Org. Chem.* **1966**, *31* (12), 3980.
- (104) Miyazaki, K. *Tetrahedron Lett.* **1968**, *9* (23), 2793.
- (105) Kaji, A.; Araki, Y.; Miyazaki, K. *Bull. Chem. Soc. Jpn.* **1971**, *44* (5), 1393.
- (106) Moseley, J. D.; Sankey, R. F.; Tang, O. N.; Gilday, J. P. *Tetrahedron* **2006**, *62* (19), 4685.
- (107) Kusch, D. *Spec. Chem.* **2003**, November, 41.
- (108) Moseley, J. D.; Lenden, P. *Tetrahedron* **2007**, *63* (19), 4120.
- (109) Kwart, H.; Evans, E. R. *J. Org. Chem.* **1966**, *31* (2), 410.
- (110) Flores-Figueroa, A.; Arista-M, V.; Talancon-Sanchez, D.; Castillo, I. *J. Braz. Chem. Soc.* **2005**, *16* (3a), 397.
- (111) Cooper, J. E.; Paul, J. M. *J. Org. Chem.* **1970**, *35* (6), 2046.
- (112) Wagenaar, A.; Engberts, J. B. F. N. *Recl. Trav. Chim. Pays-Bas* **2010**, *101* (3), 91.
- (113) Percec, V.; Bera, T. K.; De, B. B.; Sanai, Y.; Smith, J.; Holerca, M. N.; Barboiu, B.; Grubbs, R. B.; Fréchet, J. M. J. *J. Org. Chem.* **2001**, *66* (6), 2104.
- (114) Miller, M. W.; Mylari, B. L.; Howes, H. L.; Figdor, S. K.; Lynch, M. J.; Lynch, J. E.; Koch, R. C. *J. Med. Chem.* **1980**, *23* (10), 1083.
- (115) Sebok, P.; Timar, T.; Eszenyi, T.; Patonay, T. *J. Org. Chem.* **1994**, *59* (21), 6318.
- (116) Brooker, S.; Caygill, G. B.; Croucher, P. D.; Davidson, T. C.; Clive, D. L. J.; Magnuson, S. R.; Cramer, S. P.; Ralston, C. Y. *J. Chem. Soc., Dalton Trans.* **2000** (18), 3113.
- (117) Renny, J. S. The Newman-Kwart Rearrangement Molecularity and Catalysis, Ph.D. Thesis, University of Bristol, 2010.
- (118) Harvey, J. N.; Jover, J.; Lloyd-Jones, G. C.; Moseley, J. D.; Murray, P.; Renny, J. S. *Angew. Chem., Int. Ed.* **2009**, *48* (41), 7612.
- (119) Mitchell, M. *personal communication* **2014**.
- (120) Perkowski, A. J.; Cruz, C. L.; Nicewicz, D. A. *J. Am. Chem. Soc.* **2015**, *137* (50), 15684.
- (121) Prabhakar, S.; Kar, P.; Mirza, S. P.; Lakshmi, V. V. S.; Nagaiah, K.; Vairamani, M. *Rapid Commun. Mass Spectrom.* **2001**, *15* (22), 2127.
- (122) Tou, J. C.; Rodia, R. M. *Org. Mass Spectrom.* **1972**, *6* (5), 493.
- (123) Thomson, J. B.; Brown, P.; Djerassi, C. *J. Am. Chem. Soc.* **1966**, *88* (17), 4049.
- (124) Overman, L. E.; Carpenter, N. E. *Org. React.* **2005**, *66*, 1.
- (125) Overman, L. E. *Angew. Chem., Int. Ed.* **1984**, *23* (8), 579.

- (126) Schenck, T. G.; Bosnich, B. *J. Am. Chem. Soc.* **1985**, *107* (7), 2058.
- (127) Ikariya, T.; Ishikawa, Y.; Hirai, K.; Yoshikawa, S. *Chem. Lett.* **1982** (11), 1815.
- (128) Anderson, C. E.; Overman, L. E. *J. Am. Chem. Soc.* **2003**, *125* (41), 12412.
- (129) Overman, L. E.; Owen, C. E.; Pavan, M. M.; Richards, C. J. *Org. Lett.* **2003**, *5* (11), 1809.
- (130) Kirsch, S. F.; Overman, L. E.; Watson, M. P. *J. Org. Chem.* **2004**, *69* (23), 8101.
- (131) Stick, R. V.; Williams, S. J. *Carbohydrates: The Essential Molecules of Life*, 2nd ed.; Elsevier: Oxford, 2009.
- (132) Davis, B. G.; Fairbanks, A. J. *Carbohydrate Chemistry*; Oxford University Press: Oxford, 2002.
- (133) Shohda, K.; Wada, T.; Sekine, M. *Nucleos. Nucleot.* **1998**, *17* (12), 2199.
- (134) Larsen, K.; Olsen, C. E.; Motawia, M. S. *Carbohydr. Res.* **2008**, *343* (2), 383.
- (135) Mercer, G. J.; Yang, J.; McKay, M. J.; Nguyen, H. M. *J. Am. Chem. Soc.* **2008**, *130* (33), 11210.
- (136) Park, N. H.; Nguyen, H. M. *Org. Lett.* **2009**, *11* (11), 2433.
- (137) Yu, B.; Tao, H. *Tetrahedron Lett.* **2001**, *42* (12), 2405.
- (138) Adinolfi, M.; Iadonisi, A.; Ravidà, A. *Synlett* **2006** (4), 583.
- (139) Nakajima, N.; Saito, M.; Kudo, M.; Ubukata, M. *Tetrahedron* **2002**, *58* (18), 3579.
- (140) Lander, G. D. *J. Chem. Soc., Trans.* **1903**, *83*, 406.
- (141) Cramer, F.; Hennrich, N. *Chem. Ber.* **1961**, *94* (4), 976.
- (142) McElvain, S. M.; Fajardo-Pinzón, B. *J. Am. Chem. Soc.* **1945**, *67* (4), 690.
- (143) MacKenzie, C. A.; Schmidt, G. A.; Webb, L. R. *J. Am. Chem. Soc.* **1951**, *73* (10), 4990.
- (144) Il'in, V. V.; Kim, A. C.-V.; Ignatenko, A. V.; Ponomarenko, V. A. *B. Acad. Sci. USSR CH+* **1989**, *38* (5), 1083.
- (145) Buckle, F. J.; Heap, R.; Saunders, B. C. *J. Chem. Soc.* **1949**, 912.
- (146) Bozhkova, N.; Heimgartner, H. *Helv. Chim. Acta* **1989**, *72* (4), 825.
- (147) Brown, H. C.; Wetzol, C. R. *J. Org. Chem.* **1965**, *30* (11), 3724.
- (148) Koppes, W. M.; Adolph, H. G. *J. Org. Chem.* **1981**, *46* (2), 406.
- (149) Pinner, A.; Klein, F. *Ber. Dtsch. Chem. Ges.* **1877**, *10* (2), 1889.
- (150) Houben, J. *Ber. Dtsch. Chem. Ges.* **1926**, *59* (11), 2878.
- (151) Hartwig, J. F. *Organotransition Metal Chemistry: From Bonding to Catalysis*; University Science Books: Sausalito, 2010.
- (152) Ikawa, T.; Barder, T. E.; Biscoe, M. R.; Buchwald, S. L. *J. Am. Chem. Soc.* **2007**, *129* (43), 13001.
- (153) Baker, R. T.; Kristjansdottir, S. S. Patent no.: WO9800399A1, 1998.
- (154) Li, Z.; Zhang, S.-L.; Fu, Y.; Guo, Q.-X.; Liu, L. *J. Am. Chem. Soc.* **2009**, *131* (25), 8815.
- (155) Weskamp, T.; Kohl, F.; Hieringer, W.; Gleich, D.; Herrmann, W. *Angew. Chem., Int. Ed.* **1999**, *38* (16), 2416.
- (156) Schwarz, J.; Bohm, V.; Gardiner, M.; Grosche, M.; Herrmann, W.; Hieringer, W.; Raudaschl-Sieber, G. *Chem. Eur. J.* **2000**, *6* (10), 1773.
- (157) Peris, E.; Crabtree, R. H. *Coord. Chem. Rev.* **2004**, *248* (21-24), 2239.

- (158) Hopkinson, M. N.; Richter, C.; Schedler, M.; Glorius, F. *Nature* **2014**, *510* (7506), 485.
- (159) Köhl, O. *Functionalised N-Heterocyclic Carbene Complexes*; John Wiley & Sons, Ltd: Chichester, 2010.
- (160) Kantchev, E. A. B.; O'Brien, C. J.; Organ, M. G. *Aldrichim. Acta* **2006**, *39* (4), 97.
- (161) Valente, C.; Calimsiz, S.; Hoi, K. H.; Mallik, D.; Sayah, M.; Organ, M. G. *Angew. Chem., Int. Ed.* **2012**, *51* (14), 3314.
- (162) Nielsen, D. J.; Cavell, K. J. In *N-Heterocyclic Carbenes in Synthesis*; Nolan, S. P., Ed.; Wiley-VCH Verlag GmbH & Co. KGaA: Weinheim, 2006; pp 73–102.
- (163) Marion, N.; Nolan, S. P. *Acc. Chem. Res.* **2008**, *41* (11), 1440.
- (164) O'Brien, C. J.; Kantchev, E. A. B.; Valente, C.; Hadei, N.; Chass, G. A.; Lough, A.; Hopkinson, A. C.; Organ, M. G. *Chem. Eur. J.* **2006**, *12* (18), 4743.
- (165) Navarro, O.; Kelly, R. A.; Nolan, S. P. *J. Am. Chem. Soc.* **2003**, *125* (52), 16194.
- (166) Mitchell, E. A.; Baird, M. C. *Organometallics* **2007**, *26* (21), 5230.
- (167) Jackstell, R.; Harkal, S.; Jiao, H.; Spannenberg, A.; Borgmann, C.; Röttger, D.; Nierlich, F.; Elliot, M.; Niven, S.; Cavell, K.; Navarro, O.; Viciu, M. S.; Nolan, S. P.; Beller, M. *Chem. Eur. J.* **2004**, *10* (16), 3891.
- (168) Jackstell, R.; Gómez Andreu, M.; Frisch, A.; Selvakumar, K.; Zapf, A.; Klein, H.; Spannenberg, A.; Röttger, D.; Briel, O.; Karch, R.; Beller, M. *Angew. Chem., Int. Ed.* **2002**, *41* (6), 986.
- (169) Selvakumar, K.; Zapf, A.; Spannenberg, A.; Beller, M. *Chem. Eur. J.* **2002**, *8* (17), 3901.
- (170) Frisch, A. C.; Zapf, A.; Briel, O.; Kayser, B.; Shaikh, N.; Beller, M. *J. Mol. Catal. A: Chem.* **2004**, *214* (2), 231.
- (171) Navarro, O.; Oonishi, Y.; Kelly, R. A.; Stevens, E. D.; Briel, O.; Nolan, S. P. *J. Organomet. Chem.* **2004**, *689* (23), 3722.
- (172) Fraser, A. W.; Besaw, J. E.; Hull, L. E.; Baird, M. C. *Organometallics* **2012**, *31* (6), 2470.
- (173) Fraser, A. W.; Jaksic, B. E.; Batcup, R.; Sarsons, C. D.; Woolman, M.; Baird, M. C. *Organometallics* **2013**, *32* (1), 9.
- (174) Borjian, S.; Tom, D. M. E.; Baird, M. C. *Organometallics* **2014**, *33* (15), 3928.
- (175) Norton, D. M.; Mitchell, E. A.; Botros, N. R.; Jessop, P. G.; Baird, M. C. *J. Org. Chem.* **2009**, *74* (17), 6674.
- (176) Trnka, T. M.; Morgan, J. P.; Sanford, M. S.; Wilhelm, T. E.; Scholl, M.; Choi, T.-L.; Ding, S.; Day, M. W.; Grubbs, R. H. *J. Am. Chem. Soc.* **2003**, *125* (9), 2546.
- (177) Nyce, G. W.; Csihony, S.; Waymouth, R. M.; Hedrick, J. L. *Chem. Eur. J.* **2004**, *10* (16), 4073.
- (178) Marion, N.; Navarro, O.; Mei, J.; Stevens, E. D.; Scott, N. M.; Nolan, S. P. *J. Am. Chem. Soc.* **2006**, *128* (12), 4101.
- (179) Sergeev, N. M. *Prog. Nucl. Mag. Res. Sp.* **1973**, *9* (2), 71.
- (180) Bielinski, E. A.; Dai, W.; Guard, L. M.; Hazari, N.; Takase, M. K. *Organometallics* **2013**, *32* (15), 4025.

- (181) Jin, Z.; Guo, S.-X.; Gu, X.-P.; Qiu, L.-L.; Song, H.-B.; Fang, J.-X. *Adv. Synth. Catal.* **2009**, *351* (10), 1575.
- (182) Dai, W.; Chalkley, M. J.; Brudvig, G. W.; Hazari, N.; Melvin, P. R.; Pokhrel, R.; Takase, M. K. *Organometallics* **2013**, *32* (18), 5114.
- (183) Arduengo III, A. J.; Calabrese, J. C.; Davidson, F.; Rasika Dias, H. V.; Goerlich, J. R.; Krafczyk, R.; Marshall, W. J.; Tamm, M.; Schmutzler, R. *Helv. Chim. Acta* **1999**, *82* (12), 2348.
- (184) Blum, A. P.; Ritter, T.; Grubbs, R. H. *Organometallics* **2007**, *26* (8), 2122.
- (185) Bedford, R. B.; Betham, M.; Bruce, D. W.; Danopoulos, A. A.; Frost, R. M.; Hird, M. J. *Org. Chem.* **2006**, *71* (3), 1104.
- (186) Grasa, G. A.; Viciu, M. S.; Huang, J.; Zhang, C.; Trudell, M. L.; Nolan, S. P. *Organometallics* **2002**, *21* (14), 2866.
- (187) Anderson, C. E.; Donde, Y.; Douglas, C. J.; Overman, L. E. *J. Org. Chem.* **2005**, *70* (2), 648.
- (188) Tamura, K.; Mizukami, H.; Maeda, K.; Watanabe, H.; Uneyama, K. *J. Org. Chem.* **1993**, *58* (1), 32.
- (189) Uneyama, K. *J. Fluorine Chem.* **1999**, *97* (1-2), 11.
- (190) Gallis, D. E.; Crist, D. R. *Magn. Reson. Chem.* **1987**, *25* (6), 480.
- (191) Satterthwait, A. C.; Jencks, W. P. *J. Am. Chem. Soc.* **1974**, *96* (22), 7045.
- (192) Clement, N. D.; Routaboul, L.; Grotevendt, A.; Jackstell, R.; Beller, M. *Chem. Eur. J.* **2008**, *14* (25), 7408.
- (193) Yin, G.; Kalvet, I.; Schoenebeck, F. *Angew. Chem.* **2015**, *127* (23), 6913.
- (194) Hruszkewycz, D. P.; Balcells, D.; Guard, L. M.; Hazari, N.; Tilset, M. *J. Am. Chem. Soc.* **2014**, *136* (20), 7300.
- (195) Chalkley, M. J.; Guard, L. M.; Hazari, N.; Hofmann, P.; Hruszkewycz, D. P.; Schmeier, T. J.; Takase, M. K. *Organometallics* **2013**, *32* (15), 4223.
- (196) Werner, H.; Kühn, A. *Angew. Chem., Int. Ed.* **1977**, *16* (6), 412.
- (197) Werner, H. *Adv. Organomet. Chem.* **1981**, *19*, 155.
- (198) Werner, H. *Angew. Chem., Int. Ed.* **1977**, *16* (1), 1.
- (199) Werner, H.; Kraus, H.-J. *Angew. Chem., Int. Ed.* **1979**, *18* (12), 948.
- (200) Busch, M.; Blume, G.; Pungs, E. *J. Prakt. Chem.* **1909**, *79* (1), 513.
- (201) Vowinkel, E. *Chem. Ber.* **1963**, *96* (6), 1702.
- (202) Pinol, A. C.; Manas, M. M. *Chem. Commun.* **1967** (5), 229a.
- (203) Allen, M.; Moir, R. Y. *Can. J. Chem.* **1963**, *41* (2), 252.
- (204) El-Faham, A.; Albericio, F. *Chem. Rev.* **2011**, *111* (11), 6557.
- (205) DeTar, D. F.; Silverstein, R. J. *Am. Chem. Soc.* **1966**, *88* (5), 1013.
- (206) Stewart, F. *Aust. J. Chem.* **1968**, *21* (2), 477.
- (207) Suttle, N. A.; Williams, A. J. *Chem. Soc., Perkin Trans. 2* **1983** (9), 1369.
- (208) Esser, F.; Brandt, K.; Pook, K.-H.; Forster, H.-J.; Koppen, H.; Leger, J.-M.; Carpy, A. J. *Chem. Soc., Perkin Trans. 1* **1988** (12), 3311.
- (209) Khorana, H. G. *Can. J. Chem.* **1954**, *32* (3), 227.
- (210) Däbritz, E. *Angew. Chem., Int. Ed.* **1966**, *5* (5), 470.
- (211) Schmidt, E.; Moosmüller, F. *Liebigs Ann. Chem.* **1955**, *597* (3), 235.

- (212) Mathias, L. J. *Synthesis* **1979** (8), 561.
- (213) Moffatt, J. G.; Khorana, H. G. *J. Am. Chem. Soc.* **1957**, 79 (14), 3741.
- (214) Vowinkel, E. *Chem. Ber.* **1962**, 95 (12), 2997.
- (215) Short, W. F.; Smith, J. C. *J. Chem. Soc., Trans.* **1922**, 121, 1803.
- (216) Forman, S. E.; Erickson, C. A.; Adelman, H. J. *Org. Chem.* **1963**, 28 (10), 2653.
- (217) Farrissey, W. J.; Ricciardi, R. J.; Sayigh, A. A. R. *J. Org. Chem.* **1968**, 33 (5), 1913.
- (218) Vowinkel, E.; Wolff, C. *Chem. Ber.* **1974**, 107 (3), 907.
- (219) Kovacs, J.; Kisfaludy, L.; Ceprini, M. Q. *J. Am. Chem. Soc.* **1967**, 89 (1), 183.
- (220) Schmidt, E.; Däbritz, E.; Thulke, K.; Grassmann, E. *Liebigs Ann. Chem.* **1965**, 685 (1), 161.
- (221) Schmidt, E.; Carl, W. *Liebigs Ann. Chem.* **1961**, 639 (1), 24.
- (222) Heinisch, G.; Matuszczak, B.; Rakowitz, D.; Mereiter, K. *J. Heterocycl. Chem.* **2002**, 39 (4), 695.
- (223) Stumpe, M. C.; Grubmüller, H. *J. Phys. Chem. B* **2007**, 111 (22), 6220.
- (224) Christenson, I. *Act. Chem. Scand.* **1964**, 18, 904.
- (225) Bordwell, F. G.; McCallum, R. J.; Olmstead, W. N. *J. Org. Chem.* **1984**, 49 (8), 1424.
- (226) Bordwell, F. G.; Algrim, D. J. *J. Am. Chem. Soc.* **1988**, 110 (9), 2964.
- (227) Ulrich, H. *Chemistry and Technology of Carbodiimides*; John Wiley & Sons, Ltd: Chichester, 2007.
- (228) Ishida, S.; Fukushima, Y.; Sekiguchi, S.; Matsui, K. *Bull. Chem. Soc. Jpn.* **1975**, 48 (3), 956.
- (229) Lee Webb, R.; Eggleston, D. S.; Labaw, C. S.; Lewis, J. J.; Wert, K. *J. Heterocycl. Chem.* **1987**, 24 (1), 275.
- (230) Trani, A.; Bellasio, E. *J. Heterocycl. Chem.* **1974**, 11 (2), 257.
- (231) Mues, P.; Buysch, H.-J. *Synthesis* **1990** (3), 249.
- (232) Khorana, H. G. *Chem. Rev.* **1953**, 53 (2), 145.
- (233) Kurzer, F.; Douraghi-Zadeh, K. *Chem. Rev.* **1967**, 67 (2), 107.
- (234) Schmidt, E.; Hitzler, F.; Lahde, E. *Ber. Dtsch. Chem. Ges.* **1938**, 71 (9), 1933.
- (235) Wdowik, T.; Samojłowicz, C.; Jawiczuk, M.; Zarecki, A.; Grela, K. *Synlett* **2010** (19), 2931.
- (236) Ayala, J. D.; Bombieri, G.; Del Pra, A.; Fantoni, A.; Vicentini, G. *Inorg. Chim. Acta* **1998**, 274 (1), 122.
- (237) Woodward, C. P.; Spiccia, N. D.; Jackson, W. R.; Robinson, A. J. *Chem. Commun.* **2011**, 47 (2), 779.
- (238) Chen, Y.; Dias, H. V. R.; Lovely, C. J. *Tetrahedron Lett.* **2003**, 44 (7), 1379.
- (239) Gracias, V.; Gasiecki, A. F.; Djuric, S. W. *Org. Lett.* **2005**, 7 (15), 3183.
- (240) Fürstner, A.; Langemann, K. *J. Am. Chem. Soc.* **1997**, 119 (39), 9130.
- (241) Ghosh, A. K.; Cappiello, J.; Shin, D. *Tetrahedron Lett.* **1998**, 39 (26), 4651.
- (242) Brown, H. C.; Pfaffenberger, C. D. *J. Am. Chem. Soc.* **1967**, 89 (21), 5475.
- (243) Hennings, D. D.; Iwama, T.; Rawal, V. H. *Org. Lett.* **1999**, 1 (8), 1205.
- (244) Cepanec, I. *Synthesis of Biaryls*; Elsevier: Oxford, 2004.
- (245) Johansson Seechurn, C. C. C.; Kitching, M. O.; Colacot, T. J.; Snieckus, V. *Angew. Chem., Int. Ed.* **2012**, 51 (21), 5062.

- (246) ChemAxon pKa predictor. www.chemicalize.org.
- (247) Guthrie, J. P. *Can. J. Chem.* **1978**, *56* (17), 2342.
- (248) Raamat, E.; Kaupmees, K.; Ovsjannikov, G.; Trummal, A.; Kütt, A.; Saame, J.; Koppel, I.; Kaljurand, I.; Lipping, L.; Rodima, T.; Pihl, V.; Koppel, I. A.; Leito, I. *J. Phys. Org. Chem.* **2013**, *26* (2), 162.
- (249) Hartung, C. G.; Snieckus, V. In *Modern Arene Chemistry*; Astruc, D., Ed.; Wiley-VCH Verlag GmbH & Co. KGaA: Weinheim, 2002; pp 330–367.
- (250) Lennox, A. J. J.; Lloyd-Jones, G. C. *Chem. Soc. Rev.* **2014**, *43* (1), 412.
- (251) Liebeskind, L. S.; Srogl, J. *Org. Lett.* **2002**, *4* (6), 979.
- (252) Hooper, J. F.; Young, R. D.; Pernik, I.; Weller, A. S.; Willis, M. C. *Chem. Sci.* **2013**, *4* (4), 1568.
- (253) Nicolaou, K. C.; Bulger, P. G.; Sarlah, D. *Angew. Chem., Int. Ed.* **2005**, *44* (29), 4442.
- (254) Angiolelli, M. E.; Casalnuovo, A. L.; Selby, T. P. *Synlett* **2000** (6), 905.
- (255) Otsuka, S.; Fujino, D.; Murakami, K.; Yorimitsu, H.; Osuka, A. *Chem. Eur. J.* **2014**, *20* (41), 13146.
- (256) Srogl, J.; Liu, W.; Marshall, D.; Liebeskind, L. S. *J. Am. Chem. Soc.* **1999**, *121* (40), 9449.
- (257) Gangjee, A.; Zeng, Y.; Talreja, T.; McGuire, J. J.; Kisliuk, R. L.; Queener, S. F. *J. Med. Chem.* **2007**, *50* (13), 3046.
- (258) Llauger, L.; He, H.; Kim, J.; Aguirre, J.; Rosen, N.; Peters, U.; Davies, P.; Chiosis, G. *J. Med. Chem.* **2005**, *48* (8), 2892.
- (259) Sun, Z.-Y.; Botros, E.; Su, A.-D.; Kim, Y.; Wang, E.; Baturay, N. Z.; Kwon, C.-H. *J. Med. Chem.* **2000**, *43* (22), 4160.
- (260) Pasquini, S.; Mugnaini, C.; Tintori, C.; Botta, M.; Trejos, A.; Arvela, R. K.; Larhed, M.; Witvrouw, M.; Michiels, M.; Christ, F.; Debyser, Z.; Corelli, F. *J. Med. Chem.* **2008**, *51* (16), 5125.
- (261) Sciabola, S.; Carosati, E.; Baroni, M.; Mannhold, R. *J. Med. Chem.* **2005**, *48* (11), 3756.
- (262) Clader, J. W.; Billard, W.; Binch, H.; Chen, L.-Y.; Crosby, G.; Duffy, R. A.; Ford, J.; Kozłowski, J. A.; Lachowicz, J. E.; Li, S.; Liu, C.; McCombie, S. W.; Vice, S.; Zhou, G.; Greenlee, W. J. *Bioorg. Med. Chem.* **2004**, *12* (2), 319.
- (263) Wang, Y.; Chackalamannil, S.; Hu, Z.; Clader, J. W.; Greenlee, W.; Billard, W.; Binch, H.; Crosby, G.; Ruperto, V.; Duffy, R. A.; McQuade, R.; Lachowicz, J. E. *Bioorg. Med. Chem. Lett.* **2000**, *10* (20), 2247.
- (264) Nielsen, S. F.; Nielsen, E. Ø.; Olsen, G. M.; Liljefors, T.; Peters, D. *J. Med. Chem.* **2000**, *43* (11), 2217.
- (265) Fink, J. K. *High Performance Polymers*; Elsevier: Oxford, 2008.
- (266) Ko, T.; Kim, K.; Jung, B.-K.; Cha, S.-H.; Kim, S.-K.; Lee, J.-C. *Macromolecules* **2015**, *48* (4), 1104.
- (267) Masaki, S.; Sato, N.; Nishichi, A.; Yamazaki, S.; Kimura, K. *J. Appl. Polym. Sci.* **2008**, *108* (1), 498.
- (268) Park, N.; Park, K.; Jang, M.; Lee, S. *J. Org. Chem.* **2011**, *76* (11), 4371.

- (269) Hajipour, A. R.; Pourkaveh, R.; Karimi, H. *Appl. Organomet. Chem.* **2014**, *28* (12), 879.
- (270) Kuhn, M.; Falk, F. C.; Paradies, J. *Org. Lett.* **2011**, *13* (15), 4100.
- (271) Eichman, C. C.; Stambuli, J. P. *Molecules* **2011**, *16* (1), 590.
- (272) Bichler, P.; Love, J. A. In *C-X Bond Formation*; Vigalok, A., Ed.; Topics in Organometallic Chemistry; Springer Berlin Heidelberg: Berlin, Heidelberg, 2010; Vol. 31, pp 39–64.
- (273) Farmer, J. L.; Pompeo, M.; Lough, A. J.; Organ, M. G. *Chem. Eur. J.* **2014**, *20* (48), 15790.
- (274) Kosugi, M.; Shimizu, T.; Migita, T. *Chem. Lett.* **1978** (1), 13.
- (275) Fernández-Rodríguez, M. A.; Shen, Q.; Hartwig, J. F. *Chem. Eur. J.* **2006**, *12* (30), 7782.
- (276) Murata, M.; Buchwald, S. L. *Tetrahedron* **2004**, *60* (34), 7397.
- (277) Fernández-Rodríguez, M. A.; Hartwig, J. F. *J. Org. Chem.* **2009**, *74* (4), 1663.
- (278) Fernández-Rodríguez, M. A.; Shen, Q.; Hartwig, J. F. *J. Am. Chem. Soc.* **2006**, *128* (7), 2180.
- (279) Eichman, C. C.; Stambuli, J. P. *J. Org. Chem.* **2009**, *74* (10), 4005.
- (280) Fernández-Rodríguez, M. A.; Hartwig, J. F. *Chem. Eur. J.* **2010**, *16* (8), 2355.
- (281) Mao, J.; Jia, T.; Frensch, G.; Walsh, P. J. *Org. Lett.* **2014**, *16* (20), 5304.
- (282) Van den Hoogenband, A.; Lange, J. H. M.; Bronger, R. P. J.; Stoit, A. R.; Terpstra, J. W. *Tetrahedron Lett.* **2010**, *51* (52), 6877.
- (283) Bruno, N. C.; Tudge, M. T.; Buchwald, S. L. *Chem. Sci.* **2013**, *4* (3), 916.
- (284) Munjanja, L.; Brennessel, W. W.; Jones, W. D. *Organometallics* **2015**, *34* (18), 4574.
- (285) Takagi, K. *Chem. Lett.* **1987** (11), 2221.
- (286) So, C. M.; Lau, C. P.; Chan, A. S. C.; Kwong, F. Y. *J. Org. Chem.* **2008**, *73* (19), 7731.
- (287) Lee, C.-F.; Liu, Y.-C.; Badsara, S. S. *Chem. Asian J.* **2014**, *9* (3), 706.
- (288) BouzBouz, S.; Boulard, L.; Cossy, J. *Org. Lett.* **2007**, *9* (19), 3765.
- (289) Nolte, C.; Mayer, P.; Straub, B. F. *Angew. Chem., Int. Ed.* **2007**, *46* (12), 2101.
- (290) Thomson, J. E.; Campbell, C. D.; Concellón, C.; Duguet, N.; Rix, K.; Slawin, A. M. Z.; Smith, A. D. *J. Org. Chem.* **2008**, *73* (7), 2784.
- (291) Dai, C.; Fu, G. C. *J. Am. Chem. Soc.* **2001**, *123* (12), 2719.
- (292) Mukaiyama, T.; Tokizawa, M.; Takei, H. *J. Org. Chem.* **1962**, *27* (3), 803.
- (293) Fors, B. P.; Davis, N. R.; Buchwald, S. L. *J. Am. Chem. Soc.* **2009**, *131* (16), 5766.
- (294) Bedford, R. B.; Betham, M.; Blake, M. E.; Frost, R. M.; Horton, P. N.; Hursthouse, M. B.; López-Nicolás, R.-M. *Dalton Trans.* **2005** (16), 2774.
- (295) Lee, J.; Chubb, A. J.; Moman, E.; McLoughlin, B. M.; Sharkey, C. T.; Kelly, J. G.; Nolan, K. B.; Devocelle, M.; Fitzgerald, D. J. *Org. Biomol. Chem.* **2005**, *3* (20), 3678.
- (296) Mohanta, P. K.; Dhar, S.; Samal, S. K.; Ila, H.; Junjappa, H. *Tetrahedron* **2000**, *56* (4), 629.
- (297) Shiro, D.; Fujiwara, S.; Tsuda, S.; Iwasaki, T.; Kuniyasu, H.; Kambe, N. *Chem. Lett.* **2015**, *44* (4), 465.
- (298) Liang, Y.; Fu, G. C. *J. Am. Chem. Soc.* **2014**, *136* (14), 5520.

- (299) Chun, J.-H.; Morse, C. L.; Chin, F. T.; Pike, V. W. *Chem. Commun.* **2013**, 49 (21), 2151.
- (300) Ke, F.; Qu, Y.; Jiang, Z.; Li, Z.; Wu, D.; Zhou, X. *Org. Lett.* **2011**, 13 (3), 454.